ISBN: 978-3-95450-192-2 doi:10.18429/JACoW-IBIC2017-MO1AB1

FRIB PROJECT STATUS AND BEAM INSTRUMENTATION CHALLENGES*

J. Wei#, H. Ao, S. Beher, N. Bultman, F. Casagrande, J. Chen, S. Cogan, C. Compton, L. Dalesio, K. Davidson, A. Facco[1], F. Feyzi, V. Ganni, A. Ganshyn, P. Gibson, T. Glasmacher, L. Hodges, K. Holland, H.-C. Hseuh[2], A. Hussain, M. Ikegami, S. Jones, R.E. Laxdal[3], S. Lidia, G. Machicoane, I. Malloch, F. Marti, S. Miller, D. Morris, J. Nolen[4], P. Ostroumov, J. Popielarski, L. Popielarski, E. Pozdeyev, T. Russo, K. Saito, S. Stanley, H. Tatsumoto, R. Webber, T. Xu, Y. Yamazaki, Facility for Rare Isotope Beams, Michigan State University, East Lansing, MI, USA
K. Dixon, M. Wiseman, Thomas Jefferson National Laboratory, Newport News, VA, USA
M. Kelly, Argonne National Laboratory, Argonne, IL, USA
K. Hosoyama, KEK, Tsukuba, Japan
S. Prestemon, Lawrence Berkeley National Laboratory, Berkeley, CA, USA
A. Aleksandrov, Oak Ridge National Laboratory, Oak Ridge, TN, USA
N. Eddy, Fermi National Accelerator Laboratory, Batavia, IL, USA
[1] also at INFN - Laboratori Nazionali di Legnaro, Legnaro (Padova), Italy
[2] also at Brookhaven National Laboratory, Upton, NY, USA
[3] also at TRIUMF, Vancouver, Canada
[4] also at Argonne National Laboratory, Argonne, IL, USA

Abstract

With an average beam power two orders of magnitude higher than operating heavy-ion facilities, the Facility for Rare Isotope Beams (FRIB) stands at the power frontier of the accelerator family. This paper summarizes the status of design, technology development, construction, commissioning, as well as path to operations and upgrades. We highlight beam instrumentation challenges including machine protection of high-power heavy-ion beams and complications of multi-charge-state and multi-ion-species accelerations.

INTRODUCTION

During the past decades, accelerator-based neutron-generating facilities, such as SNS [1], J-PARC [2], PSI [3], and LANSCE [4], advanced the frontier of proton beam power to the 1 MW level, as shown in Fig. 1. FRIB is designed to advance the power frontier for heavy ions by more than two orders of magnitude, to 400 kW [5].

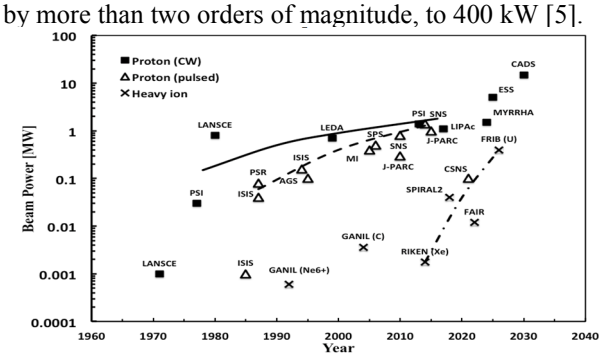

Figure 1: Achieved and planned average beam power on target for proton and heavy ion facilities.

*Work supported by the U.S. Department of Energy Office of Science under Cooperative Agreement DE-SC0000661 and the National Science Foundation under Cooperative Agreement PHY-1102511.
#wei@frib.msu.edu

The FRIB driver accelerator is designed to accelerate all stable ions to energies >200 MeV/u with a beam power on the target of up to 400 kW (Table 1). The driver accelerator consists of a 46 m long Front End [6] containing electron-cyclotron-resonance (ECR) ion sources and a room temperature RFQ followed by a 472 m long SRF linac with quarter-wave-resonators (QWR) of β_0=0.041 and 0.085 and half-wave-resonators (HWR) of β_0=0.29 and 0.53 in a folded layout to facilitate charge stripping and beam collimation and to accommodate the limited real estate footprint in the center of the MSU campus (Fig. 2). Up to 400 kW of the primary beam is focused down to a spot size of 1 mm in diameter striking the production target for rare isotope production. Following the low-loss design philosophy [7], the design average uncontrolled beam loss is below 1 W/m. For heavy ions like uranium at low energies, activation and radiation shielding is of less concern; the 1 W/m limit addresses concerns in damage on superconducting cavity surfaces and in cryogenic heat load [5].

Table 1: FRIB Driver Accelerator Baseline Parameters

Parameter	Value	Unit
Primary beam ion species	H to ^{238}U	
Beam kinetic energy on target	> 200	MeV/u
Maximum beam power on target	400	kW
Macropulse duty factor	100	%
Beam current on target (^{238}U)	0.7	emA
Beam radius on target (90%)	0.5	mm
Driver linac beam-path length	517	m
Average uncontrolled beam loss	< 1	W/m

ISBN: 978-3-95450-192-2 doi:10.18429/JACoW-IBIC2017-MO2AB2

OVERVIEW AND STATUS OF DIAGNOSTICS FOR THE ESS PROJECT

T. J. Shea*, R. Baron, B. Cheymol, C. Derrez, T. Grandsaert, A. Jansson, H. Hassanzadegan, I. Dolenc-Kittelmann, H. Kocevor, S. Molloy, C. Thomas
European Spallation Source, Lund, Sweden
E. Adli, U. Oslo, Oslo, Norway
M. Poggi, INFN, Legnaro, Italy
M. Ferianis, Sincrotrone Trieste, Trieste, Italy
I. Bustinduy, ESS Bilbao, Bilbao, Spain
P. Aden, STFC, Daresbury, UK
T. Papaevangenlou, J. Marroncle, L. Segui, CEA, Saclay, France
S. Vilcins, DESY, Hamburg, Germany
A. J. Johannson, LTH, Lund, Sweden

Abstract

The European Spallation Source, now under construction in Lund, Sweden, aims to be the world's most powerful pulsed neutron scattering facility. Driving the neutron source is a 5 MW superconducting proton linear accelerator operating at 4 percent beam duty factor and 14 Hz repetition rate. Nineteen partner institutions from across Europe are working with the Accelerator Division in Lund to design and construct the accelerator. The suite of accelerator instrumentation consists of over 20 unique system types developed by over 20 partners and collaborators. Although the organizational complexity presents challenges, it also provides the vast capabilities required to achieve the technical goals. At this time, the beam instrumentation team is in transition, completing the design phase while scaling up to the deployment phase. Commissioning of the ion source has commenced in Catania, preparations for installation on the Lund site are ramping up, and basic R&D on target instrumentation continues. Beam commissioning results from the systems immediately following the ion source will be presented, along with technical highlights and status of the many remaining instrumentation systems.

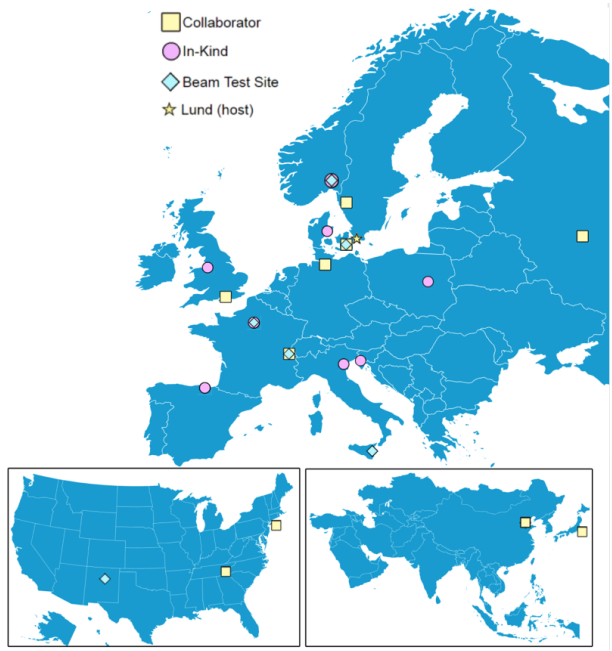

Figure 1: Map of In-kind partners, collaborators, and test sites.

OVERVIEW

The Project Organization

Like the ESS project itself, the beam diagnostics project is executed by an international partnership. Figure 1 illustrates the breadth of this organization, consisting of in-kind contributors from partner countries, collaborators that participate via memorandum or contract, and finally, several institutes that provide beam test facilities. From this partnership of over 20 institutions, all designs, components and completed systems are eventually delivered to the host facility, ESS in Lund, Sweden.

The Diagnostic Suite

As itemized in Table 1, the beam diagnostics team will deliver a comprehensive suite of instrumentation that supports commissioning and operations of the ESS accelerator. Reading from left to right in the table, the devices are deployed in the 75 keV transport line (LEBT) following the ion source, in the normal-conducting section ending with the drift tube linac (DTL), in the superconducting section ending with the high beta linac (HBL), and finally in the transport lines to the tuning dump and the target.

MEASUREMENT CAPABILITIES

The diagnostic systems provide three categories of measurement, the first being beam accounting. Throughout the machine, various diagnostic devices measure the beam current and where it is lost, starting from constituents of beam extracted from the ion source, then the proton current and losses throughout the accelerator, and finally the beam leaving aperture in the region of the tuning dump and the target.

* thomas.shea@esss.se

ISBN: 978-3-95450-192-2 doi:10.18429/JACoW-IBIC2017-MO2AB3

SESAME STORAGE RING DIAGNOSTICS AND COMMISSIONING

H. Al-Mohammad, K. Manukyan, SESAME, Allan, Jordan

Abstract

SESAME Storage Ring is a 2.5 GeV Synchrotron Light Source in Allan, Jordan. The commissioning of the Storage Ring has been done in spring 2017. The storage ring is equipped with 64 BPMs whereas 48 connected to Libera-Brilliance+, three fluorescent screens, one FCT, one DCCT, four BLMs, two Bunch by Bunch kickers and one Synchrotron Radiation Monitor. This paper gives an overview of the Diagnostics elements and our experience during the commissioning.

INTRODUCTION

The SESAME Storage Ring (SR) shown in Fig. 1 is a 2.5 GeV Light Source of 133.2 m circumference composed of 8 DBA cells with dispersion in all straight sections (8*4.4 m and 8*2.4 m), offers a maximum capacity of 25 beamlines [1]. The RF system consists of four 500 MHz ELETTRA cavities powered by four 80 kW Solid State Amplifiers [2]. A 800 MeV Booster Synchrotron (original from BESSY I) injects the beam into the SR with 1 Hz repetition frequency. The SR main parameters are listed in Table 1.

Table 1: Storage Ring Main Parameters

Energy (GeV)	2.5
Circumference (m)	133.2
RF Frequency (MHz)	499.654
Repetition freq.(Hz)	1
Betatron tunes Q_X / Q_Y	7.23 / 6.19
Horizontal emittance ε_x (nm.rad)	26
Momentum compaction factor	0.0083
Circulating Current(mA)	250
Energy loss per turn (keV)	603

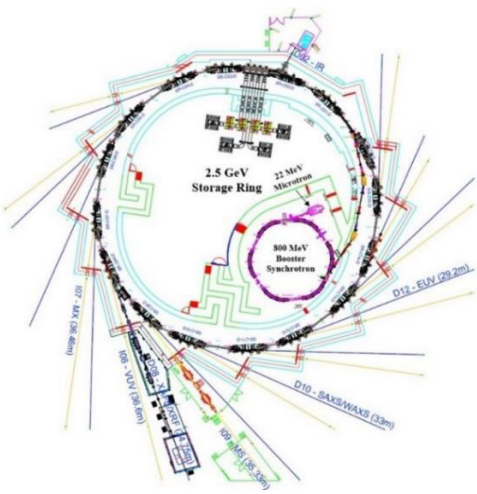

Figure 1: SESAME Facility.

Commissioning of the Microtron had been done in 2012, commission of the Booster in 2014 and of the SR in 2017. Throughout the commissioning, the Diagnostics components are key elements to check SR performance a set of equipment's are installed in the machine in order to measure electron beam current, transverse shape, position inside the vacuum chamber and orbit, tune, chromaticity and emittance. In the following, we present the different diagnostics elements installed in the SR and our experience during the commissioning.

BPM SYSTEM

There are 64 button type beam position monitor (BPM) in SR, which are distributed around the ring as 4 BPMs/cell, two of them flanking the bending magnet and two at beginning and end of the straight sections, 48 of them are connected to Libera Brilliance + [3] and one BPM is connected to a Spectrum Analyser. The BPMs are connected to the Libera B+ by low attenuation RF cables with different lengths (20 m-45 m). 8 Libera B+ units are equipped with GDX (Gigabit Data eXchange) module for FOFB which will be done by using 32 BPM, 4 GDX modules are donated from Instrumentation Technologies as a support to SESAME project. For early stage of the commissioning (first turn(s)), the BPMs could not be used for indication of beam position, due to the low beam intensity, but ADC buffer data and sum signal were used to indicate the passage of the beam. The signal of BPM1 for the first turns is shown in Fig. 2 exemplarily. Once a beam of about mA was stored, transverse beam position could be evaluated and orbit correction was done via SVD method using initially the theoretical and later the measured response matrix. By doing beam based alignment and tuning RF frequency it was possible to correct horizontal orbit to 0.3mm and to 0.17 mm rms, as shown in Fig. 3 [1] then BPMs can be calibrated in positon relative to magnet centres.

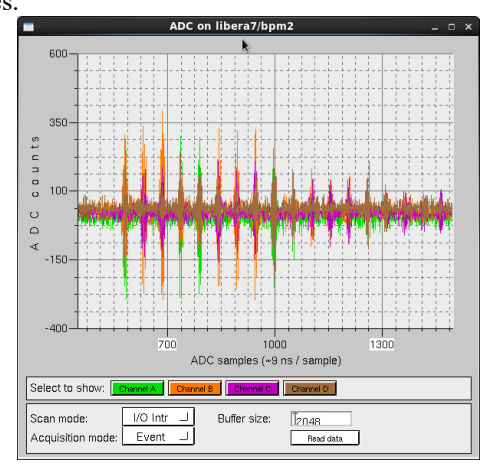

Figure 2: ADC Buffer Data for Few Turns in SR.

ISBN: 978-3-95450-192-2 doi:10.18429/JACoW-IBIC2017-MO3AB1

CHARACTERIZING THE COUPLED BUNCH DRIVING TERMS IN A STORAGE RING *

Katherine C. Harkay†, Tim Berenc, Louis Emery, Ulrich Wienands, ANL, Argonne, IL, USA
Dmitry Teytelman, Dimtel, Inc., San Jose, CA, USA
John Byrd, LBNL, Berkeley, CA, USA
Rohan Dowd, Australian Synchrotron, Clayton, Australia

Abstract

Stable operation of a modern high current storage rings requires attention to the sources of coupling impedance. Methods ranging from EM modeling to bench and beam measurements are routinely used to characterize accelerator components. The beam-based method presented here complements existing approaches, and allows precise measurements and identification of narrowband resonances in structures such as RF cavities or in-vacuum undulators. We combine the well-established approach of characterizing eigenvalues of coupled-bunch instabilities with modern high-throughput data acquisition tools and automatic analysis methods. By sequentially exciting low-amplitude oscillation of individual modes below the instability threshold and observing open-loop damping, we automatically map the eigenvalues of all even-fill eigenmodes. Repeating the measurements while changing operating conditions, such as cavity temperatures or undulator gaps, provides a detailed mapping of the impedance source. These measurements are used to extract impedance parameters as well as to optimize accelerator settings. Experimental results from the Advanced Photon Source and other accelerators illustrate the technique.

INTRODUCTION

In this paper we present a beam-based method for measuring narrowband coupling impedances in a storage ring. Such narrow resonant modes, typically parasitic modes in vacuum structures or higher-order modes (HOMs) in RF cavities, can potentially excite severe coupled-bunch instabilities. Precise characterization of these resonances is important for optimizing the operation of existing machines as well as for planning of upgrades.

MEASUREMENT METHOD

Instabilities and Impedances

In order to characterize the coupling impedances we measure the eigenvalues of the even-fill eigenmodes (EFEMs). Modal eigenvalue Λ_l defines the open-loop trajectory $A_l e^{\Lambda_l t}$ of EFEM l. The real part of the eigenvalue determines the modal growth or damping rate and the imaginary part — the oscillation frequency. In the longitudinal plane, the eigenvalues are described by the following relation:

$$\Lambda_l = \Lambda_0 + \frac{\pi\alpha e f_{\rm rf}^2 I_0}{E_0 h\omega_s} Z^{\parallel\rm eff}(l\omega_0 + \omega_s), \quad (1)$$

where $\Lambda_0 = -\lambda_{\rm rad} + i\omega_s$ is the unperturbed eigenvalue, $Z^{\parallel\rm eff}$ is the effective impedance, related to the physical impedance as follows:

$$Z^{\parallel\rm eff}(\omega) = \sum_{p=-\infty}^{\infty} \frac{p\omega_{\rm rf} + \omega}{\omega_{\rm rf}} Z^{\parallel}(p\omega_{\rm rf} + \omega) \quad (2)$$

In the transverse plane we have [1]:

$$\Lambda_l = (-\lambda_{\rm rad}^{\perp} + i\omega_\beta) - \frac{cef_{\rm rev} I_0}{2\omega_\beta E_0} Z^{\perp\rm eff}(l\omega_0 + \omega_\beta) \quad (3)$$

$$Z^{\perp\rm eff}(\omega) = \sum_{p=-\infty}^{\infty} Z^{\perp}(p\omega_{\rm rf} + \omega), \quad (4)$$

where c is the speed of light and ω_β is the betatron frequency. The transverse impedance, unlike longitudinal, does not scale with frequency when aliasing to $Z^{\perp\rm eff}$.

Modal eigenvalues sample machine impedances at synchrotron or betatron sidebands of many revolution harmonics. To characterize the resonant modes we need a way to tune their frequencies. For higher order modes in RF cavities the typical method for tuning the HOMs is to change the cavity temperature. Mechanisms to change the geometry of the structure provide another way of tuning the resonances. These include cavity tuners, in-vacuum undulators (IVUs) with movable jaws, and others.

A measurement of complex eigenvalues as a function of a tuning parameter characterizes the aliased effective impedance $Z^{\rm eff}(\omega)$. In order to reconstruct the original HOM resonance additional information is required. Aliased impedance measurement defines, with the resolution of the RF frequency, where in the spectrum the true impedance might be located. One way to localize the impedance is to compare these frequencies to the known HOM spectra, from simulations or bench measurements. If the structure in question has RF probes, it can be investigated with beam to resolve various resonances. In this case, a single-bunch fill pattern is normally used to generate a comb of revolution frequency harmonics extending beyond the beam pipe cut-off frequency.

To summarize, by scanning a resonant mode and measuring EFEM eigenvalues we can extract the response as a function of the scanning parameter. In order to translate that information to the modal frequency and bandwidth we need

* Work at supported by U. S. Department of Energy, Office of Science, under Contract No. DE-AC02-06CH11357.
† harkay@aps.anl.gov

ISBN: 978-3-95450-192-2 doi:10.18429/JACoW-IBIC2017-MO3AB2

REVIEW OF BEAM-BASED TECHNIQUES OF IMPEDANCE MEASUREMENT*

V. Smaluk†, Brookhaven National Laboratory, Upton, USA

Abstract

Knowledge of a vacuum chamber impedance is necessary to estimate limitations of particle beam intensity. For new accelerator projects, minimization of the impedance is a mandatory requirement. The impedance budgets are computed during the machine design. Beam-based measurements of the impedance are usually carried out at the beginning of the machine commissioning. Comparisons of the impedance computations and measurements often show significant discrepancies, a factor of two or even more is not something unusual. Since the accuracy of impedance computations is not sufficient, the beam-based measurements are important to estimate the machine impedance and to predict stability conditions for high-intensity particle beams.

WAKEFIELDS AND IMPEDANCES

The beam intensity in storage rings is usually limited by its interaction with electromagnetic fields induced in a vacuum chamber by the beam itself (wakefields). The beam-wakefield interaction is described in terms of wake functions defined as normalized integrals of the Lorentz forces that act on a test particle moving behind a leading particle which excites the wakefields. The velocity of both particles is $\mathbf{v}$ ($|\mathbf{v}| = c$). To analyze the beam stability in most practical cases, it is enough to consider only monopole longitudinal $W_\parallel$ and dipole transverse $\mathbf{W}_\perp$ wake functions. The longitudinal wake function is [1]:

$$W_\parallel(\tau) = -\frac{1}{q}\int_{-\infty}^{\infty} E_z(t,\tau)\ \mathrm{d}t\ , \qquad (1)$$

where q is the charge of leading particle, $\tau = s/c$, s is the distance between the leading and the trailing particles, c is the speed of light. The transverse wake function is defined similarly to the longitudinal one but the integral is normalized by the dipole moment qr of the leading particle; $\mathbf{W}_\perp$ is a vector with horizontal and vertical components:

$$\mathbf{W}_\perp(\tau) = -\frac{1}{q\,r}\int_{-\infty}^{\infty} [\mathbf{E}(t,\tau) + \mathbf{v}\times\mathbf{B}(t,\tau)]_\perp\ \mathrm{d}t\ . \qquad (2)$$

The longitudinal and transverse wake functions are related to each other by the Panofsky-Venzel theorem [1, 2].

For a beam with arbitrary charge distribution, its interaction with wakefields is described by the wake potential:

$$V(\tau) = \int_0^{\infty} W(t)\lambda(\tau - t)\mathrm{d}t\ , \qquad (3)$$

where $\lambda(t)$ is the longitudinal charge density normalized as $\int_{-\infty}^{\infty}\lambda(t)\mathrm{d}t = 1$.

* Work supported by DOE under contract DE-SC0012704
† vsmalyuk@bnl.gov

In the frequency domain, each part of the vacuum chamber is represented by a frequency-dependent longitudinal $Z_\parallel$ and transverse $Z_\perp$ impedances defined as Fourier transforms of the corresponding wake functions. For any vacuum chamber component, the impedance can be approximated by a set of equivalent resonators plus the resistive-wall impedance. The beam interaction with the narrowband impedance and with the broadband one can be analyzed separately. We can assert that the narrowband impedance leads to the bunch-by-bunch interaction and can result in multi-bunch instabilities, whereas the broadband impedance leads to the intra-bunch particle interaction and can cause single-bunch instabilities.

Computation of the impedance budget is an essential part of accelerator design. The impedance of a vacuum chamber is computed by element-wise wakefield simulations using 3D finite-difference simulation codes solving Maxwell equations with the boundary conditions determined by the chamber geometry. The fields are excited by a bunched beam with pre-defined charge distribution. The code output is a wake potential (3) and the impedance is calculated as $Z(\omega) = \tilde{V}(\omega)/\tilde{\lambda}(\omega)$, where $\tilde{V}$ and $\tilde{\lambda}$ are the Fourier transforms of the wake potential and of the longitudinal charge density, respectively. So the bandwidth of the impedance derived from the simulated wake potential is limited by the bunch spectrum width which is inversely proportional to the bunch length defined for the simulation. The mesh size of the solver is very important, it should be small enough to get reliable results for a given bunch spectrum. For a typical bunch length of few millimeters, full 3D simulation of wakefields in a big and complex structure is quite difficult.

Beam-based measurement of the impedance is an important part of a machine commissioning. Comparisons of impedance computations and beam-based measurements show significant discrepancies for many machines, a factor of two or even more. There are many publications describing thorough calculations of impedance budgets and finally the total impedance is multiplied by a "safety factor" of two. Some accelerator facilities have not achieved their design beam currents because the collective effects nave not been predicted correctly at the design stage. Since the accuracy of impedance computations is not sufficient, the beam-based measurements are important to estimate the machine impedance and to predict stability conditions for high-intensity particle beams.

LONGITUDINAL BROADBAND IMPEDANCE

For the longitudinal broadband impedance, the measurable single-bunch effects are: current-dependent bunch lengthening, synchronous phase shift, and energy spread

ISBN: 978-3-95450-192-2 doi:10.18429/JACoW-IBIC2017-MO3AB3

BEAM DIAGNOSTIC CHALLENGES FOR FACET-II*

S. Z. Green†, M. J. Hogan, N. Lipkowitz, B. O'Shea, G. White, V. Yakimenko, G. Yocky
SLAC National Accelerator Laboratory, Menlo Park, CA 94025, USA

Abstract

FACET-II, the Facility for Advanced Accelerator Experimental Tests II, is a new accelerator R&D test facility to be constructed at SLAC. It will provide high-energy, high-density electron and positron beams to advance the development of beam driven plasma wakefield acceleration and support a broad range of experiments. The FACET-II beams are expected to have 10 GeV energy, contain 2 nC of charge, have a transverse normalized emittance of 7 microns, be compressed to about 1 micron long and focused to about 6 micron wide at the interaction point. The nominal peak current is 20 kA and is expected to fluctuate up to 200 kA. Most experiments desire complete knowledge of the incoming beam parameters on a pulse-to-pulse basis. However, the extreme beam densities and strong fields of the beam current will destroy any diagnostics intercepting the beam in a single shot and impose unique challenges for beam diagnostics. Moreover, non-intercepting diagnostics are desirable to provide feedback for machine setup and characterization. We need to look beyond conventional diagnostics to seek new solutions for measurements of the high charge, small beam size, short bunch length, and low emittance.

INTRODUCTION

FACET-II, the Facility for Advanced Accelerator Experimental Tests II, is a new accelerator research and development test facility to be constructed at SLAC National Accelerator Laboratory. It's an upgrade of the FACET User Facility that delivered 20 GeV electron and positron beams for experimental programs from April 2012 to April 2016. Experiments at FACET produced high impact results on efficient acceleration of electrons and positrons in plasma. Highlights of these results include mono-energetic electron acceleration, high efficiency electron acceleration [1] and the first high-gradient positron plasma wakefield acceleration (PWFA) [2].

In April 2016, the Linac Coherent Light Source-II (LCLS-II) began construction for the second phase of SLAC's x-ray laser in the first kilometer (Sectors 0 to 10) of the SLAC Linac that previously housed the first half of the FACET accelerator. This represented an opportunity to rebuild and upgrade FACET. FACET-II will occupy the second kilometer of the SLAC Linac from Sectors 10 to 20 and use existing experimental infrastructure in Sector 20 (S20). A schematic layout of FACET-II relative to LCLS and LCLS-II is shown in Fig. 1. FACET-II will operate as a national user facility with experimental programs between 2019 and 2026.

FACET-II will continue to support advanced accelerator PWFA experiments. PWFA research priorities at FACET-II include emittance preservation with efficient acceleration, high brightness beam generation and characterization, positron acceleration, and staging studies. High-gradient high-efficiency acceleration was demonstrated at FACET and will be used to benchmark FACET-II. Full pump depletion of the drive beam and preservation of emittance at the micron level are planned as the first high impact experiments. Emittance preservation at the 10's of nm level is necessary for collider applications. Ultra-high brightness plasma injectors may lead to first applications of PWFA technology and allow the study of emittance preservation at this level. The delivery of positron beams to FACET-II will enable the only positron capability in the world for PWFA research. The emphasis will be to develop techniques for positron acceleration in PWFA stages. An independent witness injector will be added to FACET-II at a later stage as an Accelerator Improvement Project (AIP) to enable studies of high transformer ratio and staging challenges such as timing and alignment.

FACET-II ACCELERATOR

The goal of FACET-II is not only to restore beam capabilities for experimental programs but also to provide beams with greatly improved quality. A schematic of the FACET-II electron and positron systems is shown in Fig. 2. The FACET-II accelerator begins with the radio frequency (RF) photocathode gun and injection system at Sector 10 (S10) that enable delivery of low emittance beams. The 4.3 MeV electron beam goes through the first accelerating section L0 and reaches 134 MeV when injected into the linac for further acceleration through L1, L2, and L3 in Sectors 11–19. Three compression stages BC11, BC14 and BC20 are required to achieve the desired bunch length for compressed electron beams to be delivered to the experimental area in Sector 20 (S20). The design of the injector complex up to BC11 is based on the LCLS S20 injector.

Beam Dynamics

The FACET-II beams were modeled and tested with the 6D particle tracking models *IMPACT-T* [3] and *Lucretia* [4]. Simulation of the injector uses *IMPACT-T* which includes three dimensional space charge effect and is the simulation tool used for LCLS and LCLS-II. The rest of the FACET-II beam dynamics modeling was performed with *Lucretia* for tracking that includes effects of incoherent synchrotron radiation (ISR), coherent synchrotron radiation (CSR), longitudinal and transverse wakefields in structures, and longitudinal space charge. This Matlab-based toolbox was benchmarked against other tracking engines in the context of Linear Col-

* Work supported by DOE Contract DE-AC02-76SF00515
† selina@slac.stanford.edu

ISBN: 978-3-95450-192-2 doi:10.18429/JACoW-IBIC2017-MOPCC01

ADVANCES IN DIAGNOSTICS FOR MEDICAL ACCELERATORS*

C.P. Welsch†, University of Liverpool and Cockcroft Institute, UK

Abstract

The Optimization of Medical Accelerators (OMA) is the aim of a new pan-European project. As one of the largest initiatives of its kind, OMA joins more than 30 universities, research centers and clinical facilities with industry partners to address the challenges in treatment facility design and optimization, numerical simulations for the development of advanced treatment schemes, and beam imaging and treatment monitoring. This paper starts with an overview of the project's research into beam diagnostics and imaging. It then presents specific research outcomes from investigations into applying detector technologies originally developed for high energy physics experiments (VELO and Medipix) for medical applications; identification of optimum detector configurations and materials for high resolution spectrometers for proton therapy and radiography; ultra-low-charge beam current monitors. Finally, it summarizes the interdisciplinary training program that OMA provides to its 15 Fellows, as well as the wider medical accelerator community.

INTRODUCTION

In 1946 R.R. Wilson introduced the idea of using heavy charged particles in cancer therapy. In his seminal paper [1] he pointed out the distinct difference in depth dose profile between photons and heavy charged particles: While photons deposit their energy along the beam path in an exponentially decreasing manner, heavy charged particles like protons and ions show little interaction when they first enter the target and deposit the dominant portion of their energy only close to the end of their range. This leads to an inverse dose profile, exhibiting a well-defined peak of energy deposition (the Bragg Peak). The depth of the Bragg Peak in the target can be selected precisely by choosing the initial energy of the particles. This allows for a significant reduction of dose delivered outside the primary target volume and leads to substantial sparing of normal tissue and nearby organs at risk. The field of particle therapy has steadily developed over the last 6 decades, first in physics laboratories, and starting in the late 90's in dedicated clinical installations. By March 2013 about 110,000 people had received treatment with particle beams, the vast majority having been treated with protons and around 15,000 patients with heavier ions (helium, carbon, neon, and argon). The latter are considered superior in specific applications since they not only display an increase in physical dose in the Bragg peak, but also an enhanced relative biological efficiency (RBE) as compared to protons and photons. This could make ions the preferred choice for treating radio-resistant tumors and tumors very close to critical organs. Proton- and ion therapy is now spreading rapidly to the clinical realm. There are currently 43 particle therapy facilities in operation around the world and many more are in the proposal and design stage. The most advanced work has been performed in Japan and Germany, where a strong effort has been mounted to study the clinical use of carbon ions. Research in Europe, particularly at GSI, Germany and PSI, Switzerland must be considered outstanding. Initial work concentrated predominantly on cancers in the head and neck region using the excellent precision of carbon ions to treat these cancers very successfully [2]. Also, intensive research on the biological effectiveness of carbon ions in clinical situations was carried out and experiments, as well as Monte Carlo based models including biological effectiveness in the treatment planning process were realized [3]. This work has directly led to the establishing of the Heavy Ion Treatment center HIT in Heidelberg, Germany [4]. HIT started patient treatment in November 2009 and continues basic research on carbon ion therapy in parallel to patient treatments. Several other centers offering carbon ion and proton therapy are under construction or in different stages of development across Europe, e.g. five proton therapy centers are being built in the UK, one more has been commissioned in Marburg, Germany and the Medaustron facility has also started patient treatment recently. The OMA network presently consists of 14 beneficiary partners (three from industry, six universities, three research centers and 2 clinical facilities), as well as of 17 associated and adjunct partners, 8 of which are from industry.

RESEARCH

Continuing research into the optimization of medical accelerators is urgently required to assure the best possible cancer care for patients and this is one of the central aims of OMA [5]. The network's main scientific and technological objectives are split into three closely interlinked work packages (WPs):

- Development of novel beam imaging and diagnostics systems;
- Studies into treatment optimization including innovative schemes for beam delivery and enhanced biological and physical models in Monte Carlo codes;
- R&D into clinical facility design and optimization to ensure optimum patient treatment along with maximum efficiency.

The following paragraphs give three examples of R&D results already obtained by Fellows in the OMA diagnostics work package.

LHCb VELO as an Online Beam Monitor

A non-invasive beam current monitor based on the multi-strip LHCb Vertex Locator (VELO) silicon detector has been developed at the Cockcroft Institute/University of

*This project has received funding from the European Union's Horizon 2020 research and innovation programme under the Marie Skłodowska-Curie grant agreement No 675265.

†c.p.welsch@liverpool.ac.uk

ISBN: 978-3-95450-192-2 doi:10.18429/JACoW-IBIC2017-MOPCC03

A METHOD OF LOCAL IMPEDANCE MEASUREMENT BY SINE-WAVE BEAM EXCITATION *

V. Smaluk†, X. Yang, A. Blednykh, Y. Tian, K. Ha, Brookhaven National Laboratory, Upton, USA

Abstract

We have developed and tested a technique, which significantly improves the accuracy of the orbit bump method of local impedance measurement. This technique is based on in-phase sine-wave (AC) excitation of four fast correctors adjacent to the vacuum chamber section, impedance of which is measured. The narrow-band sine-wave signals provide better signal-to-noise ratio. Use of fast correctors to the beam excitation eliminates the systematic error caused by hysteresis. The systematic error caused by orbit drift is also suppressed because the measured signal is not affected by the orbit motion outside the excitation frequency range. The measurement technique is described and the result of experimental testing carried out at NSLS-II is presented.

INTRODUCTION

The beam intensity in storage rings is limited by collective effects of beam dynamics resulting from the interaction of a particle beam with electromagnetic fields induced in a vacuum chamber by the beam itself. This interaction can result in serious troubles affecting accelerator performance such as overheating of vacuum chamber components or instability of the beam motion.

The beam-impedance interaction manifests itself in several effects, which can be measured quite precisely using modern beam diagnostic instruments and measurement techniques. So the impedance can be measured experimentally using beam- based techniques. For the longitudinal broadband impedance, the measurable effects are current-dependent bunch lengthening, synchronous phase shift, and energy spread growth due to microwave instability. For the transverse broadband impedance, the measurable effects are current-dependent shift of betatron tunes and rising/damping time of chromatic head-tail interaction.

The impedance distribution along the ring is not uniform and beam-based measurement of local impedance is a subject of importance for accelerator physicists. For example, low-gap light-generating insertion devices make significant contributions to the total impedance of a light sources. Thus, measurement of impedances of already installed insertion devices is helpful to predict the impedance evolution of light sources while installing new insertion devices.

* Work supported by DOE under contract DE-SC0012704
† vsmalyuk@bnl.gov

ORBIT BUMP METHOD

The interaction of a bunched beam with the transverse broadband impedance is characterized by the kick factor:

$$k_\perp = \frac{1}{2\pi}\int_{-\infty}^{\infty} Z_\perp(\omega)\, h(\omega)\mathrm{d}\omega\,, \qquad (1)$$

where $Z_\perp(\omega)$ is the frequency-dependent transverse impedance; $h(\omega) = \tilde{\lambda}(\omega)\tilde{\lambda}^*(\omega)$ is the bunch power spectrum; $\tilde{\lambda}(\omega) = \int_{-\infty}^{\infty} \lambda(t)e^{-i\omega t}\mathrm{d}t$ is the Fourier transform of the bunch longitudinal density $\lambda(t)$ normalized as $\int_{-\infty}^{\infty} \lambda(t)\mathrm{d}t = 1$. A transverse dipole kick $\Delta x'$ caused by the beam-impedance interaction is

$$\Delta x' = \frac{q}{E/e}k_\perp x\,, \qquad (2)$$

where $q = Ne$ is the beam charge, N is the number of particles, x is the beam transverse offset, E is the beam energy, e is the electron charge.

A local transverse impedance acts on the beam as a defocusing quadrupole, strength of which depends on the beam intensity. The orbit bump method [1, 2] is based on the measurement of a wave-like orbit distortion created by the wakefield kick $\Delta x'$ (2) proportional to the beam charge and its transverse position at the impedance location. If a local orbit bump is created at the impedance location, the intensity-dependent orbit distortion is:

$$\Delta x(s) = \frac{\Delta q}{E/e}k_\perp x_0 \frac{\sqrt{\beta(s)\beta(s_0)}}{2\sin\pi\nu_\beta}\cos\left(|\mu(s)-\mu(s_0)|-\pi\nu_\beta\right)\,, \qquad (3)$$

where x_0 is the orbit bump height, s_0 is the impedance location, Δq is the bunch charge variation, ν_β is the betatron tune, β is the beta function, and μ is the betatron phase advance. This wave-like orbit distortion can be measured using beam position monitors, and the wave amplitude is proportional to the kick factor at the bump location. To reduce the systematic error caused by intensity-dependent behavior of the BPM electronics, this error is also measured and then subtracted.

The orbit bump method is more sensitive than the method [3] based on the measurement of intensity-dependent betatron phase advance along the ring because the beam position monitors (BPMs) are used in the narrowband orbit mode rather than in the broadband turn-by-turn mode, and the noise is much smaller.

Evolution of BPM electronics resulted in great improvement of the bump method accuracy from 20 – 40 μm at the very beginning of the method development [4] to

ISBN: 978-3-95450-192-2 doi:10.18429/JACoW-IBIC2017-MOPCC04

SIMULATION OF BEAM-BEAM TUNE SPREAD MEASUREMENT WITH BEAM TRANSFER FUNCTION IN RHIC*

Y. Luo†, W. Fischer, X. Gu
Brookhaven National Laboratory, Upton, NY, USA

Abstract

Head-on beam-beam compensation had been successfully implemented routinely in the 2015 polarized proton operation in the Relativistic Heavy Ion Collider at Brookhaven National Laboratory. Two electron lenses have been used to reduce the incoherent beam-beam tune spread to allow a larger proton bunch intensity and therefore a higher luminosity. Beam transfer function was used to determine the beam-beam incoherent tune spread. In this article, we carry out numeric simulations to compare the tune spreads derived from tune histogram and the beam transfer function. Then we present the experimental beam transfer function measurements and extract the tune spreads due to beam-beam interaction and electron lens. Experimental results show that the electron lens reduced the beam-beam tune spread.

INTRODUCTION

The luminosity is limited by the beam-beam interaction in the polarized proton operation operation in the Relativistic Heavy Ion Collider (RHIC) at Brookhaven National Laboratory. To have good beam and polarization lifetimes, the working point is constrained between 2/3 and 7/10 in the tune space. To minimize the head-on beam-beam tune spread and to compensate the nonlinear beam-beam resonance driving terms, two electron lenses (e-lenses) have been installed in RHIC, one for each ring. In 2015, head-on beam-beam compensation had been implemented routinely for the first time in the RHIC 100 GeV polarized proton operation [1–3]. With beam-beam compensation, both the peak and integrated luminosities had been doubled comparing to the previous energy proton operation in 2012.

In the article, we present a fast and efficient way to experimentally determine the incoherent beam-beam tune shift with beam transfer function (BTF) measurement. We first carry out numerical simulations to compare the tune spreads from the BTF calculation and from the tun histogram and the beam-beam parameter. Then we present the BTF measurements during electron current scans without and with beam-beam interaction. The tune spreads introduced by the e-lens are extracted. The experimental results show that the e-lens reduced the beam-beam tune spread.

NUMERICAL SIMULATION

We developed both weak-strong and strong-strong beam-beam codes to numerically calculate BTF and tune histogram [4]. The advantage of weak-strong code is that the particles can be tracked element-by-element through the ring and all the lattice nonlinearities can be included. In the RHIC operation, coherent beam-beam modes can only be detected with external excitation. In the following, we will use the weak-strong beam-beam interaction model. The proton bunch is represented by macro-particles while the other beam by a rigid Gaussian charge distribution. The e-lens is modeled as 4 segments with each one represented by a drift – a 4-d beam-beam kick – a drift.

In one test, the 2015 100 GeV blue ring lattice is used. The lattice tunes are set to (0.69, 0.685). To minimize the tune spread from the chromatic effect, the linear chromaticities are set to (0, 0). The proton bunches collide at IP6 and IP8. The e-lens is switched off. The proton bunch intensity is scanned up to 2.0×10^{11} or a total beam-beam parameter of -0.02.

Figure 1 shows the calculated imaginary part of BTF and the tune histogram with a beam-beam parameter of -0.01. The imaginary part of BTF is wider than that directly calculated tune histogram since BTF is related to the amplitudes of particles. In the following, to compare the width of tune spreads derived from the imaginary part of BTF and the tune histogram, we define the tune spread as the full width of 10% maximum [5]. We choose the full width of 10% maximum other than the well-known full width of half maximum (FWHM) because the former is close to the full span of the tune distribution, and also 10% maximum is a practical choice for experimental BTF measurements to overcome the noise floor.

Figure 2 shows the correlation between the tune spreads derived from the imaginary part of BTF and tune histogram. The horizontal and vertical axises are the tune spreads from the tune histogram and BTF respectively. The tune spread derived from BTF can be fitted linearly with that from the tune histogram, although the tune spread from BTF is about 8% larger than that from the tune histogram in this test. We also found that both the tune spreads from BTF and from the tune histogram can be fitted linearly with the beam-beam parameter, too. They are about half of the beam-beam parameter within a relative error of 12%.

The linear correlations between the tune spreads from the imaginary part of BTF and the tune histogram and the beam-beam parameter provide us a fast and convenient way to estimate the tune spread experimentally based on the high signal-to-noise BTF measurement.

* Work supported by Brookhaven Science Associates, LLC under Contract No. DE-AC02-98CH10886 with the U.S. Department of Energy.
† yluo@bnl.gov

ISBN: 978-3-95450-192-2 doi:10.18429/JACoW-IBIC2017-MOPCC05

MEASURING BEAM ENERGY WITH SOLENOID*

I. Pinayev†, D. Kayran, V.N. Litvinenko, G. Wang, BNL, Upton, NY 11973, U.S.A.

Abstract

We have developed a method of measuring electron beam energy based on the measurement of the Larmor angle. In this paper, we describe the experimental set-up and obtained results.

INTRODUCTION

Measuring energy of the electron beam with few MeV energy is a challenging task. Conventional approach utilizing energy spectrometer has a disadvantage of low magnetic field in a bending magnet, which is hard to measure accurately and it is affected by the residual magnetic fields. Electron beam is also sensitive to the stray magnetic fields. Time-of-flight technique requires precise measurement of arrival time because the velocity variation is inversely proportional to the square of the relativistic factor.

Low-energy beamlines usually implement solenoids for the focusing of the beam (the usage of the quadrupoles is limited due the same reasons as for the spectrometer dipole). The solenoids are rotating the plane of the betatron oscillations [1] and the rotation angle is directly proportional to the axial field integral, which is usually known with high accuracy, and inversely proportional to the beam rigidity.

The electron beam energy is found from the change in the response matrix with varying excitation current of the solenoid.

MEASUREMENT TECHNIQUE

The transfer matrix of a hard edge solenoid can be represented as multiplication of the rotation matrix M_{rot} and focusing matrix M_f:

$$\begin{pmatrix} \tilde{x} \\ \tilde{x}' \\ \tilde{y} \\ \tilde{y}' \end{pmatrix} = M_{rot} M_f \begin{pmatrix} x \\ x' \\ y \\ y' \end{pmatrix} \quad (1)$$

where rotation matrix is:

$$M_{rot} = \begin{pmatrix} cos\theta & 0 & sin\theta & 0 \\ 0 & cos\theta & 0 & sin\theta \\ -sin\theta & 0 & cos\theta & 0 \\ 0 & -sin\theta & 0 & cos\theta \end{pmatrix} \quad (2)$$

and $\theta = \int eB_{\parallel}(s)/2p\, ds$, where e is electron charge, p is its momentum, and $B_{\parallel}(s)$ is axial field. The focusing matrix can be calculated from the following equation:

$$M_f = \begin{pmatrix} cos\theta & sin\theta/k & 0 & 0 \\ -ksin\theta & cos\theta & 0 & 0 \\ 0 & 0 & cos\theta & sin\theta/k \\ 0 & 0 & -ksin\theta & cos\theta \end{pmatrix} \quad (3)$$

where k is $eB_{\parallel}(s)/2p$.

The real solenoid can be represented as series of hard edge solenoids with different magnetic fields. Because rotation and focusing matrices commute and focusing matrix does not mix horizontal and vertical plane the Larmor angle will be sum of the rotation angles for the parts of solenoid and Eq. 2 is valid for any solenoid.

In our experiment, we steered the electron beam with a trim located prior a solenoid and measured the tilt of the beam trajectory in the X-Y plane (see Fig. 1).

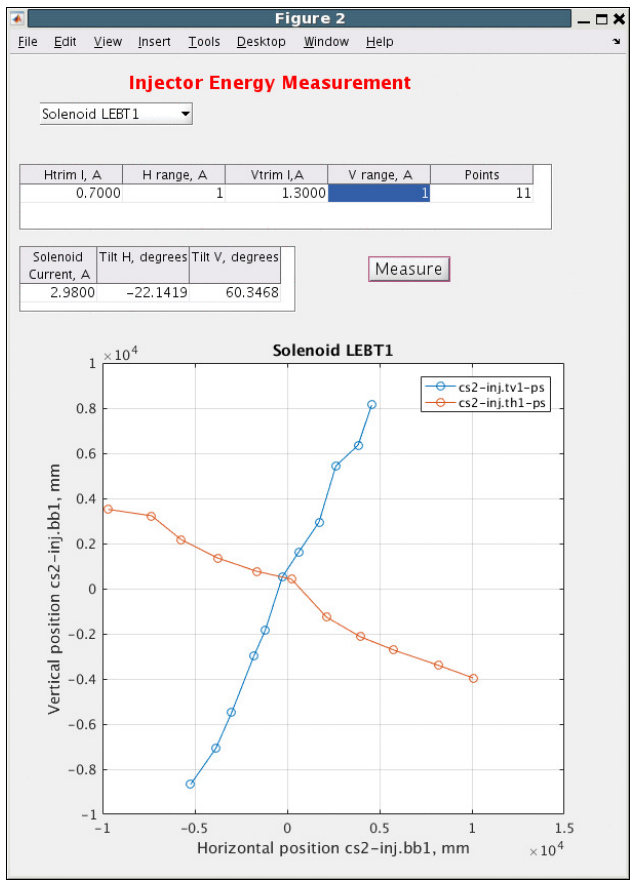

Figure 1: First scan of the orbit tilt in the X-Y plane caused by solenoid's rotation of the orbit. Measured beam position is in microns.

The measurements were performed using an automated MATLAB script. Operator can choose the solenoid (with corresponding beam position monitor (BPM) and trim),

* Work supported by the US Department of Energy under contract No. DE-SC0012704
† pinayev@bnl.gov

ISBN: 978-3-95450-192-2 doi:10.18429/JACoW-IBIC2017-MOPCC06

BEAM BASED ALIGNMENT OF SOLENOID*

I. Pinayev†, Y. Jing, D. Kayran, V.N. Litvinenko, I. Petrushina, K. Shih, G. Wang,
BNL, Upton, NY 11973, U.S.A.

Abstract

In this paper, we present the procedure and experimental results of measuring electron beam position and angle relative to the solenoid axis.

INTRODUCTION

Preserving low emittance of the beam in the transport line require good alignment of the beam trajectory with axis of the focusing element [1]. Axis of a quadrupole can be easily found either buy using array of the Hall probes or vibrating wire measurements [2, 3]. Location of the solenoid axis is much less straightforward due to quadratic dependence of file on the deviation from axis. Situation becomes more complicated because beam coming through a center but with angle with respect to the axis is also deflected by solenoid. Therefore, method of determining beam trajectory vs. solenoid axis with beam itself becomes a necessity.

In [1] the solenoid current was scanned and downstream beam position was recorded. The obtained data were fit using the transfer matrix of solenoid calculated by a special script [4].

We utilize similar approach but since we do not have overlapping magnetic and electrical fields the transfer matrix can be calculated from the magnetic measurement data and beam energy. We also generalized the method to an arbitrary transfer function between solenoid and beam position monitor.

METHODE DESCRIPTION

Calculation of Solenoid Transfer Function

The transfer function of a hard edge solenoid (uniform field of certain length) is well known [5]:

$$\begin{pmatrix} \tilde{x} \\ \tilde{x}' \\ \tilde{y} \\ \tilde{y}' \end{pmatrix} = M_{rot} M_f \begin{pmatrix} x \\ x' \\ y \\ y' \end{pmatrix} \quad (1)$$

where rotation matrix is:

$$M_{rot} = \begin{pmatrix} cos\theta & 0 & sin\theta & 0 \\ 0 & cos\theta & 0 & sin\theta \\ -sin\theta & 0 & cos\theta & 0 \\ 0 & -sin\theta & 0 & cos\theta \end{pmatrix} \quad (2)$$

and $\theta = \int eB_{\parallel}(s)/2p\, ds$, where e is electron charge, p is its momentum, and $B_{\parallel}(s)$ is axial field. The focusing matrix can be calculated from the following equation:

$$M_f = \begin{pmatrix} cos\theta & sin\theta/k & 0 & 0 \\ -ksin\theta & cos\theta & 0 & 0 \\ 0 & 0 & cos\theta & sin\theta/k \\ 0 & 0 & -ksin\theta & cos\theta \end{pmatrix} \quad (3)$$

where k is $eB_{\parallel}(s)/2p$.

The real solenoid can be represented as series of hard edge solenoids with different magnetic fields.

The rotation of beam trajectory was utilized for beam energy measurement.

Transfer Matrix Calculation

We treated focusing elements as infinitesimally short, separated by known drift space. In this case transfer matrix from the solenoid under test to BPM can be found as:

$$M_{tr} = M_{driftBPM} \prod \left(M_{foci} M_{drifti} \right) M_{sol} \quad (4)$$

where $M_{driftBPM}$ is matrix o drift space between the last focusing element and beam position monitor (BPM) used for position observation, M_{foc} is matrix of the focusing element (either solenoid or quadrupole), and M_{sol} is matrix of the solenoid being scanned.

Transfer matrix of the solenoid was calculated using the magnetic measurement data:

$$M_{sol} = M_{drift2} \prod \left(M_{rot} M_f \right) M_{drift1} \quad (5)$$

where M_{drift1} and M_{drift2} are transfer matrices of drifts with negative length transporting beam from the solenoid center to the start of the data and from the end of the data to the solenoid center, respectively.

Data Processing

For each solenoid current the transfer matrix was calculated according to the Eq. (4). Then two *4×N* matrices $\boldsymbol{R}_x$ and $\boldsymbol{R}_y$ were formed:

$$X = \begin{bmatrix} x_1 \\ \cdots \\ x_N \end{bmatrix} = R_x \begin{bmatrix} x_0 \\ x'_o \\ y_0 \\ y'_0 \end{bmatrix} \quad (6)$$

$$Y = \begin{bmatrix} y_1 \\ \cdots \\ y_N \end{bmatrix} = R_y \begin{bmatrix} x_0 \\ x'_o \\ y_0 \\ y'_0 \end{bmatrix} \quad (7)$$

where *X* and *Y* are *1×N* vectors of recorded positions, and vector *W,* appearing on the right side, has offsets and angles of the beam with respect to solenoid axis (X and Y are also relative to this axis). The matrices are formed

* Work supported by the US Department of Energy under contract No. DE-SC0012704
† pinayev@bnl.gov

ISBN: 978-3-95450-192-2 doi:10.18429/JACoW-IBIC2017-MOPCC07

DIAGNOSTICS OF ELBE SRF GUN - STATUS AND FUTURE DESIGN

P. Lu, A. Arnold, P. Murcek, J. Teichert, H. Vennekate, R. Xiang, HZDR, Dresden, Germany

Abstract

Since 2015, Mg photocathodes have been applied for the ELBE SRF gun. In 2016, user experiments with a bunch charge of 100 pC and beam transport experiments with 200 pC have been performed. Beams diagnose methods are presented in this article, mainly including measurements of transverse emittance and bunch length. Measurements and corresponding simulations show that the operation parameters of the SRF gun significantly affects the beam quality. A gun lab has been proposed to run as an analog optimizer aiming to explore the potentials of the SRF gun. With the experience of former beam diagnostics, the design of a diagnostics beamline for the future gun lab is described. The purpose is to rebuild phase space projections, either transversely or longitudinally, in a short time scale of several seconds to support analog optimizations for multiple operation parameters.

INTRODUCTION

The concept of SRF (Superconducting Radio Frequency) gun was first proposed in 1988 at the University of Wuppertal [1] and realized in 2002 at HZDR (Helmholtz Zentrum Dresden Rossendorf) [2]. To achieve CW beams with good quality and high bunch charge has always been motivating SRF gun projects. However, the development of SRF guns is still challenged by the processing of cavities, the performance of photocathodes and their lifetime, as well as the risk of cavity contamination [3]. In spite of these challenges, since 2015 an SRF gun has been operating with a magnesium cathode and a 4 MeV, 100 kHz electron beam with the bunch charge up to 200 pC was available in 2016.

As proof of principle, a 100 pC beam was applied in ELBE (superconducting Electron Linac for beams with high Brilliance and low Emittance) for neutron time-of-flight experiments and generation of THz radiation. The beam with the maximum bunch charge of 200 pC was transported in the main beamline of ELBE with negligible beam loss. The energy, energy spread, beam profile and transverse emittance of the beam were measured in a dedicated diagnostics after the SRF gun. The bunch length and slice emittance were measured with the ELBE accelerator modules.

In addition to the design of gun cavity, several operation parameters dominate the beam quality. In general, the phase difference between the RF and the driving laser determines the orientation in the longitudinal phase space; The distance from the cathode surface to the entrance of cavity sets up a trade-off between bunch length and transverse emittance; The transverse size of the laser could be optimized for balancing thermal emittance and space-charge-induced emittance; Moreover, a longer laser pulse reduces the space charge effect but introduces longitudinal nonlinearity to the electron bunch. The working point of all these parameters should be optimized according to a specific requirement.

A new gun lab has been proposed to support the research and development of SRF guns. It will be separated from the ELBE accelerators and therefore offer more experimental time for the gun. The gun lab will consist of an SRF gun and a diagnostics beamline. The beam diagnostics include energy measurement and distribution measurement in both transverse and longitudinal phase spaces. Among them the phase space diagnostics are required to be fast (in 10 seconds) so that gun parameters can be analog and automatically optimized. Longitudinal phase space diagnostics will be probably realized by a transverse deflecting cavity which is possible of single bunch measurement. For transverse phase space diagnostics, different setups based on one dimensional scanning are discussed in the following sections.

CURRENT DIAGNOSTICS BEAMLINE

A diagnostics beamline is connected directly behind the SRF gun at ELBE. Its setup is shown in Figure 1. A Faraday cup is installed to measure the total current. After that three quadrupoles focus the beam for further transport, followed by Screen-station 2 and 3 for beam observation and slit-scan emittance measurement. A 180° horizontal dipole (C-bend) is installed following Screen-station 3 for energy and energy spread measurement, which images the input beam reversely. The distance from its entrance to Screen-station 4 is the same as the distance from its exit to Screen-station 5, as shown in Figure 1. Therefore, projections of a monoenergetic beam on both screens should be the same.

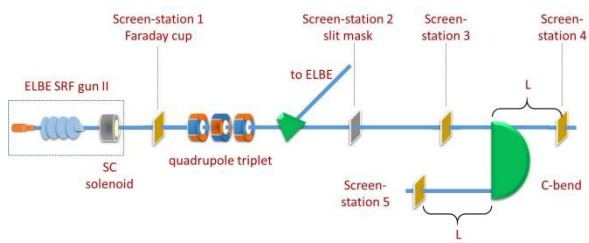

Figure 1: The diagnostics beamline of ELBE SRF gun.

The principle of distribution measurement in transverse phase space is shown in Figure 2. A slit mask is installed at the position of Screen-station 2. It is vertically moveable with a horizontal slit, which has the dimension of 10 mm × 0.1 mm. Screen 3 is located 77 cm after the slit mask to record the sampled beamlet, with the screen installed at 45° to the beam. The scanning step is usually set to 0.1 mm, which is the width of the slit, and thus the entire beam is sampled. The exposure time of the camera should be adjusted to avoid saturation on a normally used YAG (Yttrium Aluminium Garnet) screen for every beamlet. In case of single pulse saturation at high energy

ISBN: 978-3-95450-192-2 doi:10.18429/JACoW-IBIC2017-MOPCC08

TIME-OF-FLIGHT MEASUREMENTS AND ANALYSIS OF THE LONGITUDINAL DISPERSION AT THE S-DALINAC*

T. Bahlo†, F. Schließmann‡, M. Arnold, J. Pforr, N. Pietralla
Institut für Kernphysik, Darmstadt, Germany

Abstract

The Superconducting Darmstadt Linear Accelerator S-DALINAC is capable of accelerating electrons to kinetic energies of up to 130 MeV. Due to its three recirculating beamlines the 30 MeV main linac can be used up to four times. The electron beam is recirculated non-isochronously with a distinct longitudinal dispersion to conserve the energy spread of the injector accelerator. Time-of-flight measurements at the beamline connecting injector and main linac will be presented, showing a non-linear dependency on the energy. This effect can be reproduced by simulations using *elegant* [1] and are caused by traversing accelerating cavities with a small transversal displacement and a small angular deviation. Adjusting the magnetic parameters of the beamline compensates this effect. Besides the first recirculation beamline does not provide enough degrees of freedom to set the desired longitudinal dispersion for the non-isochronous recirculation mode. This has to be compensated in succeeding recirculation beamlines or by installation of additional magnets at the first recirculation beamline. Possible beamline modifications and time-of-flight measurements representing the longitudinal dispersion will be presented.

S-DALINAC

The S-DALINAC [2], shown in Fig. 1, is a superconducting, recirculating linear electron accelerator providing kinetic energies of up to 130 MeV. Due to its three recirculation beamlines the main accelerator can be used up to four times in order to reach the design energy. By using a non-isochronous recirculation mode the energy spread of the beam provided by the superconducting injector linac can be conserved over several recirculations. To use this mode a destinct momentum deviation within the electron bunch has to be introduced and a matching longitudinal dispersion R_{56} has to be implemented by quadrupole magnets. The momentum deviation can be introduced by accelerating off-crest with a phase offset of Φ_S.

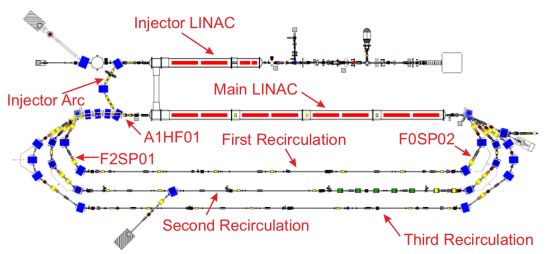

Figure 1: Floorplan of the S-DALINAC. Relevant devices are highlighted.

DETERMINING THE OPERATING POINT

Since the setup of the S-DALINAC has been upgraded from two to three recirculation beamlines [3] a new operating point for the non-isochronouly recirculated mode had to be found. A operating point consists of all quantities influencing longitudinal beam dynamics. Off-crest-acceleration introduces a quasi-proportional energy deviation in respect to the reference particle within a electron bunch since the longitudinal bunch length is short in comparison to one RF period [4]. The slope of this energy deviation can be characterized by the slope of the energy gain ΔE of each particle

$$\Delta E = \hat{E}_z \cos\left(2\pi \cdot f_{\mathrm{RF}} \cdot t + \Phi_S\right)$$

with the maximum energy gain $\hat{E}_z$, the RF frequency f_{RF}, the time t and the synchrotronphase Φ_S. The longitudinal position of an electron in respect to the reference particle can be manipulated by the longitudinal dispersion R_{56} of the beamline, which is associated with the 6×6 beam transport matrix R. This matrix describes the tracking of the particle vector $\vec{x}(s)$ at position s_1 to position s_2:

$$\vec{x}(s_2) = R \cdot \vec{x}(s_1).$$

Assuming all longitudinally coupling components of R to be zero the longitudinal position Δl relative to the reference particle can be expressed by

$$\Delta l = R_{56} \cdot \frac{\Delta p}{p_0}$$

and the optimal operating point using the (I)njector, the (F)irst, (S)econd, and (T)hird recirculation can be calculated:

Φ_S	$R_{56,\mathrm{I}}$	$R_{56,\mathrm{F}}$	$R_{56,\mathrm{S}}$	$R_{56,\mathrm{T}}$
−5.8°	0.21 m	0.2 m	0 m	0.54 m

Several states of the longitudinal phase space for acceleration using all recirculations are plotted in Fig. 2.

Requirements for Optimal Beam Tuning

As mentioned above the electron beam should fulfill specific properties when entering a cavity. Especially the correct alignment of the longitudinal phase space ellipse is crucial for an optimal acceleration process. This is ensured if the longitudinal dispersion outside the cavity is only influenced

* funded by DFG through RTG 2128, INST163/383-1/FUGG and INST163/384-1/FUGG.
† tbahlo@ikp.tu-darmstadt.de
‡ fschliessmann@ikp.tu-darmstadt.de

ISBN: 978-3-95450-192-2 doi:10.18429/JACoW-IBIC2017-MOPCC11

DIAGNOSTICS FOR TRANSVERSE COUPLED BUNCH INSTABILITIES AT ALBA

U. Iriso, A. Olmos, A. A. Nosych, and L. Torino
ALBA-CELLS, Cerdanyola del Vallés, Spain

Abstract

Transverse Couple Bunch Instabilities (TCBI) have been identified at ALBA as one of the main beam current limitations since its early commissioning in 2011. In these last years, we have developed several diagnostics tools that allow us a better characterization of these instabilities. The Synchrotron Radiation Interferometry has been equipped with a Fast Gated Camera (FGC) to measure the bunch-by-bunch beam size evolution, which, in combination with the diagnostics tools of the Transverse Multibunch Feedback system, provides us with a fruitful insight of these phenomena. This paper describes these diagnostics tools, and as an example, compares the emittance and tune evolution switching on/off some of the vacuum pumps at the Storage Ring.

INTRODUCTION

Beam current limitations have been observed at ALBA since its early commissioning in 2011. They are mainly related with Transverse Coupled Bunch Instabilities (TCBI), which appear above certain current thresholds and they could be cured by increasing the beam chromaticity. The origin of these beam instabilities is mainly related with the Geometrical and Resistive Wall impedances [1], although the influence of ion effects due to large pressures inside the chamber is not ruled out. In these phenomena, the perturbing field produced by a given bunch affects the subsequent bunches and therefore, bunch-by-bunch (BbB) instrumentation is required to obtain reliable diagnostics of these effects.

During these last years, we have developed two bunch-by-bunch instruments that provide us with a better insight into these effects. First, we have equipped our visible light interferometry [2] with a Fast Gated Camera with gating times as short as 2 ns [3], which provides a bunch-by-bunch emittance monitor. Second, we have set-up into operation our Transverse Multi-Bunch Feedback [4], which allows tune measurements to be performed also on a BbB basis. With these instruments, we have performed several experiments switching on/off the vacuum pumps in different sectors of the storage ring in order to evaluate the influence of ion effects on these beam instabilities. This paper reviews this BbB instrumentation and shows the results of these beam experiments.

BEAM SIZE MONITOR

In addition to the X-ray pinhole camera, since 2013 ALBA has been developing a beam size monitor using the Synchrotron Radiation Interferometry (SRI) with visible light [5–7]. Imaging with the X-ray pinhole has two main timing limitations: a)the YAG:Ce screen decay time is typically in the order of 100 ns [8]; and b) the minimum CCD exposure time (around 100 µs). This is obviously too much for ALBA's storage ring, where the bucket length is 2 ns. Since the SRI uses visible light (not X-rays), only the latter one affects the SRI. This can be circunvented by using a FGC with gatings as short as 2 ns.

The general principle of FGCs is as follows: when the light impinges on the photo-cathode of an image intensifier, photo-electrons are emitted and guided through a Multi-Channel Plate by an electric field. A high potential (whose duration can be as short as 2 ns) is applied across the MCP to accelerate and multiply the primary electrons. The final electron avalanche reaches a phosphor screen, whose light is read by a CCD.

The main FGC limitation stems from the space-charge effects produced when the electrons exit the photo-cathode, which enlarges the inteferograms fringes and so the measured beam size is larger. Figure 1 shows interferograms produced by a standard CCD (left) and two types of FGC: the Hamamatsu II C9546 (middle) and the Andor iStar 334T (right). Compared with the CCD camera, the visibility produced by FGCs is lower due to space charge effects, hence the measured beam size is larger. A thorough explanation, as well as a comparison for different cameras is shown in [3].

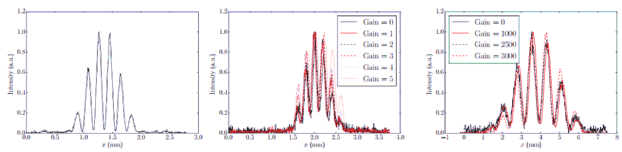

(a) Standard CCD (b) Image Intensifier C9546-01 (c) FGC iStar 334T

Figure 1: Comparison of interferograms produced by a standard CCD camera (left) and two types of FGC. The lower visibility (with higher valleys) is due to space charge effects, and increases the measured beam size.

Nevertheless, this beam size enlargement can be calibrated using the beam itself: we measure the beam size with both the standard CCD and the FGC by changing the beam coupling in a controlled way. This shows a linear relation (see Fig. 2), which we use to calibrate the FGC measurements. Our SRI system is equiped with the Andor FGC camera.

Figure 3 shows the measured bunch-by-bunch beam size with 130 mA in routine operation at ALBA. The calibrated beam size is consistent with the theoretical one. Nevertheless, the resulting size oscillates due to bunch-by-bunch shot noise, which explains the large error bars in Fig. 2. Due to low amount of light, the bunch size is not obtained from a single shot (i.e. single bunch passage), but rather by integrating the light produced by many (typically ~100) passages, for which the gating and trigger are carefully synchronized.

ISBN: 978-3-95450-192-2 doi:10.18429/JACoW-IBIC2017-MOPCC12

UPGRADE OF BPMS AND SRMS FOR THE BTS TRANSFER LINE AT ALBA

U. Iriso, M. Alvarez, G. Benedetti, A. A. Nosych, A. Olmos, X. Rodriguez
ALBA-CELLS, Barcelona, Spain

Abstract

The beam position and size of the electron beam in the ALBA Booster-To-Storage (BTS) transfer line are monitored using Beam Position Monitors (BPMs) and Synchrotron Radiation Monitors (SRMs). However, their performance was not fully optimized and the beam trajectory in the transfer line was not properly controlled. Consequently, the transfer efficiency in the BTS has been fluctuating since day one, so more studies and precise beam measurements were critically needed to optimize it. Firstly, the SRMs mechanics and automation were significantly improved to provide a more robust optics alignment. Secondly, BPM electronics have been upgraded for single-pass beam detection, showing a factor 10 better position resolution than the former units. Both SRMs and BPMs are now routinely used to keep transmission efficiency along the BTS above 90%.

INTRODUCTION

ALBA's booster and storage ring have a concentric layout with a short (~15 m) transfer line between them. Following the extraction elements (kicker, dipole and septum), the BTS consists of 2 dipoles (in blue in Fig. 1), 7 quads (in purple) and 3 H/V correctors. It follows into an injection section consisting of 2 kicker pairs (in yellow) and a septum (in green) in between them. The booster ramps up the energy of a 0.2 nC Linac charge from 110 MeV to 3 GeV and fires at a 3.125 Hz rate. The BTS diagnostics are quite numerous: 4 BPMs (red crosses), 3 SRMs (yellow stars), 3 FSOTRs and 2 FCTs.

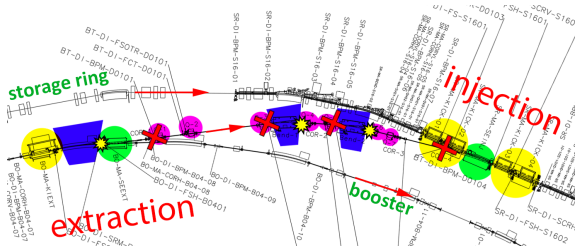

Figure 1: Layout of booster-to-storage transfer line of ALBA.

The injection efficiency measured from the Booster to the Storage Ring has been, for a long time, maximized by scanning mostly the pulsed elements and the BTS last pair of correctors, without paying much attention to the electron beam trajectory in the BTS. This worked reasonably well when we were operating the accelerators in decay mode, injecting only two times per day with the Front Ends (FE) closed. Nevertheless, once we had moved to top-up operation, the instabilities of the injector became an issue since the injection times could be significantly extended and disturb some beamline experiments.

In order to improve and stabilize the injection efficiency, we first performed a beam alignment campaign based on the FSOTRs. This already improved the injection efficiency stability. Nevertheless, since these components are beam destructive elements, we decided to work on the non-destructive instrumentation (SRMs and BPMs) in order to improve the diagnostics and provide a real-time monitoring tool during routine operation. These should not only provide a better understanding of the transmission oscillations, but also should help in finding more stable beam trajectories. This paper describes the improvements in the SRMs and BPMs, and shows the results obtained with them.

SRM UPGRADE

As a non-destructive diagnostic tool, the SRM uses the synchrotron radiation produced when the electron beam traverses a bending magnet. The visible light is guided away by a 45° mirror into the CCD optics, producing a transverse beam image in real-time. The diffraction limit does not significantly affect the beam imaging in the BTS, since the beam size is in the order of ~(200, 100) µm.

There are 3 locations of SRMs in the transfer line [1, 2]. One is placed after a booster dipole in between the extraction elements, and two more SRMs are located after each dipole in the BTS. The SRM setup and optics are all identical: a telephoto zoom lens (Sigma 70-300 mm) is used with a commercial CCD (Basler scA1300-32gm). Each is focused at 1.5 m distance to a source point in the center of the corresponding upstream dipole. Even though the set-up is the same as the one working since day-one in the Booster [3], the SRMs in the BTS did not properly function due to problems with alignment and low visibility, and consequently, the BTS-SRM system received a major upgrade taking care of its a) mechanical stability and b) centering on beam.

Initially, the SRM optics were lightly attached to the girder (Fig. 2, left), and its alignment relied on the viewport. However, in this configuration the SRM weight was partially supported in the viewport as well, thus risking bending it downwards. Moreover, any manipulation of the optics would mean losing any reference of the CCD position with respect to the viewport. Instead, the new generation of ALBA's SRM supports have been designed to be firmly clamped to the girder (Fig. 2, right), allowing independent mechanical adjustment of its optics without forcing the viewport. On the contrary, the viewport is now a stable reference for SRM optics alignment.

ISBN: 978-3-95450-192-2 doi:10.18429/JACoW-IBIC2017-MOPCC13

BEAM ENERGY MEASUREMENTS WITH AN OPTICAL TRANSITION RADIATION FOR THE ELI-NP COMPTON GAMMA SOURCE

M. Marongiu*[1], A. Giribono[1], A. Mostacci[1], L. Palumbo[1], M. Pompili, Sapienza University, Rome, Italy
E. Chiadroni, F. Cioeta, G. Di Pirro, G. Franzini, V.Shpakov, A. Stella, C. Vaccarezza, A. Variola
LNF-INFN, Frascati, Italy
D. Cortis, INFN, Rome, Italy
A. Cianchi, Università di Roma II Tor Vergata, Rome, Italy
[1]also at INFN, Rome, Italy

Abstract

A high brightness electron LINAC is being built in the Compton Gamma Source at the ELI Nuclear Physics facility in Romania. To achieve the design luminosity, a train of 32 bunches, 16 ns spaced, with a nominal charge of 250 pC will collide with the laser beam in the interaction point at two electron beam energies, namely 280 MeV and 720 MeV. Electron beam spot size is measured with optical transition radiation (OTR) profile monitors. The paper deals with the possibility of using the OTR monitors to measure also beam energy along the machine; such measurements may help monitoring the accelerating sections performances, especially when the whole bunch train is being accelerated. We discuss the measurement principle, the expected accuracy and the main characteristic of the optical line to retrieve the angular distribution of the emitted radiation.

INTRODUCTION

The Gamma Beam Source [1] (GBS) machine is an advanced source of up to ≈20 MeV Gamma Rays based on Compton back-scattering, i.e. collision of an intense high power laser beam and a high brightness electron beam with maximum kinetic energy of about 740 MeV. The Linac will provide trains of bunches in each RF pulse, spaced by the same time interval needed to recirculate the laser pulse in a properly conceived and designed laser recirculator, in such a way that the same laser pulse will collide with all the electron bunches in the RF pulse, before being dumped. The final optimization foresees trains of 32 electron bunches separated by 16 ns, distributed along a 0.5 µs RF pulse, with a repetition rate of 100 Hz.

The goal of this paper is to verify the possibility of implement an energy measurement technique based on the OTR and to study its expected accuracy; furthermore, the main characteristics of the optical line will be discussed.

In a typical monitor setup, the beam is imaged via OTR or YAG screen using standard lens optics, and the recorded intensity profile is a measure of the particle beam spot [2]. In conjunction with other accelerator components, it will also be possible to perform various measurements on the beam, namely: its energy and energy spread (with a dipole or corrector magnet), bunch length [3] (with a RF deflector), Twiss parameters [4] (by means of quadrupole scan) or in general 6D characterization on bunch phase space [5]. Such technique is common in conventional [6] and unconventional [7, 8] high brightness LINACs.

The optical acquisition system is constituted by the CCD camera "Basler scout A640-70gm" or by the "Hamamatsu Orca-Fash4" with a macro lens. A movable slide is used to place the lens plus camera system closer or farer from the OTR target; such distance is between 60 cm and 130 cm from the OTR target due to mechanical and geometric constraints. In order to avoid possible damage of the optics devices due to the radiation emitted by the beam, a 45° mirror is placed at 40 cm from the target leading to a minimum distance achievable of 60 cm; since the beam pipe is placed 1.5 m from the floor, the maximum distance is instead 130 cm.

OTR RADIATION

Optical Transition Radiation (OTR) monitors are widely used for profile measurements at LINACs. The radiation is emitted when a charged particle beam crosses the boundary between two media with different optical properties [9], here vacuum and a thin reflecting screen (silicon). For beam diagnostic purposes the visible part of the radiation is used; the recorded intensity profile is a measure of the particle beam spot. Advantages of OTR are the instantaneous emission process enabling fast single shot measurements, and the good linearity (neglecting coherent effects). Disadvantages are that the process of radiation generation is invasive, i.e. a screen has to be inserted in the beam path, and that the radiation intensity is much lower in comparison to scintillation screens.

ENERGY MEASUREMENT

Another advantage of the OTR is the possibility to measure the beam energy by means of observation of its angular distribution (see Figures 1 and 2); this can be expressed by the well known formula 1.

$$\frac{dI^2}{d\omega d\Omega} = \frac{e^2}{4\pi^3 c\epsilon_0} \frac{\sin^2\theta}{\left(\frac{1}{\gamma^2} + \sin^2\theta\right)^2} R(\omega,\theta) \qquad (1)$$

Where $R(\omega,\theta)$ is the reflectivity of the screen; the peak of intensity is at $\theta = 1/\gamma$.

Due to the beam divergence, the angular distribution of the whole beam will be different from 0 at the center (see

* marco.marongiu@uniroma1.it

ISBN: 978-3-95450-192-2 doi:10.18429/JACoW-IBIC2017-MOPCC14

PHYSICS MODEL OF AN ALLISON PHASE-SPACE SCANNER, WITH APPLICATION TO THE FRIB FRONT END*

Chun Yan Jonathan Wong†, National Superconducting Cyclotron Laboratory, East Lansing, USA
Scott Cogan, Yue Hao, Steven Lidia, Steven M. Lund, Tomofumi Maruta‡, Diego Omitto,
Peter Ostroumov, Eduard Pozdeyev, Haitao Ren, Rebecca Shane, Takashi Yoshimoto, Qiang Zhao
Facility for Rare Isotope Beams, East Lansing, USA

Abstract

We study Allison-type phase-space scanners by extending analytic models to include two important geometric features that are conventionally omitted, namely asymmetric slit-plate to dipole-plate gaps at the two ends and finite slit-plate thickness. Their effects can be significant for high-resolution Allison scanners and lead to two corrections in the measurement data relative to more idealized descriptions: 1) a change in the voltage-to-angle conversion relation, and 2) a data point weight compensation factor. These findings are corroborated by numerically integrated single-particle trajectories in a realistic 2D field map of the device. The improved model was applied to the Allison scanner used to measure a 12 keV/u heavy-ion beam in the front-end of the Facility for Rare Isotope Beams (FRIB) at Michigan State University. Preliminary measurements show that the improved model results in significant ($\gtrsim$10%) modifications to beam moments, thus rendering the corrections important for accurate phase-space characterizations.

INTRODUCTION

Allison scanners [1] are widely used to efficiently measure slit-transmitted phase-space projections of low-energy beams. An Allison scanner (see Fig. 1) consists of an entrance slit-plate (slit width s), an aligned exit slit-plate (slit width s) with an integrated Faraday cup, and a bipolar-biased electric dipole (voltage V_0) placed between the two slits. The scanner is translated mechanically (typically in steps) to change the slit position, and the dipole voltage V_0 is varied to select transmittable angles by varying the bending strength. For a particular coordinate and dipole voltage, the scanner samples a point in the beam phase-space. The density of the point is taken to be proportional to the current collected at the Faraday cup.

Idealized analytic formulas relating Allison scanner geometry and voltages to phase-space measures were derived in Refs. [1,2]. These idealized results assume thin slit-plates, an ideal (no-fringe) dipole field, and a symmetric geometry. This paper extends idealized model results by considering two additional geometric features that can lead to significant corrections: 1) asymmetric slit-plate to dipole-plate gaps at the two ends, and 2) finite slit-plate thickness.

* Work supported by the U.S. DOE Office of Science under Cooperative Agreement DE-SC0000661 and the NSF under Grant No. PHY-1102511.
† wong@nscl.msu.edu
‡ On leave from KEK/J-PARC

Asymmetry commonly arises, probably unintentionally, in Allison scanners because relief cuts on thick entrance- and exit-plates have been made in the same direction [3,4]. This asymmetry is also present in the FRIB Allison scanner where relief cuts on both plates face the incoming beam as shown in Fig. 1. Due to this issue, the effective slit-plate to dipole-plate gap on the exit end is more than double that on the entrance end. We find such asymmetries significantly impact angle selection calibration with V_0.

Slit-plate thickness can be neglected when it is much smaller than the slit width. This idealization can break down as Allison scanners decrease slit widths to improve resolution. Recent examples include slit widths of $s \leq 100\,\mu$m planned at GSI FAIR [5] and $s = 38\,\mu$m implemented at TRIUMF [6]. Fig. 1 details the slit plate presently employed in the FRIB scanner where $s = 60\,\mu$m and the effective (not including irrelevant thickness spanning the 30° relief cut) plate-thickness is 254 µm. This approximately 4 : 1 aspect ratio is effectively a small channel, which can scrape particles that would have passed through a slit-plate with no thickness.

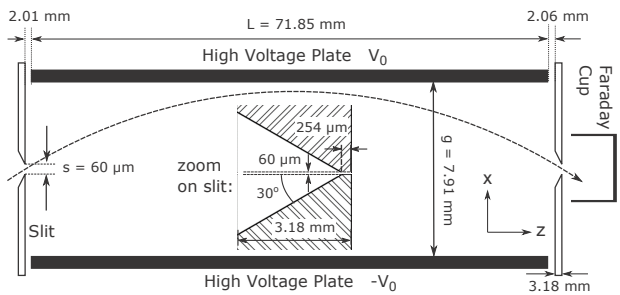

Figure 1: FRIB Allison scanner geometry.

ANALYTIC MODEL

Four geometric models of an Allison scanner are presented in Fig. 2. The models cover combinations of symmetric/asymmetric end-plate to slit-plate gaps with thin/thick slit-plates to study effects of asymmetry and slit-plate thickness. As illustrated in the Fig. 2, a range of angles can be transmitted at each voltage setting due to the finite slit width. We define:

$x'_{\rm ref}$: the angle at which a particle enters and exits the chamber at the same x-position,

$x'_{\rm max\,/\,min}$: maximum/minimum transmittable angle,

$\Delta x' = x'_{\rm max} - x'_{\rm min}$: angular resolution,

ISBN: 978-3-95450-192-2 doi:10.18429/JACoW-IBIC2017-MOPCF01

BEAM DIAGNOSTICS FOR LOW ENERGY ANTIPROTON BEAMS*

C. P. Welsch†, University of Liverpool/Cockcroft Institute, UK

Abstract

Beams of low energy antiprotons in the keV energy range are very difficult to characterize due to their low intensity of only 10^7 particles per shot, annihiliation, and low repetition rate. The project AVA [1] (Accelerators Validating Antimatter physics) is an Innovative Training Net-work within the H2020 Marie Skłodowska-Curie actions. It enables an interdisciplinary and cross-sector program on antimatter research across 3 scientific work packages. These cover facility design and optimization, advanced beam diagnostics and novel low energy antimatter exper-iments. This paper presents the AVA R&D into beam profile, position and intensity measurements, as well as detector tests which will provide an order of magnitude improvement in the resolution and sensitivity in closely related areas. It also summarizes the interdisciplinary training program that AVA will provide to its 15 Fellows, as well as to the wider antimatter and accelerator commu-nities.

INTRODUCTION

In July 1983, the very first ions were stored in the Low Energy Antiproton Ring (LEAR) at CERN in Geneva, Switzerland [2]. It was the first storage ring that was explicitly designed to address physics with low-energy antiprotons and opened the door to a field were several very fundamental questions in physics can be directly addressed. When this machine was prematurely shut down in 1996 to free resources for the Large Hadron Collider (LHC) project, an international user community pushed for the continuation of this unique research program. This led to the construction of the Antiproton Decelerator (AD) facility that became operational in 2000 [3]. This storage ring is presently the only facility in the world to allow the realization of experiments with low energy antiproton beams. It has led to the successful production of cold antihydrogen, which has been widely acknowledged in the scientific community, as well as in the public media. The successful storage of antihydrogen over an extended period [4] was selected as top physics highlight in 2010 by physics world. Other recent breakthroughs include successful two-photon laser spectroscopy of antiprotonic helium and the measurement of the antiproton-to-electron mass ratio [5], measurement of resonant quantum transitions in trapped antihydrogen atoms [6], one-particle measurement of the antiproton magnetic moment [7], the production of antihydrogen for in-flight hyperfine spectroscopy [8], direct measurements into the antihydrogen charge anomaly [9] and the comparison of antiproton-to-proton charge-to-mass ratio [10] in 2015. Due to the low intensity of only ~10^5 antiprotons/s and the availability of only pulsed extraction – one pulse every 85 seconds - the physics program is presently limited to the spectroscopy of antiprotonic atoms and antihydrogen formed in charged particle traps or by stopping antiprotons in low-density gas targets. Since the output energy of the AD (5 MeV kinetic energy) is far too high to be of direct experimental use, the standard deceleration cycle of the antiprotons consists of the following steps:

- Deceleration in the AD from 3.5 GeV/c down to 0.1 GeV/c;
- Degrading by a foil from 5 MeV kinetic energy down to a few keV;
- Electron and positron cooling of the particles trapped to meV energies.

The drawback of this procedure is the rather large increase of the beam divergence and momentum spread and the high loss rate of antiprotons in the degrader foil. These effects limit the capture efficiency to about 10^{-4} or even less. An improvement was achieved by the installation of a decelerating rf quadrupole structure (RFQ-D) used by the ASACUSA collaboration [11] that today provides beams at 100 keV energy. However, the rather large emittance ε=100 mm mrad and energy spread $\Delta E/E$ = 10% of the output antiproton beam require a large stopping volume and a high-power pulsed laser to induce transition for high precision spectroscopy. A cooled antiproton beam at such energy would greatly improve this situation and even CW laser spectroscopy may become feasible. The scientific demand for low-energy antiprotons at the AD continues to grow. By now there are six experiments at the AD, the most recent ones being AEgIS and BASE, and a seventh (GBAR) has recently been approved. These experiments, however, require significant improvements in the underpinning accelerator technology, beam cooling and handling techniques, novel instrumentation, as well as significant upgrades to the experiments themselves. The AD was not able to provide the required number of cooled antiprotons at lowest energies. CERN is currently finalizing the construction of a new Extra Low ENergy Antiproton ring (ELENA) [12] which promises a significant improvement over this situation. Commissioning of this machine started in 2016.

The *AVA* project focuses on R&D benefiting low energy antimatter facilities. The project will offer its Fellows the unique opportunity to make contributions to the ELENA machine development and physics R&D programs. Beyond the opportunities that ELENA will immediately provide it would be desirable to make experiments using the antiproton as a hadronic probe to study the nuclear structure [13] and to have RF bunching tools to switch between ns and long beam pulses for studies into the collision dynamics of matter and antimatter [14]. This range of experiments could be realized after appropriate

*This project has received funding from the European Union's Horizon 2020 research and innovation programme under the Marie Skłodowska-Curie grant agreement No 721559.
†c.p.welsch@liverpool.ac.uk

ISBN: 978-3-95450-192-2 doi:10.18429/JACoW-IBIC2017-MOPCF03

PRELIMINARY DESIGN OF BEAM DIAGNOSTIC SYSTEM IN THE HUST-PTF BEAMLINE*

X. Liu†, QS. Chen†, B. Qin, K. Tang, State Key Laboratory of Advanced Electromagnetic Engineering and Technology, School of Electrical and Electronic Engineering
W. Chen, Huazhong University of Science and Technology, Wuhan 430074, China

Abstract

Proton therapy is now recognized as one of the most effective radiation therapy methods for cancers. A proton therapy facility with multiple gantry treatment rooms is under development in HUST (Huazhong University of Science and Technology), which is based on isochronous superconducting cyclotron scheme. The 250MeV/500nA proton beam will be extracted from a superconducting cyclotron and injected into the beam-line. Many beam diagnostic instruments are distributed throughout the beam line to measure the beam profile, position, current, loss, energy and energy spread. Some of them will send the beam information to the treatment control system (TCS) and serve as the safety interlock. This paper presents the considerations for the distribution of beam diagnostic instruments and shows the layout of beam diagnostics monitors in the beamline.

INTRODUCTION

A proton therapy facility based on an isochronous superconducting cyclotron is under development in HUST, by a collaborative team from HUST, CIAE (China Institute of Atomic Energy), Tongji Hospital and Union Hospital affiliated to HUST. For HUST proton therapy facility (HUST-PTF), a 250 MeV proton beam with 500 nA will be extracted from a superconducting cyclotron. After passing through the energy selection system (ESS) in which the energy will be modulated in the range of 70~240 MeV, it will be switched and delivered to three treatment rooms: two gantry rooms and one room with fixed beam line. The main specifications [1] are listed in Table 1.

Many beam diagnostic instruments are distributed throughout the beam line to measure the beam profile, position, current, loss, energy and energy spread. In this paper, the primary design considerations of beam diagnostics system within one gantry beamline are described and the layout of beam diagnostics monitors in the beamline is presented.

* Work supported by The National Key Research and Development Program of China, with grant No. 2016YFC0105305, and by National Natural Science Foundation of China (11375068).
† Email address: lxhustliu@hust.edu.cn, chenqushan@hust.edu.cn

Table 1: Main Specifications of HUST-PTF

Parameter	Specification
Max. Beam Energy	250 MeV
Max. Beam Current	500 nA
Energy Range for ESS	70-240 MeV
Energy Modulation Time	≤150 ms per step
Gantry Type	360 degree, normal conducting
Treatment scheme	Pencil beam scanning (PBS)
Max. Dose Rate	3 Gy/L/min
Field Size	30 cm × 30 cm

OPERATION MODE

For a proton therapy facility, beam diagnostics system shall perform functions covering functions beam parameters measurement, and guarantee of the treatment safety. Several beam parameters shall be measured in real – time.to ensure the safety of treatment. Thus in the HUST-PTF system, the beam diagnostic instruments will operate in two modes: debugging mode and treatment mode. These two modes can arbitrary switch. The overview of this two modes is shown in Fig. 1.

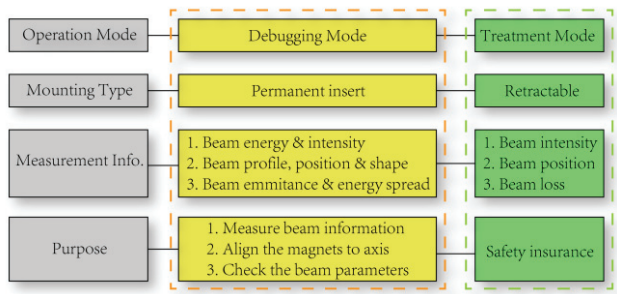

Figure 1: Overview of two operation modes.

Debugging Mode

In the debugging mode, all monitors are retractable and locate at the axis to measure the beam information. Based on the reading data, all dipole and quadrupole magnets can be aligned in the beam line. In addition, the beam envelop is rebuilt to check the beam optics.

ISBN: 978-3-95450-192-2 doi:10.18429/JACoW-IBIC2017-MOPCF05

BEAM INSTRUMENTATIONS AND COMMISSIONING OF LINAC IN CSNS

W. L. Huang†, T. G. Xu, P. Li, F. Li, J. L. Sun, J. M. Tian, M. Meng, L. Zeng, R. Y. Qiu, Z. H. Xu, T. Yang, J. Peng, S. Wang, S.N Fu
Dongguan Campus, Institute of High Energy Physics, Dongguan, China

Abstract

China Spallation Neutron Source (CSNS), the biggest platform for neutron scattering research in China, will be finished built and run in the end of 2017. It mainly consists of an 80MeV H- linac and an 80MeV to 1.6GeV Rapid Cycling Synchrotron, two beam transport lines, one target station and relative ancillary facilities. The linac beam commissioning with beam loss monitors, current transformers, BPMs, beam profile monitors and beam emission measurement has been the main task since last year. Beam instrumentations, commissioning of the temporary 60 MeV linac will be discussed in this paper.

INTRODUCTION

Beam instrumentations distributed on the CSNS linac are presented in Fig. 1. After the 50keV H- source, there are 2 beam current monitors and an emission monitor installed on the low energy beam transport line (LEBT). At the middle energy beam transport line (MEBT) there are 2 self-made FCTs to monitor the beam current, 7 strip-line beam position monitors and 4 wire scanners to monitor the beam profile for measuring the Twiss parameters of the RFQ output beam. The 4-tank 324MHz drift tube linac (DTL) is designed to accelerate the H- beam from 3MeV to 80MeV. At the exit of the 4th tank of an 80MeV drift tube linac (DTL), 5 Bergoz FCTs are used to monitor the beam phase for energy measurement by means of TOF. At present commissioning period, only 3 of the 4 klystrons are available to feed 3MW power into the corresponding DTL tank, therefore tank 1 to 3 have been commissioned and the beam was successfully accelerated to 61MeV. After that, the beam was transported through the last DTL tank and the linac to RCS Beam Transport line (LRBT), and finally directly to the LRDMP1. Until May 2017, four runs of linac beam commissioning have been performed [1].

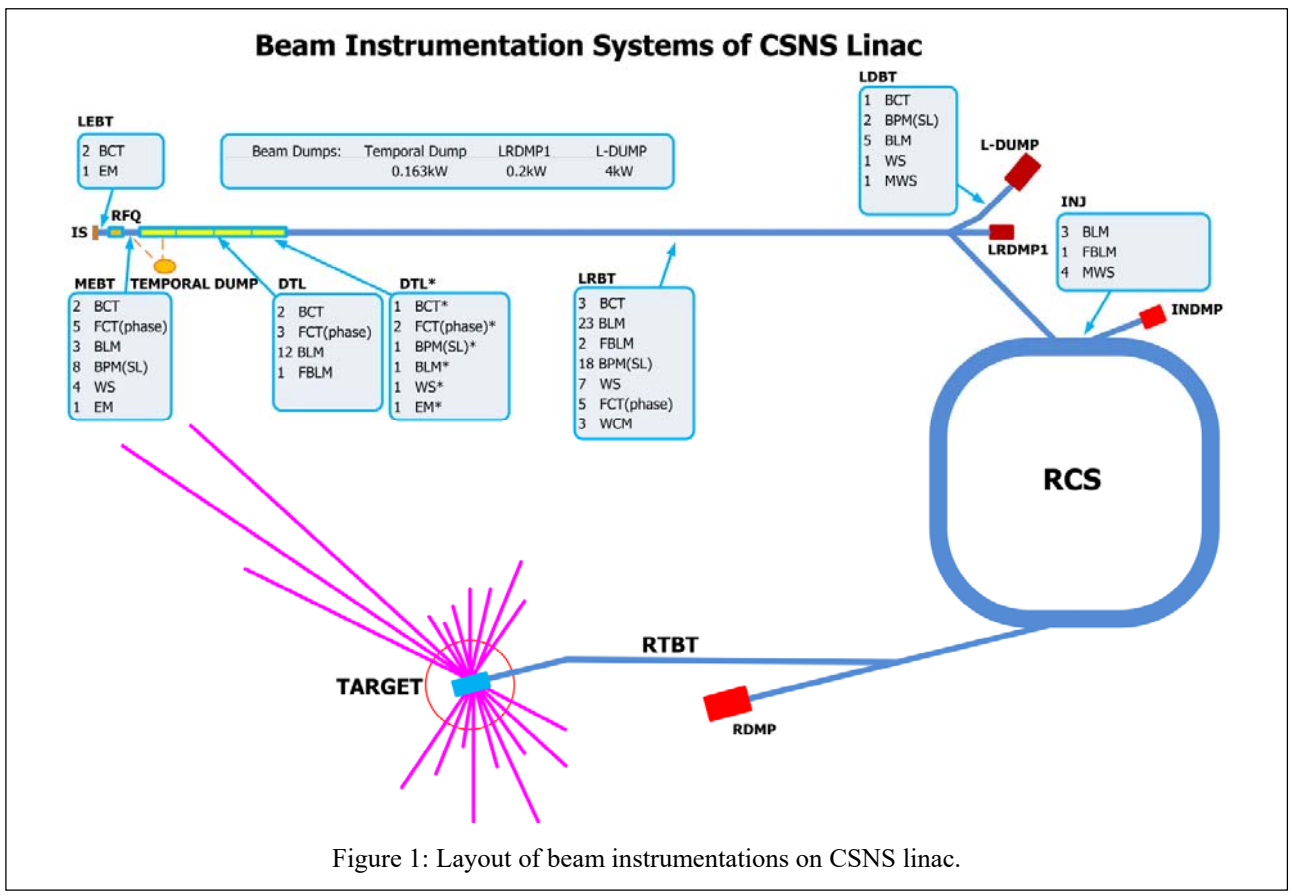

Figure 1: Layout of beam instrumentations on CSNS linac.

† huangwei@ihep.ac.cn

ISBN: 978-3-95450-192-2 doi:10.18429/JACoW-IBIC2017-MOPCF09

BEAM DIAGNOSTICS SYSTEMS FOR SIRIUS LIGHT SOURCE

S. R. Marques*, LNLS, Campinas, Brazil
on behalf of the LNLS Accelerator and Engineering Divisions

Abstract

This paper gives an overview of Sirius diagnostics systems under commissioning or in planning phase. It includes beam position monitors for electron and photon beams, visible and X-ray synchrotron light monitors, transverse profile monitors, streak camera, beam loss monitors, current monitors, charge monitors, tune and filling pattern measurements. The paper focuses on the specification of the beam diagnostics systems and their motivation, parts selection, accompanying data acquisition systems, control software capabilities and development status.

INTRODUCTION

The Sirius light source facility is based on a 518 m circumference 5BA 3 GeV electron storage ring (SR), designed to achieve a bare lattice emittance of 0.25 nm·rad [1]. The machine is under construction at LNLS, in Campinas, Brazil. Machine installation is expected to start at the end of 2017 and beam commissioning in the middle of 2018.

The injector is composed of a 497 m circumference full energy booster synchrotron (BO) installed in the same tunnel as the SR, with a 3.5 nm·rad emittance at 3 GeV, a 150 MeV LINAC supplied by SINAP, LINAC-to-booster (LTB) and booster-to-storage ring (BTS) transfer lines.

The LINAC operates in single and multi-bunch modes, with 1 ns / 1 nC and 150 ns / 3 nC pulse length / charge, respectively. Maximum repetition rate is 10 Hz, but booster cycling will occur at 2 Hz.

The SR and BO rings operate at 500 MHz and have harmonic numbers 864 and 828, respectively. The LINAC operates at the 6th RF frequency harmonic (3 GHz). All of the instrumentation has been designed to allow injection in multi, single or hybrid bunch modes.

For brevity, LINAC diagnostics are not covered herein.

SIRIUS DIAGNOSTICS

In order to monitor the quality of the electron and photon beams, several diagnostics equipment will be installed along the accelerators and transfer lines. Parameters like bunch charge, transverse and longitudinal profiles, beam orbit, tunes, beam emittance and beam loss, the injection efficiency and beam stability will be constantly monitored. Table 1 briefly shows the main beam diagnostics devices of the accelerator complex.

Flags

In total 19 fluorescent screens (or beam flags) will be used in the commissioning phase and for general troubleshooting. In the transfer lines the fluorescent screens will be installed together with 6 cm stripline BPMs in order to provide beam profile measurements and non-destructive beam position measurements in the same location.

Table 1: Summary of Beam Diagnostics Components

	Linac	LTB	BO	BTS	SR
DCCT			1		2
FCT		1		1	
ICT	2	2		2	
Beam Flag	5	6	3	6	
Horizontal Slit		1			
Vertical Slit		1			
Button BPM			50		160
Stripline BPM	3	6		5	
Front-End Photon BPM					80
Filling Pattern Monitor					1
Horizontal scraper					1 pair
Vertical scraper					1 pair
Tune shaker			1		2
Tune pick-up			1		1
Bunch-by-Bunch kicker					2
Bunch-by-Bunch BPM					1
X-ray port					2
Visible light port					1
Streak camera					1
Beam Loss Monitor		tbd	tbd	tbd	
Gas Bremsstrahlung Monitor					tbd

The booster fluorescent screens are installed right after the injection point, a few meters apart from each other, in order to monitor the position and angle of the injected beam.

Cerium-doped Yttrium Aluminium Garnet (YAG:Ce) 0.1 mm thick screens, produced by Crytur, were selected for the flags. The screen is placed inside a bellows, which can be moved to intercept the beam.

The bellows is attached to a Huber 5101.20 X1 linear translation stage moved by a Vexta PK-266-02B stepper motor. The linear stage also contains a rotary encoder provided by Huber. This allows the usage of more than one screen, as the motor can move the bellows with micrometer precision, enough to place one of the available screens in the correct position to intercept the beam. The current approach is to use a YAG:Ce screen to intercept the beam and an additional screen with markers to calibrate the optics.

The stepper motor is driven by a single-axis Galil DMC-30017 controller. An IOC [2], communicating with the controller through Ethernet, is used to integrate the motion controller to the accelerator control system via EPICS [3].

* sergio@lnls.br

ISBN: 978-3-95450-192-2 doi:10.18429/JACoW-IBIC2017-MOPCF10

ESTIMATION OF HEAVY ION BEAM PARAMETERS DURING SINGLE EVENT EFFECTS TESTING

V.S. Anashin, P.A. Chubunov, G.A. Protopopov, United Rocket and Space Corporaton, Institute of Space Device Engineering, Moscow, Russia
S.V. Mitrofanov, V.A. Skuratov, Y.G. Teterev, Joint Institute for Nuclear Research, Dubna, Russia

Abstract

During flight mission onboard electronic equipment of spacecraft exposed to outer space radiation. Impact of charged particles leads to errors and failures in electronic components (EC). The most critical problem for spacecraft engineers is heavy ions influence which cause single event effects (SEE) in EC [1,2]. To be assure that spacecraft electronics will work properly during the mission ground SEE testing is needed. For these purposes heavy ions accelerators are used. In this paper, we present facility for SEE testing including requirements to heavy ions beams, techniques and equipment used for control heavy ion beam parameters during SEE testing.

BASIC PRINCIPLES OF SEE TESTING

SEE are such effects, the cause of which is the interaction of the single charged particle with active area of semiconductor device. Such effects have a probabilistic nature and are not related to radTatTon "history" of the device. SEE can be classified into Destructive, Residual and Transient effects, by types of failures. Destructive SEE are Single event latch up (SEL) - inclusion of the parasitic four- layer p-n-p-n structure leading to harsh increase circuit current; Single event burnout (SEB) - secondary induced breakdown of p-n junction leading to its destruction; Single event gate rapture (SEGR) - breakdown of gate insulator along nuclear track of particle; Single event snapback (SESB) - secondary induced breakdown, determined the performance spurious bipolar structure in MOS transistor. Residual SEE are Single event upset (SEU) - inversion of logical state of memory unit or trigger circuit; Multiply byte upset (MBU) - inversion of logical state of several neighboring memory unit or trigger circuit; Single event functional interruption (SEFI) - inversion of logical state of memory unit or trigger circuit operation leading to violation of program progress (for example, program hangup). Transient SEE are analogue and digital Single event transient (ASET, DSET) - Short- time pulse in output element of linear or digital semiconductor devices.

General SEE testing foundation is The principle of equivalence thresholds LET for space heavy charged particles and monoenergetic ions, in which the electronic components having SEE :equality thresholds LET under the influence of space heavy charged particles, containing ions of different chemical elements with different spectral and energetic characteristics and any monoenergetic ion having a given value of LET, under the influence of which in electronic components appears SEE. Main SEE hardness characteristics are following: Threshold LET; Effect cross-section (saturation); Dependence of effect cross-section from ions LET, usually Weibull curve (see example on Fig. 1).

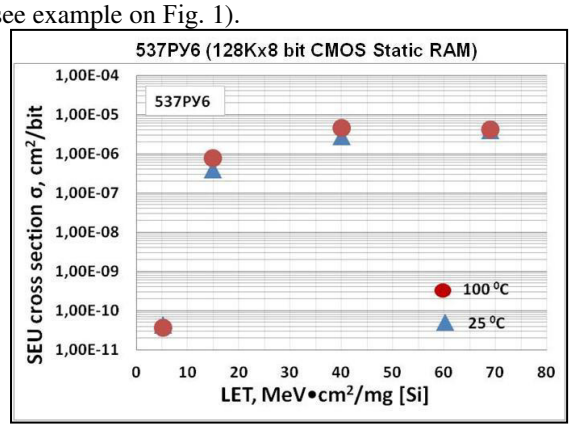

Figure 1: Dependence of SEU cross-section from ions LET for Russian-made SRAM at different temperatures.

TEST FACILITIES

A number of heavy ion test facilities are created under TCe BrancC of JSC "UnTted Rocket and Space Corporation" – "Institute of Space Device Engineerng" authorizing on the base of cyclotrons U400 and U400M (Flerov Laboratory of Nuclear Reactions (FLNR), Joint Institute for Nuclear Research (JINR), Dubna city, Moscow region) which have differential in the composition of output ions and their energy, the radiation area, range of temper-atures, by changeover time from one ion to another, vacu-um pumping time (see Table 1 for details). Currently our test facilities provide test operations of all EC functional classes on hardness to all types of SEE. Since 2010, by the effort of the five testing laboratories have been tested more than 3000 EC part types All test facilities are avail-able to carrying out tests (on request); there are no re-strictions for foreign organizations. Some pictures of test facilities are shown on Figs. 2-4.

Figure 2: Low energy test facility (IS OE PP).

ISBN: 978-3-95450-192-2 doi:10.18429/JACoW-IBIC2017-MOPWC01

BUILDING THE THIRD SRF GUN AT HZDR

H. Vennekate[1]*, A. Arnold, P. Lu, P. Murcek, J. Teichert, R. Xiang
Helmholtz-Zentrum Dresden-Rossendorf, Germany
[1]also at Technical University Dresden, Germany

Abstract

The multipurpose accelerator ELBE at HZDR which is delivering a large set of secondary beams, is driven by a thermionic DC injector. In order to enhance the beam quality of the machine, the development of superconducting RF injector has been pursued since the early 2000's. The corresponding ELBE SRF Gun I of 2007 and Gun II of 2014 already delivered beam for the operation of several user beamlines, such as the FEL, positron generation, and THz facility. Currently, the next version – Gun III – and its cryomodule are being assembled, characterized, and prepared for the final commissioning throughout late 2017/early 2018. The new module benefits from the experiences gained with regard to emittance compensation and monitoring of operation variables made with the two predecessors.

MOTIVATION

The unique feature of the ELBE accelerator is its ability to run all its modules in continuous wave (CW) mode while delivering electron bunches at a frequency of up to 13 MHz. Hence, a flexible CW source is required for its operation. A superconducting radio frequency (SRF) electron gun represents the ideal solution for this task. Itcombines the advantages of RF injectors and DC guns, which are high field gradients causing enhanced beam parameters and large beam currents due to increased repetition rates, respectively. The ELBE SRF Gun project is an R&D effort to provide such an injector. The two implemented prototypes — Gun I and Gun II — successfully provided beam for several of the beamlines during machine tests as well as for user operation [1]. Due to a degradation of available maximum gradient of the cavity of the currently installed Gun II, the construction of the third version of the photoinjector was initiated. For this purpose, the niobium resonator of Gun I is being refurbished at DESY, Hamburg. In combination with a newly built cryomodule, this cavity is designated to be put in operation as the ELBE SRF Gun III within 2018.

EMITTANCE COMPENSATION

An important aspect of the beam dynamics of an SRF injector is the optimization of the emittance of the electron bunches, which presents more challenges than for a normal conducting gun. In the case of the ELBE SRF gun this is solved by a combination of RF focusing at the photocathode and a superconducting solenoid being integrated into the injector's cryomodule, as shown in the scheme in Figure 1. The use of these two mechanisms has shown a significant reduction of the particle beam's transverse emittance and extent in both, simulation (see Figure 2) as well as in experiment (see Figure 3) [2]. This is of substantial importance for the successful integration into an accelerator's beam dynamics framework.

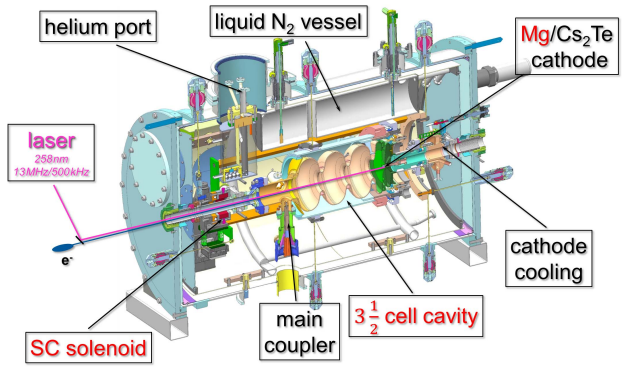

Figure 1: The current ELBE SRF Gun design featuring a 3.5 cell gun cavity and a superconducting solenoid at about 70 cm from the cathode.

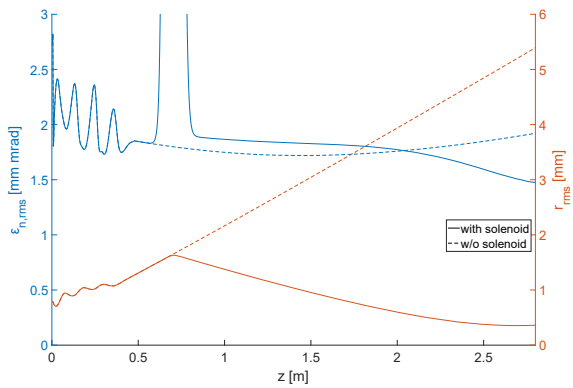

Figure 2: Simulation results of the evolution of a 250 pC bunch in emittance and radius along the first 3 m of beamline [2].

In addition to the characterization of the intentional displacement of the photocathode inside the superconducting cavity to control RF focusing [3], the superconducting magnet requires separate thorough examination and testing prior to its installation inside the module. The corresponding measurements conducted so far are described in the following.

* h.vennekate@hzdr.de

ISBN: 978-3-95450-192-2 doi:10.18429/JACoW-IBIC2017-MOPWC02

MICROTCA.4-BASED LLRF FOR CW OPERATION AT ELBE – STATUS AND OUTLOOK

M. Kuntzsch†, R. Steinbrück, R. Schurig, Helmholtz-Zentrum Dresden-Rossendorf, Dresden, Germany
M. Hierholzer, M. Killenberg, C. Schmidt, M. Hoffmann, DESY, Hamburg, Germany
C. Iatrou, J. Rahm, Technische Universität Dresden – Chair of Distributed Control Engineering, Dresden, Germany
I. Rutkowski, M. Grzegrzółka, Warsaw University of Technology - Institute of Electronic Systems, Warsaw, Poland

Abstract

The superconducting linear accelerator ELBE at Helmholtz-Zentrum Dresden-Rossendorf is operated in continuous wave (CW) operation [1]. The analogue LLRF (low level radio frequency) system, used since 2001, is going to be replaced by a digital solution based on MicroTCA.4. The new system enables a higher flexibility, better performance and more advanced diagnostics. The contribution shows the performance of the system at ELBE, the hardware and the software structure. Further it will summarize the last steps to bring it into full user operation and give an outlook to the envisioned beam-based feedback system that will take advantage of the capabilities of the digital LLRF system.

SYSTEM STRUCTURE

Hardware

The ELBE injector uses a thermionic gun followed by two normal conducting (NRF) buncher cavities operating at 260 MHz and 1.3 GHz. The main accelerator consists of two cryo-modules, each is equipped with two TESLA-type superconducting cavities (SRF) that are operated routinely in CW mode.

For high bunch charge and high current beams with good beam properties a superconducting photo gun is currently being developed. It contains a 3.5-cell structure operating at 1.3 GHz [2].

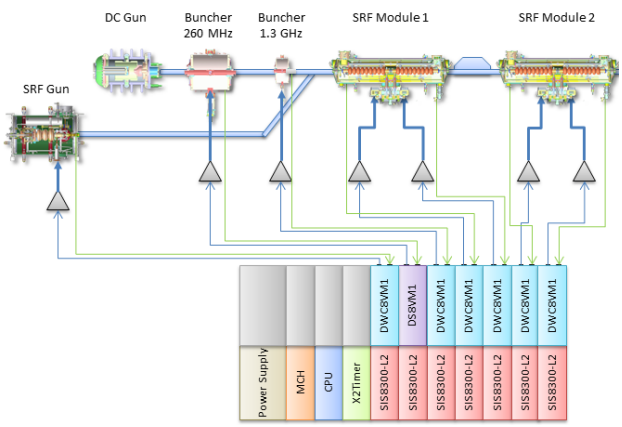

Figure 1: Digital LLRF schematic.

In Figure 1 the main components and the associated hardware are shown. The digital LLRF system at ELBE is based on a modular system using MicroTCA.4 compatible hardware [3]. The standard separates the analogue circuits from the digital data processing. This allows an adaption of the analogue frontend to the desired application, while the digital part remains the same. For all cavities a SIS8300-L2 digitizer board is used which contains fast analogue-to-digital converters (ADCs) and a powerful Virtex 6 field programmable gate array (FPGA).

For the 260 MHz buncher cavity a direct sampling scheme is applied using the DS8VM1 analogue board [4]. For all 1.3 GHz cavities a mixer configuration with DWC8VM1 has been realized [5]. The cavity pickup signals are mixed with a local oscillator (LO) to an intermediate frequency (IF) which is sampled by the ADC sitting on the SIS8300-L2 [6]. The data processing and control loop is done inside the FPGA which allows parallel execution of processes with high data rate.

Software

All digitizer boards are connected to a CPU-board through a PCIe link. Status information and data traces are provided to a server application while this sets all the controller parameters and offers high level features.

For the first test phase a stand-alone DOOCS server application was used to control the system. It could only be accessed by remote login on to the MicroTCA.4-CPU and had no interface to the ELBE control system which is a network of programmable logic controllers (PLCs) and the graphical user interface (GUI) provided by a WinCC server-client system.

In order to overcome these limitations a new server application has been developed using the ChimeraTK framework [7]. This universal toolkit allows development of applications for different control systems like DOOCS and EPICS or the OPC-UA protocol. ChimeraTK enables collaboration and joint software development of institution that are using different control system architectures.

OPC-UA is a powerful protocol for industrial automation and is supported by many commercial suppliers [8]. The features integrated in the ChimeraTK framework are based on the open source implementation open62541 [9] that has been designed to run on different operating systems and hardware platforms.

† m.kuntzsch@hzdr.de

ISBN: 978-3-95450-192-2 doi:10.18429/JACoW-IBIC2017-MOPWC03

COMMISSIONING RESULTS AND FIRST OPERATIONAL EXPERIENCE WITH SwissFEL DIAGNOSTICS

V. Schlott†, V. Arsov, M. Baldinger, R. Baldinger, G. Bonderer, S. Borelli, R. Ditter, D. Engeler, F. Frei, N. Hiller, R. Ischebeck, B. Keil, W. Koprek, R. Kramert, D. Llorente Sancho, A. Malatesta, F. Marcellini, G. Marinkovic, G.L. Orlandi, C. Ozkan-Loch, P. Pollet, M. Roggli, M. Rohrer, M. Stadler, D. Treyer, Paul Scherrer Institut, Villigen, Switzerland

Abstract

SwissFEL is a free electron laser user facility at the Paul Scherrer Institute in Villigen, Switzerland designed to provide FEL radiation at photon energies ranging from 0.2 to 12 keV. Beam commissioning of the hard x-ray line ARAMIS has started in October 2016 and first lasing at 300 eV was achieved in May 2017. First pilot user experiments at photon energies ≥ 2 keV are foreseen for the end of 2017. This contribution comprehends commissioning results and first operational experience of various SwissFEL diagnostics systems, such as beam position monitors, charge and loss monitors as well as transverse profile measurements with screens and wire scanners. It also provides first results from the BC-1 compression monitor and summarizes the status of the electron and laser bunch arrival time monitors.

STATUS OF THE SWISSFEL PROJECT

The compact free electron laser user facility SwissFEL is presently under commissioning at the Paul Scherrer Institut (PSI) in Villigen, Switzerland. In its first project stage, the installation of the hard X-ray branch ARAMIS, which is designed to provide linearly polarized SASE radiation at photon energies between 2 and 12 keV to three user end stations, has been completed and the accelerator has been equipped with all required beam diagnostics systems. The soft X-ray branch ATHOS, which will deliver variably polarized radiation at photon energies between 0.2 and 2 keV, will be realized during a second construction phase during 2018 and 2020. All diagnostics systems for the ATHOS bypass line have been designed and successfully tested and most of the components are already ordered.

Since the delivery schedule for the solid-state modulators of the C-band LINACs drives the SwissFEL commissioning schedule, a staged commissioning approach has been chosen.

- In August 2016 first electrons at beam energies of 7.9 MeV have been generated by the 2 ½ cell S-band photo-injector RF gun and transported to the injector beam dump, including the first successful acceleration through one of the LINAC-1 C-band accelerator modules.
- In November 2016 first beam has been transported through the ARAMIS undulators with achievement of first lasing at 24 nm with moderate beam energies of 345 MeV, just in time for the SwissFEL inauguration ceremony on December 5th 2016.
- After a two months winter shut down, where some final installation and consolidation work was done, first SASE lasing in the nominal SwissFEL wavelength range (0.1 – 5 nm) could be achieved at 4.1 nm mid of May 2017. The electron beam energy was set to 910 MeV at bunch charges of 145 pC and bunch length of 400 fs (rms).

The accelerator set-up for lasing included careful optimization of the RF gun and photo-cathode laser operating points, transverse beam optics measurements and matching in the injector, tuning of the first bunch compressor (BC-1) with the S-band deflecting cavity, implementation of the computed beam optics in the LINACs and undulators and steering of the beam according to the BPM centres. Figure 1 shows the FEL gain curve at 4.1 nm, which was measured with a Neon gas photon intensity monitor.

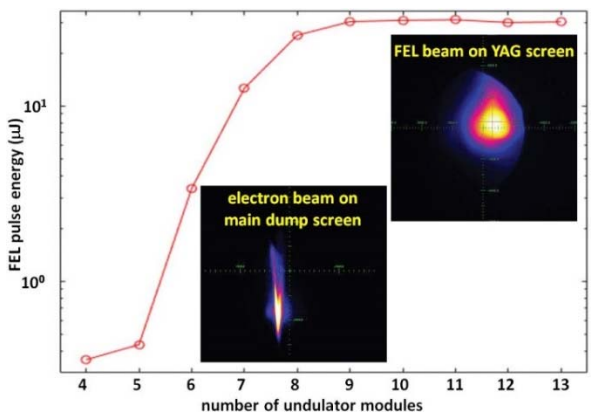

Figure 1: Gain curve for first lasing at SwissFEL at 4.1 nm. The inlets show the FEL beam on an ARAMIS front end YAG screen and the electron beam on the main dump screen monitor (LYSO screen).

After the first lasing attempts, which demonstrated the operability of most of the SwissFEL sub-systems, the commissioning is ongoing, presently focusing on the set-up of the bunch compression stages, beam optics matching and further characterization and calibration of diagnostics systems with beam. With further increase in beam energy by consecutively adding more C-band accelerator stations, a first pilot ("friendly user") experiment at photon energies ≥ 2 keV is envisaged for the end of 2017.

DIAGNOSTICS COMMISSIONING

Although the performance of the diagnostics monitors could be successfully demonstrated at the SwissFEL Injector Test Facility [1] and the front end, data acquisition and

† volker.schlott@psi.ch

ISBN: 978-3-95450-192-2 doi:10.18429/JACoW-IBIC2017-MOPWC05

ATF FACILITIES UPGRADES AND DEFLECTOR CAVITY COMMISSIONING*

C. Swinson†, M. Fedurin, M. A. Palmer, I. Pogorelsky, Brookhaven National Lab, NY, USA

Abstract

The Accelerator Test Facility (ATF) at Brookhaven National Lab is an Office of Science user facility focusing on advanced acceleration techniques. It houses several electron beamlines synchronized to high power lasers, including a TW-class carbon dioxide (10 μm) laser. Here we outline ongoing upgrades to both the accelerator and laser systems, give a brief overview of the experimental landscape, and report on the recent commissioning of a newly installed X-band deflector cavity [1]. The deflector cavity is implemented as a longitudinal electron beam diagnostic, which will allow us to measure the structure of ultra-short bunches.

INTRODUCTION

The mission of the ATF is to provide the advanced accelerator community with state-of-the-art facilities and scientific support. We also host beam instrumentation and transport R&D, laser research, and materials/condensed matter physics programs. Figure 1 highlights the major components of the ATF complex.

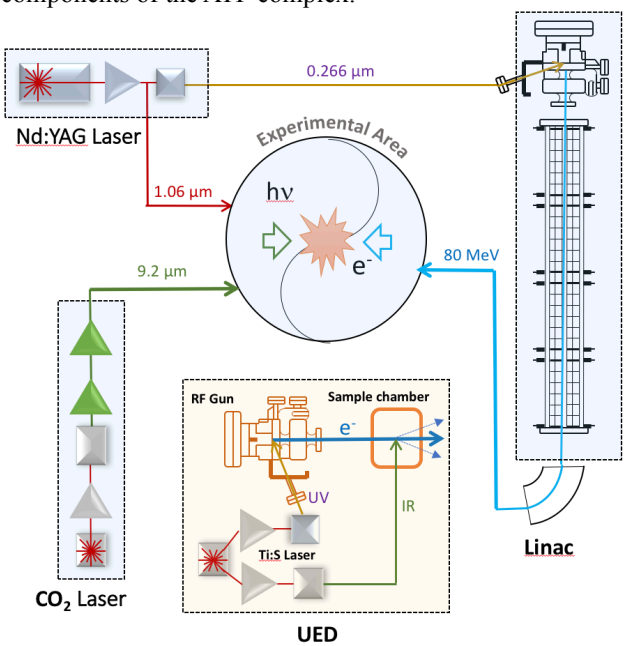

Figure 1: Schematic of the ATF, featuring the four ma-jor components. We plan to add a strong field laser to the ATF portfolio, in the near future.

* The ATF is a U.S. Department of Energy, (DOE) Office of Science User Facility operated for the DOE, Office of Science by Brookhaven National Laboratory under Contract No. DE-AC02-98CH10886

†cswinson@bnl.gov

PRESENT STATUS

The ATF is presently hosting a full user program. Table 1 shows the presently available electron beam parameters at the ATF. A maintenance program, currently underway and continuing over the next few months, will allow us to routinely reach the highest achievable beam parameters. This paper outlines upcoming R&D, designed to expand the CO_2 laser parameter space, shown in Table 2.

Table 1: Presently Electron Beam Parameters at ATF

Beam Property	Nominal	Best Achievable
Energy (MeV)	57	80
Rep. Rate (Hz)	1.5	3
IP Beam Size (μm)	50	5
Bunch Charge (nC)	0.01-1.5	3

Table 2: Present CO_2 Laser Parameters

Laser Property	Value
Energy (J)	7
Pulse length (ps)	3.5
Power (TW)	1.5
Power delivered IP (TW)	0.5
Rep. Rate (Hz)	1/20

Accelerator Improvements

The ATF is presently undergoing a program of accelerator improvements aimed at improving RF stability and beam reproducibility. Alongside such improvements, we report the recent commissioning of an X-band deflector cavity as a longitudinal bunch diagnostic, and a focus on providing <100 fs long electron bunches through magnetic bunch compression.

X-band Deflector Commissioning

An X-band (11.4 GHz), Traveling Wave, Deflection Mode Cavity [2] for Ultra-Fast Beam Manipulation and Diagnostics (fig. 2), developed and manufactured by Radiabeam Technologies, was recently installed in one of the ATF experimental beam lines. The system has been commissioned and has already been utilized by two user groups.

An initial estimate of time resolution showed better than 10 fs. This was done by using a microbunched beam of known spacing, produced using a mask technique [3]. The microbunched beam was used to calibrate a yag crystal screen downstream of the deflecting cavitiy. The measurement was limited by the resolution of the beam profile monitor camera.

ISBN: 978-3-95450-192-2 doi:10.18429/JACoW-IBIC2017-MOPWC06

BEAM DIAGNOSTICS FOR NEW BEAM TRANSPORT LINE OF PF-AR

R. Takai*, T. Honda, T. Obina, M. Tadano, H. Sagehashi,
KEK Accelerator Laboratory and SOKENDAI, 1-1 Oho, Tsukuba, Ibaraki, Japan

Abstract

The beam transport line (BT) for the Photon Factory Advanced Ring (PF-AR), which is a 6.5-GeV light source of KEK, has been recently renewed. The new BT dedicated to PF-AR allows not only simultaneous operation with the SuperKEKB storage ring, which has a much shorter Touschek lifetime, but also the top-up operation via 6.5-GeV full-energy injection. The construction, including tunnel excavation, was completed by the end of 2016, and the commissioning was performed for one month from February 2017. Standard beam monitors, such as stripline beam position monitors, screen monitors, beam loss monitors, and fast current transformers are installed in the new BT and contribute greatly to accomplishing the commissioning in a short period of time. This paper discusses details of these monitors and some commissioning results obtained by using them.

INTRODUCTION

The Photon Factory Advanced Ring (PF-AR), which is a 6.5-GeV electron storage ring of KEK, is a dedicated light source for generating pulsed hard X-rays. The beam transport line (BT) for injecting electron beams to PF-AR has been renewed recently [1]. Before the renewal, the continuous injection for KEKB, which is an electron-positron collider of KEK, had to be interrupted for about 15 min at each injection for PF-AR, because a part of the BT was shared with it. Following the upgrade of KEKB to SuperKEKB, the Touschek lifetime is shortened to ~10 min [2]; therefore, such interruptions should be avoided. This is the main reason why the dedicated BT for PF-AR was constructed. The principal parameters of PF-AR are listed in Table 1.

Table 1: Principal Parameters of PF-AR

Beam Energy	6.5 GeV
Max. Stored Current	60 mA
RF Frequency	508.57 MHz
Circumference	377.26 m
Harmonic Number	640
Number of Bunches	1
Revolution Frequency	795 kHz
Tunes (x/y/s)	10.17/10.23/0.05
Damping Time (x/y/s)	2.5/2.5/1.2 ms
Natural Emittance	294 nm rad
Natural Bunch Length	18.6 mm (62 ps)
Max. Injection Frequency	12.5 Hz
Operation Mode	Decay
Number of Stations	8

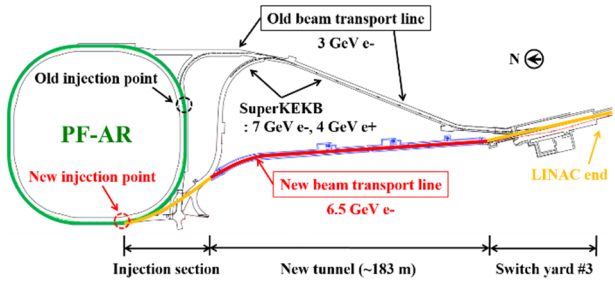

Figure 1: Schematic view of the old and new BTs for PF-AR. The total length of the new BT, from the LINAC end to the new injection point, is about 320 m.

The construction was started in FY2013, followed by the excavation of the new BT tunnel, the development of infrastructure in the tunnel, and the design and production of the required BT components sequentially. The final construction works, such as the deconstruction of the old BT, the relocation of magnets to be reused, the installation of the new BT components, and the reconstruction of the new injection point of PF-AR were proceeded in parallel for seven months from July 2016 to January 2017, and completed on schedule. Following these, the commissioning of the new BT was started and the necessary preparation to resume the user operation could be made in about one month. The new BT is designed for 6.5-GeV full-energy injection and enables not only the simultaneous operation with SuperKEKB but also top-up operations in near future. Besides, it resolves the difficult problems with stacking and accelerating of the 3-GeV short-bunch beam, such as the beam loss due to severe beam instabilities and the heat generation of beam ducts.

In this paper, we describe the beam monitors installed in the new BT for PF-AR in detail and some commissioning results obtained by them.

BEAM MONITORS FOR THE NEW BEAM TRANSPORT LINE OF PF-AR

Figure 1 shows a schematic of the old and new BTs for PF-AR. The new BT is about 320 m long and can be classified into three main sections: Switch Yard #3 for distributing beams to the lower rings at the end of LINAC (SY3), the new BT tunnel dedicated for PF-AR, and the beam injection section connected to the new injection point at the southwestern part of the ring after crossing the existing BT for SuperKEKB. The beam monitors installed in the new BT are listed in Table 2. As the three sections are separated from each other, the control systems of these monitors are arranged sporadically in several local control rooms (LCRs), and the output signals from each monitor are collected through the control network after being digitized at

* ryota.takai@kek.jp

ISBN: 978-3-95450-192-2 doi:10.18429/JACoW-IBIC2017-MOPWC07

COMMISSIONING OF THE BEAM INSTRUMENTATION FOR THE HALF SECTOR TEST IN LINAC4 WITH 160 MeV H- BEAM

G. Guidoboni†, J.C. Allica Santamaria, C. Bracco, S. Burger, G.J. Focker, B. Mikulec, A. Navarro Fernandez, F. Roncarolo, L. Soby, C. Zamantzas, CERN, Geneva, Switzerland

Abstract

In the framework of the LHC Injector Upgrade (LIU) project, the Proton Synchrotron Booster (PSB) will be extensively modified during the Long Shutdown 2 (LS2, 2019-2020) at CERN [1]. This includes a new injector, Linac4, which will provide a 160 MeV H- beam and a complete new injection section for the PSB composed essentially of a chicane and a stripping foil system. The equivalent of half of this new injection chicane, so-called Half-Sector Test (HST), was temporarily installed in the Linac4 transfer line to evaluate the performance of the novel beam instrumentation, such as, stripping foils, monitoring screens, beam current transformers, H^0/H^- monitor and dump, beam loss monitors, and beam position monitors. The results of the instrumentation commissioning of the HST are presented in this paper.

INTRODUCTION

The Half Sector Test project (HST) [2] aimed to test the new injection scheme of the PSB that will be installed during LS2. The beam instrumentation needed to commission the HST was temporarily installed in the Linac4 transfer line as shown in Fig. 1. In particular, the HST was composed by:

- The stripping foil system (TKSTR) and a beam imaging system based on a scintillating screen with radiation-hard camera (BTV1).
- Half of the injection chicane (BSW3 and BSW4 magnets).
- The monitor measuring the partially stripped and unstripped particles (H^0/H^- monitor) and the H^0/H^- dump integrated with BSW4.
- Beam Loss Monitors (BLMs) in the vicinity of the H^0/H^- dump, one ionisation chamber and one diamond detector for fast time-resolved measurements.
- One Beam Current Transformer upstream (BCT1) and one downstream (BCT2) of the HST for transfer efficiency measurements.
- A second beam imaging system (BTV2) for beam profile measurements and steering to the final (temporarily installed) dump.
- Beam Position Monitors (BPMs) installed along the Linac4 and the transfer line up to the HST.
- Vacuum equipment and services.

In the next section, the instrumentation will be described in more detail and their performance illustrated.

HST INSTRUMENTATION

Stripping oil and ptical eam Systems

The stripping foil system is composed by:

- A stripping foil loader holding up to six foils that can be remotely interchanged and fine-adjusted to reduce the time for machine intervention (e.g. foil substitution) and thus less dose absorbed by the personnel [3].
- A retractable optical beam observation system (BTV), consisting of a 1 mm thick Chromox (Al_2O_3 doped with Cr_2) scintillating screen that can be placed at a distance of 6 mm in front of the foil.

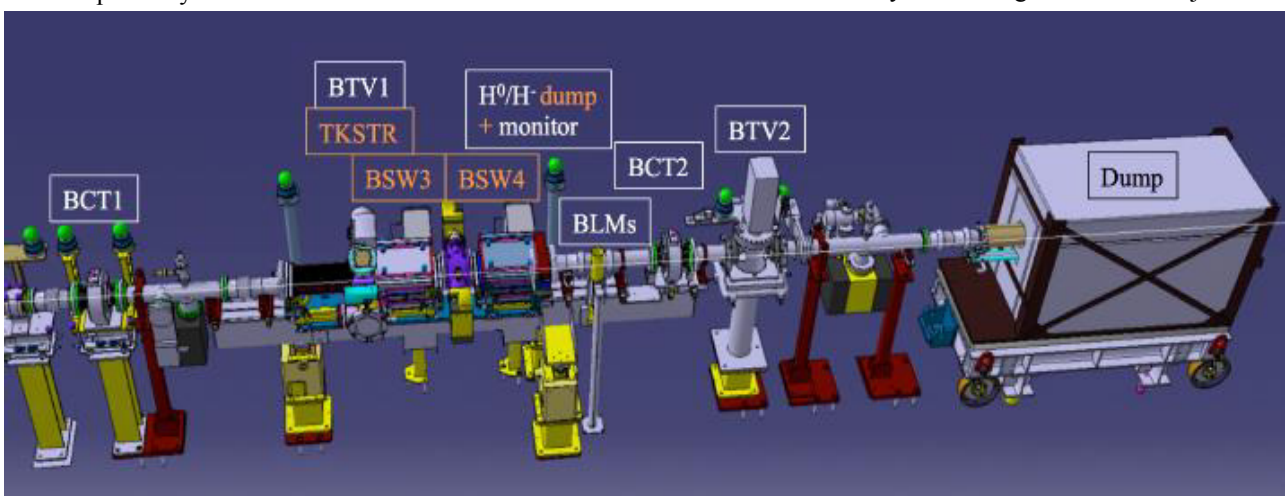

Figure 1: 3D drawing of the HST installation in the Linac4 transfer line (beam from left to right).

† greta.guidoboni@cern.ch

ISBN: 978-3-95450-192-2 doi:10.18429/JACoW-IBIC2017-TU1AB2

HIGH REPETITION-RATE ELECTRO-OPTIC SAMPLING: RECENT STUDIES USING PHOTONIC TIME-STRETCH

C. Evain, C. Szwaj, E. Roussel, M. Le Parquier, S. Bielawski*
PhLAM, Université Lille 1, France
Eléonore Roussel, J.-B. Brubach, L. Manceron, M.-A. Tordeux, M. Labat, P. Roy,
Synchrotron SOLEIL, Gif-Sur-Yvette, France
Nicole Hiller, Paul Scherrer Institute, PSI (Switzerland)
Edmund Blomley, Stefan Funkner, Erik Bründermann, Michael Johannes Nasse,
Gudrun Niehues, Patrik Schönfeldt, Marcel Schuh, Johannes Leonard Steinmann, Sophie Walter,
and Anke-Susanne Müller
Karlsruhe Institute of Technology (Germany)

Abstract

Single-shot electro-optic sampling (EOS) is a powerful characterization tool for monitoring the shape of electron bunches, and coherent synchrotron radiation pulses. For reaching high acquisition rates, an efficient possibility consists in associating classic EOS systems with the so-called *photonic time-stretch* technique. We present several setups that may be used for adding the time-stretch functionality to existing EOS systems, and focus on experimental tests made in two situations. At SOLEIL, we present a setup which is optimized for high SNR recording of THz CSR pulses. At KARA (Karlsruhe Research Accelerator), the storage ring of the test facility and synchrotron radiation source ANKA at KIT, we show how the time-stretch strategy can be tested using almost no modification of an existing spectrally-encoded EOS system. Finally we present recent results on CSR and the microbunching instability that have become accessible using photonic time stretch.

INTRODUCTION: HIGH REPETITION RATE EOS

Single-shot Electro-Optic Sampling [1] (EOS) is an efficient technique for monitoring electron bunch shapes [2–4] by recording the electric field in the near-field of the bunch, and is also capable of recording the Coherent Synchrotron Radiation emitted by the electrons [5]. The principle (Fig. 1a) consists of modulating a stretched laser pulse with the electric pulse to be characterized. As a result, the information is imprinted in the spectrum of the laser pulse, and the information can be retrieved by recording the spectrum shape. In classical spectral encoding EOS, the spectrum is typically recorded using a diffraction grating and a camera.

Although this technique is particularly efficient, operation of EOS at high repetition rates (1 MHz or more) remined up to recently a largely open challenge. The main bottleneck in high-speed EOS was the readout part, as commercial linear cameras are typically limited to the 100 KHz range. Two approaches to this problem have been undertaken recently: (i) one direction has been to develop specific cameras that can operate at several Megahertz, the KALYPSO project at Karlsruhe Institute of Technology [6, 7], (ii) a second research direction has been devoted to an alternate type of readout: photonic time-stretch [8–10].

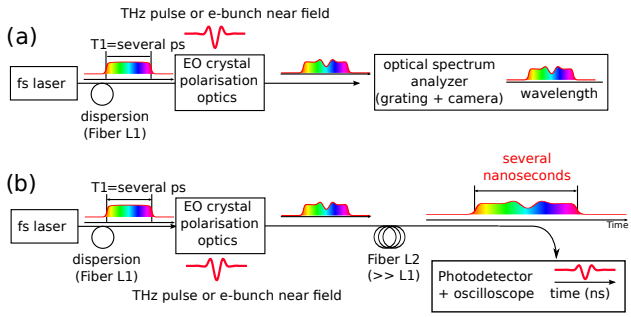

Figure 1: Principles of (a) usual spectrally-encoded EOS (b) photonic time-stretch EOS. In both cases a chirped laser pulse is modulated by the electric pulse under investigation, and the main difference concerns the readout. In classical spectral encoding, the output spectrum is recorded using a single-shot optical spectrum analyzer (usually composed of a grating and a camera). In photonic time-stretch, a long fiber (typically few kilometers-long) stretched the output signal, so that it can be recorded by a single pixel photodetector and an oscilloscope (typically with few GHz bandwidth).

In photonic time-stretch EOS [8–10], the output pulse (Fig. 1b) is dispersed in a long fiber (typically with few kilometers length). As a result, the EOS signal appears as slowed-down replica of the THz electric field, and can be recorded using a single pixel commercial photodetector and an oscilloscope (or acquisition board) with few GHz bandwidth. The acquisition rate can thus be pushed to the hundreds of MHz range, using commercial devices.

Historically, the photonic time-stretch technique has been introduced by the B. Jalali team in 1999 [11, 12] for increasing the bandwidth of A/D digitizers in general. Variants of the technique have also been widely used for recording optical spectra at hundreds of MHz rates [13] (a technique known as Dispersive Fourier Transform, or DFT), as well as high repetition-rate imaging [14–16].

* serge.bielawski@univ-lille1.fr

ISBN: 978-3-95450-192-2 doi:10.18429/JACoW-IBIC2017-TU1AB3

THE OPTICAL DISSECTOR BUNCH LENGTH MEASUREMENTS AT THE METROLOGY LIGHT SOURCE

D. Malyutin†, A. Matveenko, M. Ries, Helmholtz-Zentrum Berlin, Berlin, Germany
O. Anchugov, V. Dorokhov, S. Krutikhin, O. Meshkov, Budker Institute of Nuclear Physics, Novosibirsk, Russia

Abstract

The bunch longitudinal profile measurements using an optical dissector are introduced in the paper. The principles of the dissector operation are briefly discussed. The first measurements using the optical dissector at the Metrology Light Source are presented. Results are analyzed and compared with the bunch profiles from the streak camera measurements. Measurement errors and limitations of the both methods are estimated. Possible applications for the presented technique are discussed.

INTRODUCTION

Practically all present synchrotron radiation sources and electron-positron colliders use streak cameras as an important diagnostic tool, which may provide high spatial resolution (up to tens of micrometers) as well as ultimate temporal resolution up to hundreds of femtoseconds [1, 2]. In the seventies of the last century, the LI-602 dissector [3, 4] was developed at BINP to measure the longitudinal beam profile at circular accelerators. This electron-optical device is based on a stroboscopic approach and is designed for measurement of periodic light pulses of sub-nanosecond and picosecond duration. This dissector is used now for permanent control of the bunch length at the VEPP-2000, VEPP-4M electron-positron colliders and SIBERIA-2 synchrotron light source [5, 6]. However, the LI-602 dissector provides a limited temporal resolution of 20 ps, which is at least one order of magnitude higher than required for modern accelerator diagnostics. Later a new generation of picosecond dissectors was developed based on the PIF-01/S1 picosecond streak-image tube [7, 8] designed and manufactured at the GPI Photoelectronics Department [9, 10]. The experimentally determined temporal resolution of such dissector approaches 3.5 ps [11]. This value was obtained illuminating the tube-input photocathode with femtosecond laser pulses at 800 nm wavelength [12]. In this paper, we describe the test of this new dissector under real experimental conditions at the Metrology Light Source (MLS) [13]. A comparison between the dissector and a Hamamatsu streak camera C10910 [14] was undertaken.

DISSECTOR

The dissector is a device similar to the streak camera. The main difference is in the detector part. The basic schematic layout of the dissector is shown in Fig. 1 and a photo of the dissector vacuum tube is shown in Fig. 2.

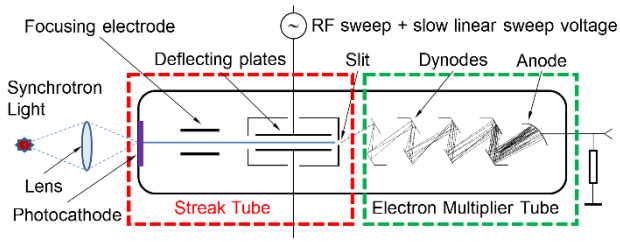

Figure 1: Dissector basic layout.

Figure 2: Dissector vacuum tube.

The synchrotron light pulse is focused on the photocathode and produces photoelectrons. These electrons are accelerated, focused and deflected transversely in a linear dependence of their longitudinal position. As a result, the vertical profile of the electron image at the slit plane will give directly the initial synchrotron light temporal profile, like in a streak camera. In the dissector a narrow slit cuts a small fraction of the electron image and this fraction of electrons is amplified in the electron multiplier tube. The amplified signal is measured by an oscilloscope or an ADC module.

Introducing a slow linear sweep voltage to the deflecting plates allows to scan the full electron image through the slit. The vertical profile is then measured as a function of time on the oscilloscope trace.

With a permanent light source like a flashlight the dissector can be calibrated: a typical signal from the dissector output will have the following appearance, Fig. 3.

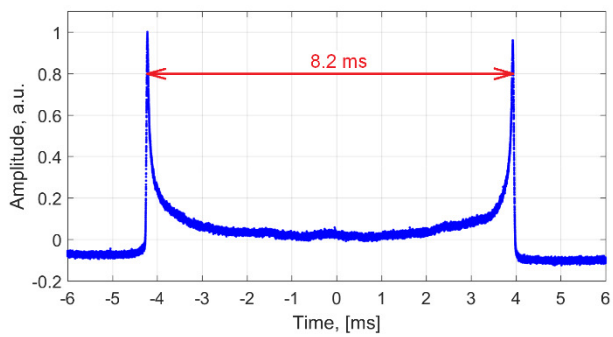

Figure 3: Dissector calibration. Signal from the dissector output for the permanent light source as an input.

† dmitriy.malyutin@helmholtz-berlin.de

ISBN: 978-3-95450-192-2 doi:10.18429/JACoW-IBIC2017-TU2AB1

INTEGRATED PHOTONICS TO THE RESCUE OF FEMTOSECOND BEAM DIAGNOSTICS

Franz X. Kärtner
Center for Free-Electron Laser Science, Deutsches Elektronen-Synchrotron and
Universität Hamburg, Germany
also at Research Laboratory of Electronics, Massachusetts Institute of Technology, Cambridge, USA

Abstract

Beam instrumentation has always been using results from neighbouring communities. Over the last 10 years, a number of beam instruments and systems have successfully adopted optical solutions, pushing performances from ps to fs, exploiting optical set-ups or photonic components. A major advance for beam diagnostics and instrumentation was the introduction of an optical pulsed timing distribution system using low jitter mode-locked lasers. An outlook on future advances using integrated optical components will be given. The ultra low jitter optical pulse trains already present in today's facilities may also lend themselves to advanced photonic analogto-digtial convertors. Progress towards such devices especially in a practical integrated format and first demonstrations are discussed.

INTRODUCTION

Modern photon science facilities, such as X-ray Free-Electron Lasers (XFEL) are becoming more and more combined accelerator and laser facilities. Lasers play an essential role starting from the photo injector laser creating the electron bunch in the gun, over a potential seed laser down to the experimental station, which usually houses a pump and/or probe lasers to excite the sample under investigation or probe it at optical frequencies. Over the last decade great progress has been made in synchronizing all lasers as well as critical microwave sources in such facilities within 10 fs rms using optical techniques. This is at least one order of magnitude better than possible with microwave techniques. In this tutorial, we first review the principles behind the optical synchronization techniques and show their further development to the sub-femtosecond level. Then we give an outlook how the low jitter properties of mode-locked lasers can be further harnessed to advance beam diagnostics at the example of photonic analog-to-digital conversion (ADC), which becomes only useful in an integrated optical package. This is made possible by exploiting the low jitter properties of mode-locked lasers. More precisely photonically assisted ADC, where optics is only used to eliminate aperture jitter and enable demultiplexing to lower rate channels, which then can be electronically digitized with the required number of bits may potentially enable a thousand fold enhancement in the resolution-sampling rate product when compared to current electronic ADCs.

JITTER OF MODE-LOCKED LASERS

The noise properties of mode-locked lasers were theoretically studied in the framework of soliton perturbation theory by Haus and Mecozzi in their seminal paper published in 1993 [1]. It successfully predicted the noise behavior of many mode-locked solid-state and fiber lasers [2–5]. Recently, it was discussed that the scaling of phase diffusion found in the Haus/Mecozzi model is generally applicable, independent from soliton effects [6]. Here, we present a simple intuitive picture of the timing jitter scaling when transitioning from the traditional case of a microwave oscillator generating a microwave signal at let's say 10 GHz to the case of a mode-locked laser generating an optical pulse train with 100-fs pulses [7].

Figure 1 shows the time-domain picture of microwave signals and optical pulse trains when emitted from an ensemble of microwave oscillators and mode-locked lasers, respectively. The zero crossings of the microwave signal and the pulse positions of the optical pulse train undergo a random walk due to the fundamental noise sources in the signal generation processes such as output coupling and compensation of cavity losses by gain. For the microwave oscillator, this fundamental noise is additive noise due to the losses of the passive cavity (internal as well as output coupling losses) and the reservoirs in the amplifying medium. Clearly, the noise contributions of gain and loss are uncorrelated. The noise energy added to the cavity field within a cavity decay time due to the losses is determined by the fluctuation-dissipation theorem, and it must be equal to kT in thermal equilibrium.

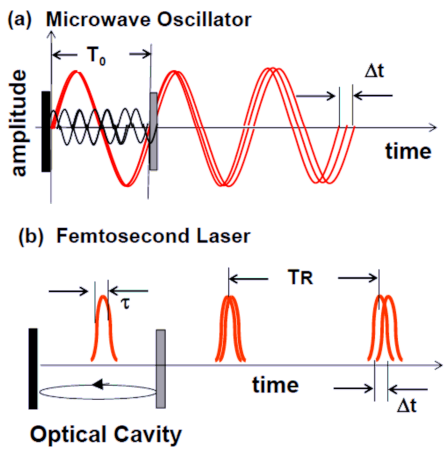

Figure 1: Random walk of (a) the phase in a microwave oscillator and (b) the pulse position in a mode-locked laser due to noise sources in the generation process [7]

ISBN: 978-3-95450-192-2 doi:10.18429/JACoW-IBIC2017-TU2AB3

SINGLE-SHOT LONGITUDINAL BEAM PROFILE AND TERAHERTZ DIAGNOSTICS AT MHz- TOWARDS GHz-RATES WITH HIGH-THROUGHPUT ELECTRONICS

M. Caselle*, L. Rota†, M. Balzer, M. Brosi, S. Funkner, B. Kehrer, M. J. Nasse, G. Niehues, M. Patil, P. Schönfeldt, M. Schuh, J. L. Steinmann, M. Yan, E. Bründermann, M. Weber, A.-S. Müller, Karlsruhe Institute of Technology (KIT), Karlsruhe, Germany
G. Borghi, M. Boscardin, S. Ronchin, Fondazione Bruno Kessler (FBK), Trento, Italy

Abstract

Accelerators with high bunch-repetition rates require high-throughput detector electronics to diagnose each individual bunch. KALYPSO with a 256-pixel detector line-array integrated in an fs laser-based electro-optical set-up allows longitudinal bunch profiling with sub-ps resolution as demonstrated at the storage ring KARA for single-bunch mode operation at 2.7 MHz and also at the European XFEL with a 4.5-MHz micro-bunch train. Improvements will enhance fs-time accuracy, reduce noise, and increase frame-rate. A custom front-end with an application-specific integrated circuit (ASIC) has been developed to operate with 10-MHz frame-rates at low noise. Several linear arrays with up to 1024 pixel and smaller pixel pitch were submitted for production. The development of a low-gain avalanche diode (LGAD) sensor will further improve the time resolution. Detector data is transmitted in the DAQ framework to external GPU-based clusters and processed in real-time at 7 GBytes/s with a few µs latency. For beam dynamics studies we also develop KAPTURE capable to analyze terahertz detector pulses at GHz-repetition rates. These developments open new possibilities in beam diagnostics of modern accelerators.

INTRODUCTION

The investigation of bunch-to-bunch interactions and beam dynamics during micro-bunching poses several challenges to both accelerator physicists and detector developers [1, 2]. The short bunch lengths and the dimension of substructures on the bunch profile impose tight requirements in the temporal resolution of detectors and front-end electronics technologies. Furthermore, if beam diagnostics setups require single-shot measurements on a turn-by-turn basis for long observation times, the front-end electronics and the Data Acquisition (DAQ) system must be able to sustain data rates of several GBytes/s.

At the Karlsruhe Institute of Technology (KIT), we are developing new experimental techniques and detector systems to meet the requirements of modern accelerators and enable ultra-fast beam diagnostics at high repetition rates. The development of new technological components is carried out in close cooperation with the accelerator facilities of KARA (Karlsruhe Research Accelerator) [3] and soon FLUTE (Fern-infrarot Linac- und Test-Experiment) [4], where the novel detectors systems are fully characterized and tested in a real accelerator environment, before their commissioning at other research centers.

In this paper we report about recent developments on two detector systems which have been developed for time-resolved beam diagnostics. The first system is KALYPSO, an ultra-fast camera developed for turn-by-turn longitudinal and transverse beam profile measurements. The second one is KAPTURE, a detector system which has been widely employed in the investigation of the fluctuations of terahertz (THz) Coherent Synchrotron Radiation (CSR) by micro-bunching instability (bursting). Both detectors have been integrated in a custom DAQ framework for real-time data processing based on Field Programmable Gate Arrays (FPGAs) and Graphic Processing Units (GPUs), in order to achieve high data throughput with low latency.

KALYPSO

KALYPSO (Karlsruhe Linear Array Detector for MHz repetition rate spectroscopy) is an ultra-fast 1D camera with a continuous frame rate of 2.7 Mfps [5]. KALYPSO has been originally developed for the upgrade of the Electro-Optical Spectral Decoding experimental setups at KARA and at the European XFEL. The front-end electronic components are mounted on the detector mezzanine card shown in Figure 1. Two types of semiconductor linear arrays can be employed, depending on the specific application. The first one is a Si microstrip sensor, originally developed at the Paul Scherrer Institute (PSI) for charge integrating X-ray

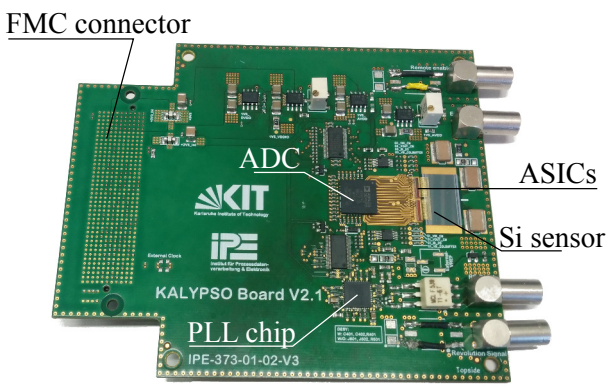

Figure 1: Photograph of the KALYPSO mezzanine board.

* Contact: michele.caselle@kit.edu
† Contact: lorenzo.rota@kit.edu

ISBN: 978-3-95450-192-2 doi:10.18429/JACoW-IBIC2017-TU3AB1

OPTICS MEASUREMENTS AT SuperKEKB USING BEAM BASED CALIBRATION FOR BPM AND BEAM BASED EXPERIMENT

Hiroshi Sugimoto, Yukiyoshi Ohnishi, Haruyo Koiso, Akio Morita, Masaki Tejima
KEK, Tsukuba, Japan

Abstract

SuperKEKB is an electron-position collider realizes a new luminosity frontier. The target luminosity is $8\times10^{35}\mathrm{cm}^{-2}\mathrm{s}^{-1}$. The initial beam commissioning started in February 2016 and operated until June 2016. Low Emittance Tuning (LET) is an important issue in the beam commissioning. The Beam-Based Calibration (BBC) scheme for Beam-Position-Monitor (BPM) has been applied in order to establish reliable beam measurement system. In the BBC, a response model among beam position, charge and output signals of the BPM electrodes are introduced to calibrate the relative gain of each electrodes. The gains are adjusted by least squares fitting so that the model reproduces the measured BPM signals. The Beam-Based Alignment (BBA) is also performed to determine the magnetic center of each quadrupole magnet. Using the BBC, the performance of the BPM system and optics correction has been successfully improved. After the series of the optics tuning and the BPM calibration, the vertical emittance of about 10 pm is achieved in the positron ring. This paper presents what we experienced during the beam commissioning focusing on the beam optics measurement and the BBC scheme for the BPM system.

INTRODUCTION

SuperKEKB [1] is an upgrade project of KEKB [2], which has been successfully finished at 2010 after about 10 years of operation with the world luminosity record of $2.1\times10^{34}\ \mathrm{cm}^{-2}\mathrm{s}^{-1}$. SuperKEKB consists of electron (HER) and positron (LER) storage rings with an injector linac and a newly constructed positron damping ring. The target peak luminosity is $8\times10^{35}\mathrm{cm}^{-2}\mathrm{s}^{-1}$.

The design concept is based on the nano-beam scheme [3], in which colliding beams are squeezed to nano-scale sizes in the vertical direction at the interaction point (IP). The key changes of machine parameters from KEKB are 2 times higher beam current, 1/20 times smaller vertical betatron function at the IP with a larger crossing angle. Low emittance beams are essential for the nano-beam scheme as well as squeezing the betatron function.

The SuperKEKB commissioning has stared after over 5 years of the upgrade work. The initial beam commissioning started on February 1st 2016 and finished on June 28th 2016. The final focus system to collide two beams is not installed in this commissioning period. The commissioning is devoted to the vacuum scrubbing and the setup of both hardware and software. The LET is the one of the most important issue. The nominal machine parameters in this commissioning period are listed in Table 1.

Table 1: Machine Parameters as of June 2016

Parameter	HER	LER	Unit
E	7	4	GeV
I	0.87	1.01	A
N_{bunch}	1576	1576	
ε_x	4.6	1.8	nm
α_p	4.44×10^{-4}	2.45×10^{-4}	
σ_E	6.30×10^{-4}	7.52×10^{-4}	
V_c	12.61	7.65	MV
U_0	2.43	1.76	MeV
τ_s	29	23	msec
σ_z	5.3	4.6	mm
ν_s	-0.0253	-0.0192	
ν_x	45.530	44.430	
ν_y	43.570	46.570	

Calibration of the BPM system is a key issue for better control of beam orbit and optics. We employ the BBC technique to the BPM system as at KEKB [4] . In BBC, both the relative gain of the BPM electrodes and the relative offset between the BPM electrical center and the magnetic center of a quadrupole are determined using measured BPM signals. In this paper we show the idea and results of BBC together with experience on the LET in the initial beam commissioning.

BPM SYSTEM

The SuperKEKB accelerator has about 900 quadrupole magnets, and BPM is attached to each quadrupole magnets for precise orbit control. Most of the BPMs installed in the HER are based on 1 GHz narrow-band system [5] reused KEKB since most of the vacuum chambers are same as those of KEKB. On the other hand, the vacuum chambers of LER are replaced with new ones with ante-chamber structure, and the cutoff frequency is lower than 1 GHz in SuperKEKB. Therefore a newly developed narrow-band system is installed in the LER.

TheBPM system is successfully used in the beam tuning with an averaging mode of 0.25 Hz. In addition to closed-orbit measurement, more than 100 BPMs can be used as gated turn-by-turn BPMs. The gated turn-by-turn BPM system was very helpful in the first injection tuning at the very early stage of the beam commissioning. Although optics measurement with turn-by-turn beam position data was performed in the initial commissioning and some results are already obtained, we concentrate on the BBC and beam measurement based on closed orbit analysis in this paper.

ISBN: 978-3-95450-192-2 doi:10.18429/JACoW-IBIC2017-TU3AB3

DIGITAL SIGNAL PROCESSING TECHNIQUES TO MONITOR BUNCH-BY-BUNCH BEAM POSITIONS IN THE LHC FOR MACHINE PROTECTION PURPOSES

J. Pospisil*, O. Bjorkqvist, A. Boccardi, M. Wendt, CERN, Geneva, Switzerland

Abstract

This paper presents the development of an upgrade to the beam position interlock system for the Large Hadron Collider (LHC) at the European Organization for Nuclear Research (CERN). The beam orbit at the beam dump kicker is continuously monitored by 16 beam position monitors that are part of the machine protection system. In case of unacceptable orbit movement the system has to trigger the beam abort immediately to prevent damage to the machine. An upgrade of the present system is underway with the aim of handling a larger dynamic range of bunch intensities, and coping with different bunch time structures (both the standard bunch spacing of 25 ns and special doublet bunches spaced by 5 ns).

The proposed architecture combines the analogue signals from opposite pickup electrodes on a single read-out channel, and stretches it with a delay-line based comb-filter. The resulting signal, covering a dynamic range of 60 dB, is digitized at 3.2 GSa/s and processed inside a Field-programmable Gate Array (FPGA) to extract a position value. Different signal processing techniques are compared on simulated ideal beam signals, and preliminary results of a prototype installation is presented.

INTRODUCTION

The interlock Beam Position Monitor (BPM) system is used to protect the aperture of the two LHC beam dump channels (one for each beam) by ensuring that the position of the circulating beam never exceeds what is considered to be a safe value whenever a beam dump is requested. It continually monitors the beam position of all bunches and will itself trigger a beam dump if the beam position lies outside a ±3.5 mm window for a predefined number of bunches over a predefined number of turns (linked to expected damage thresholds with respect to beam intensity and energy). It comprises 16 stripline BPMs, and at present is read-out using the standard *Wide-Band Time Normalizer* (WBTN) LHC position system electronics combined with dedicated FPGA firmware [1, 2]. This system performs bunch-by-bunch position measurements with a nominal resolution ranging from 150 µm to 50 µm, while covering a respective range of bunch intensities from 2×10^9 to 1.5×10^{11} charges per bunch (cpb). This is achieved using two sensitivity settings, one from 2×10^9 to 5×10^{10} cpb and the other from 2×10^{10} to 1.5×10^{11} cpb. The current system has several downsides:

- The need to switch sensitivity means that the system cannot effectively operate with bunches of very different intensity in the machine at the same time.
- The system suffers from performance degradation due to temperature drifts.
- The limited flexibility in terms of beam filling patterns, requiring a minimum bunch-to-bunch spacing of 25 ns.

This latter point is a major limitation for beam scrubbing runs, when the LHC is filled with 5 ns so-called "doublet bunches", i.e. a pair of bunches spaced by 5 ns, themselves spaced by a 25 ns from the next pair [3]. This operational mode and the other limitations mentioned call for a new read-out system for the LHC interlock BPMs.

SINGLE CHANNEL DIGITIZATION

In the proposed architecture shown in Fig. 1, the signals from both electrodes are time multiplexed onto a single read-out channel using a 12.5 ns delay transmission-line, Delay Multiplex Single Path Technology (DMSPT), where some minimum signal conditioning is applied before the conversion to the digital domain. This analog RF signal conditioning is limited to a delay-line based band-pass comb filter, an anti-aliasing low-pass filter and gain/attenuator stages. Most of the processing then takes place in a subsequent FPGA.

The two main advantages of this architecture are the direct digitization, which allows doublet bunches to be processed, and the single channel read-out scheme, which reduces beam position offset effects caused by asymmetries in the signal processing electronics [4–6].

Analog Signal Processing

The single bunch response from a stripline electrode is a bipolar pulse, which in the case of the LHC is, to first approximation, a single 500 MHz sinusoidal oscillation of ~2 ns duration. A band-pass comb filter, operating at the same central frequency combines four time-shifted replicas of the input signal from opposite electrodes to generate two ~8 ns sine-wave like bursts of four oscillation periods at 500 MHz. This can be seen in Fig. 2a with results of a beam measurement performed in the Super Proton Synchrotron (SPS) on a single bunch. In this case the ADC was running at 3.2 GSa/s giving up to 30 usable samples per electrode to reconstruct the signal amplitudes.

In the case of doublet bunches only some parts of each 8 ns bursts are unaffected by the doublet structure leaving only ~ 10 samples for signal reconstruction, see Fig. 2b.

* j.pospisil@cern.ch

ISBN: 978-3-95450-192-2 doi:10.18429/JACoW-IBIC2017-TUPCC01

CURRENT STATUS OF CVD DIAMOND BASED BEAM DETECTOR DEVELOPMENTS AT THE S-DALINAC*

A. Rost[1†], T. Galatyuk[12], J. Pietraszko[2]
[1]Institut für Kernphysik, TU Darmstadt, Darmstadt, Germany
[2]GSI Helmholtzzentrum für Schwerionenforschung GmbH, Darmstadt, Germany

Abstract

In this contribution a field-programmable gate array (FPGA) based read-out concept for diamond based beam monitoring detectors will be introduced. Furthermore for research and development of diamond based detectors a test setup will be installed at the Superconducting Darmstadt Electron Linear Accelerator (S-DALINAC) of TU Darmstadt. The preparatory work, with particular focus on beam transport simulations will be shown.

INTRODUCTION

For future experiments with the HADES [1] and CBM [2] detectors at the FAIR facility in Darmstadt, a radiation hard and fast beam detector is required. On the one hand the detector should handle high current beams, especially the CBM experiment plans to operate at up to 10^9 ions/s. On the other hand the detector has to perform precise T0 measurements ($\sigma_{T0} < 50$ ps) and should offer beam monitoring capabilities. These tasks can be fulfilled by utilizing single-crystal Chemical Vapor Deposition (scCVD) diamond based detectors. This material is well known for its radiation hardness and high drift velocity of both electrons and holes, making it ideal not only as Time-of-Flight (ToF) detectors placed in the beam but also as luminosity monitors. Challenging is the detection of minimum-ionizing particles (MIPS) traversing the diamond detector. The very small induced charges and expected high rates require special emphasis on the read-out electronics. The developed technology of producing mono-crystalline diamond material, which is almost free of structural defects and chemical impurities and thus provides very high charge collection efficiency, allows for building detectors for MIP based on single-crystalline diamond material. With the help of stripped read-out electrodes or by arranging several diamond detectors in a mosaic, a position information can be obtained for beam monitoring purposes. An example of such a diamond based mosaic detector is shown in Fig. 1.

TRB3 BASED BEAM MONITORING SYSTEM

A read-out concept for diamond based beam monitoring and diagnostic detectors is currently under development. It will be based on the already well established TRB3 (Trigger and readout board - version 3) platform [3, 4], developed at GSI Helmholtzzentrum für Schwerionenforschung in Darmstadt. The board provides 260 high precision (RMS < 12 ps) multi-hit FPGA-TDCs and serves as a flexible data acquisition system (DAQ). The available comprehensive software package allows on-line monitoring capabilities including basic analysis. A large variety of front-end electronics is available in order to extend its functionality. One of those front-end boards is the PADIWA discriminator board. It is designed to discriminate 16 detector signals. Due to its flexible analog input stage, it is possible to adjust it to a wide range of detector signals i.e. different Photomultiplier (PMT) types. A photography of the PADIWA board and the simplified read-out scheme is shown in Fig. 2. The input signals are amplified and afterward discriminated by the low-voltage differential signaling (LVDS) input buffers of an FPGA. Thresholds can be set via pulse width modulation in combination with a low pass filter. The arrival time and the time-over-threshold (ToT) is encoded in the leading edge and the width of a digital pulse. The digital pulse is afterwards sent via differential lines to the TRB3 for time measurements.

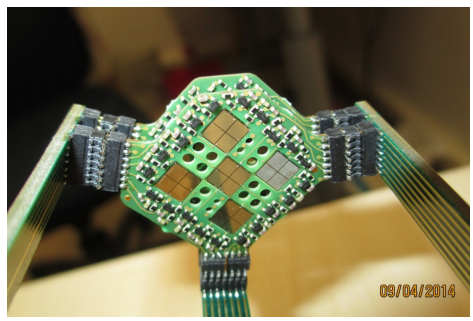

Figure 1: Diamond based mosaic detector which was located in front of the HADES target in a pion production beam time. An total area of 14 mm × 14 mm was covered. The first transistor based pre-amplification stage is located very close to the diamond material.

The read-out concept was already successfully employed to read out the Hodoscope detector in the HADES experiment, which is located at GSI Helmholtzzentrum für Schwerionenforschung (Darmstadt). The Hodoscope was placed behind the HADES spectrometer and was mainly used for beam-monitoring purposes during the beam-tuning. It consists of 16 stacked plastic scintillator rods with sizes of 10 mm × 5 mm × 100 mm. The scintillation light produced in the rods is read out from both sides by Hamamamtsu R3478 PMTs. The PADIWA-AMPS [5] front-end board (which is similar to the PADIWA board, with additional

* Work supported by the DFG through GRK 2128 and VH-NG-823
† a.rost@gsi.de

ISBN: 978-3-95450-192-2 doi:10.18429/JACoW-IBIC2017-TUPCC03

ONLINE LONGITUDINAL BUNCH PROFILE AND SLICE EMITTANCE DIAGNOSTICS AT THE EUROPEAN XFEL

Ch. Gerth*, B. Beutner, O. Hensler, F. Obier, M. Scholz, M. Yan†
Deutsches Elektronen-Synchrotron DESY, Hamburg, Germany

Abstract

The longitudinal current profile and slice emittance are important bunch parameters for the operation of an X-ray free-electron laser. At the European XFEL, dedicated diagnostic sections equipped with transverse deflecting RF structures (TDS) have been installed for the control and optimisation of these parameters. Travelling-wave TDS in combination with fast kicker magnets and off-axis screens allow for the study of individual bunches without affecting the other bunches in the super-conducting linear accelerator which can generate bunch trains of up to 2700 bunches at 4.5 MHz within 600 microsecond RF pulses at a repetition rate of 10 Hz. The measurement of the slice emittance is realised in a static F0D0 lattice equipped with four individual screen stations.

Variations of the longitudinal bunch profile or slice emittance along the bunch train may lead to degraded FEL performance for parts of the train which reduces the effective available number of bunches for FEL operation. By gradually adjusting the timing, individual bunches along the bunch train can be measured in order to optimise the overall beam parameters for all bunches in the train. In this paper, we describe in detail the diagnostic concept and present first measurement results of the projected and slice emittance along the bunch train.

INTRODUCTION

The European XFEL, which is currently under commissioning, will deliver ultra-short X-rays in the photon energy range 0.25 keV to 25 keV [1]. The superconducting linear accelerator that will drive 3 FEL undulator beamlines will generate beam energies of up to 17.5 GeV. As is illustrated in Fig. 1, the RF accelerating field is pulsed at a frequency of 10 Hz with a flat-top duration of up to 600 µs, in which a train of electron bunches is accelerated. The bunch repetition rate can be up to 4.5 MHz (equal to a bunch spacing of 220 ns), which corresponds to a maximum of 2700 bunches per bunch train. In future, it is envisioned to operate the accelerator with constant bunch filling patterns that are advantageous in terms of operation stability. The photon pulse pattern can be chosen by sending unwanted electron bunches with fast kicker magnets into a local dump upstream of the FEL undulator beamlines.

Variations during the RF flat-top duration of either the laser pulse properties of the photo-cathode laser or the RF parameters of the accelerator modules in the injector may result in variations of beam matching or emittance of the bunches in the bunch train. This in turn may lead to substantial variations along the bunch train of the photon pulse energies of the X-rays that are delivered to the user experiments. Hence, there is a strong demand for diagnostic techniques with which electron bunch parameters such as the longitudinal current profile or slice emittance can be measured along the bunch train. This has been realised by utilising a transverse deflecting RF structure (TDS) in combination with kicker magnets and off-axis screens.

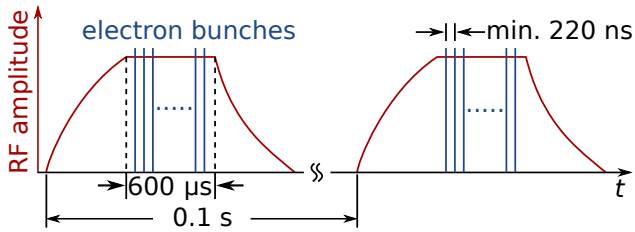

Figure 1: RF timing structure and electron bunch pattern of the European XFEL.

The RF field of the TDS induces a time-dependent transverse deflection of the electrons of one bunch in the bunch train by which the longitudinal bunch shape is transformed to the transverse plane. A fast kicker magnet downstream of the TDS is then used to deflect this bunch onto an off-axis screen without affecting the remaining bunches in the bunch train. The diagnosed bunch is taken out of the bunch train before the FEL undulators while the remaining bunches continue for the generation of FEL radiation. By utilising four kicker magnets with four off-axis screens in a static F0D0 lattice, the longitudinal bunch profile and slice emittance can be measured. Finally, these bunch parameters can be measured along the bunch train by properly adjusting the timing of the TDS, kicker magnets and camera systems of the screen stations. In this paper, we present the results of projected and slice emittance measurements obtained in the injector section of the European XFEL.

DIAGNOSTIC SECTION

Three dedicated beamline sections equipped with TDS have been designed for the measurement of the longitudinal profile and slice emittance as well as the longitudinal phase space [2]. A schematic layout of the TDS diagnostics sections, which are located downstream of the laser heater system in the injector section and downstream of the second and third bunch compressor chicane, is depicted in Fig. 2. Each section comprises a TDS, four kicker magnets, four screen stations with off-axis and on-axis screens, one dipole

* christopher.gerth@desy.de
† Current address: Karlsruher Institut für Technologie, 76131 Karlsruhe, Germany, minjie.yan@kit.edu

ISBN: 978-3-95450-192-2 doi:10.18429/JACoW-IBIC2017-TUPCC05

CONCEPT FOR THE MINIMIZATION OF THE ELECTRON BUNCH ARRIVAL-TIME JITTER BETWEEN FEMTOSECOND LASER PULSES AND ELECTRON BUNCHES FOR LASER-DRIVEN PLASMA WAKEFIELD ACCELERATORS*

S. Mattiello†, Andreas Penirschke, Technische Hochschule Mittelhessen, Friedberg, Germany
Holger Schlarb, DESY, Hamburg, Germany

Abstract

Using laser driven plasma wakefield accelerators, the synchronization between electron bunch and the ultrashort laser is crucial to obtain an stable acceleration. In order to minimize the electron bunch arrival-time jitter, the development of a new shot to shot feedback system with a time resolution of less than 1 fs is planned. As a first step, stable Terahertz (THz) pulses should be performed by optical rectification of high energy femtosecond laser pulses in a nonlinear crystal. It is planed that the generated THz pulses will energy modulate the electron bunches shot to shot before the plasma to achieve the time resolution of 1fs. The selection of the nonlinear material is a critical aspect for the development of laser driven THz sources. In this contribution we investigate systematically the influence of the optical properties, and in particular adsorption coeffient, of lithium niobate crystal on the conversion efficiency of the generation of THz pulses.

INTRODUCTION

The investigation of new concepts for accelerator technology is a challenging task for science as well as society. Particle accelerators allow to achieve crucial new discoveries, e.g. the Higgs boson or the strong interacting Quark Gluon Plasma. On the other side, they have several applications in material science, biology, medicine and industry. The size of conventional accelerators is extremely large and costly. Therefore, new concepts as well as the realization of compact and less expensive accelerators are needed. Plasma-based particle accelerators driven by either lasers or particle beams allow to overcome these problems because of the extremely large accelerating electric fields. This method is known as plasma wakefield acceleration (PWA). The period of these fields is in the range of 10 fs to 100 fs. In the case of laser driven plasma wakefield accelerators a stable synchronization of the electron bunch and of the plasma wakefield in the range of few femtoseconds is needed in order to optimize the acceleration.

Consequently, the central aim is the minimizing the electron bunch arrival-time jitter. In order to achieve this goal we are developing a new shot to shot feedback system with a time resolution of less than 1 fs. As a first step, stable Terahertz (THz) pulses should be performed by optical rectification of high energy laser pulses in a nonlinear crystal. With the generated THz-pulses an energy modulation of the electron bunch can be performed, in order to achieve the required resolution. In this contribution we focus on the first step of the feedback system, i.e. the generation of THz pulses.

Intense ultrashort terahertz pulses are an important tool, not only for our planed feedback system, but also for many new applications, in state solid physics, spectroscopy, chemistry and biology, for security purposes and point-to point communications [1]. Therefore, the development of robust and efficient strong THz pulses is strongly needed. Consequently, the main focus is to maximize the conversion efficiency of the THz generation defined by [2],

$$\eta = \frac{F_\mathrm{T}}{F_\mathrm{p}}, \tag{1}$$

where F_p and F_T indicate the pump and the THz fluence respectively. From this point of view the optical rectification (OR) is one of the best method for this purpose and the selection of the nonlinear material is a critical aspect. Because of its high nonlinear optic coefficient, is lithium niobate ($LiNbO_3$, LN) a suitable material for THz generation, by using tilted-pulse-fronts (TPF) as well as a periodically poled crystal (PPLN) [4]. In general, three main factors lead to increase the efficiency of the THz generation: *(i)* longer pump pulses, *(ii)* large pump size and energy, and *(iii)* cooling of the crystal [3].

Evidently, the first two factors are fixed by the laser properties. Therefore, although it has been shown that longer (1.3 ps) pulses lead to a sizeable enhancement about 2.5% of the efficiency, these factors cannot be modified in our setup [3]. Indeed, for our feedback system only the third point can play a significant role. In fact the cooling of the crystal reduce the value of the intensity adsorption coefficient of the THz radiation $\alpha_\mathrm{T}(\Omega)$, which leads to the suppression of η. The optical properties of the material and in particular of $\alpha_\mathrm{T}(\Omega)$ are important not only for the optimization of the efficiency, but also for its stability. Therefore, in this contribution we give a first estimation of the influence of refractive index $n(\Omega)$ and adsorption coefficient, on the efficiency. Firstly, we present the models for the description of the THz generation as well as for the calculation of the optical properties of the material. Therefore we investigate in this framework the influence of the optical properties of lithium niobate crystal on the conversion efficiency of the generation of THz pulses. The Conclusions finalize this work.

* The work of S. Mattiello is supported by the German Federal Ministry of Education and Research (BMBF) under contract no. 05K16ROA.
† stefano.mattiello@iem.thm.de

ISBN: 978-3-95450-192-2 doi:10.18429/JACoW-IBIC2017-TUPCC06

INJECTION AND BUNCH LENGTH STUDIES AT THE BESSY II STORAGE RING

D. Malyutin†, T. Atkinson, P. Goslawski, A. Jankowiak, A. Matveenko, M. Ries,
Helmholtz-Zentrum Berlin, Berlin, Germany

Abstract

To improve the injection process into the BESSY II storage ring and allow for high injection efficiencies in all operational modes, one needs to know the development of the bunch length during acceleration in the booster synchrotron up to the extraction point. It will become even more important for the future BESSY VSR upgrade, when high efficiency injection into much shorter RF buckets needs to be guaranteed.

Measurements of bunch phase and energy during injection in the storage ring are presented. Studies of the bunch length evolution during the energy ramp of the booster synchrotron are described. Results are compared with numerical simulations and discussed.

INTRODUCTION

To provide new possibilities for time resolved experiments at the synchrotron light source BESSY II an innovative upgrade scheme to store both long and short bunches simultaneously in the storage ring is under realisation: the Variable pulse length Storage Ring BESSY VSR [1].

The most prominent aspect with respect to the injector is the evidence, that the bunch length on injection into the storage ring needs to be reduced from its present value, by at least a factor two in order to keep the by radiation protection required high injection efficiencies of above 90 % on an 4 h average. The problem arises from the large difference in the bunch lengths on injection and the reduced longitudinal bucket length (phase acceptance) due to the proposed VSR [2] technique as depicted in Figure 1.

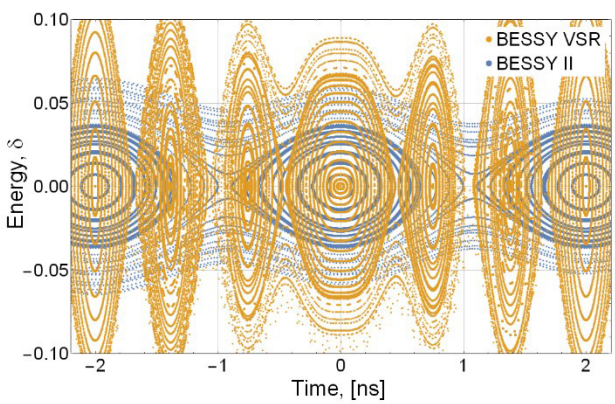

Figure 1: Longitudinal phase space comparison between BESSY II (blue) and the alternating bucket length scheme of BESSY VSR (yellow).

Presently the bunch length of the injected beam on injection into the storage ring is approximately 60 ps FWHM. Such bunch lengths will unfortunately not allow the required high efficient injection into the short BESSY VSR buckets. An upgrade of the injection systems to produce shorter bunches is foreseen.

Today there is no diagnostics at the BESSY II booster synchrotron to directly measure the bunch length during the energy ramp. One possible solution is to extract the beam during the ramp of the booster and to measure the bunch length just after injection into the storage ring. This can be achieved by reducing the energy of the storage ring, as well as the transfer line, and extracting the bunch earlier or later from the booster (with respect to a nominal energy). Then, a synchrotron light from a storage ring dipole magnet is used to get a bunch length with a dual-sweep synchroscan streak camera.

BUNCH LENGTH EVOLUTION

Figure 2 shows the evolution of the bunch length, the bunch energy and cavity voltage from elegant [3] simulations during the acceleration stage of the 10 Hz booster cycle.

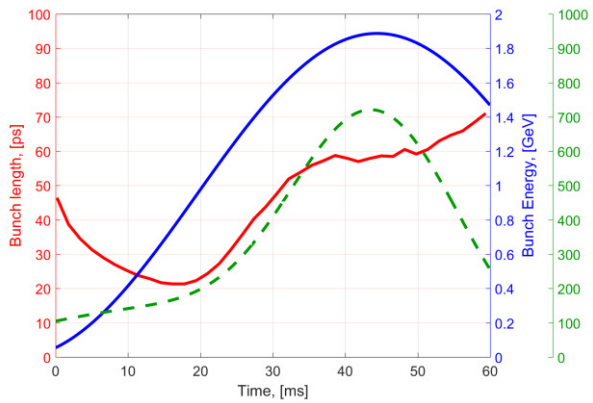

Figure 2: Simulation of the bunch length as a function of time over the 10 Hz booster cycle, the red curve, and the bunch energy, the blue curve and the cavity voltage the green dashed curve.

The beam energy is increased from 50 MeV on injection to 1.7 GeV at 35 ms on extraction. The simulation starts with parameters of the injected beam as measured during the site acceptance tests of the injector LINAC. The peak voltage in the cavity is set to 720 kV, the nominal values for booster operation. The voltage pedestal is none zero, so that the phase and with it the synchrotron frequency are also time dependent to match recent measurements in the booster.

The variation of the bunch length over the booster ramp is due to its inherent energy dependent parameters. The dy-

† dmitriy.malyutin@helmholtz-berlin.de

ISBN: 978-3-95450-192-2 doi:10.18429/JACoW-IBIC2017-TUPCC08

IMPROVING THE SENSITIVITY OF EXISTING ELECTRO-OPTIC SAMPLING SETUPS BY ADDING BREWSTER PLATES: TESTS OF THE STRATEGY AT SOLEIL

C. Szwaj, C. Evain, M. Le Parquier, S. Bielawski*
PhLAM, Université Lille 1, France
J.-B. Brubach, L. Manceron, M.-A. Tordeux, M. Labat, P. Roy,
Synchrotron SOLEIL, Gif-Sur-Yvette, France

Abstract

For improving the sensitivity of electro-optic sampling (EOS), several techniques are used. Operation of the set of polarizing elements "close to extinction" is a technique used routinely for obtaining high responsivity (i.e., a large output signal for a given input electric field). This technique is widely used for monitoring electron bunches in linear accelerators and FELs. We show that a simple modification of these EOS systems enables to increase further the SNR, by cancelling out the laser noise. The idea is to introduce a set of Brewster plates, following the idea Ahmed, Savolainen and Hamm [1] in the EOS path, and performing balanced detection. We present detailed tests of this type of upgrade on the PhLAM-SOLEIL EOS system, destined to studies of THz CSR pulse dynamics [2, 3].

INTRODUCTION: CLASSICAL SNR IMPROVEMENT METHODS AND THEIR LIMITATIONS

For recording ultrafast electric field transient in single-shot, a particularly efficient method consists in using the spectrally encoded Electro-Optic Sampling (EOS) [4,5,5–8]. The electric field transient is imprinted onto a chirped laser pulse, by electro-optic modulation. Then the output pulse is analyzed using a single-shot spectrum analyzer.

High Responsivity Using Near-Extinction EOS Setups

In order to reach high SNR, a popular way consists in operating the setup in a configuration known as *near extinction* EOS [9, 10] (Fig. 1a). In these conditions, an important limit to the SNR comes from the shot-to-shot fluctuations of the laser, which can be well above the shot-noise limit. This is particularly the case for laser systems with a fiber amplifier, which is known to add Amplified Spontaneous Emission noise.

Noise Cancellation Using Balanced Detection

Laser noise cancellation is possible using balanced detection [11–14] (Fig. 1b). However the combination with near-extinction (for reaching high responsitivety) is not trivial to realize.

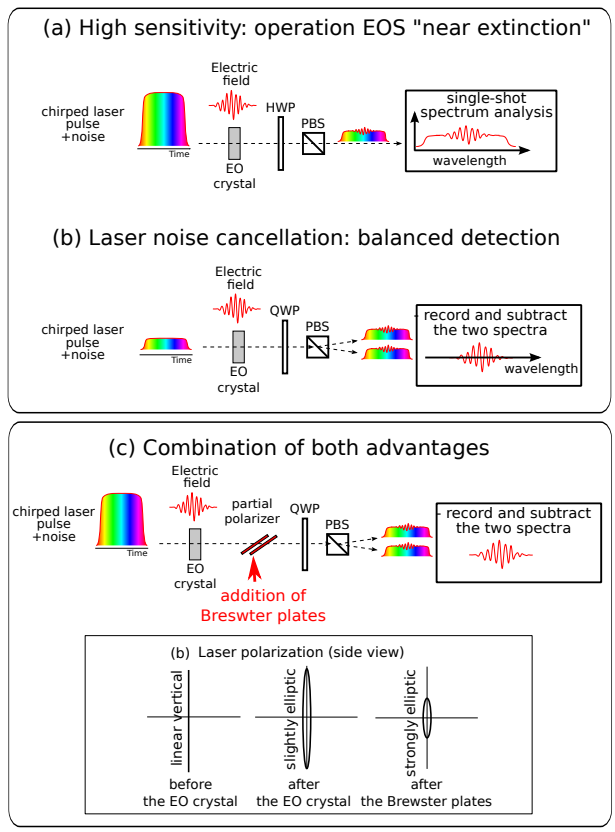

Figure 1: (a) and (b): classical EOS setups. In (a) operation near extinction can provide high responsivity (defined as the detected signal per unit electric field in the EO crystal). The balanced detection scheme (b) provides laser noise cancellation capability, but has a moderate responsivity. The EO setup (c) provides both advantages, i.e., high responsivity and laser noise cancellation. Lower inset represents the polarization states of the light in the setup.

PRINCIPLE OF THE METHOD

In a different context (scanned EOS), Ahmed Savolainen and Hamm demonstrated that the advantages of (i) near-extinction and (ii) balanced detection can be associated in a very simple way. The principle consists of introducing a partial polarizer (e.g., a set of Brewster plates) in a classical balanced detection EOS system, between the EO crystal and the polarizer [1, 1]. We tried to test this strategy in the case of single-shot spectrally-encoded detection. The basic principle is represented in Figure 1c.

* serge.bielawski@univ-lille1.fr

ISBN: 978-3-95450-192-2 doi:10.18429/JACoW-IBIC2017-TUPCC09

ELECTRON BUNCH PATTERN MONITORING VIA SINGLE PHOTON COUNTING AT SPEAR3*

B. Xu, E. Carranza, A. Chen, S. Condamoor, A.S. Fisher and J.Corbett †
SLAC National Accelerator Laboratory, Menlo Park, CA, 94025, USA

Abstract

In recent years the synchrotron radiation program at SPEAR3 has moved toward laser/x-ray pump-probe experiments which utilize a single timing 'probe' bunch isolated by a ± 60 ns dark space on either side. In order to quantify bunch purity in the region near the timing bunch, time-correlated single photon counting is used. In this paper we investigate methods to optimize the fill pattern and resolve satellite bunches in the region near the timing bunch. Integration of the Matlab measurement and data processing software into EPICS is reported.

INTRODUCTION

SPEAR3 is a 234 m circumference electron storage ring with a 476MHz RF frequency. The electron beam can be injected into any of 372 RF buckets separated by 2.1 ns. As shown in Fig. 1, the 500 mA electron beam is configured in four electron bunch 'trains' each containing 70 bunches. The 30 ns gap between bunch trains allows for ion clearing to optimize beam lifetime. By design, the bunches in the four bunch trains contain equal charge. The single isolated timing bunch seen to the right is separated by ±60 ns dark space for time-resolved pump/probe experiments. With a 9 hr beam lifetime, the 1% beam loss is replenished every 5 min by a 10 Hz injector delivering single-bunches with ~50 pC charge/pulse.

For the injection process, a linear accelerator (linac) with a thermionic cathode gun transfers 120 MeV electrons to a booster ring which by design accelerates a single bunch of charge to 3 GeV prior to injection into SPEAR3. To avoid charge spill, the timing of each charge transfer process must be accurate to the sub-nanosecond level.

A visible-light diagnostic beam line on SPEAR3 is used to measure beam cross section, bunch length and injected beam dynamics. Time-Correlated Single Photon Counting (TCSPC) was added to monitor electron charge stored in each bunch [1-7]. With TCSPC, the bunch charge can be resolved with high dynamic range. The TCSPC data is used to monitor satellite bunches adjacent to the pump-probe timing bunch and to monitor evenness of charge in the bunch trains. The TCSPC system reported here uses a combination of Matlab for data acquisition and processing and EPICS for control. In this paper we report on recent developments with the data processing algorithm and the software environment.

* Work sponsored by U.S. Department of Energy, Office of Science, under Contract DE-AC02-76SF00515 and the DOE SULI.

† corbett@slac.stanford.edu

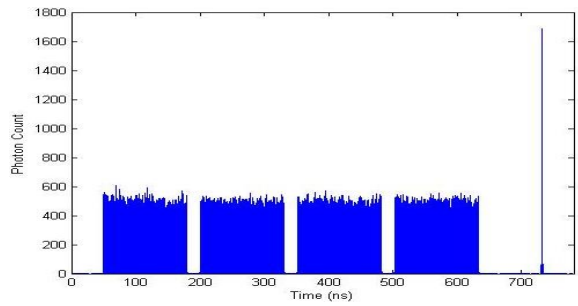

Figure 1: SPEAR3 timing bunch pattern with 4 bunch trains and 1 timing bunch (tall spike at right).

SPEAR3 TCSPC SYSTEM

Time Correlated Single Photon Counting is a slow yet accurate measurement process that can provide the dynamic range needed to detect low-charge bunches. The measurement depends on the fact that the rate of SR photon emission is proportional to the total charge in each bunch, and produces much higher resolution compared to conventional techniques such as oscilloscope sampling of a beam position monitor.

The SPEAR3 TCSPC detection system uses a PMA Hybrid single-photon detector with a PicoHarp300 pulse detector, both manufactured by PicoQuant [8]. The PicoHarp300 operates by detecting the arrival time of single photon emission events relative to a trigger, in this case the periodic beam revolution clock. For SPEAR3, the beam revolution time is 781 ns and the corresponding revolution rate is f=c/L=1.28 MHz. At each trigger event, the first photon arrival event is recorded in one of 65535 discrete 16 ps time bins which is sufficient to resolve the 2.1 ps bunch separations. The accumulation of counts in each time bin integrated over the total measurement interval generates a histogram of the electron beam bunch pattern in time.

Since the PicoHarp300 only records the first photon arrival event each trigger cycle, it is important to reduce the single photon arrival rate to avoid measurement pileup [5, 9]. An average photon arrival rate of one count per every 10 beam revolution triggers provides high accuracy.

SATELLITE ELECTRON BUNCHES

In practice, small inaccuracies in the charge acceleration process can cause electrons to be captured in RF buckets adjacent to the target bunch, a process referred to charge spill. These 'satellite' bunches can grow over time with repeated topup cycles.

The plot in Fig. 2 shows TCSPC data expanded around the timing bunch after approximately 10 days of periodic

ISBN: 978-3-95450-192-2 doi:10.18429/JACoW-IBIC2017-TUPCC10

TIME-RESOLVED ELECTRON-BUNCH DIAGNOSTICS USING TRANSVERSE WAKEFIELDS*

J. Wang†, D. Mihalcea[1], P. Piot[1]
Department of Physics, Northern Illinois University, DeKalb, IL 60115, USA
[1]also at Fermi National Accelerator Laboratory, Batavia, IL 60510, USA

Abstract

The development of future free electron lasers (FELs) requires reliable time-resolved measurement of variable ultrashort electron-bunchs characteristics. A possible technique is to streak the bunch in the transverse direction by means of time-dependent external fields. In this paper we explore the possible use of self-generated electromagnetic fields. A passive deflector, consisting of a dielectric-lined waveguide, is used to produce wakefields that impart a time-dependent transverse kick to the relativistic electron bunch passing off-axis. We investigate the technique and its performances and explore its possible application at the Fermilab Accelerator Science and Technology (FAST) facility.

INTRODUCTION

Modern physics accelerators sever a variety of science from high-energy physics and nuclear physics to radiation sources and electron microscopes. Conventional methods used in the preparation of beams for accelerator application often cannot keep pace with the new demands, thus, new approaches continue to emerge. Techniques to tailor the electron beam phase space distribution by means of external and internal fields have come to play an increasingly important role in linear accelerators over the last decade. Precise control of beam phase space distribution is foreseen for beam-driven advanced acceleration techniques and for novel radiation sources including free-electron lasers and THz radiators. A wide of techniques has been developed to utilize the fields to influence the beam distribution. One of the manipulations operates within one degree of freedom, e.g., those based on the use of external and internal fields to control the distribution in one of three 2D phase-spce planes: $(x - p_x)$, $(y - p_y)$, $(z - p_z)$.

In this paper, the self-generated wakfields, as the internal fields, is used as a tool to provide the transverse kick on the beam so as to introduce a correlation between time and the transverse beam distribution. The first part of this paper is to review the transverse equations of motion in the presence of wakefield and explore the use of a passive deflector to provide time-dependent deflecting kick to a relativistic electron bunch. Such a capability could enable the development of new passive (and cheap) beam diagnostics [1]. The passive deflector does not need to be powered and it is easier to be manufactured compared to a rf transverse deflecting structure, thus, resulting in a considerable cost saving. The passive deflector is self-synchronized with the beam by design, being the wakefield excited by the bunch itself when it travels through a dielectric tube. Thus, we could use it to perform time-resolved measurements of a relativistic electron bunch based on the self-transverse wakefield interaction of the beam itself passing off-axis through a dielectric-lined tube and reconstruct the beam profile from the resulting image of the streaked beam on the downstream profile monitor. The second part of this paper is to explore some possible ways to reconstruct the profile of the beam as a way of beam diagnostics.

* Work supported by the DOE award DE-SC0011831 to NIU. Fermilab is operated by the Fermi Research Alliance, LLC for the DOE under contract DE-AC02-07CH11359.
† Email:wangjinlong97888@gmail.com

BASIC EQUATIONS

We first introduce the coordinate system under consideration and take an electron propagating along an accelerator beam line with applied external fields. The transverse coordinates are x and y while the longitudinal laboratory coordinate along the straight beamline is z. In order to quantify the bunch dynamics, it is often convenient to introduced $\zeta(t) \equiv z(t) - c\int_0^t \beta(t')dt'$ where ζ represents the axial position of an electron with respect to the bunch centre ($\zeta = 0$) at the time t. Since the beam dynamics also involves the momenta we introduce p_i the conjugate momenta associated to the spatial coordinates $i = x, y, \zeta$ and note that for a bunch $p_\zeta \gg (p_x, p_y)$. For convenience we also introduce the angular divergence as $x' \equiv \frac{p_x}{p_z}$ and $y' \equiv \frac{p_y}{p_z}$. Finally we introduce the relative momentum spread as $\delta \equiv \frac{p}{\langle p \rangle}$ where $p^2 = p_x^2 + p_y^2 + p_z^2$.

In order to describe the dynamics of a bunch in presence of transverse wakefield it is often useful to describe the bunch as an ensemble of axial slices. The transverse position of these slices at a given position z along the beamline is a function of ζ and parameterized as $\boldsymbol{x}(\zeta, z)$ where the vector $\boldsymbol{x} \equiv (x, y)$. Considering the case of a transverse wakefield giving rise to the transverse Green's function $w_\perp(\zeta)$ along, e.g., the x direction we can write the corresponding transverse horizontal force as

$$F_x(\zeta, z) = e^2 \int_\zeta^\infty d\zeta' \rho(\zeta') w_\perp(\zeta - \zeta') x(\zeta', z) d\zeta' \qquad (1)$$

where e is the electronic charge. Consequently the transverse equation of motion can be written as [2, 3]

$$\frac{d}{dz}\left[\gamma(z)\frac{d}{dz}x(\zeta, z)\right] + K^2\gamma(z)x(\zeta, z) = r_0 \int_\zeta^\infty d\zeta' \rho(\zeta') w_\perp(\zeta - \zeta') x(\zeta', z) d\zeta' \qquad (2)$$

ISBN: 978-3-95450-192-2 doi:10.18429/JACoW-IBIC2017-TUPCC12

BUNCH SHAPE MONITORS FOR MODERN ION LINACS

S. Gavrilov†, A. Feschenko
Institute for Nuclear Research of Russian Academy of Sciences, Troitsk, Moscow, Russia

Abstract

In recent years several Bunch Shape Monitors were designed for new modern ion linacs, such as Linac4 CERN, Proton and CW-linac FAIR GSI, FRIB MSU, ESS ERIC. Each of these accelerators has its own requirements for a phase resolution, mechanical design and operating conditions of the monitor. An overview of the most interesting features of different monitors is presented. Some results of laboratory tests and on-site beam measurements are discussed.

INTRODUCTION

The technique of a coherent transformation of a temporal bunch structure into a spatial charge distribution of low energy secondary electrons through RF-modulation was initially implemented by R. Witkover [1] for BNL linac. An energy (longitudinal) RF-modulation of secondary electrons was used. In the Bunch Shape Monitor (BSM) [2], developed in INR RAS, a transverse RF-scanning is used. The general principle of BSM operation has been described many times previously and is clear from Fig. 1.

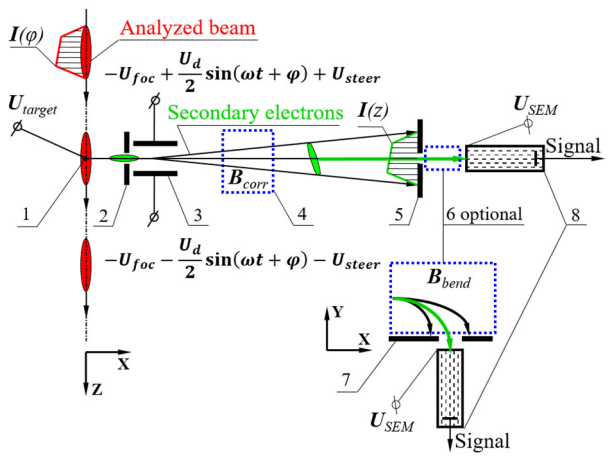

Figure 1: BSM scheme: 1 – tungsten wire target, 2 – inlet collimator, 3 – RF-deflector, 4 – correcting magnet, 5 – outlet collimator, 6 – optional bending magnet, 7 – registration collimator, 8 – secondary electron multiplier.

The series of the analysed beam bunches crosses the wire target 1 which is at a high negative potential. Interaction of the beam with the target results in emission of low energy secondary electrons. The electrons are accelerated by electrostatic field and move almost radially away from the target. A fraction of the electrons passes through inlet collimator 2 and enters RF-deflector 3. The field in the deflector is a superposition of electrostatic focusing and steering field and RF-deflecting field Ud with a frequency equal (or multiple) to the bunch sequence frequency.

† s.gavrilov@gmail.com

CURTAIN RANGE EXTENDER

Two groups of electrons passing the deflector with the phase shift of 180° get through the outlet collimator and their intensity is detected (Fig. 2).

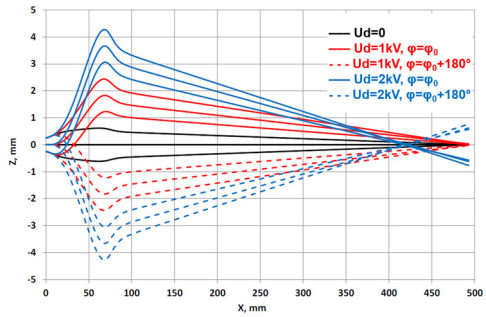

Figure 2: Trajectories of electrons in BSM.

If the bunch length is bigger than 180°, then the signals corresponding to two longitudinal points shifted by 180° are superimposed and the results of the measurements are distorted. Hence the standard phase range of measurements of BSM is equal to half a period of the deflecting field. The range of the measurements can be increased to a full period if one of the two groups of electrons is blocked. To do it the flag-type rotatable curtain can be used at the exit of the RF-deflector. The idea of the curtain was initially proposed by A. Tron and one of the paper's authors, however it was realized in practice for the first time in BSM for FAIR GSI linacs (Fig. 3).

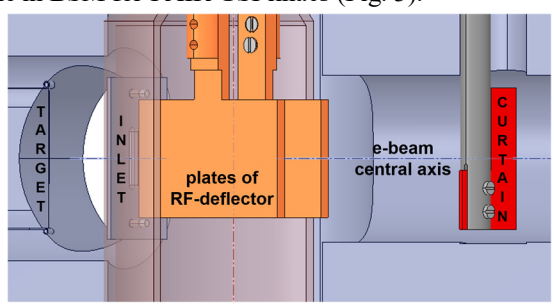

Figure 3: Internal layout of BSM for GSI with curtain.

Rotating the curtain, one can absorb the electrons (Fig. 4) corresponding to one of the two half-periods of the deflecting field thus avoiding superimposing of the signals corresponding to the particles shifted by half a period.

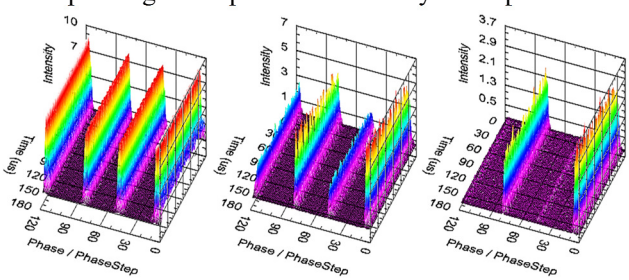

Figure 4: Experimental results for curtain rotation.

ISBN: 978-3-95450-192-2 doi:10.18429/JACoW-IBIC2017-TUPCC13

DESIGN AND DEVELOPMENT OF BUNCH SHAPE MONITOR FOR FRIB MSU

S. Gavrilov†, A. Feschenko, Institute for Nuclear Research of Russian Academy of Sciences, Troitsk, Moscow, Russia

Abstract

Bunch Shape Monitor was developed and tested in INR RAS for the Facility for rare isotope beams to fulfil the requirements of a half a degree phase resolution for 80.5 MHz FRIB operating frequency. The configuration of the λ/4-type RF-deflector based on the parallel wire lines with the shorting jumper and capacitive plates was selected. Special separation of secondary electrons by energy is foreseen to decrease a possible influence of the electrons detached from the ions in the wire target. Peculiarities of the design and development process are described. Results of laboratory tests are presented.

INTRODUCTION

The operation principle of the Bunch Shape Monitor (BSM), developed in INR RAS, is based on the technique of a coherent transformation of a temporal bunch structure into a spatial charge distribution of low energy secondary electrons through a transverse RF-scanning [1, 2] and is clear from Fig. 1.

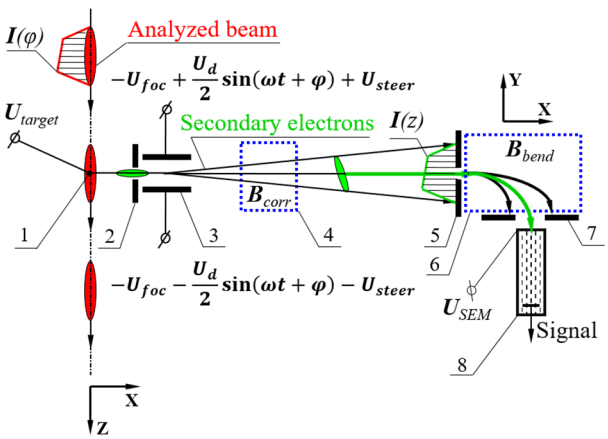

Figure 1: BSM scheme: 1 – tungsten wire target, 2 – inlet collimator, 3 – RF-deflector combined with electrostatic lens, 4 – correcting magnet, 5 – outlet collimator, 6 – bending magnet, 7 – registration collimator, 8 – secondary electron multiplier.

The series of the analysed beam bunches crosses the wire target 1 which is at a high negative potential about -10 kV. Interaction of the beam with the target results in emission of low energy secondary electrons, which characteristics of importance for bunch shape measurements are practically independent of beam energy and charge states of ions, so the monitor can be used for any location along the accelerator without design modification (Fig. 2).

† s.gavrilov@gmail.com

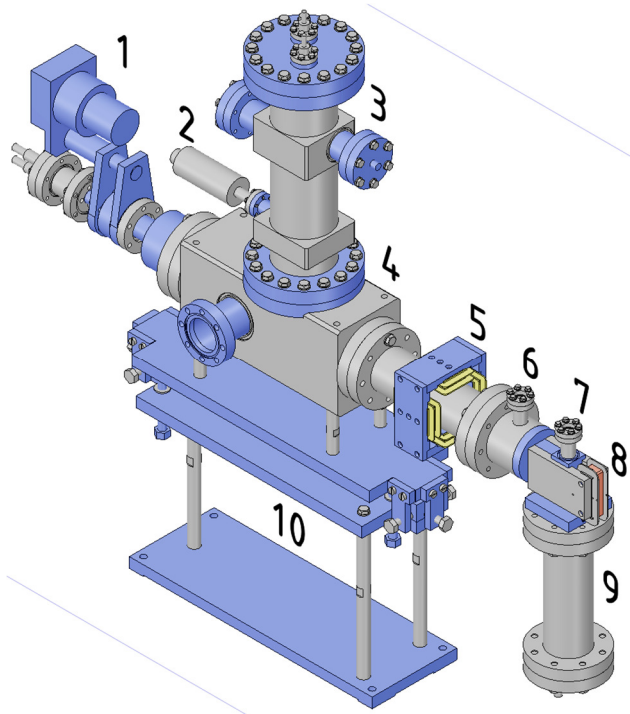

Figure 2: BSM design: 1 – target actuator, 2 – tuner, 3 – RF-deflector, 4 – BSM box, 5 – quadrupole + dipole correcting magnet, 6, 7 – viewports for optical control of e-beam, 8 – bending magnet, 9 – SEM-detector, 10 – support with 3D-adjustment.

The electrons are accelerated by electrostatic field and move almost radially away from the target. A fraction of the electrons passes through inlet collimator 2 and enters RF-deflector 3, where electric field is a superposition of electrostatic focusing and steering fields and RF-deflecting field with a frequency equal to the second harmonic of RF-field frequency in the linac: 161 MHz.

Passed electrons are scanned by the RF-field and an intensity of electrons passed through outlet collimator 5 represents a fixed point of the longitudinal phase distribution of the primary beam. Another points can be obtained by changing the phase of the deflecting field with respect to the RF-reference. If the phase of the deflecting field is adjusted in a wide range, then the bunch can be observed twice per the period of the deflecting field.

By adjusting the steering voltage one can change the measured phase position of the observed bunches and obtain the periodicity of bunches to be exactly equal to π. If the bunch duration is larger than π, the intensities corresponding the phase points differed by π are superimposes and the results of bunch shape measurements become wrong.

ISBN: 978-3-95450-192-2 doi:10.18429/JACoW-IBIC2017-TUPCC15

DESIGN AND COMMISSIONING OF THE BUNCH ARRIVAL-TIME MONITOR FOR SwissFEL

V. Arsov†, F. Buechi, P. Chevtsov, M. Dach, M. Heiniger, S. Hunziker, M. Kaiser, R. Kramert, A. Romann, V. Schlott, Paul-Scherrer-Institute (PSI), Villigen, Switzerland

Abstract

The Bunch Arrival-Time Monitor for SwissFEL (BAM) is based on the concept which was successfully tested at the SwissFEL Test Facility (SITF). During the gap between the SITF decommissioning and the start of SwissFEL, all key components underwent design improvement. In this paper, we report on some of these new developments and on the commissioning progress.

INTRODUCTION

SwissFEL is an X-ray free-electron laser user facility with two beamlines. The first one, Aramis, designed for electron energies between 2.1 and 5.8 GeV and for hard X-rays in the range 1.8 to 12 keV, has been inaugurated in December 2016 [1] and is presently under commissioning to reach its final design parameters. The second beamline, Athos, designed for energies between 2.65 and 3.4 GeV and for soft X-rays between 0.2 and 2 keV, is scheduled for commissioning in 2018-20.

According to the initial concept, totally five BAMs had been foreseen for the Aramis and two more BAMs for the Athos beam lines. These BAMs are capable for two bunch operation with 28 ns bunch separation at 100 Hz with <10 fs resolution in the charge range of 10 to 200 pC (simultaneous, single-shot non-destructive measurement).

Presently all pick-ups, most of the electronics and cabling, including the optical fibres, have been installed. Two stations, BAM1 at the laser heater and BAM3 after LINAC1 between the two bunch compressors, are fully equipped and presently under commissioning.

DESIGN OVERVIEW AND IMPROVEMENTS

The BAM concept was successfully demonstrated with two stations in SITF [2,3]. In view of the different girder and space limitations, for SwissFEL the BAM-box underwent a redesign. In SwissFEL the boxes are located under the granite girder, which serves as a radiation shield. Lead and boron-doped polyethylene sheaths are used for additional shielding. For servicing the box can be lifted up on wheels and pulled from below the girder. The last few meters of the cable tree and the optical fibres are laid in a flexible cable chain and are retracted together with the box. The housing lids provide additional isolation against acoustical noise and radiation. They are easily removable to allow servicing.

Pick-up and RF-Front End

The BAM pick-ups are cone-shaped buttons with 2.39 mm base (DESY design [4]), but modified for the SwissFEL beam pipe, 8 mm behind the undullator lines (BAM5 and 7) and 16 mm for the rest of the BAMs. The vacuum chamber mounts have five micrometer screws for vertical and lateral fine centring of the chamber axis to the beam.

The button pairs in each of the two orthogonal axis are combined together to minimize the orbit dependence. The 20 mm long PhaseMaster160 cables (Teledyne) and the couplers, type PS2-55-450/17S, Pulsar Microwave, are fixed in dedicated mounts close to the pick-up chamber. The output of the coupler is connected to the EOMs with armoured PM160 cables, 0.7 m for the EOM1 (high resolution branch) and 1.2 m for the EOM2.

To prevent orbit dependence and spoiling of the pick-up RF-transient quality, the relative group delay of the two branches from the pickup to the combiner has to be minimized. Initially the combiners were measured separately and then matched to a cable pair, which best compensated the relative group delay of the two combiner ports. An example from BAM4, located after LINAC3, is shown on Fig. 1. Up to 40 GHz the pk-pk relative phase between the combiner inputs is 5.5 deg (380 fs mean group delay difference), red curve. A cable pair from many samples has been selected to have 5.4 deg relative phase difference (384 fs mean group delay), blue curve. The entire package has 3.0 deg pk-pk relative phase difference (103 fs mean group delay), green curve. This best possible match is not perfect. The reason is the amplitude and phase relations at higher frequencies for the high bandwidth PS2-55-450 combiners (1 - 40 GHz).

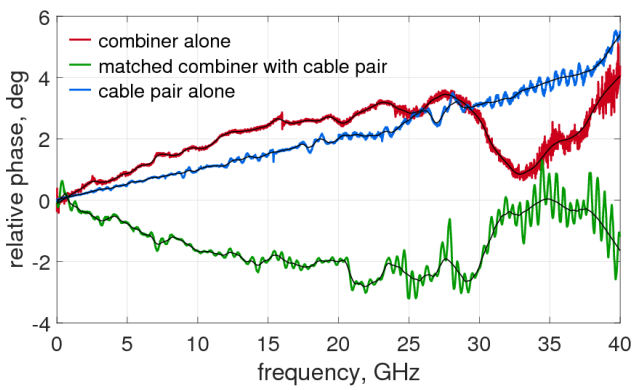

Figure 1: Phase match of the RF combiner and cables (BAM4).

Optomechanical Front End (BAM-Box)

The BAM-box is temperature stabilized with 8 large surface Peltiers. The mechanical design was improved to reduce the shear stress between the regulated base plate and the heat sinks by using flexible fixtures. Typical temperature stability for the components in contact with

† vladimir.arsov@psi.ch

ISBN: 978-3-95450-192-2 doi:10.18429/JACoW-IBIC2017-TUPCC16

STATUS OF THE THZ STREAKING EXPERIMENT WITH SPLIT RING RESONATORS AT FLUTE

V. Schlott†, M. Dehler, R. Ischebeck, M. Moser, Paul Scherrer Institute, Villigen, Switzerland
T. Feurer, M. Hayati, Z. Ollmann, R. Tarkeshian, University of Berne, Berne, Switzerland
E. Bründermann, S. Funkner, A.-S. Müller, M.J. Nasse, G. Niehues, R. Ruprecht, T. Schmelzer, M. Schuh, M. Schwarz, M. Yan, Karlsruhe Institute of Technology, Karlsruhe, Germany

Abstract

THz streaking with split ring resonators (SRR) promise ultra-high (sub-femtosecond) temporal resolution even for relativistic electron bunches. A proof-of-principle experiment in collaboration between the University of Bern, the Paul Scherrer Institute (PSI) and the Karlsruhe Institute of Technology (KIT) is currently prepared at the FLUTE facility (Ferninfrarot Linac und Test Experiment) at KIT. Most of the critical components have been designed, tested and set-up in the 7 MeV diagnostics part of FLUTE. In this contribution we will present an update on the experimental set-up and report on SRR configurations which have been optimized for highest THz deflection, while simultaneously accounting for the restrictions of the manufacturing process. Test measurements characterizing the SRR samples and the THz source, which has been matched to the FLUTE gun laser, will also be presented.

INTRODUCTION

Low charge operation of electron accelerators opens up the possibility of generating highly brilliant beams with micrometre transverse sizes and femto-second bunch length. Beam instrumentation for single-shot measurement of such ultra-short electron bunches is either limited in time resolution to some tens of femto-seconds for electro-optical methods [1, 2] or requires quite complex and expensive infrastructure as in case of RF deflectors, which are capable of providing the desired time resolution even for highly relativistic beams [3].

The test accelerator for far-infrared experiments (FLUTE) at the Karlsruhe Institute of Technology [4] is presently being set-up and commissioned to generate ultra-short and intense THz pulses and to provide a test infrastructure for femto-second electron beam studies aiming for the development of advanced diagnostics. Based on the proposal of using high frequency THz fields, which are enhanced in a split ring resonator (SRR), to streak an electron beam for its temporal characterization [5], a proof-of-principle experiment is presently prepared at FLUTE, intending to make use of the 7 MeV beam from the RF photo-injector gun in order to demonstrate the applicability of this method in a real accelerator facility [6, 7]. The tasks in this research collaboration between the University of Berne, KIT and PSI are distributed in the following way:

- KIT provides the FLUTE accelerator, the photo-injector laser system to generate the electron beam and the THz radiation as well as beam optics simulations for ultra-low charge operation.
- The University of Berne provides the SRR and the THz pulse generation.
- PSI participates in the design optimizations of the SRR and provides the beam diagnostics for the FLUTE experiment.

STATUS OF THE SRR EXPERIMENTAL SET-UP AT FLUTE

The UHV-chamber for the SRR experiment has been installed at about 1.7 m behind the photo-cathode, where ASTRA simulations indicate, that transverse rms beam sizes of ≤ 10 µm can be achieved at low ($\leq$ 100 fC) bunch charges [7]. In the experimental chamber, a set of SRRs can be accurately positioned to the electron beam path by means of UHV-compatible translation stages. A scintillator screen in combination with a high resolution optical telescope allows matching of the beam through the SRRs. Presently all components are interfaced to the FLUTE control system. The Ti:Sa FLUTE laser system, which provides the ps long UV (266 nm) pulses for the RF photo-injector gun and which is used to generate the short and intense THz pulses for exciting the SRRs, is in operation and the laser transfer line from the optics hutch to the FLUTE accelerator bunker is presently under commissioning. The THz pulse generation is set-up on an optical breadboard outside of the experimental chamber, from which the THz radiation is imaged through a CF-40 z-cut crystalline quartz UHV-window onto the SRRs by using an off-axis parabolic mirror. Overlap of the electron bunches with the sub-ps rise times of the THz streaking field is achieved with a motorized delay stage, while the synchronization is inherently provided through the use of the same laser for the electron beam and THz pulse generation. RF conditioning of the FLUTE gun is ongoing so that first acceleration of electrons is expected by October 2017.

THZ PULSE GENERATION

The intense single-cycle THz pulses for exciting the SRRs are generated by optical rectification [8-10] of the ultrashort FLUTE gun laser pulses (Coherent Astrella provides pulse energies of 6 mJ at a wavelength of 800 nm and a FWHM pulse length of < 35 fs with 1 kHz repetition rate) in a $LiNbO_3$ crystal.

Tilted Pulse Front Generation

Optical rectification, as any other nonlinear frequency conversion process, requires excellent phase matching in order to be efficient. Proper phase matching in $LiNbO_3$

† volker.schlott@psi.ch

ISBN: 978-3-95450-192-2 doi:10.18429/JACoW-IBIC2017-TUPCC17

ULTRA-STABLE FIBER-OPTIC REFERENCE DISTRIBUTION FOR SwissFEL C-BAND LINACS BASED ON S-BAND RADIO-OVER-FIBER LINKS AND FREQUENCY DOUBLER / POWER AMPLIFIERS

S. Hunziker†, V. Arsov, F. Buechi, M. Dach, M. Heiniger, M. Kaiser, R. Kramert, A. Romann, V. Schlott, Paul Scherrer Institut, CH-5232 Villigen, Switzerland

Abstract

The reference distribution for the SwissFEL accelerator is based on ultra-stable Libera Sync 3 fiber-optic links operating at 3 GHz with <2.4 fs added timing jitter. While s-band injector RF stations are directly supplied with these actively stabilized reference signals at 2.9988 GHz, the same 3 GHz optical links are used to transmit reference signals at 2.856 GHz (half c-band frequency) to the c-band LINACs, combined with a frequency doubler-amplifier at the link end. A novel zero AM/PM-conversion frequency doubler and an amplitude-/phase-controlled power amplifier have been implemented in a compact 1HU 19inch unit. Key design concepts and measurement results will be presented. It will be shown that this inexpensive doubler-amplifier system adds only insignificant jitter and drift to the transmitted reference signals. As the same actively stabilized 3 GHz links can be used for s- and c- band RF stations, development of a more expensive 6 GHz fiber-optic link could be avoided. A higher quantity of the same link type can thus be manufactured and the number of spares is reduced as only one link type is utilized for the SwissFEL injector and LINAC RF reference signals.

SwissFEL C-BAND REFERENCE DISTRIBUTION

The concept of the reference distribution for the SwissFEL accelerator RF stations and first performance measurements of the group delay stabilized Instrumentation Technologies Libera Sync 3 (3 GHz) prototype fiber-optic links have been presented in [1]. It is based on using 3 GHz radio-over-fiber links for distributing s-band (2.9988 GHz) as well as c-band (5.712 GHz) reference signals. For the c-band links the basic idea is not to transmit the c-band frequency itself but half of it (2.856 GHz) by means of a 3 GHz Libera Sync 3 link and then double and ampli-fy the transmitted signal frequency at the end of the link (Fig. 1). So we can use the same links for both s-band and c-band stations, which saves development and production costs for the fiber-optic links and simplifies testing and inventory.

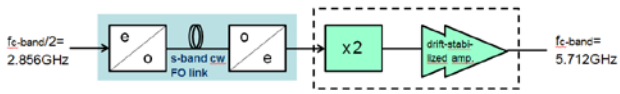

Figure 1: Concept of the radio-over-fiber based c-band link for the SwissFEL RF reference distribution. Dashed: frequency doubler / power amplifier. The timing jitter and gain / timing drift performance of the actual Libera Sync 3 link used in SwissFEL is shown in Figs. 2 and 3.

† stephan.hunziker@psi.ch

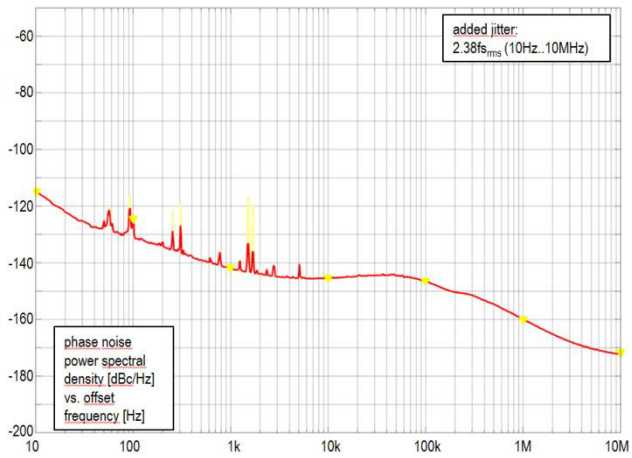

Figure 2: Libera Sync 3 fiber-optic link Added jitter at 2.9988 GHz for 500 m link span (standard SM fiber).

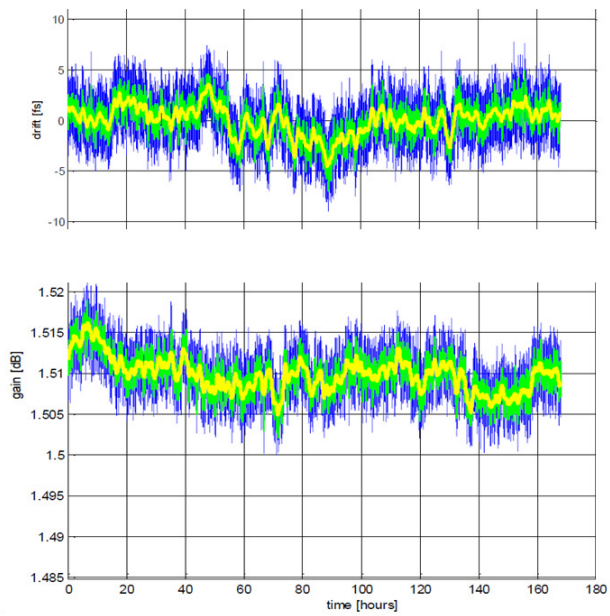

Figure 3: Libera Sync 3 drift measurement at 2.9988 GHz. Lower: Timing drift over 7 days: 11.9 fs_{p-p} (2.2 min avg.), 8.2 fs_{p-p} (1 h avg.), 2.6 fs_{rms}. Upper: Gain variation over 7 days, 0.017 dB_{p-p} (2.2 min avg.), 0.011 dB_{p-p} (1 h avg.).

As no frequency doubler / power amplifiers with the desired performance (particularly low phase drift and at the same time low jitter at high output power) are available on the market, such a device has been developed at PSI.

ISBN: 978-3-95450-192-2 doi:10.18429/JACoW-IBIC2017-TUPCC18

BEAM ARRIVAL TIME MEASUREMENT AT SXFEL*

S. S. Cao†, Y. B. Leng‡, R. X. Yuan, J. Chen
SSRF, SINAP, Shanghai, China

Abstract

Shanghai Soft X-ray Free Electron Laser (SXFEL) is a fourth-generation light source which could provide coherent X-rays for various scientific researches. One of the key issues of its operation is the measurement of bunch arrival time because it is important for the synchronization of a bunch and seeded laser. The measurement utilized a newly designed beam arrival time monitor (BAM). The BAM contains two different frequencies of cavities. Thus a new scheme, dual-cavities mixing method, can be applied in this experiment to evaluate the beam arrival time resolution. In this paper, we presented the scheme, calculated the measured resolution with this method and evaluated the stability of the new monitor.

INTRODUCTION

SXFEL is a XFEL facility and it is under construction [1]. For this facility, it is of importance to measure the beam arrival time within 100 fs to keep the synchronization of a bunch and a seeded laser. One method to conduct the measurement is to compare the phase difference between reference signal and measured signal. To reduce the noise introduced by the reference signal during transmission, a dual-cavity BAM was applied in this experiment. Since the high energy electron beam almost reaches the speed of light and the cavities distance is very short, the phase difference measured at the two cavities is constant. Thus the system errors from cavities cables and RF front-end electronics can be evaluated. In the preliminary work, we are committed to minimize these system errors as much as possible.

To carry out this experiment, a dual-cavities BAM was designed and the pickups were based on C-band monopole cavities [2]. Figure 1 shows the photograph of the prototype BAM.

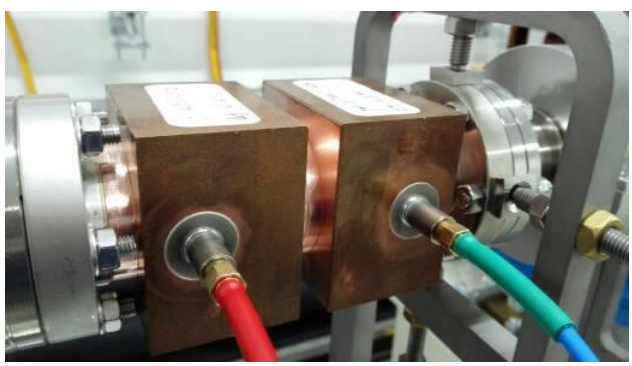

Figure 1: Photograph of the prototype BAM.

* Work supported by National Natural Science Foundation of China (No.11575282)
† caoshanshan1992@sinap.ac.cn ‡ lengyongbin@sinap.ac.cn

The prototype BAM has been developed and installed at SXFEL. The two pickups work at 4.685GHz and 4.72GHz, respectively. The frequency difference of the two cavities is about 35 MHz. The distance between the two cavities is more than 60 mm to avoid the cavity crosstalk. Table 1 shows the parameters of the BAM pickups. The parameters were calculated by Computer Simulation Technology (CST) Microwave Studio.

Table 1: BAM Pickup Parameters

Parameter	Value (#1)	Value (#2)	Unit
Frequency	4.685	4.72	GHz
Unloaded quality factor (Q_0)	4796	4835	-
External quality factor (Q_e)	1.8e5	1.9e5	-
Loaded quality factor (Q_L)	4671	4716.4	-
R over Q	107.2	107.9	Ohm
Bandwidth (BW)	1.002	1.025	MHz
Decay time constant (τ)	317.7	318	ns

In this study, the beam induced signal from downstream pickup served as a local oscillator signal input to the mixer. And the RF signal form upstream pickup was used as input signal for the mixer. Thus an intermediate frequency (IF) signal of about 35 MHz were obtained.

MEASUREMENT

There are four BAMs on the SXFEL facility. Two of them are installed at the drift section after the injection; the other two are placed in the modulator section. The experiment was conducted near the modulator because the noise in the experiment hall compared to the injection is smaller. Figure 2 presented the schematic diagram of the beam arrival time resolution evaluation [3]. An RF signal is generated when an electron beam passes through the BAM cavities. The RF signal was extracted with four antennas in the BAM wall and delivered to the RF front end in the experiment hall with long cables. The signals were processed with four channels of the RF front end system. In this system, two set of frequency mixer were applied for down conversion. The signals from port 1 and port 2 were used as local oscillator (LO) signal of mixer; signals from port 3 and port 4 were served as RF input signal. Then the low pass filters were used to filter out the high frequency signal, thus the IF signal was retained. A 12 bit Analog-to-Digital Converter (ADC) with a sampling rate of 500 MHz was then adopted to sample the IF signal.

ISBN: 978-3-95450-192-2 doi:10.18429/JACoW-IBIC2017-TUPCF02

MODELING THE FAST ORBIT FEEDBACK CONTROL SYSTEM FOR APS UPGRADE*

P. Kallakuri†, D. Paskvan, J. Carwardine, N. Sereno, and N. Arnold,
Argonne National Lab, Lemont, USA.

Abstract

The expected beam sizes for APS Upgrade (APS-U) are in the order of 4 microns for both planes. Orbit stabilization to 10% of the beam size with such small cross-sections requires pushing the state of the art in Fast Orbit Feedback (FOFB) control, both in the spatial domain and in dynamical performance; the latter being the subject of this paper. In this paper, we begin to study possible performance benefits of moving beyond the classic PID regulator to more sophisticated methods in control theory that take advantage of a-priori knowledge of orbit motion spectra and system non-linearities. A reliable model is required for this process. Before developing a predictive model for the APS Upgrade, the system identification methodology is tested and validated against the present APS storage ring. This paper presents the system identification process, measurement results, and discusses model validation.

INTRODUCTION

The current APS real-time orbit feedback system has been in routine operation for more than 20 years and was the first digital truly global orbit feedback system to be implemented at a light-source. A distributed array of DSPs compute orbit corrections at 1.6 kHz using a matrix of 160 bpms x 38 correctors per plane. Unity-gain bandwidth is 60-80 Hz [1]. The regulator uses just the integral term of a classical PID, and is tuned for minimum residual broad-band rms orbit motion. A higher K_i than optimal gives better attenuation at lower frequencies but comes at the expense of amplifying residual motion at higher frequencies. The optimum value of K_i therefore depends on the spectral content of the orbit motion. A new orbit feedback system is under development for the APS Upgrade, where the smaller beam size drives orbit stability requirements that are considerably more stringent than the present APS. The new orbit feedback system will use a distributed array of DSPs to compute orbit corrections at 22.6 kHz (12x faster than the present system) and using a matrix of 560 bpms and 160 correctors. The target unity-gain bandwidth is 1 kHz. We need to study the possible performance benefits of moving beyond classic PID regulator and investigate different controller design methods in advanced control theory that are applicable to electron beam stabilization. A reliable model is required for this process since most of the advanced control algorithms are model based. We start this investigation by first modeling the FOFB system. Prototype feedback controllers, and fast corrector power supplies developed under R&D for APS-U have been integrated in prototype feedback system in APS Sector 27/28 for beam stability studies [2]. This system uses present storage ring corrector magnets. The modeling results are tested and validated against this prototype before developing the predictive model for APS-U.

Main tasks involved in the system modeling are: to develop a open loop system model, to create a simulation model of the DSP controller, and use them to implement a real time simulation setup that represents FOFB control system for APS-U. The layout of the FOFB system in closed loop is shown in Fig. 1. The open loop dynamics are represented by the process transfer function from corrector power supply set point to BPM read backs. Let $H[z]$ be the transfer function of open loop system with present corrector magnet. We assume,

$$H[z] = H_1[z] \cdot H_M[z] \tag{1}$$

where $H_M[z]$ is the transfer function of the present corrector magnet, and rest of the dynamics are represented by the transfer function $H_1[z]$. Then, the predicted open loop dynamics of the FOFB system for APS-U can be represented by,

$$H_U[z] = H_1[z] \cdot H_{UM}[z] \tag{2}$$

where, $H_{UM}[z]$ is the transfer function of the prototype fast corrector magnet. Developing the simulink model of the DSP controller is the next step in the process. BPM readbacks are the input to this model and the outputs are the corrector set points to power supply.

In this work, Matlab System Idendification Toolbox is used for model estimation. Data pre-processing, model validation are done in Matlab and Simulink environment.

SYSTEM IDENTIFICATION PROCEDURE

In this modeling we assume the FOFB system in open loop is linear time-invariant. The model application in our case is to use it for control design, so having accurate model around the crossover frequency is important.

Data Collection

The modelling process starts with collecting the data required for matlab system identification tool. Experiments are conducted to measure open loop time and frequency response data. For open loop measurements, input is the corrector setpoint to power system and output measured is BPM readbacks. Time response is measured with an unit step signal input at corrector drive. The measured step response data is preprocessed by smoothing and removing the zero offset. For open loop frequency response measurements, sine sweep signal with step changes in frequency

* Work supported by the U.S. Department of Energy, Office of Science, under Contract No. DE-ACO2-O6CH11357.
† pkallakuri@anl.gov

ISBN: 978-3-95450-192-2 doi:10.18429/JACoW-IBIC2017-TUPCF03

THE RF BPM PICKUP ELECTRODES DESIGN FOR THE APS-MBA UPGRADE*

X. Sun†, R. Lill, B. Stillwell, ANL, Argonne, IL 60439, U.S.A.

Abstract

The Advanced Photon Source (APS) is currently in the preliminary design phase for a multi-bend achromat (MBA) lattice upgrade. Beam stability is critical for the MBA and will require roughly 570 rf beam position monitors (BPMs) to provide the primary measurement of the electron beam trajectory through the insertion device (ID) straight sections and in the storage ring arcs. The BPM assembly features 8 mm diameter pickup electrodes that are welded to a stainless steel chamber and integrated shielded bellows both upstream and downstream of the chamber to decouple the BPM electrodes from mechanical motion of adjacent chambers. The design, simulations, and prototype test results will be presented.

INTRODUCTION

The APS Upgrade project (APS-U) requires rf BPMs at roughly 570 locations in the APS storage ring to achieve the beam stability requirements outlined in Table 1 [1]. For the preliminary design, the horizontal AC rms beam stability requirement is based on 10% the rms beam size at the ID source points from 0.01 to 1000 Hz, while the vertical requirement in microns will remain at the conceptual design values, with 10% of beam size being an operational goal. In addition, long-term drift over a 7 day period may be no more than 1 μm.

Table 1: MBA Beam Stability Requirements

Plane	AC rms Motion (0.01 – 1000 Hz)	Long-term Drift (100 s – 7 days)
Horizontal	1.3 μm 0.25 μrad	1.0 μm 0.6 μrad
Vertical	0.4 μm 0.17 μrad	1.0 μm 0.5 μrad

THE RF BPM PICKUP ELECTRODES R&D OVERVIEW

The four pickup electrodes used in each BPM are evenly distributed circumferentially around the circular MBA beam pipe and provide the primary measurement of the electron beam trajectory in the storage ring. Their sensitivities, charge induced voltages and wake impedance are all critical for the beam stability.

"As-built" 10.8 mm diameter APS button pickup electrodes and the elliptical APS standard chamber were modelled as shown in Fig. 1. The simulation was made using CST Microwave Studio (MWS) [2] for 24-siglet fill pattern 102 mA (15 nC per bunch, rms bunch length 10 mm). Measurements on as-built BPM electrodes installed in the existing APS storage ring were also made to validate the simulation model. Simulation results agreed well with the measured data, as shown in Fig. 2.

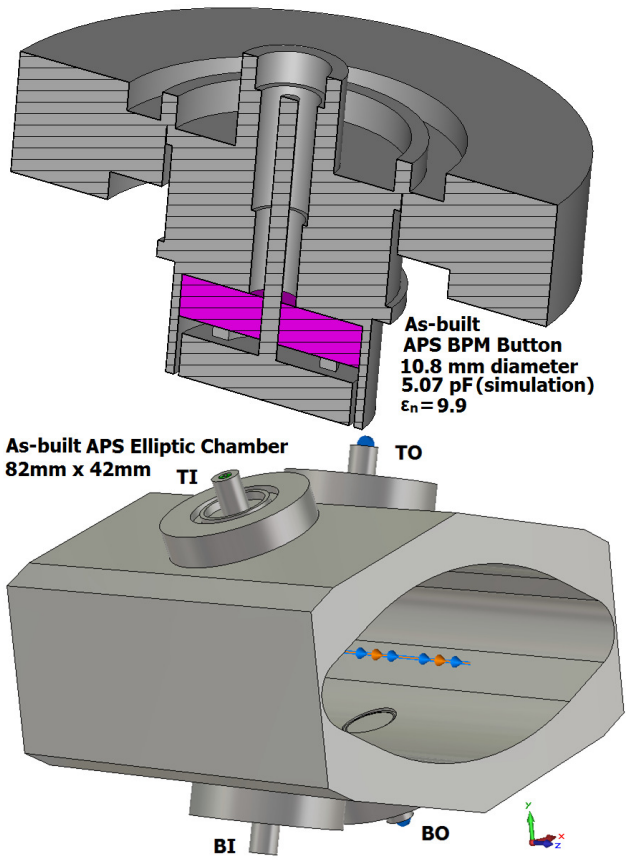

Figure 1: As-built APS BPM button and elliptic chamber.

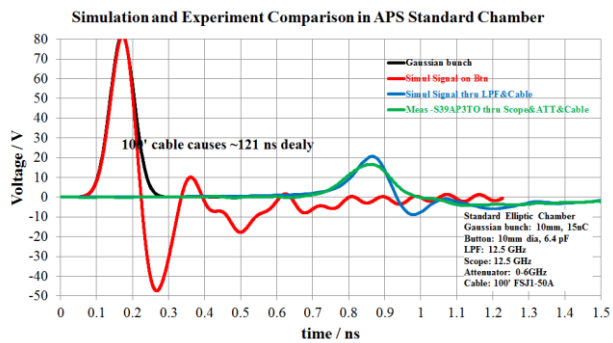

Figure 2: Simulation and experiment in APS elliptic chamber with BPM.

An MBA pickup electrode design has been developed which is essentially a scaled version of that for existing APS BPMs to match the planned MBA beam pipe aperture.

To help validate the new design, two sets of four prototype button pickup electrodes were purchased from two independent suppliers (vendors A and B) and then bench

* Work supported by the U. S. Department of Energy, Office of Science, Office of Basic Energy Sciences, under Contract No. DE-AC02-06CH11357.
† xiang@aps.anl.gov

ISBN: 978-3-95450-192-2 doi:10.18429/JACoW-IBIC2017-TUPCF04

FEEDBACK CONTROLLER DEVELOPMENT FOR THE APS-MBA UPGRADE*

H. Bui†, D. Paskvan, A. Brill, S. Veseli, A. Pietryla, T. Fors, S. Shoaf, S. Xu, N. Sereno, R. Lill, N. Arnold, J. Carwardine, G. Decker

Advanced Photon Source, Argonne National Laboratory, Argonne, IL 60439, USA

Abstract

The Advanced Photon Source (APS) is currently in the preliminary design phase for the multi-bend achromat (MBA) lattice upgrade. Broadband Root Mean Square (rms) orbit motion should stay within 10% of a beam cross-section of the order 4 µm x 4 µm rms at the insertion device source-points. In order to meet these stringent AC beam stability requirements, a new orbit feedback system is under development and is being tested on the existing APS storage ring. The controller prototype uses Commercial Off-The-Shelf (COTS) hardware that has both high-performance Xilinx Field-Programmable Gate Array (FPGA) and two high-performance Texas-Instruments Digital Signal Processors (DSP) onboard. In this paper, we will discuss the rationale for a combined DSP/FPGA architecture and how functions are allocated. We then present the FPGA architecture and the results of using Infinite Impulse Response (IIR) filtering to mitigate Beam Position Monitor (BPM) switching noise and aliasing.

INTRODUCTION

The Feedback Controller (FBC) receives turn-by-turn (TbT or 271 kHz) BPM data from commercial Instrumentation Technologies Libera Brilliance+ BPM electronics [1], decodes and performs data integrity check, notifies the DSPs to generate corrector setpoints, and forwards corrector setpoints to the fast corrector power-supply interface.

Currently, the prototype Feedback Controller uses a CommAgility AMC-V7-2C6678 [2] module as a base development platform. The AMC-V7-2C6678 is a single width, mid-size Advanced Mezzanine Card (AMC), is comprised of two Texas Instrument (TI) TMS320C6678 DSPs, each with 8 cores running at 1.25 Giga Hertz (GHz), and a Xilinx Virtex-7 VX415T [3] FPGA. The combined architecture of a FPGA and a DSP shortens the development cycle time by taking full advantage of a vast library of highly-optimized DSP code and algorithms developed over the past 20 years for the present APS real-time feedback system (RTFB), which is running on a previous-generation of TI DSP. Investigations may be performed in the future to determine if any functionalities handled by the external DSPs can be implemented using resources inside the FPGA to improve system performance.

Figure 1 shows the simplified block diagram of the prototype FBC system. Light-blue blocks represent functionalities that are implemented inside the Virtex-7 FPGA, while orange blocks represent the two external TI DSP devices.

Xilinx FPGA's Gigabit transceivers and Peripheral Component Interconnect Express (PCIe) 2.0 are used to transfer data between the FPGA and DSP subsystem.

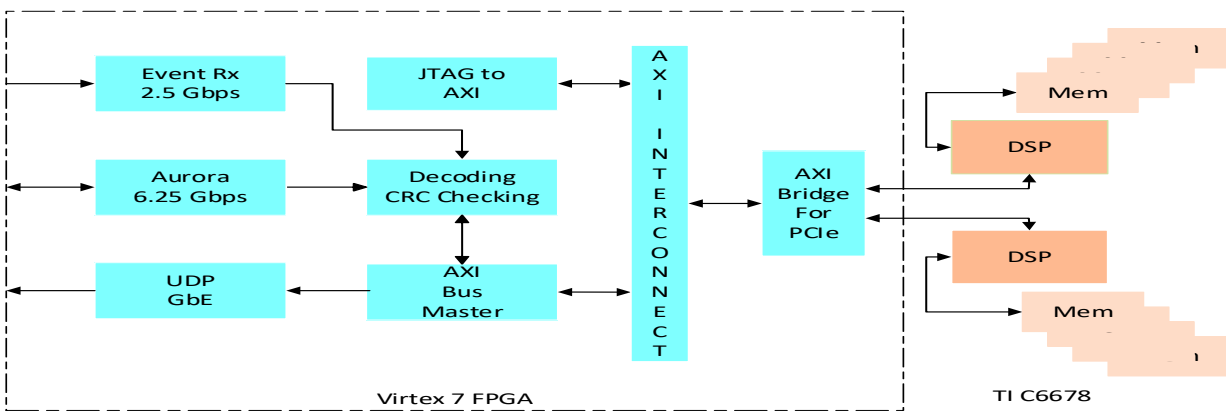

Figure 1: Simplified Block Diagram for the prototype FBC.

* Work supported by the U.S Department of Energy, Office of Science, under Contract No. DE-AC02-06CH11357
† hbui@aps.anl.gov

ISBN: 978-3-95450-192-2 doi:10.18429/JACoW-IBIC2017-TUPCF05

THE ORBIT MEASUREMENT SYSTEM FOR THE CERN EXTRA LOW ENERGY ANTIPROTON RING

O. Marqversen†, R. Ruffieux, L. Søby, J. Molendijk, M.E. Angoletta, J. Quesada, M. Jaussi, CERN, Geneva, Switzerland
R. Marco-Hernandez††, IFIC, Valencia, Spain

Abstract

The CERN Extra Low ENergy Antiproton ring (ELENA), intended to further decelerate anti-protons coming from the CERN Antiproton Decelerator (AD) from a momentum of 100 MeV/c to 13.7 MeV/c, has been equipped with an orbit measurement system consisting of 10 horizontal and 10 vertical electrostatic pick-ups. Using charge amplifiers the signals are converted into sum and difference signals that, once digitized, are down converted to baseband and used to calculate intensity independent beam positions. The system is implemented on seven VME switched serial based (VXS) FPGA / DSP boards carrying direct digital synthesisers and analogue to digital converters on standard FPGA mezzanine cards. The switched serial high-speed bus allows intercommunication between DSPs and thus averaging of the signals from all pick-ups in real-time to be used either in the RF radial feedback system or for longitudinal Schottky diagnostics. The system implementation and initial orbit measurements with the H^- beam used for ELENA commissioning will be presented, as well as future upgrades for trajectory and longitudinal Schottky measurements.

INTRODUCTION

An overview of the ELENA Orbit system is given in [1]. The system is being implemented in steps; the closed orbit measurement, the trajectory measurement and the longitudinal Schottky measurement. The analogue and digitization electronics are common to all measurements, the difference coming from the subsequent treatment of this data in the Field Programmable Gate Array (FPGA) and Digital Signal Processing (DSP) code. The orbit measurement is already operational and is being used for the ELENA commissioning, with first measurements presented here. Trajectory and longitudinal Schottky measurements will follow in the future.

The ELENA orbit system is built with the same VXS-DSP-FMC-carriers and FMC boards as the CERN AD orbit system [2] and the Firmware, DSP code and real-time software share a common base.

ELENA is CERNs Extra Low ENergy Antiproton ring intended to decelerate antiprotons injected at an energy of 5.3 MeV from the CERN AD to 100 keV. To minimize impact on the CERN AD physics program the ELENA ring is initially being commissioned using H^- ions injected at the intended antiproton extraction energy. Due to problems with the H^- source the achieved energy has only reached 85 keV, challenging the low energy end of the RF system, and forcing the system to run at the second RF harmonic (2·132 kHz). The orbit measurement system, measuring the beam position from a signal down mixed to baseband, has been designed to follow this.

The system

The orbit system consists of electrostatic pick-ups equipped with charge amplifiers, preamplifiers and VXS-DSP-FMC-Carriers [3]. The charge amplifiers send sum and difference signals from the pick-ups, via preamplifiers to ADCs placed on FMC boards. The ELENA RF system sends the actual revolution frequency as an integer value via an optical gigabit link, from which the orbit system will generate its own local oscillator frequency on the wanted harmonic used for digital down mixing of the sum and difference signals. Position calculations are performed in DSP modules and the results are sent to the real-time software that makes the data available to the control room. The orbit system also computes a real-time mean radial horizontal position for the RF radial feedback. The system is only capable of producing beam position data during the times when the beam is bunched.

INITIAL MEASUREMENTS

All pick-up signals after the charge and pre-amplifier are also made available to the CERN Oasis system (an online oscilloscope) allowing operators to plot the beam sum or difference signal from any pick-up. During commissioning of ELENA the H^- beam is injected using a 700 ns kicker pulse, which for a revolution frequency of 132 kHz (energy 85 keV) results in a bunch like structure even before RF is applied (Figure 1). The number of charges, N_q Eq (1) has been estimated, knowing the charge amplifier feedback capacitance and following amplifier gains. The voltage integrated over the bunch length is divided by the time where a single charge is contributing to the voltage i.e. the effective length of the pick-up divided by the particle speed. The effective length of the pick-up is obtained from the shape of the image charge for a given relativistic β, assuming a centred beam [4].

$$N_q = \frac{C_{feedback} \int V(t)dt}{e \cdot Gain \cdot \frac{l_{PU\_eff}}{v}} \qquad (1)$$

Where $C_{feedback}$ is the feedback capacitance in the charge amplifier, $\int V(t)dt$ the voltage integrated over the bunch length at the output of the amplifier (Figure 1, trace 2), e the electric charge, l_{PU_eff} the effective length of the pick-up, and v the speed of the particle. The effective length of the pick-up is given by

† Ole.marqversen@cern.ch
†† Ricardo.Marco@ific.uv.es

ISBN: 978-3-95450-192-2 doi:10.18429/JACoW-IBIC2017-TUPCF06

PERFORMANCE OF THE AWAKE PROTON BEAM LINE BEAM POSITION MEASUREMENT SYSTEM AT CERN

M. Barros Marin*, A. Boccardi, T. Bogey, J. L. Gonzalez, L. K. Jensen,
T. Lefevre, D. Medina Godoy, M. Wendt, CERN, Geneva, Switzerland
J. Boix Gargallo, UAB-IFAE, Barcelona, Spain

Abstract

The Advanced Proton Driven Plasma Wakefield Acceleration Experiment (AWAKE), based at CERN, explores the use of a proton driven plasma wake-field to accelerate electrons at high energies over short distances. This paper introduces the Beam Position Measurement (BPM) system of the proton beamline and its performance. This BPM system is composed of 21 dual plane button pickups distributed along the 700 m long transfer line from the CERN Super Proton Synchrotron (SPS) extraction point to beyond the plasma cell. The electrical pulses from the pickups are converted into analogue signals proportional to the displacement of the beam using logarithmic amplifiers, giving the system a high dynamic range (>50 dB). These signals are digitized and processed by an FPGA-based front-end card featuring an ADC sampling at 40 MSps. Each time a bunch is detected, the intensity and position data is sent over 1km of copper cable to surface electronics through a serial link at 10 Mbps. There, the data is further processed and stored. The dynamic range, resolution, noise and linearity of the system as evaluated from the laboratory and 2016 beam commissioning data will be discussed in detail.

INTRODUCTION

The Advanced Proton Driven Plasma Wakefield Acceleration Experiment (AWAKE) [1] is a proof-of-principle experiment installed in the former CERN Neutrinos to Gran Sasso (CNGS) facility and is the first proton driven plasma wake-field acceleration experiment world-wide. The AWAKE experiment aims to accelerate electrons from low energy (~15 MeV) up to the multi-GeV energy range over short distances (~10m). This is achieved using the wake-field of a plasma to accelerate electrons. The wake-field is induced in the plasma by a high-energy (~400GeV) proton bunch extracted from the CERN Super Proton Synchrotron (SPS) via a 700 m long transfer line.

THE PROTON BPM SYSTEM

The Beam Position Monitor (BPM) system of the AWAKE proton beam line, is composed of 21 dual plane button pickups, distributed along a 700 m beam transfer line. The read-out electronics is divided into two parts: the front-end electronics located close to the pick-ups in the tunnel and the back-end electronics sitting in a service gallery. The back-end communicates with all the different front-ends and concentrates the BPM control and data acquisition to a single point. The communication between the front-end and back-end is performed using a custom protocol running at 10 Mbps over 1 km of copper cable. This system has been optimized for the low repetition rate (~30 s) and high dynamic range (~40 dB) of the AWAKE proton beam. Its target resolution is better than 100 µm for nominal bunches ($3.5e^{11}$ protons).

Front-End Electronics

For each BPM, the front-end electronics is composed of two analogue, logarithmic amplifier boards (LogAmp), a Digital Front-End board (DFE) and a power supply unit. The LogAmp board receives the electrical pulses from the pick-up and shapes them using 30 MHz band-pass filters, before processing them with logarithmic amplifiers and sending the resulting analogue signals to the DFE board for digitization. The LogAmp board also features an on-board calibrator emulating pickup signals of known displacement. The DFE is an FPGA-based digital board featuring a multi-channel ADC sampling at 40 MSps. Due to the low radiation levels expected in the AWAKE beam line, radiation-tolerant components are not required. An image of the pick-up and front-end electronics under test in the laboratory is shown in Figure 1.

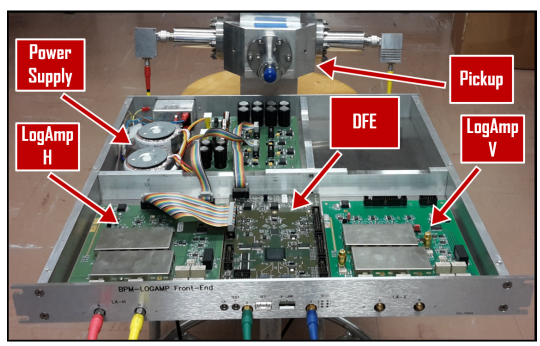

Figure 1: Pickup and front-end electronics.

The front-end electronics provides both a difference signal (Dif) and a summation signal (Sum) per plane. As for all BPM systems based on logarithmic amplifiers, the Dif signal is obtained from the difference in the logarithm of opposite electrodes, Log[electrode1] – Log[electrode2] = Log[electrode1/electrode2] and is directly proportional to the normalized beam position. The Sum signal is obtained by summing the logarithmic signal of both electrodes and is a function of the beam intensity. The Sum signal is used for auto-triggering the acquisition system. All signals are

* manoel.barros.marin@cern.ch

ISBN: 978-3-95450-192-2 doi:10.18429/JACoW-IBIC2017-TUPCF07

THE DESIGN IMPROVEMENT OF TRANSVERSE STRIPLINE KICKERS IN TPS STORAGE RING

P.J. Chou†, C.K. Chan, C.C. Chang, K.T. Hsu, K.H. Hu, C.K. Kuan and I.C. Sheng
National Synchrotron Radiation Research Center, Hsinchu 30076, Taiwan

Abstract

An improved design of horizontal stripline kicker for transverse feedback system has been replaced in January 2017. A rapid surge of vacuum pressure near the old horizontal kicker was observed when we tested the high current operation in TPS storage ring in April 2016. A burned vacuum feedthrough of the horizontal kicker was discovered during a maintenance shutdown. The improved design has reduced the reflection of the driving power from horizontal feedback system and the beam induced RF heating. Based on the experience learned from this improved design of horizontal stripline kicker, we also work out the improved design for the vertical kickers as well. The major modifications of the improved designs for both the horizontal and the vertical stripline kickers are described. The results of RF simulation performed with the electromagnetic code GdfidL are also reported.

INTRODUCTION

The designs of both the horizontal and the vertical stripline kickers for bunched beam feedback in Taiwan Photon Source (TPS) were adapted from the SLS/ALBA design [1, 2]. The type-N vacuum feedthroughs of horizontal kicker were found damaged due to over heating during high current operation in 2016. The original horizontal kicker was replaced by an improved design in January 2017. Details of the design improvement of horizontal stripline kicker have been reported [3]. Since the same type of vacuum feedthroughs are used in the vertical kickers, there is a concern whether we will encounter similar problems as the original horizontal kicker did or not. To ensure a reliable operation at the designed beam current 500 mA in the future, we embark on the design improvement for the vertical stripline kicker.

From the beam experiments conducted with the improved horizontal kicker, we discover that the beam induced signal is the dominant source which could damage the drive amplifier connected at the downstream ports. The priority is given to the matching of even mode impedance when we improve the design of vertical kicker. The same design concept that is effective in greatly reducing the loss factor of horizontal kicker [3] is also applied to the vertical kicker. A 3-D electromagnetic code GdfidL [4] is used for the simulation studies of this improved vertical kicker.

† pjchou@nsrrc.org.tw

DESIGN IMPROVEMENT

Since there is limited space available for the installation of transverse kickers in TPS storage ring, there is no taper section in the design of stripline kickers. The transverse profile of kicker electrodes should be flushed to the inner surface of racetrack beam pipe in order to reduce the broadband impedance. A section view of the existing vertical stripline kicker is shown in Fig. 1. The width of electrodes is 42.7 mm, the length is 280 mm and the cross section of racetrack beam pipe is 68 mm x 20 mm.

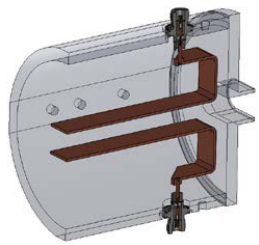

Figure 1: The section view of the existing vertical stripline kickers in TPS storage ring. The longitudinal gap between the electrodes and the end plate is 10 mm.

Impedance Matching

To prevent the beam induced signal propagating towards the downstream ports, the even mode impedance Z_{even} should be matched to the terminating line impedance (typically 50Ω). For maximum transmission of signal coming from the drive amplifier at the downstream ports, the necessary condition given by the theory of coupled transmission lines should be satisfied [5, 6]:

$$Z_{even}Z_{odd} = Z_0^2 \quad (1)$$

where Z_0 is the terminating line impedance.

For beam pipes of small cross section, it is difficult to satisfy both conditions for a good impedance matching of stripline electrodes. We choose to match the even mode impedance in order to minimize the beam induced signal at the downstream ports where the drive amplifier of feedback system is connected to.

The geometry of proposed improvement of vertical stripline kicker is shown in Fig. 2. The stripline electrodes are flushed to the inner surface of racetrack beam pipe for the reduction of broadband impedance. The summary of mode impedance for the existing vertical stripline kicker and the proposed improvement is listed in Table 1. The distribution of electrical fields of the odd mode of the improved design is shown in Fig. 3. The comparison of simulated results of the time domain reflectometry (TDR) for the existing and the improved vertical kicker is shown in Fig. 4.

ISBN: 978-3-95450-192-2 doi:10.18429/JACoW-IBIC2017-TUPCF08

BEAM STABILITY DIAGNOSTICS WITH X-RAY BEAM POSITION MONITOR IN THE TAIWAN PHOTON SOURCE

C. H. Huang†, P. C. Chiu, C. Y. Wu, Y. Z Lin, Y. M. Hsiao, J. Y. Chuang, Y. S. Cheng, C. Y. Liao, C. K. Kuan, K. H. Hu, K. T. Hsu
NSRRC, Hsinchu 30076, Taiwan

Abstract

To monitor the stability of photon beams, X-ray beam position monitors (BPMs) with quadrant PIN photodiodes or blades are installed in the beam lines and front ends. Although there are about 200 electron BPMs installed in the storage ring, the beam-line managers or users prefer X-ray BPMs to monitor beam stability. Among the beam lines, different electronics are used to acquire data at various sampling rates. A method to calculate the beam intensity fluctuation within different frequency ranges is described in this report. The results of calculations are shown in the control system and saved in the archive system thus helping to monitor and analyse beam quality on- and off-line. Initial experiences with this system will be discussed in this report.

INTRODUCTION

An X-ray beam position monitor (BPM) is a device used to measure the centroid of the synchrotron radiation. Many devices have been used to detect the beam position such as: fluorescent screens, split plate ionization chamber, blade-type BPM, quadrant PIN photodiodes BPMs (QBPMs) and so on. For continuous use, non-destructive blade-type BPMs and QBPMs are installed in the front ends and beam lines of the Taiwan Photon Source (TPS) to monitor the beam position and density fluctuation.

The first blade-type BPM is used in the front end of an insertion device (ID) reported by Mortazavi et al. in 1986. Shu et al. at the Advanced Photon Source used chemical vapour deposition (CVD) diamond as the blade material with metal (Au, Pt and Ti) coating for good photoemission [1]. This blade-type BPM provides submicron resolution at high power density absorption capability. The heat load in a beam line becomes greatly reduced downstream of the double crystal monochromator making the QBPM a good candidate to monitor the beam position due to its reduced sensitivity to beam profile [2].

In the TPS, two blade-type BPMs are installed in each front end with one being located at the entrance to the front end and the other downstream of the fast closing valve as shown in Fig. 1. Numbers and types of X-ray BPMs are different for most beam lines, due to different consideration.

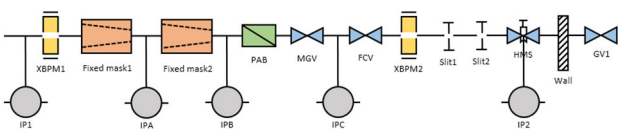

Figure 1: Layout out of front-end instrumentation.

† huang.james@nsrrc.org.tw

In this paper, the data acquisition electronics for X-ray BPMs is introduced first, followed by a discussion of beam position observations with X-ray BPMs. In order to define a reference to quantify beam stability, we discuss this issue in the third part.

SYSTEM SETUP

For the X-ray BPMs (XBPM) in the front end, we use two kinds of electronics to acquire and evaluate the beam position with the old and new version of the Libera Photon system. These devices provide several acquisition types for different sampling rates. An input/output controller (IOC), based on the experimental physics and industrial control system (EPICS), is embedded in these devices and the acquisition data are transferred to the control network through process variables (PVs). For example, the slow acquisition (SA) data is 10/25 Hz and the fast acquisition data is 160 Hz/5 kHz for the old/new version electronics. The layout of the XBPM in the front end is shown in the Fig. 2. For the XBPMs in the beam line, there are three types of electronics in use now. One uses the FMB Oxford F-460 to convert the current to voltage and read the voltage with a NI-9220. For this type of electronics, the data can only be read by the local computer and the sampling rate is 2 kHz now. Another type of electronics is a home-made device with 0.5 Hz update rate and its data are published in the control system while fast data can only be acquired by local instruments now. A third type is used with a new Libera Photon system. The display of the position with various sampling rates is done by the extensible display manager (EDM) and Matlab, shown in Fig. 3. The spectrum of the beam motion can also be shown in the control console as shown in Fig. 4.

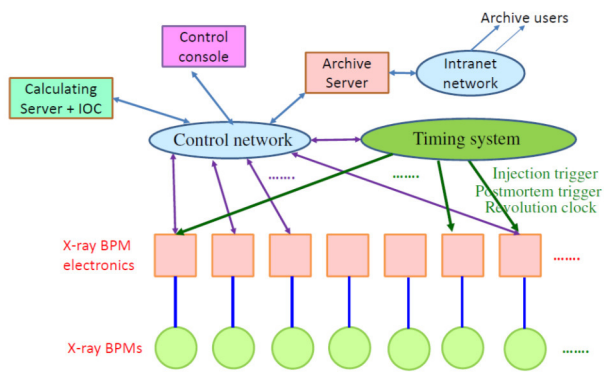

Figure 2: Layout of the XBPM electronics setup in the front end.

ISBN: 978-3-95450-192-2 doi:10.18429/JACoW-IBIC2017-TUPCF09

TURN-BY-TURN TIMING SYSTEMS FOR SuperKEKB DAMPING RINGPOSITION MONITORS

Makoto Tobiyama* and Hitomi Ikeda,
KEK Accelerator Laboratory, 1-1 Oho, Tsukuba 305-0801, Japan
Graduate University for Advanced Studies (SOKENDAI), 1-1, Oho, Tsukuba 305-0801, Japan

Abstract

Turn-by-turn timing systems for SuperKEKB beam position monitors using Xilinx Zynq FPGA have been developed. The RF frequency divider with external synchronization circuit creates a fiducial signal synchronized to the accurate injection timing from the injector event system. As the Log-Ratio turn-by-turn monitors (Digitex 18k11) need clock timing deviation to the beam signal within 8 ns, the cable length from the BPM heads to the detectors have been adjusted with the maximum deviation less than 1 ns using TDR. The time delay to adjust each cable lengths and the BPM placements have been created by using 32-ch RF timing delay with the step of 2 ns. The start trigger to the 18k11 has been made by using the digital delay (SRS DG645) from the injection trigger. The measured performance of the frequency divider, the 32-ch RF timing delay and start trigger system will be shown.

INTRODUCTION

The KEKB collider has been upgraded to the SuperKEKB collider with a final target of 40 times higher luminosity than that of KEKB. It consists of a 7 GeV high energy ring (HER, electrons) and a 4 GeV low energy ring (LER, positrons). About 2500 bunches per ring will be stored at total beam currents of 2.6 A (HER) and 3.6 A (LER) in the final design goal.

Due to strong focus at the interaction point, the dynamic apertures of both rings will be spoiled with the squeezing of the beam. To cure the LER injection efficiency and to reduce the beam noise coming from injected beam, the positron damping ring (DR) has been constructed in the linac with energy of 1.1 GeV after the production target, to damp the emittance of the positron beam. Table 1 shows the main parameters of the SuperKEKB damping ring.

Since the beam circulating time in the normal operation is short, from 40 ms to 200 ms depending on the injection repetition, and since the bucket filling pattern and injected bucket changes due to the bucket selection system to fill the beam as uniform as possible at LER, we have decided to use turn-by-turn beam position detector with Log-Ratio detection scheme using Digitex 18K11 [1]. As it is the time-domain detection system, we need to prepare following timing signals:

- Position data acquisition start trigger with good time relationship from the injected beam.
- Master clock timing for the ADC of 18K11 (Fiducial, 2.21 MHz) synchronized to the measuring bunch.
- Delayed timing to compensate the BPM placements in the ring and cable delays for each BPM.

To generate such timing signals, we have developed following timing generation circuits:

- RF frequency divider with external synchronization circuit using Zynq FPGA.
- Multi-channel (32-channels) digital delay working with the RF timing using Zynq FPGA.
- Start trigger generator with fine digital delay starting from the external signal (injection timing) under the software control (enable /disable start).

The measured performance of the systems such as the jitter of the timing will be shown in this paper.

Table 1: Major Parameters of SuperKEKB Rings

	DR
Energy (GeV)	1.1
Circumference(m)	135.5
Max. Beam current (mA)	70.8
Max. Number of bunches	4
Bunch separation (ns)	>96.3
Natural bunch length (mm)	6.5
RF frequency (MHz)	508.887
Harmonic number (h)	230
T. rad. damping time (ms)	11
x-y coupling (%)	5
Beam emittance at Inj (nm)	1700
Equilibrium emittance (nm)	41.4/2.07
Max. injection rate (Hz)	50
Number of BPMs	83
Number of BPM stations	4

BEAM POSITION MONITORS

Since the storage time of a beam in DR is normally short, less than 200 ms, we have constructed the turn-by-turn based beam position monitor systems with Log-Ratio detector (Digitex 18K11). From the measured narrow pulse response of 18K11 detector shown in Fig. 1, we have adjusted the timing deviations between the four signal-

*makoto.tobiyama@kek.jp

ISBN: 978-3-95450-192-2 doi:10.18429/JACoW-IBIC2017-TUPCF10

MEASUREMENT OF THE LONGITUDINAL COUPLED BUNCH INSTABILITIES IN THE J-PARC MAIN RING

Y. Sugiyama*, M. Yoshii, KEK/J-PARC, Tokai, Ibaraki, Japan
F. Tamura, JAEA/J-PARC, Tokai, Ibaraki, Japan

Abstract

The J-PARC Main Ring (MR) is a high intensity proton synchrotron, which accelerates protons from 3 GeV to 30 GeV. Its beam power for the fast extraction reached 470 kW, which corresponds to 2.4×10^{14} protons per pulse, in February 2017, and the studies to reach higher beam intensities are in progress. We observed the longitudinal dipole coupled bunch instabilities in the MR for the beam power beyond 470 kW. To investigate the source of the instabilities and to mitigate them, we analyzed the beam signals throughout the acceleration cycle to obtain the oscillation modes and their growth by using two methods. One focuses the motion of the bunch centers and the other used the frequency spectrum of the beam signal. We describe the methods and the measurement results of the longitudinal coupled bunch instabilities in the J-PARC MR.

INTRODUCTION

The Japan Proton Accelerator Research Complex (J-PARC) is a high intensity proton accelerator facility, which consists of the 400 MeV linac, the 3 GeV Rapid Cycling Synchrotron (RCS), and the 30 GeV Main Ring (MR). The MR delivers the proton beams to the neutrino experiment by the fast extraction (FX), and to the hadron experiments by the slow extraction (SX). The operation parameters of the J-PARC MR and the RF system for the fast extraction are shown in Table 1.

Table 1: Operation Parameters of the J-PARC MR and the RF System for the Fast Extraction

energy	3–30 GeV
repetition period	2.48 s
accelerating period	1.4 s
accelerating frequency f_{RF}	1.67–1.72 MHz
revolution frequency f_{rev}	185–191 kHz
harmonic number h_{RF}	9
number of bunches N_b	8
maximum rf voltage	300 kV
fundamental harmonic cavities	7
second harmonic cavities	2
Q-value of rf cavity	22

The MR delivers 2.4×10^{14} protons per pulse, which corresponds to the beam power of 470 kW, to the neutrino experiment as of February 2017, and studies toward higher beam intensity are in progress. During studies, the longitudinal bunch oscillation appeared to be an issue to achieve higher beam intensities than 500 kW.

* yasuyuki.sugiyama@kek.jp

LONGITUDINAL BUNCH OSCILLATION IN THE J-PARC MR

The beam signal from an Wall Current Monitor (WCM) [1] is recorded by an oscilloscope, LeCroy WP715Zi, with the sampling frequency of 500 MHz.

Figure 1 shows the typical mountain plot of the beam signal at the beam power of 480 kW for the fast extraction during the studies. The bunches start the dipole oscillations from the middle of the acceleration and their amplitudes keep increasing until the extraction. One can notice that the amplitudes and the phases of the oscillations of the bunches are different.

This kind of the oscillations is called the coupled bunch (CB) oscillation, and the instability caused by the CB oscillation is called the CB instability (CBI). The identification of the CB oscillation mode is necessary to find the source of the CBI.

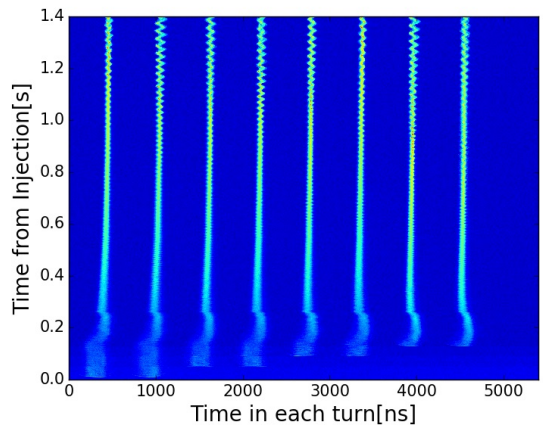

Figure 1: The mountain plot for the fast extraction in the J-PARC MR with the beam power of 480 kW during the studies.

COUPLED BUNCH OSCILLATION

For M bunches, there are M modes of the CB oscillation with the mode number $n = 0...M-1$. The phase difference of the synchrotron oscillation between adjacent bunches is $2\pi n/M$. For each mode, all bunches oscillate with the same frequency and the amplitude but with different phases.

The CB modes can also be seen in the spectrum of the beam signal as sidebands of the harmonic components [2].

ISBN: 978-3-95450-192-2 doi:10.18429/JACoW-IBIC2017-TUPCF11

UPGRADE OF THE BEAM POSITION MONITORING SYSTEM AT THE J-PARC MAIN RING FOR HIGH INTENSITY OPERATION *

Aine Kobayashi†, Takeshi Toyama, Kenichiro Satou, Hironori Kuboki,
High Energy Accelerator Research Organization (KEK),
J-PARC Center, Tokai-mura, Naka, Ibaraki, Japan

Abstract

For the T2K neutrino oscillation experiment an upgrade programs of J-PARC are on-going for higher beam intensity. The goal of 10-year upgrade plan is to achieve a beam power of 1.3 MW in the main ring [1], a significant increase compared to the presently achieved power of 470 kW. Beam loss causes the limitation on the proton bunch intensity. A precise orbit correction is necessary in order to reduce the beam loss. Beam position monitor (BPM) is a vital element providing accurate measurements of the beam positions for the control of closed orbit distortion (COD). The current position resolution is a few 10 μm in the COD mode, a few 100 μm in the turn-by-turn mode [2], and the goal is make one tenth of it. Currently an apparent dependence of RMS of COD on the beam intensity is observed (about 100 ~ 200 μm). In order to understand the nature of the phenomenon, investigations are being made on the BPM response and its intensity dependence as well as on the effects of wake field, local orbit bumps to COD and septum. Status of the studies will be discussed.

PROCESSING CIRCUIT FOR THE MR BPMS

The BPM of the MR is a diagonal cut which is nondestructive to the beam, readout from both horizontal and vertical electrodes as shown in Fig. 1. The number of BPM is 186, placed around the MR. After signal processing with Fourier transformation, the position of the beam is defined. The calibration such as beam based alignment (BBA) and beam based gain calibration (BBGC) are implemented [3].

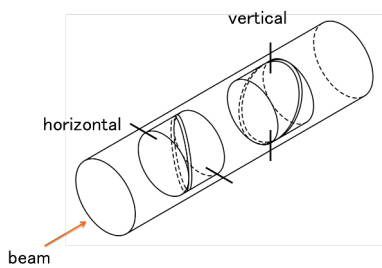

Figure 1: The schematic view of the MR BPM.

COD WITH INTENSITY DEPENDENCE

There are 9 RF buckets in the MR and up to 8 bunches can be filled. The kickers [4] inject bunches every 40 ms at K1, K2, K3 and K4 timing. After 10 ms of the K4 timing, acceleration is started. Usually, the RMS of COD is not dependent on the number of bunches. But an apparent dependence on the beam intensity is observed [5]. When the beam intensity exceeds about 10^{14} ppp, the RMS of COD is observed to grow by 100 ~ 200 μm as shown in Fig. 2.

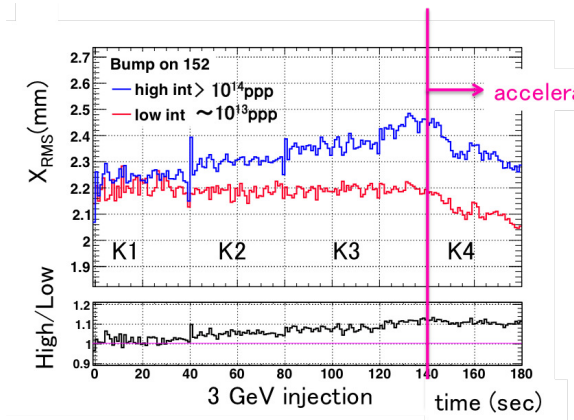

Figure 2: COD excursion of high intensity (> 10^{14} ppp) compared to low intensity (~ 10^{13} ppp) with bump on QFR152.

MEASUREMENTS

Referring to the study which investigated the COD made by a transverse impedance of a local bump in VEPP-4M accelerator, Russia [6], a measurement menu was contained with changing the local bump as well as changing a beam intensity. The fast extraction (FX) kicker and the septum are chosen as the position of the local bump. The size of bumps were arranged with the aperture and not to exceed beam loss about 10^{12} ppp. The taken sets with high beam intensity ($> 2.4 \times 10^{14}$ ppp) are: without bump, with a bump on QFR152 with 10 mm for the FX kicker, with a bump on QFR152 with 4 mm for the septum, and with bumps on both QFR152 (10 mm) and QFR82 (4 mm). Also, the data of low beam intensity (~ 6.0×10^{13} ppp) with a bump on QFR152 wih 10 mm. About 10 to 20 shots were taken for each sets. The MR power was 470 kW at most, with 3 GeV extraction. The number of bunches was up to 8.

BPM RESPONSE

It is necessary to examine BPM signals that are processed to the COD. The typical signals of high intensity beam are shown in Fig. 3, the number of counts from horizontal (upper) and vertical (bottom) electrodes. This measurement

* Work supported by JSPS-JP16H06288
† aine.kobayashi@kek.jp

ISBN: 978-3-95450-192-2 doi:10.18429/JACoW-IBIC2017-TUPCF12

MEASUREMENT OF EACH 324 MHz MICRO PULSE STRIPPING EFFICIENCY FOR H⁻ LASER STRIPPING EXPERIMENT IN J-PARC RCS

P.K. Saha*, K. Okabe, A. Miura, N. Hayashi, H. Harada and M. Yoshimoto
J-PARC Center, KEK & JAEA, Japan

Abstract

In 3-GeV RCS (Rapid Cycling Synchrotron) of J-PARC (Japan Proton Accelerator Research Complex), a proof-of-principle experiment for 400 MeV H⁻ stripping to protons by using only lasers is under preparation. The experiment requires precise measurements of all three charge fractions of only a single H⁻ micro pulse of 324 MHz at the downstream of laser and H⁻ interaction point (IP). It is very essential to establish a new measurement method for that purpose, which has not yet been studied anywhere in that direction. We consider measuring BPM (beam position monitor) pickup signal by using a fast oscilloscope with more than 4 GHz bandwidth. To test the system, we have done some experimental studies, where charge-exchange type beam halo scrapper, placed at the L-3BT (linac to 3-GeV beam transport) was used for H⁻ stripping. The un-stripped H⁻ and stripped proton (p) separated by bending magnets at the downstream of IP were simultaneously measured by two BPMs. The stripping efficiency of each 324 MHz micro pulse is precisely and separately obtained from the measured H⁻ and p pulses depending on the scrapper position settings. A detail of the present study results are presented.

INTRODUCTION

In 3-GeV RCS (Rapid Cycling Synchrotron) of J-PARC (Japan Proton Accelerator Research Complex), carbon stripper foil is used for multi-turn H⁻ stripping injection [1]. The injected beam energy is 0.4 GeV, while it is accelerated up to 3-GeV and simultaneously delivered to the muon and neutron production targets at the Material and Life Science Facility as well as injected into the Main Ring Synchrotron. At present RCS beam power for operation is much lower than its designed 1 MW, and no serious issues yet with foil lifetime. However, real lifetime and rapid foil failure due to overheating of the foil, especially at high intensity are always serious concerns [2]. The real lifetime means, how long a foil can be put in service until when foil degradation is tolerable. Foil degradation such as, change of foil thickness, pinhole formation as well as deformation of the foil deteriorate the stripping efficiency rapidly, resulting a significant increase of the waste beam at the injection beam dump. It is then determine the foil lifetime even if a foil failure does not occur [3]. On the other hand, residual activation near the stripper foil due to foil scattering beam losses during injection is also another uncontrollable factor and a serious issue for facility maintenance [4].

In order to overcome realistic issues and limitations involved in the conventional H⁻ stripping injection by using stripper foil, a POP (proof-of-principle) experiment for 400 MeV H⁻ stripping to proton (p) by using only lasers is under preparation at J-PARC [5]. Figure 1 shows a schematic view of present method [6]. Similar to the laser-assisted H⁻ stripping method [7], it also has 3 steps, but high field magnetic stripping in the 1st (H⁻ to H⁰) and 3rd (H⁰* to p) steps are replaced by lasers. Widely available high power Nd:YAG lasers can be used for those purposes in order to utilized large photo-detachment and photo-ionization cross sections [8], in the former and later steps, respectively. The 2nd step is an excitation of ground state (n=1) H⁰ atoms to two level higher (n=3) states, where we considered ArF Excimer laser of 193 nm for that purpose. The strategy of

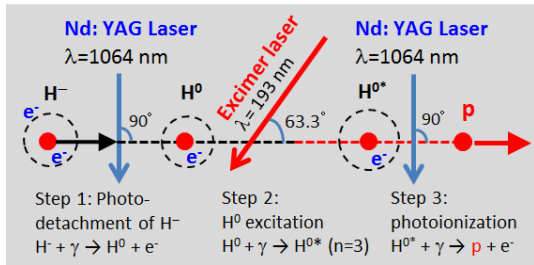

Figure 1: Schematic view of principle for H⁻ stripping to proton by using only lasers. Noted parameters are typical ones estimated for 400 MeV H⁻ beam energy.

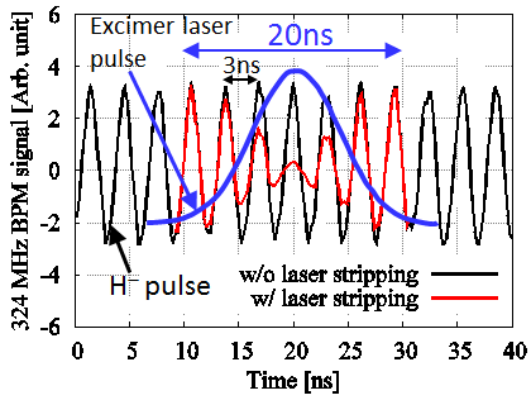

Figure 2: The H⁻ (black) micro pulse signal measured by BPM pickup. The blue curve is a typical laser pulse. The red curve is an expected H⁻ signal out of the laser pulses.

POP experiment is to strip only a single H⁻ micro pulse of 324 MHz. This is because, the whole micro pulses (~ 10^5) can be covered by using laser storage ring [9], which is under development for this purpose. The POP experiment requires precise measurements of not only the stripped protons but also (if any) neutral H⁰ and H⁻ of only a single micro pulse at the downstream of laser and H⁻ interaction

* E-mail address: saha.pranab@j-parc.jp

ISBN: 978-3-95450-192-2 doi:10.18429/JACoW-IBIC2017-TUPCF13

NEW DESIGN OF A TAPERED-COUPLER BPM TOWARD SIMPLER GEOMETRY AND FLATTER FREQUENCY RESPONSE*

T. Toyama†, T. Koseki, H. Kuboki, M. Okada, KEK, Ibaraki, Japan
W. Uno, A. Ichikawa, K. Nakamura, T. Nakaya, Kyoto University, Kyoto, Japan

Abstract

The tapered-coupler stripline beam position monitor has been used for the intra-bunch feedback system in the J-PARC MR. It should be realized with a special shaped stripline whose width is tailored exponentially and whose gap distance between the inner surface of the beam pipe should be also decreasing as a exponential function in order to keep the characteristic impedance at 50 ohm. This 3D varying geometry makes it difficult to achieve the good balance between the electrode responses to the beam. We propose a new design method with a groove, which may give simpler geometry and flatter frequency response.

INTRODUCTION

In J-PARC (Japan Proton Accelerator Research Complex) a 10-year upgrade plan is running in which a proton beam power is to be upgraded from 470 kW to 1.3 MW in the Main Ring [1]. In this process an intra-bunch transverse feedback system plays an important role [2,3]. As operating beam intensity gets higher, growth rate of collective instabilities becomes larger. In addition a wider operating condition search in which betatron tune and/or chromaticity are optimized for a stable incoherent motion sometimes conflicts with the stability of collective motions. It is, therefore, crucial to get the stronger damping of the collective instabilities. We observe the larger Δ-signal in the vertical plane as shown in Fig.1. We are using the tapered-coupler BPM as a position sensor (Fig.2) [3]. Investigation of the bench test data with TDR indicates that one vertical electrode is deformed. Due to the wideband characteristic of this monitor and its high pass filter response, the unbalance seems to become large in high frequencies. It is still unclear because the FIR filter in the signal processing system should reduce the revolution signal, yet we have larger output in the vertical system and cannot raise the loop gain. A good balanced electrode pair needs better machining and assembling of the three dimensionally shaped electrodes, which seems not straightforward. This motivates the new design of a tapered-coupler BPM toward simpler geometry. This design can also achieve flatter frequency response that was difficult in the previous design.

PROPERTIES OF STRIPLINE PICKUPS

The stripline pickup with straight electrode is schematically shown in Fig. 3. The signal is terminated with resistors at both ends. The coupling constant of the pickup which is defined as the induced voltage on the pickup per unit beam current, is constant, k_0, in this case [4]. With the relativistic beam ($v \approx c$) and the electrode length ℓ, we obtain the frequency response as

$$F(\omega) = jk_0 e^{-j\omega\ell/c} sin(\omega\ell/c).$$

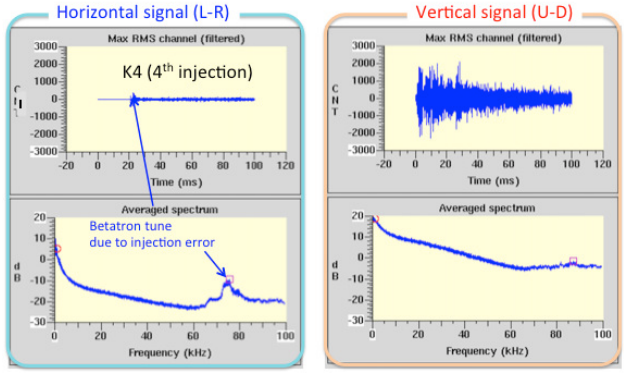

Figure 1: Signals from the left-right pair (left plots) and up-down pair (right plots). Upper plots are time domain signals and lower plots are frequency domain signals.

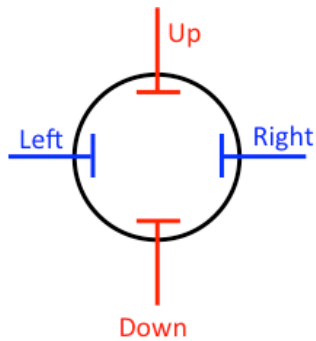

Figure 2: Layout of the BPM electrodes.

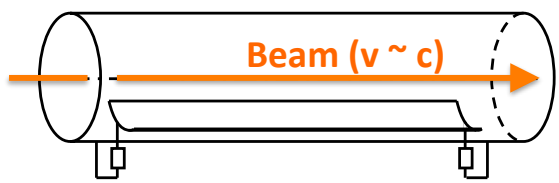

Figure 3: Stripline pickup with a constant electrode width.

In the case of an exponentially tapered stripline as Fig. 4, the coupling constant is $k(z) = k_0\, e^{-\alpha z/\ell}$ and the frequency response is

* Work partially supported by MEXT KAKENHI Grant Number 25105002
† takeshi.toyama@kek.jp

ISBN: 978-3-95450-192-2 doi:10.18429/JACoW-IBIC2017-TUPCF14

BENCHTOP BPM CALIBRATION USING HELICAL PULSE LINES FOR NON-RELATIVISTIC BEAMS*

C. Richard#, National Superconducting Cyclotron Laboratory, East Lansing, USA
S. Lidia, Facility for Rare Isotope Beams, East Lansing, USA

Abstract

Calibration of capacitively-coupled beam position monitors (BPMs) for use in non-relativistic beam lines has proven to be challenging. This is due to the fields generated by the beam being non-transverse causing the measured signals to depend on the measured frequency and the beam velocity [1]. In order to correct for these effects, calibration of BPMs may be done with an apparatus that is capable of simulating the fields generated by non-relativistic beams for several beam velocities. One possible method of simulating these beams is to use a helical pulse line. This paper studies the ability of helical lines to simulate the fields generated by slow beams for BPM calibration.

INTRODUCTION

Capacitative beam position monitors (BPMs) are commonly used to measure the orbit of relativistic beams in particle accelerators. They can also be used in non-relativistic beamlines, however, the measured positions from the BPMs become dependent on the beam velocity and measurement frequency [1, 2]. These effects are due to the electromagnetic fields generated by the beam no longer being pancaked by relativistic effects. For an off axis beam, this results in a difference in the extents of the fields along the pipe which cause the BPM pickups on opposite sides to measure a different frequency spectrum. This effect needs to be carefully calibrated in order to achieve accurate measurements.

Typical calibration of BPMs is performed using a straight wire strung through the BPM. Signals are sent down the wire that create electromagnetic fields that mimic the fields generated from a beam. The wire is moved along a grid of positions in the pipe and at each location the position of the wire is calculated from the BPM signals using a difference-over-sum formula. By comparing the calculated wire positions to the actual positions, non-linear effects and abnormalities in the measured positions can be determined.

However, signals on a straight wire propagate at the speed of light, therefore straight wires cannot be used to calibrate BPMs that will be used to measure non-relativistic beams. Currently, BPMs for non-relativistic beamlines are calibrated primarily with simulations to determine non-linear effects as well as frequency and velocity dependence of the measurements. Benchtop, straight wire calibrations are also performed to determine the effects of any physical abnormalities of each BPM [3].

To ensure proper calibration of BPMs for use in non-relativistic beamlines, the signals sent through the BPM should travel at the expected beam velocity to properly simulate the fields on the pick-ups.

Helical Wire Phase Velocity

One method to propagate signals at low velocities is to send pulses down a helical wire. Helical lines in free space have been shown to propagate signals at any phase velocity less than the speed of light by choosing the correct parameters for the helix [4].

A singal propagating down a helical line can be modelled using the sheath helix approximation. A sheath helix is constructed by winding a thin wire in a helix. A second thin wire is then wound directly above the first and this process

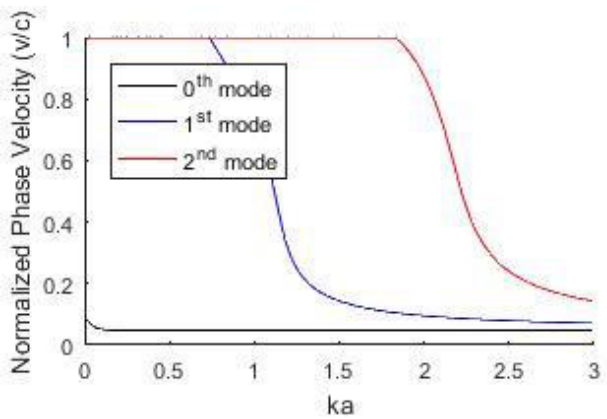

Figure 1: Normalized phase velocity of the first three modes of a sheath helix, pitch angle is 0.048 rad and R/a=4. K is the free space propagation constant and a is the helix radius.

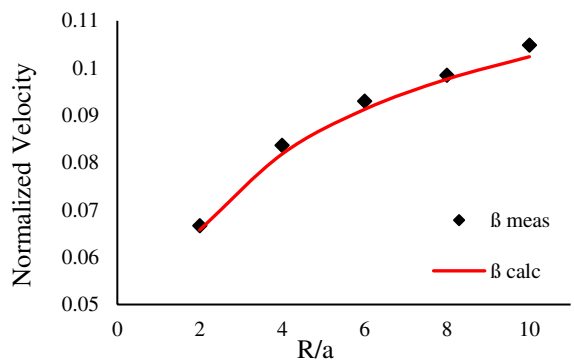

Figure 2: Velocity comparison for different ratios of pipe radii, R, to helix radius, a. Sheath helix phase velocity of 0th mode in red and results of simulations in black.

* Work supported by Michigan State University and the National Science Foundation: NSF Award Number PHY-1102511
#richard@nscl.msu.edu

ISBN: 978-3-95450-192-2 doi:10.18429/JACoW-IBIC2017-TUPCF15

S-BAND CAVITY BPM READOUT ELECTRONICS FOR THE ELI-NP GAMMA BEAM SOURCE

M. Cargnelutti, B. Baričevič, Instrumentation Technologies, Solkan, Slovenia
G. Franzini, D. Pellegrini, A. Stella, A. Variola, INFN-LNF, Frascati, Italy
A. Mostacci, Sapienza Università di Roma, Rome, Italy

Abstract

The Extreme Light Infrastructure – Nuclear Physics Gamma Beam Source (ELI-NP GBS) facility will provide an high intensity laser and a very intense gamma beam for various experiments. The gamma beam is generated through incoherent Compton back-scattering of a laser light off a high brightness electron beam provided by a 720MeV warm LINAC. The electrons are organized in compact trains with up to 32 bunches, each separated by 16ns. To optimize the laser-electron interaction and therefore the generation of the gamma rays, one big challenge is to precisely monitor the trajectory of each electron bunch.

To match this requirement, at the interaction point two S-band cavity beam position monitors will be used, and the related readout system should perform bunch-by-bunch position measurements with sub-µm resolution. Using 500MS/s ADC converters and dedicated data processing, the readout system proposes an alternative measurement concept. In this paper the architecture of the system, the implemented signal processing and the results of the first laboratory tests will be presented.

INTRODUCTION

The ELI-NP accelerator facility employs a warm C-band electron LINAC [1]. At every injection, up to 32 electron bunches are accelerated and delivered to two interaction points (IP) with energies of 280MeV and 720MeV. The beam structure at the interaction point is represented in Figure 1.

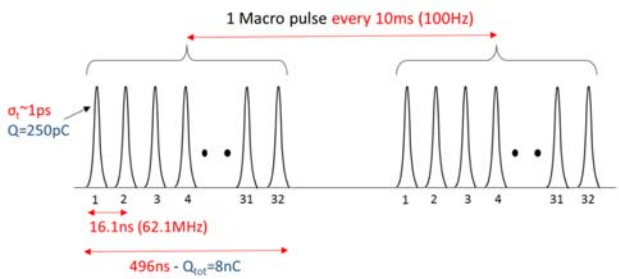

Figure 1: Electron beam structure at the interaction point.

In order to align the beam with the laser at the IP, the position of each bunch should be measured with µm resolution, in the range of ±1mm. For this purpose four low-Q cavity beam position monitors (BPMs) will be installed immediately before and after the IPs [2].

The cavity BPM pick-up is the same BPM16 used at PSI [3]. It consists of one reference cavity and one position cavity, with low quality factor (Q=40) and a resonant frequency of 3.284GHz. This makes sure that the signal excited by each bunch will decay fast enough to not interfere with the signal coming from the next bunch: this is necessary condition to perform individual bunch measurements.

THE READOUT ELECTRONICS

The concept and a first prototype of readout electronics was presented in [4] and further developed into a commercial readout electronics called Libera CavityBPM, shown in Figure 2.

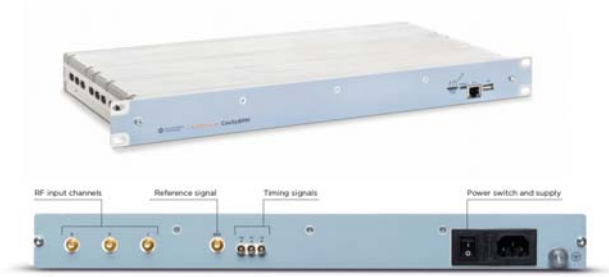

Figure 2: Cavity BPM readout electronics.

The cavity signals are processed by an RF front-end, which filters out the unwanted frequency components. A variable attenuation stage is used to adjust the position full-scale and to optimize the signal level depending on the beam conditions (e.g. charge, position). Finally the signals are down-converted to an intermediate frequency (IF) in the 2nd Nyquist zone, and filtered again to remove the signal components which are outside of the bandwidth of interest. A block-scheme of the RF front-end is shown in Figure 3.

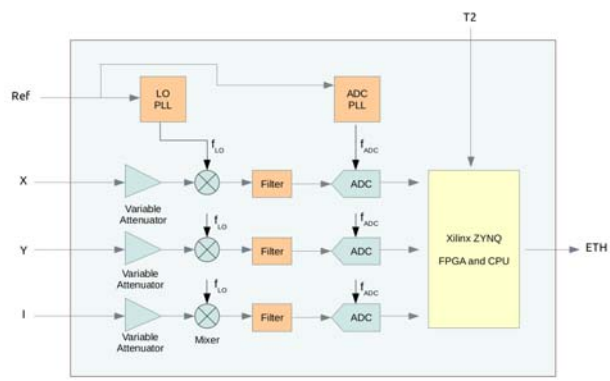

Figure 3: RF front-end of the readout electronics.

ISBN: 978-3-95450-192-2 doi:10.18429/JACoW-IBIC2017-TUPCF16

STRIPLINE BEAM POSITION MONITOR MODELLING AND SIMULATIONS FOR CHARGE MEASUREMENTS

G. Castorina*, A. Mostacci, M. Maroungiu, University of Rome "La Sapienza", Rome, Italy
G. Franzini, B. Spataro, INFN-LNF, Frascati (Rome), Italy
A. A. Nosych, ALBA-CELLS, Barcelona, Spain

Abstract

Strip line Beam Positions Monitors (BPMs) are the main devices used for non-intercepting position measurement for the electron LINAC of ELI-NP (Extreme Light Infrastructure - Nuclear Physics). All the 29 BPMs have the same design, with the exception of the one installed in one of the dump line, which has a much larger acceptance than the others. BPMs will also be used to measure the charge of the beam, by measuring the sum of the pickups signals and calibrating it with beam charge monitors installed along the LINAC. An analytical model has been developed for the proposed BPMs. This model has been checked by means of electromagnetic simulations, in order to obtain the pickups signals at the passage of the beam and to study the effects of BPMs non-linearities, particularly on charge measurements. Details of the analytical model, results of the numerical simulations and the correction algorithm proposed for charge measurements are described in this paper.

INTRODUCTION

An S-Band photo-injector and a C-band LINAC will be used at the Compton Gamma Source in construction at the ELI (Extreme Light Infrastructure) Nuclear Physics facility in Romania. They will operate with a repetition rate of 100 Hz with macro pulses of 32 electron bunches, separated by 16 ns and with 25–250 pC nominal charge range and a temporal duration of 0.91 ps [1].

Stripline BPMs will be installed along the beam path in order to measure the position of bunches. Each BPM has an approximate length of 235 mm and is composed by four steel electrodes with an angular width of 26 deg. The distance from the beam pipe is 2 mm and they have a width of 7.7 mm, see Fig. 1. The impedance of the transmission line created by the the electrode and the pipe chamber is roughly 50 Ω. The acceptance of the BPM is 34 mm. A further BPM with an acceptance diameter of 100 mm will be installed on the dump line after the low energy interaction point. [2]. The BPMs on the beam line have been calibrated on a test bench. On the contrary the dump line BPM cannot be calibrated with the test bench used for the other BPM because of its larger dimension.

These BPMs can be also employed to measure the macro pulse charge. By this way it is possible to have a non destructive estimation of the macro pulse charge along the beam line. Four Integrating Current Transfmorers (ICT) will be installed in the critical points of the machine: after the RF gun of the photo-injector, after the first six accelerating structures and before the interaction chambers. The measurement of the bunch charge is proportional to the sum of the four voltage signals from the output ports of the BPM. However, due to the non linear behaviour of the pick-up devices, a calibration curve should be applied to the readings. A full characterization of the voltage signals picked from the output port of the BPMs has been done by means of an analytical model and with full 3D simulations. Aim of this work is the development of a numerical calibration method for the charge measurement. The curve obtained with the simulation results has been compared with the experimental data and an estimation error is provided. This numerical method will be used for the calibration of the BPM for the dump line.

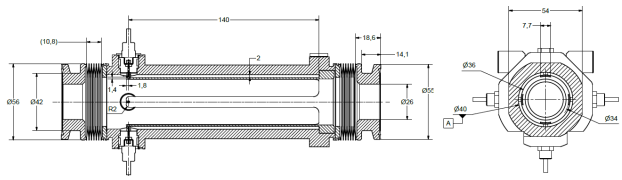

Figure 1: Main BPM CAD model for ELI-GBS. Units in mm.

CHARACTERIZATION OF A STRIP LINE BPM AS A CHARGE MONITOR

The BPMs described in the previous paragraph have been characterized with an approximate analytical method and with the aid of 3D electromagnetic simulations. The results are summarized and compared with the measurements in Fig. 2. The curves in the three analysis cases (analytical model, simulations and measurements) have been evaluated over a grid of 841 points with 29 points for both horizontal and vertical axis. The points are in the span length of ±7 mm around the centre with a fixed step of 0.5 mm. The traces have been normalized to the central value of the grid.

The excitation signal used in the measurement setup is a 500 MHz sinewave. Therefore it is not a reproduction of the ELI_NP macro pulse charge and only a comparison of the normalized curves is possible. The normalization is based on the measurements in the central position, i.e. $y = x = 0$.

The agreement between the analytical model, the simulation results and the measurements is quite good. The measurements have been carried out at ALBA with the wire stretching method [3]. The details of the analytical model and of the simulation analysis are described in the next sections.

* giovanni.castorina@uniroma1.it

ISBN: 978-3-95450-192-2 doi:10.18429/JACoW-IBIC2017-TUPCF17

FIRST BEAM COMMISSIONING EXPERIENCE WITH THE SwissFEL CAVITY BPM SYSTEM

Boris Keil, Raphael Baldinger, Robin Ditter, Daniel Engeler, Waldemar Koprek, Reinhold Kramert, Fabio Marcellini, Goran Marinkovic, Markus Roggli, Martin Rohrer, Markus Stadler, Daniel Marco Treyer, Paul Scherrer Institute, Villigen, Switzerland

Abstract

SwissFEL is a free electron laser facility designed to produce FEL radiation at wavelengths from 0.1 to 7 nm. The beam commissioning of its hard X-ray undulator line ("Aramis") started 10/2016, and first lasing was observed in 12/2016. Presently, a 2nd undulator line ("Athos") for soft X-rays is being constructed, with 1st beam scheduled for mid-2019. In the injector, linac and Aramis beam transfer lines, 95 low-Q cavity BPMs operating at 3.3 GHz are used that were designed to support the future two-bunch operation mode with 28 ns bunch spacing and 100 Hz repetition rate. The Aramis (and future Athos) undulator lines will only be operated with single bunches by means of a fast beam distribution kicker system, and are thus equipped with high-Q cavity BPMs operating at 4.9 GHz. The BPMs are not only used for beam trajectory optimization, but also for beam energy measurements (using standard cavity BPMs in the bunch compressors and beam dumps), beam charge and transmission measurements, or improvement of the performance of other monitors like wire scanners for profile measurement. This paper will report about the first operation experience with the BPM system, including a performance comparison of low-Q and high-Q BPMs.

INTRODUCTION

BPM Pickups

Table 1 gives an overview of the number and type of BPMs (119 overall) that are presently operational in SwissFEL. CBPM38 low-Q pickups are only used at a few locations where their large aperture is needed (1st bunch compressor, beam distribution area, beam dumps). Undulator intersections are equipped with high-Q CBPM8 pickups, while low-Q CBPM16 pickups are used everywhere else.

Table 1: SwissFEL BPM Types and Quantities

	CBPM38	CBPM16	CBPM8
Quantity	7	96	24
Usage	Linac, Transfer Lines		Undulators
Aperture	38 mm	16 mm	8 mm
Length	255 mm	100 mm	
#Bunches/ Train	1-3		1
Bunch Spacing	28 ns		10 ms
Frequency	3.2844 GHz		4.9266 GHz
Q_L	40		1000

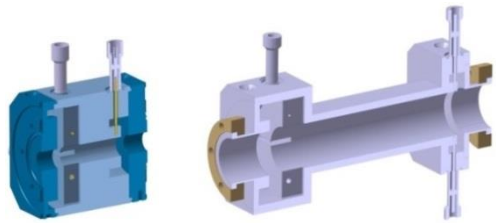

Figure 1: SwissFEL CBPM16 pickup (left) and CBPM38 pickup (right).

CBPM38 and CBPM16 pickups (shown in Figure 1 and Figure 2) differ in aperture and length, but were designed to deliver (nearly) the same sensitivity and RF parameters [1], thus providing similar performances.

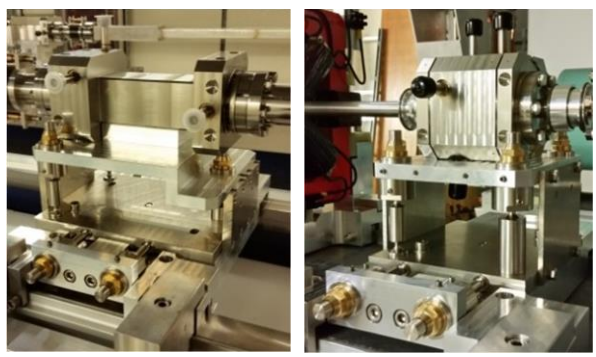

Figure 2: CBPM38 (left) and CBPM16 pickup (right) with manually adjustable supports.

Like the SwissFEL C-band accelerating structures, the BPM pickups (incl. CBPM8) have no tuners but were precision-machined to the nominal frequency and other RF parameters. The achieved very small deviations [1] have negligible impact on the performance.

The position resonators of the pickups have two ports both for the horizontal (X) and vertical (Y) position signals. The two signals in each plane are added using an external RF combiner near the pickup that is connected with short flexible low-loss cables, thus improving the position resolution at low charge.

The relevant RF parameters of all pickups and long-range ½'' Sucofeed RF cables from pickups to the electronics racks (located outside the SwissFEL accelerator tunnel) were measured before 1st beam. The results were used to verify the quality of the system and do determine scaling factors for the conversion of raw signal amplitudes to charge and position in physical units already before 1st beam, followed by a more accurate beam-based calibration that is still in progress.

ISBN: 978-3-95450-192-2 doi:10.18429/JACoW-IBIC2017-TUPCF18

THE SwissFEL HIGH-Q UNDULATOR BPM SYSTEM

M. Stadler*, B. Keil, F. Marcellini, G. Marinkovic, Paul Scherrer Institute, Villigen, Switzerland

Abstract

In 10/2016, PSI started the beam commissioning of Aramis, the hard X-ray undulator line of the SwissFEL free electron laser. The injector, linac and transfer line BPMs have 3.3 GHz low-Q cavity BPMs to support 2-bunch operation with 28ns bunch spacing. In contrast, Aramis as well as the future 2nd soft X-ray undulator line called "Athos" are equipped with 4.9 GHz high-Q cavity BPMs, since the undulator will only be operated with single bunches by means of a fast beam distribution kicker system. The undulator BPM system uses 4.9GHz double-resonator pickups having a nominal loaded-Q of 1000. The associated front-end electronics applies single-stage analog down conversion to a 135 MHz IF frequency, subsampling ADC and digital quadrature down conversion. A detailed description of the BPM pickup and front-end design and signal processing will be given. Laboratory test and calibration methods and results of pickups and electronics will be compared with first beam measurements.

INTRODUCTION

The SwissFEL Aramis beam-line BPM system uses three types of pickups: Low-Q (Q=40) at 3.3GHz having 16mm or 38mm aperture in the linac and transfer line sections, and high-Q (Q=1000) 4.9GHz with 8mm aperture in the undulator section. A detailed description of the pickup design is given in [1].

Bunch spacing is 28ns in linac and transfer sections. Hence, low-Q cavity BPMs (CBPMs) are used in order to minimize signal leakage from the first into the second bunch. In contrast, the undulator section operates only with single bunches at a maximum repetition rate of 100 Hz. A high-Q cavity pickup is adequate here and provides higher resolution.

FRONT-END ARCHITECTURE

The high-Q CBPM front-end uses a combined analog/digital two-stage frequency conversion scheme. Figure 1 shows the front-end block diagram. The BPM signal enters an RF chain consisting of a first variable attenuator, a first RF amplifier, a second variable attenuator, a second RF amplifier and a band-pass filter. The variable attenuators establish a gain range of 60dB. The band-pass filter is centered at the nominal pick-up signal frequency, which is 4926.6 MHz.

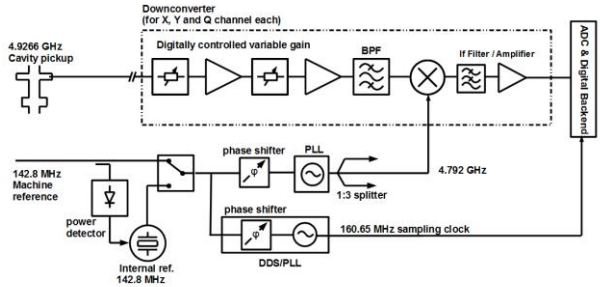

Figure 1: RFFE Block Diagram.

The band-pass filter rejects signal components and noise especially at the image frequencies, thereby improving resolution and reducing reading errors due to RF phase shifts. A local-oscillator signal at 4792 MHz is derived from a reference at 142.8 MHz. In the first (analog) down conversion stage the BPM signal is shifted to an IF frequency of 134 MHz. The IF section consist of an IF band-pass filter and an output amplifier. Both RF and IF stages are identical for position channels (x and y) and charge channel. A phase-adjustable 165.65 MHz clock used by the (separate) digitizer board is also generated on the RF front-end module. In nominal operation the reference frequency of 142.8 MHz is provided to the RFFE by the SwissFEL timing system. This signal is strictly bunch-synchronous. In case of reference failure an internal free-running reference oscillator switches in automatically. All frequencies generated are multiples of a common super-period frequency, which is 142.8MHz/72.

The second and final frequency conversion is done digitally on the separate FPGA board and will be described in the signal processing section.

Primary Design Guidelines

Development was guided by following major requirements:

- Nominal charge range: 10pC-200pC
- Useful readings below 1pC.
- No damage to the RFFE for charges up to 1nC, independent of gain setting.
- Single-shot resolution <1µm within nominal charge range
- Robust position and charge readings at varying RF phase and/or reference signal phase.

Front-End Module Construction

The front-end electronics is assembled on a 6-layer printed-circuit board. The size fits into a double width standard VME64x slot (Figure 2) of the modular BPM unit (MBU) crate. SMA connectors are provided at the

* markus.stadler@psi.ch

ISBN: 978-3-95450-192-2 doi:10.18429/JACoW-IBIC2017-TUPCF19

PRODUCTION TESTS, CALIBRATIONS, AND COMMISSIONING OF BUTTON BPMS FOR THE EUROPEAN XFEL*

D.M. Treyer, B. Keil, W. Koprek, PSI, Villigen, Switzerland
D. Lipka, DESY, Hamburg, Germany

Abstract

Commissioning of the entire European XFEL started early 2017. More than 300 button-electrode type beam position monitors (BPMs) are used in its cold Linac and warm beam transfer lines. Signal processing in the BPM RF front-end (RFFE) electronics employs signal stretching by chirp filtering, switchable gain stages, digital step attenuators, and peak detection. In this paper we present details on RF front-end production tests, calibration, and BPM beam commissioning results. Furthermore, a calibration pulser circuit that is built into each BPM electronics is presented. The setup and algorithms for production calibration of all RFFEs are described. Finally, resolution measurements obtained by correlation among all XFEL BPMs (including cavity and re-entrant types) are presented, confirming that the system can be used for orbit correction and transmission measurement down to bunch charges of a few pico-Coulombs.

INTRODUCTION

The European XFEL (E-XFEL) is a free electron laser with a 17.5 GeV superconducting linac and currently five experimental end stations with three undulators for producing trains of (sub-)fs-duration X-ray pulses with a wavelength range down to 0.1 nm. The accelerator works in train-pulsed mode at 10 Hz repetition rate. Up to 2700 bunches with a bunch spacing down to 222 ns can be produced in a single train. The accelerator is built in underground tunnels of >5 km total length. It is equipped with ~460 BPM pickups of five types: warm and cold buttons [1], cold re-entrant cavities, and warm dual-resonator cavities with two aperture sizes. More than 304 BPMs use cold and warm button pickups. The E-XFEL is an international project where Switzerland provides electronics for all electron BPMs [2] except 24 re-entrant BPM RFFEs, as well as the transverse intra-train beam based feedback system (IBFB) [3] as in-kind contributions. Production and commissioning of this comparatively large amount of BPM electronics motivated an automated production test system. The tasks of this test system include quality checks of the produced electronic boards, calibration and performance verification of complete BPM electronics, and documentation of test results as a part of the deliverables.

BUTTON BPM ELETRONICS OVERVIEW

Electronics for up to four button BPMs (four channels each) are housed in a modular BPM unit (MBU), a customized crate that can be used for different types of BPMs [4]. On the rear side it has slots for modular power supply and interface boards. On the front side it has slots for a digital carrier board (GPAC) with two analog-to-digital converter (ADC) mezzanine boards, and up to four button BPM RF front ends (RFFEs). Mixed configurations consisting of button, cavity, and/or re-entrant type BPMs are also possible.

The task of the RFFEs is to condition the signals from the beam pickups for digitization by the ADCs. Figure 1 shows the block diagram of the button BPM type RFFE [5]. One out of four identical channels is shown. In summary, the RFFE electronics first stretches the very short incoming pickup signal pulse by a dispersive chirp filter, then amplifies/or attenuates the stretched signal, and finally detects its amplitude by diode based peak detectors. An onboard pulser can generate pickup-like signals for beam emulation, self-testing, and calibration purposes. Switches at the RF inputs allow selection of the beam pickup or the on-board pulser signal.

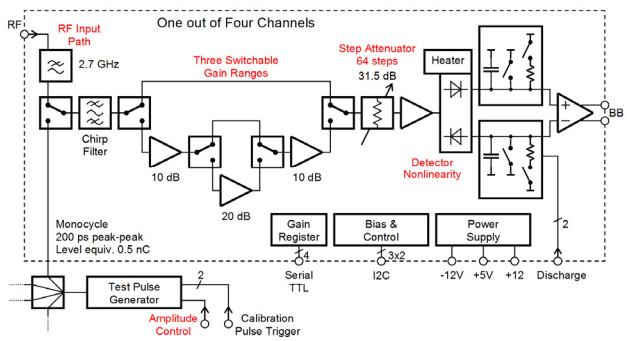

Figure 1: Block diagram of a single RFFE channel. Red labeled items need calibration.

CALIBRATION PULSER

The purpose of the onboard calibration pulser is to enable RFFE built-in test and calibration without the need for an external test signal source. The pulser should therefore ideally provide a signal having waveform, spectrum, and repetition rate matching the typical E-XFEL button pickup. An earlier design based on an avalanche transistor was later superseded by a design based on a step-recovery diode (SRD). This resulted in higher repetition rate (5 MHz), excellent pulse amplitude stability (1‰ rms), much better spectral matching to the pickup signal (peak at 2 GHz), and the ability to adjust the pulse amplitude (≈8 Vpp max.) over a wide range (26 dB).

Figure 2 shows the pulser block diagram. After the trigger rising edge, the SRD is forward biased during roughly 50 ns. Then the current is reversed and boosted

*Work supported by Swiss State Secretariat for Education, Research and Innovation.

ISBN: 978-3-95450-192-2 doi:10.18429/JACoW-IBIC2017-TUPCF20

COSY ORBIT CONTROL UPGRADE

C. Böhme, I. Bekman, V. Kamerdzhiev, B. Lorentz, S. Merzliakov, M. Simon, C. Weidemann
Forschungszentrum Jülich, Germany

Abstract

The Cooler Synchrotron COSY can store and deliver proton and deuteron beam in the momentum range from 0.3 GeV/c to 3.65 GeV/c for internal and external experiments. New requirements of the Jülich Electric Dipole Moment Investigation (JEDI) experiment requires a RMS beam orbit distortion smaller than 100 μm. This requirement lead so far to the replacement of the BPM readout electronics, an introduction of a slow beam orbit correction and feedback system and the re-alignment of the magnets. All three projects are close to completion, therefore first results are presented.

INTRODUCTION

The COoler SYnchrotron (COSY) of the Forschungszentrum Jülich is a 184 m long racetrack-shaped synchrotron and storage ring for protons and deuterons from 0.3 GeV/c (protons) or 0.6 GeV/c (deuterons) up to 3.65 GeV/c. Built in are devices for stochastic as well as electron cooling. The stored ions can be polarized or unpolarized. Commissioned in 1993, the machine was mainly used for target experiments. Therefore no special focus was laid on the beam orbit, as long as the target overlap was maximized.

With the JEDI (Jülich Electric Dipole moment Investigations) experiment new requirements concerning the overall RMS beam orbit deviation were introduced [1]. Therefore an automatized beam orbit control system was developed. Furthermore other components were identified being in need to be upgraded or to be added. One example is the analog BPM readout electronics, which offsets prevents an accurate position determination especially around the 0 position. Another example is the positioning of the magnets, which drifted out of their position over the years [2].

BPM SYSTEM

COSY is equipped with a total of 33 BPMs whereas 29 are shoebox-style BPMs utilizing a standard readout electronics. During commissioning of COSY 27 BPMs of two types were installed, a cylindrical type with 150 mm diameter and a rectangular type with 150 mm · 60 mm inner size [3]. The selection was made to fit into the beam pipe, which is round in the straight sections and rectangular in the arcs in order to fit into the dipole magnets. Recently 4 BPMs were added with special geometries. Two of them are designed to fit within the 2 MeV electron cooler [4]. Another 2 are based on Rogowski coils in order to have a minimal longitudinal length for the Wien Filter of the JEDI experiment [5]. These four use their own, non-standard electronics for readout.

Analog BPM Signal Processing

At the commissioning of COSY, a BPM readout system was build based on a mainly analog processing [6]. Pre-amplifiers are directly connected to the N-type vacuum feedthrough of the pick-ups. This pre-amplifier has a fixed gain of 13.5 dB with an input impedance of 500 kΩ and a bandwidth of 100 MHz (-3 dB). The gains and offsets of two pre-amplifiers have been exactly matched for one plane of one BPM in order to avoid incorrect measurements. The pre-amplified signals are fed into an analog processing module, where sum and delta signals are generated using a hybrid. These signals are then treated separately and can be further amplified in 6 dB steps from 0 dB to 66 dB. Both the sum and the delta branches have two signal paths. A narrowband path features 3 possible filter settings with bandwidths of 10 kHz, 100 kHz, or 300 kHz and an additional amplifier that can be set from 0 dB to 18 dB in 6 dB steps. A broadband path with 10 MHz bandwidth can be used for direct sampling of the signals. The analog outputs are unipolar, the sign of the narrowband delta signal is detected separately and the information is transmitted by a separate TTL signal line. After the analog signal processing the signals are digitized in a separate module. This is done using 20 MHz 8 bit ADCs. For the narrowband signal the sampling frequency is lowered to 1 MHz or 100 kHz, depending on the selected analog bandwidth. For the sum signal only 7 of the 8 bits of the ADC are used, the 8th bit is used to indicate the polarity of the delta signal. The digital module generally has the capability to buffer 4096 data points, while few modules can store up to 64k data points. The CPU in the VXI crate calculates out of the narrowband signal the beam position. It is also possible to transfer the raw broadband data to the control system in order to display and export it, for e.g. computation of the turn-by-turn position.

Despite the outdated digital hardware and the increasing failing rate, the main issue lays within the split signal path of the differential signal and the sign of the position. An offset of the differential signal is measured on all modules, even directly after calibration. Because of this the measured beam position never reaches the zero position [7]. Using the introduced orbit correction system this leads to incorrect correction settings.

Digital BPM Signal Processing

Because of these problems with the analog BPM signal processing system, a new system was introduced with digital signal processing. The decision was made to utilize the commercially available Libera hadron system [8]. The system was recently put into operation and commissioning is ongoing. First results are presented later in this article.

ISBN: 978-3-95450-192-2 doi:10.18429/JACoW-IBIC2017-TUPCF21

TRANSVERSE DAMPER USING DIODES FOR SLIP STACKING IN THE FERMILAB RECYCLER*

N. Eddy#, B. Fellenz, P. Prieto, S. Zorzetti, Fermilab, Batavia, IL 60510, USA.

Abstract

During slip stacking in the Recycler, up to six batches of 84 bunches each are slipped by each other to and then captured to double the intensity of the extracted beam. For nominal chromaticity settings, a bunch by bunch transverse damper system is needed to maintain beam stability but this system is blind to the bunches as they are slipping. The initial solution was to drastically raise the chromaticity to keep the beam stable. A new frequency based damper using diode detectors was developed to provide damping during slip stacking and allow the chromaticity to be reduced to nominal settings.

INTRODUCTION

Slip stacking refers to the process in which batches (84 bunches) of beam are injected and captured with slightly different RF systems so that they have slightly different energies and travel on separate orbits allowing them to slip by one another. The process was first implemented in the Main Injector to increase proton beam power for the MINOS neutrino experiment at Fermilab [1]. As part of the NOvA neutrino upgrade the Recycler anti-proton storage ring which shares the same tunnel with the Main Injector was re-purposed as a proton stacker [2]. In this configuration, slip stacking is done in the Recycler while the Main Injector is ramping which allows the overall cycle time to be reduced, further increasing the beam power.

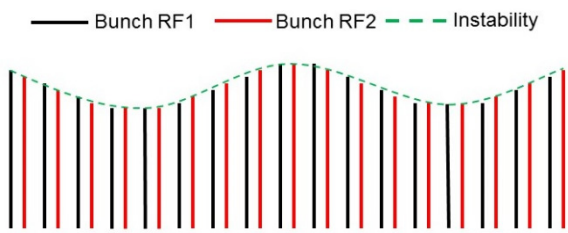

Figure 1: Cartoon showing slip stacking bunches with coupled bunch instability superimposed.

Initially the Recycler had a bunch by bunch digital damper very similar to the one used in the Main Injector [3]. These bunch by bunch systems were blind during the slipping process and needed to be disabled. This drastically increased chromaticity and subsequently tunes to provide beam stability while the dampers were off. As the Recycler struggled to reach design intensity, the high losses during the slipping forced the development of a system capable of damping the beam during the slip stacking.

* This work was supported by the DOE contract No.DEAC02-07CH11359 to the Fermi Research Alliance LLC.
# eddy@fnal.gov

As shown in Figure 1, the damper is required to suppress the coupled bunch instabilities which are dominant at low frequencies. The first mode is at about 50KHz and the expected bandwidth is a few MHz. Because the two beams are effectively coupled, we just need to detect the envelope of the instability frequency.

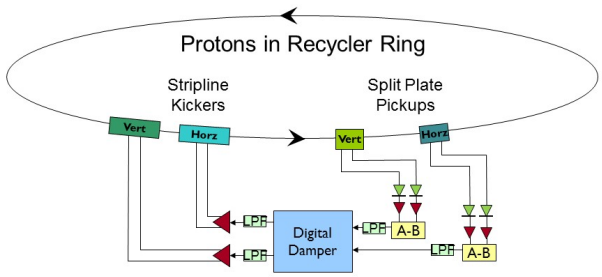

Figure 2: Overview of the current Diode Damper system in the Recycler.

SYSTEM OVERVIEW

The slip stack damper was implemented using existing components from the original Recycler anti-proton damper [4]. An overview of the system is shown in Figure 2. The system consists of a BPM pickup, input filters, digital signal processing, output amplifiers, and stripline kickers. To damp the slip stacked beam, a technique to detect the relatively low frequency coupled bunch beam instability was developed.

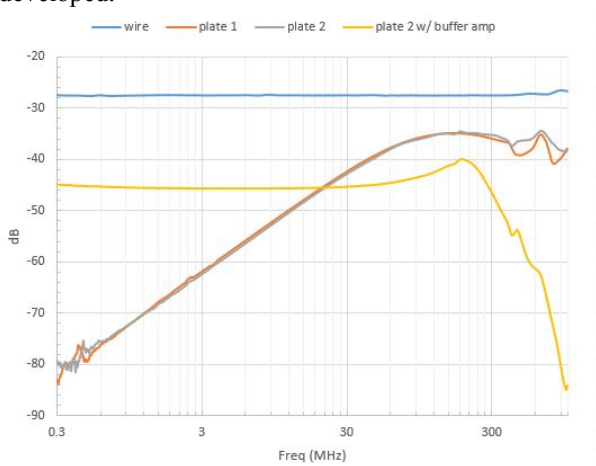

Figure 3: Measured frequency response for the split tube beam position monitor using a frequency matched wire.

The Pickup Response

The damper system uses the same split plate pickups installed in the Recycler . To measure anti-proton beam, high impedance pre-amps were installed in the tunnel to extend the frequency response of the pickup down to about 100KHz. The frequency response of the pickups is shown

ISBN: 978-3-95450-192-2 doi:10.18429/JACoW-IBIC2017-TUPCF23

FIRST BEAM TESTS AT THE CERN SPS OF AN ELECTRO-OPTIC BEAM POSITION MONITOR FOR THE HL-LHC

A. Arteche*, S. E. Bashforth, G. Boorman, A. Bosco, S. M. Gibson,
Royal Holloway, University of London, Egham, UK
N. Chritin, M. Krupa, T. Lefèvre, T. Levens, CERN, Geneva, Switzerland

Abstract

An Electro-Optic Beam Position Monitor is being developed for the High Luminosity Large Hadron Collider (HL-LHC), aimed at the detection of high order proton bunch instabilities and as a diagnostic for crabbed bunch rotation. A prototype EO-BPM was installed in the CERN SPS during 2016 and recent first beam tests of the EO pick-up are presented. The tested system comprises two opposing pick-ups, each equipped with 5 mm cubic $LiNbO_3$ crystals in vacuum, illuminated by polarized light from a fibre-coupled CW 780 nm laser. The 1 ns proton bunch induces a temporal modulation in the polarization state of light emerging from each birefringent crystal, by the Pockels effect. The modulation is analyzed, then recorded by a fibre-coupled fast photodetector in the counting room. The very first experimental signals obtained by the EO pick-ups of a passing proton bunch are reported as a proof of concept of the idea. Moreover, the expected response of the beam signal is measured with respect to remotely controlled changes in the polarizer and analyser orientations. The data are compared with analytical and electromagnetic simulations. Following the first detection, we report the latest status of the prototype design and future prospects.

MOTIVATION

The crab cavities are one of the main upgrades in the High-Luminosity LHC scenario designed to induce a bunch rotation before and after the interaction point, in order to make the bunches collide head-on and thus maximizing the luminosity [1]. The control of the bunch rotation induced by the crab cavities requires precise diagnostic techniques capable of monitoring intra-bunch transverse position for a 1 ns proton bunch. Whereas the performance of conventional head-tail (HT) monitors is typically limited with a bandwidth of 6 GHz [2], the electro-optic (EO) BPM stands out as a promising innovative candidate aiming to perform with an improved time resolution (<50 ps) due to the faster optical response, expanding the bandwidth up to 10-12 GHz, sufficient for optimizing the crab cavities performance as well as the detection of high order HT instabilities.

Currently the technology is under development and a prototype has been successfully installed at the CERN SPS, where two variants were tested during the 2016 and 2017 SPS runs, respectively [3, 4].

* alberto.arteche.2014@live.rhul.ac.uk

ELECTRO-OPTIC PICK-UP PROTOTYPE

The EO pick-up prototype includes button-like devices that comprise a compact optical system formed of a $LiNbO_3$ (LNB) crystal sample and two prisms in combination with an optical beam (OB) [5]. Figure 1 depicts the design with the optical path superimposed for both prototype variants, zero and one: the 10 mm side right-angle prisms align the laser beam propagating in free-space through the crystal and back-reflect it out of the pick-up. The button body is shielded by a flange and a viewport that permits the transmission of the OB in and out of the optical system embedded in the vacuum.

The key piece of the EO pick-up is the LNB sample assembled in the core of the opto-mechanical body. The fundamental principle of detection exploits the Pockels effect exhibited by the LNB crystals, since its birefringence is modified by the action of the Coulomb field propagating from a passing particle bunch. The system imitates an EO amplitude modulator where the initial linear polarization at 45° is rapidly modified at the emerging beam by the action of the field on the crystal [6]. The extent of the optical modulation depends on the field strength and the crystal length. The output beam is incident upon an analyser which measures this modulation. Therefore, the transverse displacement can be obtained in the same fashion as the traditional BPM layouts, taking the difference in optical response between pick-ups on the opposite sides of the beam pipe.

The prototype pick-up variants differ when comparing the dimensions of the crystal and the use of electrodes. For pick-up zero, the propagating Coulomb field decays sharply at the crystal interface due to the LNB dielectric constant $\epsilon_{33} = \epsilon_z = 30$ in the propagating direction z [4, 7]. The field strength limitation caused by the dielectric constant can be partially overcome by placing electrodes to direct more field lines towards the crystal, following the mechanism shown in Figure 1. According to the CST simulations [8] carried out for each case using SPS nominal bunch of length 4σ=1 ns and intensity of 1.15×10^{11} protons, the estimated electric field in the crystal for pick-up zero is 0.65 kV/m whereas the field strength for pick-up one will be enhanced up to 2.8 kV/m. Furthermore, given the same field the optical modulation is enlarged by a factor 1.8 for pick-up one as it holds a 9 mm long crystal while pick-up zero employs a cubic 5 mm sample. Consequently, the overall effect of the crystal elongation in combination with the field increase predicts an EO signal ~8 times higher for pick-up one with respect the first proposal pick-up zero for the same nominal bunch conditions [6].

ISBN: 978-3-95450-192-2 doi:10.18429/JACoW-IBIC2017-TUPCF26

STRIPLINE BEAM POSITION MONITOR FOR THE PAL-XFEL

C. Kim*, S. Lee, J. Hong, D. Shin, H. S. Kang, I. S. Ko
Pohang Accelerator Laboratory, POSTECH, Pohang 790-834, Korea

Abstract

The X-ray Free Electron Laser of the Pohang Accelerator Laboratory (PAL-XFEL) produces 0.1 nm wavelength X-ray with a femtoseconds pulse width by using the self-amplification of spontaneous emission (SASE). For the successful commissioning and the stable operation of the PAL-XFEL, Beam Position Monitors (BPMs) are most the impor-tant instrument among the various kinds of electron diagnos-tic tools. In this work, the BPM system for the PAL-XFEL is introduced. From the pickup to the electronics, details of the BPMs are presented.

INTRODUCTION

After upgrade of the Pohang Light Source (PLS-II), the Pohang Accelerator Laboratory (PAL) had rushed into the construction of the X-ray Free Electron Laser (PAL-XFEL) [1]. The project period was from 2011 to 2015 and the project budget was 400-million-dollar. In the PAL-XFEL, an electron beam with 200 pC charges can be generated from a photocathode RF gun with 60 Hz repetition rate and can be accelerated to 10 GeV energy by using a 780 m-long linear accelerator (linac). After the acceleration, electron beams pass through a 250 m-long undulator section to produce 0.1 nm-wavelength hard x-ray with the self-amplification of spontaneous emission (SASE) [2-4].

To send an electron beam from the gun to the linac end, transverse beam-position measurements along the linac are the most important issue in the beam diagnostics. The electron beam should pass through the center of the quadrupole magnet to keep the beam size and shape symmetrically and to make the orbit as close as possible to the ideal one. In this reason, a good performance of the Beam Position Monitor (BPM) is a critical element for the stable operation of the PAL-XFEL.

The electron beam of the PAL-XFEL has a small charge (20 pC ~ 200 pC) and a short bunch length (50 fs ~ 5 ps). In addition, In the PAL-XFEL, different BPM resolutions were required for the linac and the undulator section. 10 μm resolution is enough for the linac operation. On the other hand, 1 μm resolution is needed for the beam based alignment of the undulator section. Under these requirements, a stripline and a cavity BPMs were selected for the linac and undulator BPMs. In this paper, we introduce the stripline BPM of the PAL-XFEL. It includes the details of the pickup design, and measurement results of the resolution by using the electron beam. The hardware and the software of the BPM electronics are presented, as well.

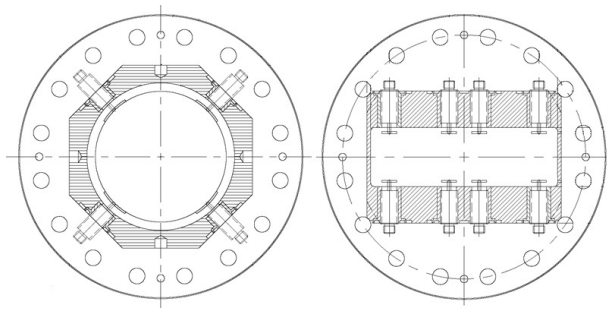

Figure 1: Transverse cross-sections of the circular (left) and the rectangular (right) chamber BPMs with CF 6 inch flanges.

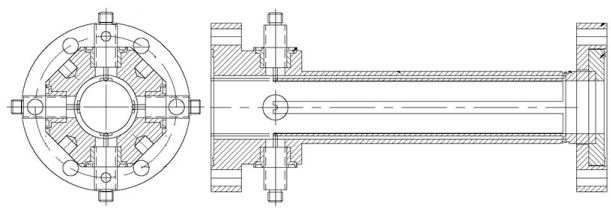

Figure 2: The transverse (left) and the longitudinal (right) cross-sections of the stripline BPM with CF 2.75 inch flanges.

PAL-XFEL STRIPLINE BPM

The stripline BPM in the linac can be separated into two groups. One is the circular chamber BPM and the other is the rectangular one for the bunch compressor. Most of the linac components have circular chambers as the aperture of the accelerating column. In the bunch compressor, however, the beam size can be increased to the horizontal direction because of the dispersion, and rectangular vacuum chambers were introduced. Even in the case of the rectangular vacuum chamber, CF flanges were used for the connection with other linac components. CF 2.75 inch, 4.5 inch, and 6 inch flanges were selected for the circular chamber, and CF 6 inch and 8 inch flanges were used for the rectangular one in the bunch compressor. Figure 1 shows transverse cross-sections of the circular and the rectangular chamber BPMs with CF 6 inch flanges.

BPMs with CF 2.75 inch flanges are widly distributed in the linac and its number is much bigger than that of BPMs with other types of flanges. A large number means that there are many requirements as well, and BPMs with CF 2.75 inch flanges have various lengths because of the limited space in the linac. Especially in the injector, lots of components were packed in a short space to minimize the emittance grow-up. Thus, the length of the BPM was reduced to a minimum

* chbkim@postech.ac.kr

ISBN: 978-3-95450-192-2 doi:10.18429/JACoW-IBIC2017-TUPWC01

THE APPLICATION OF DIRECT RF SAMPLING SYSTEM ON CAVITY BPM SIGNAL PROCESSING*

L. W. Lai, Y. B. Leng†, J. Chen, S. S. Cao, T. Shen, L. Y. Yu, R. X. Yuan, T. Wu, F. Z. Chen, J. Chen
SSRF, SINAP, Shanghai, China

Abstract

Cavity BPM signal processing system normally consists of two modules, first one is RF conditioning module(RF front end) to down convert the BPM signal to IF, second one is IF signal digitizer and digital signal processing module (DAQ) to calculate beam position and communicate with control system. The RF front end complicates the system and introduces noise. A direct RF sampling system has been constructed to process the cavity BPM signal, which structure is more concise and performance is better compared to the conventional system. The evaluation tests and an on-line RF DAQ system will be introduced in this paper.

INTRODUCTION

As the fourth-generation light source, FEL (free electron laser) is widely developed due to its outstanding performance. And in China, several FEL facilities have been built, such as DCLS (Dalian Coherent Light Source) and SXFEL (Shanghai Soft X-ray Free Electron Laser).

SXFEL is a high gain FEL. It is constructed at the bottom of 2016, now is under commissioning. The main parameters are listed in Table 1.

Table 1: SXFEL Parameters

Parameters	Value
Status	Commissioning
Wavelength	3-9 nm
Length	~300 m
FEL principle	HGHG, EEHG
Beam energy	0.84 GeV
Peak current	500 A
Normalized emittance	1 mm.mrad
Bunch length(FWHM)	1 ps
Harmonic number	30th

The improvement of FEL performance leads to higher requirement on beam-diagnose technology. Cavity beam position monitor (CBPM) is one of the important diagnostic component on FEL for its high resolution to dozens of nanometers. The output signal from CBPM is narrowband signal centralized at up to several GHz. For example, the central frequency of TM110 and TM010 signal of CBPM on SXFEL is 4.7 GHz [1], while LCLS is 11.424 GHz. This high frequency signal is hard to be sampled and processed directly limited by electronic technology. A traditional method is to down convert the RF signal to IF signal (MHz) firstly, so that the following ADC and signal processing module (data acquisition system, DAQ) can deal with the signal.

Figure 1 is the block diagram of CBPM signal processing system on SXFEL. The front end consists of preamplifier in tunnel, local oscillator (LO), mixer, filters, et al. CBPM output signal is down converted to about 500 MHz after the front end. DAQ system is an in-house designed digital beam position processor (DBPM), which central frequency is 500 MHz, four channels 16 bits ADC sampling at 119 MHz [2, 3].

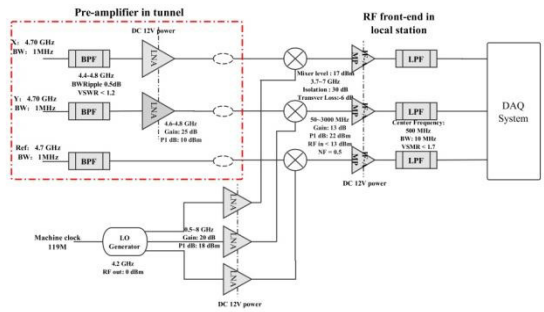

Figure 1: CBPM signal processing system on SXFEL.

This structure not only increase the costs, large numbers of RF components also make the system complex and fragile, and the components introduced extra noise will degrade the system performance. Considering this, the ideal BPM read-out electronics should contain no RF front-end [4, 5]. But this vision is infeasible in most cases, because the CBPM output signal frequency always out of the bandwidth range of most ADC. Fortunately, current electronics already enables this "ideal electronics" (6 GHz bandwidth oscilloscope) on the C band Cavity BPM system on SXFEL (4.7 GHz).

BEAM TESTS ON SXFEL

Two bunch arrival time measurement (BAM) cavities have been installed at the injection section and accelerator section to evaluate the BAM performance on SXFEL. The BAM monitor consists of two reference cavities. The central frequency of the two cavities respectively is designed to 4720 MHz and 4680 MHz. The output signal of the reference cavities can also be used to measure the bunch charge [6]. Then the BAM system can be used to evaluate the system performance by measuring the bunch charge.

RF DAQ Test

Figure 2 is the system diagram of RF direct sampling test. It consists of two BAMs in tunnel (IN-BAM01 at

*Supported by The National Science Foundation of China (Grant No.11375255, 11575282); The National Key Research and Development Program of China (Grant No. 2016YFA0401990, 2016YFA0401903).
† lengyongbin@sinap.ac.cn

ISBN: 978-3-95450-192-2 doi:10.18429/JACoW-IBIC2017-TUPWC02

THREE-DIMENSIONAL BUNCH-BY-BUNCH POSITION MEASUREMENT AT SSRF*

Y. M. Zhou†, L.W. Duan, Y. B. Leng[1], N. Zhang[1]
Shanghai Institute of Applied Physics, Chinese Academy of Sciences, Shanghai, China
[1]also at Shanghai Synchrotron Radiation Facility, Chinese Academy of Sciences, Shanghai, China

Abstract

Measurement of the bunch-by-bunch particle beam position related to dynamic instability is a useful input to accelerator optimization. And the bunch-by-bunch information has been contained in the BPM signals, including bunch charge, transverse position and longitudinal phase information. This paper reports a 3D beam position monitor system based on a high speed digital oscilloscope, which has been used to capture three-dimensional position information during the injection transient at the Shanghai Synchrotron Radiation Facility. With this information the traces of stored bunch and refilled bunch, and the mismatch of energy, transverse position and longitudinal phase between them can be precisely retrieved. The progress of this work and several particular experimental results will be discussed in this paper. The details of data processing method so-called software re-sampling technique will be discussed as well.

INTRODUCTION

In the operation of the third generation light source, the beam instability will be caused by rail noise. The beam instability, such as beam position shift, beam tune drift and beam wake field effect, will affect the effective operation of the accelerator. In the SSRF (Shanghai synchrotron radiation facility), turn-by-turn beam position measurement has been realized and the resolution has reached 2 μm [1]. In order to improve the resolution, it is important to measure the beam position bunch by bunch. At the same time, higher resolution is essential for the study of beam position shift and the mismatch of energy during the injection transient process. In this paper, the traces of the stored bunch and refilled bunch can be achieved. And the three-dimensional beam motion can be constructed according to the three-dimensional position information. The beam position can be obtained from the amplitude difference among four signals extracted by the button electrode. The difference-over-sum method is usually used in the beam transverse position measurement. However, in the longitudinal phase measurement, the bunch phase is detected from the difference between a beam pulse and a reference frequency signal. In this paper, the longitudinal phase is calculated by using the zero-crossing fitting method. Since the original signal of the storage ring button electrode already contains the transverse position and longitudinal phase information, the original signal can be extracted directly by a high sampling rate oscilloscope. The three-dimensional bunch-by-bunch position information was calculated by the off-line data processing. Shanghai light source as the third generation synchrotron radiation source, the storage ring energy reached 3.5 GeV with 432 m in circumference. There are totally 140 BPMs (Beam Position Monitor) around the storage ring. For SSRF, a practical filling pattern is a 500 −bunch train filled in the storage ring, leaves a 220 bucket empty gap. The harmonic number is 720 and the RF frequency is 499.654 MHz.

PRINCIPLE

Typical BPMs used in the storage ring are button-type electrode and strip-type electrode. When the beam passes through the button electrode, the electric quantity obtained by each electrode is closely related to the distance from the surface of the button electrode to the beam due to the electrostatic induction. The three-dimensional position information of the beam can be calculated from the original signal outputted from the electrode. Figure 1 shows the cross section of the button electrode used in the Shanghai light source storage ring. For the non-center bunch response, the amount of induced charge on the electrode is different when the bunch whose current is $I_b(t)$ passes through the non-center position of the button electrode. As shown in Fig. 1, the bunch is in the (δ, θ) position, the radius of the vacuum chamber is b, and the distance from the electrode to the vacuum chamber is a.

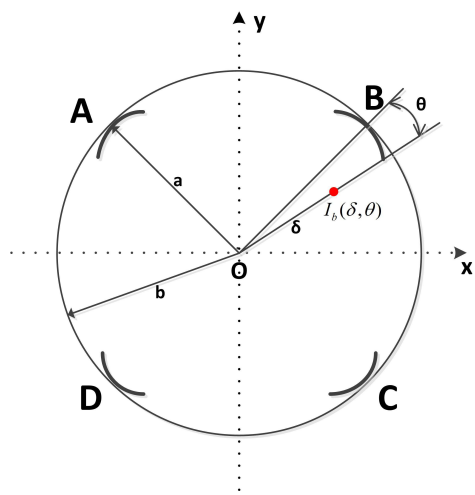

Figure 1: Cross section of button-type position monitor.

In the following analysis [2], a Gaussian distribution of the beam is used. Considering N particles of charge e in a bunch of the half width σ, the induced voltage generated by

* Work supported by National Science Foundation of China (No. 11575282, No. 11375255, No. 11305253)
† zhouyimei@sinap.ac.cn

ISBN: 978-3-95450-192-2 doi:10.18429/JACoW-IBIC2017-TUPWC03

DESIGN OF A NEW TYPE OF BEAM CHARGE MONITOR BASED BUNCH BY BUNCH DAQ SYSTEM *

F. Z. Chen , L. W. Lai†, Y. B. Yan, Y. B. Leng
SSRF, SINAP, Shanghai, China

Abstract

Beam current is one of the fundamental parameters to be measured in storage ring. The Shanghai Synchrotron Radiation Facility (SSRF), a third generation light source with the RF frequency of 499.68 MHz, used adopt commercial product to monitor beam charge. However, the maintain and upgrade is not always straightforward. Thus, a new type of beam charge monitor (BCM) based on beam positon monitor (BPM) sum signals has been developed for the online beam current measurement on SSRF storage ring. This system has been convincingly validated by mathematical analysis, and has been demonstrated with beam experiments during machine study time.

INTRODUCTION

We used to employ the commercially BCM manufactured by Acqiris, however, the maintain and upgrade is not always straightforward. In the electron accelerator, the beam position detector can be used to measure beam charge. Since BPM sum signals provide a new type of solution of beam charge monitor in SSRF, and there're 140 BPMs in the storage ring, we choose the one meet the criteria for this particular usage under particular measurement [1]. For data acquisition system, obviously, the higher the sampling rate, the more precise the original signal reconstruction. However, consider of the sampling rate measurement accuracy and equipment cost, we choose sample rate at RF frequency.

The DBPM processor system played a vital role in beam diagnostics system. The BI group of SSRF developed a new type of DBPM processor to handle the BPM data acquisitions and the position calculations. The BPM processor carry FPGA and ARM, available for further application development. The processor also could use external trigger and external clock. Under the circumstances, we design a new type of BCM based on BPM sum signals using the DBPM processor, namely, a DBPM-BCM. .We design a new type of BCM based on BPM sum signals using a new type of BCM

The DBPM-BCM consist of three parts: pick up, front-end electronics and the data acquisition. In order to monitor beam charge bunch by bunch, consider of DBPM external clock sampling rate, we divide the storage ring bunches into four parts. Using delay line to generate RF frequency interval, make the sum signal reach 4 channels at different interval, in our system which is a 2 ns interval one after one. This design of signal transmission guarantee each channel acquire a different quarter of bunch cluster in storage ring. Adjusting the sampling clock phase to acquire signals peak value is the core requirement of the system, and has a profound effect on the measurement accuracy and reliability. Therefore, the sampling phase must be cautious adjust. Another one of the key challenges of the system is to find a suitable sample frequency, and delay the signals to ensure every single bunch in the storage ring should be captured. The transmission phase also needs to be cautiously adjusted.

The main reason why the bunch-by-bunch separation sample method chosen is that independent test can extract the irrelevant four bunch clusters in storage ring. This feature assures every single bunch in the storage ring has been monitored. The total design is neat and obvious. That makes the method easy to be implemented and work online.

DESIGN AND REALIZATION OF THE SYSTEM

System Requirements Analysis

Take full use of the existing beam diagnostic equipment in the storage ring, establish a set of bunch-by-bunch BCM data acquisition system (DAQ) system, given the current intensity information of each bunch, the measurement accuracy should meet the top-up actual operational indicators.

DBPM has a 16-bit resolution, DC-700 MHz bandwidth baseband data acquisition card, which meets our present needs. The electron accelerator could provide accuracy RF frequency demultiplication, and in our system it should be a quarter of RF frequency used for external sample clock.

The Principle of BCM

According to model building and formula proving, the relationship between the average beam current and four electrode sum signals can be expressed by Eq. (1):

$$I_{avg} = \frac{k(x,y)*V_{sum}}{Z} \quad (1)$$

Where the Z is the equivalent impedance constitute detection electrode and the signal transmission network, k(x,y) is the current intensity correction factor dependent on beam position, V_{sum} is detect electrode output sum signal voltage [2]. Using the button electrode BPM and the sum signal pulse measure pulse current intensity. The equation also suit for beam charge monitor.

When the ADC sample rate could reach RF frequency, we can realize bunch-by-bunch beam charge monitor. The criteria are the following: use four channels of DBPM processor to acquire sum signals, each channel has a 2 ns

*Work supported by National Natural Science Foundation of China (No.11575282No.11305253)
†lailongwei@sinap.ac.cn

ISBN: 978-3-95450-192-2 doi:10.18429/JACoW-IBIC2017-TUPWC04

EXPERIMENTAL DAMPING SYSTEM WITH A FERRITE LOADED KICKER FOR THE ISIS PROTON SYNCHROTRON

A. Pertica*, D. W. Posthuma de Boer, ISIS, STFC, Rutherford Appleton Laboratory, Oxfordshire, OX11 0QX, UK

Abstract

The ISIS neutron and muon source, located in the UK, consists of a H^- linear accelerator, a rapid cycling proton synchrotron and extraction lines towards two target stations. Transverse beam instabilities are one of the major factors limiting the intensity of the proton beam. In order to mitigate these instabilities an experimental damping system is being developed for the ISIS synchrotron. This system uses a split electrode beam position monitor (BPM) as a pickup and a ferrite loaded kicker as a damper. This kicker is ordinarily used to excite the beam with a fast rise time pulse for tune measurements. This paper describes the utilization of this device within a fast feedback system, using the continuous waveform provided by a split electrode BPM, which is processed by an FPGA board.

INTRODUCTION

The ISIS Synchrotron

The ISIS synchrotron accelerates two proton bunches, with a total of 3×10^{13} protons, from 70 MeV to 800 MeV at a repetition rate of 50 Hz, delivering a mean beam power of 0.2 MW to two tungsten targets. Protons are accelerated over 10 ms by first and second harmonic RF cavities, with a fundamental frequency sweep of 1.3 MHz to 3.1 MHz.

Instabilities at ISIS

A coherent instability has been observed at ISIS, causing vertical emittance growth around 2 ms into the 10 ms acceleration cycle. BPM measurements taken over a number of turns have previously identified vertical oscillations along each bunch [1]; see Fig. 1. The sum signal in this figure shows the longitudinal profile of the bunch, while the difference signal provides an indication of the vertical position along the bunch. The oscillations shown in the difference signal are characteristic of a transverse $m = 1$ head-tail instability [2].

Operationally the head-tail instability is suppressed by ramping the vertical tune over the appropriate time interval. While this technique is effective, it is limited by losses as the vertical tune approaches the half-integer resonance [3].

The Feedback System

A broadband, fast feedback system based on a stripline pickup & kicker has been designed to actively damp the effects of transverse instabilities and is currently being manufactured. Progress has been made on the feedback system itself by making use of the existing equipment in the ISIS synchrotron, specifically a split-plate BPM and a ferrite loaded kicker, the betatron exciter. The general set-up of the existing system is shown in Fig. 2.

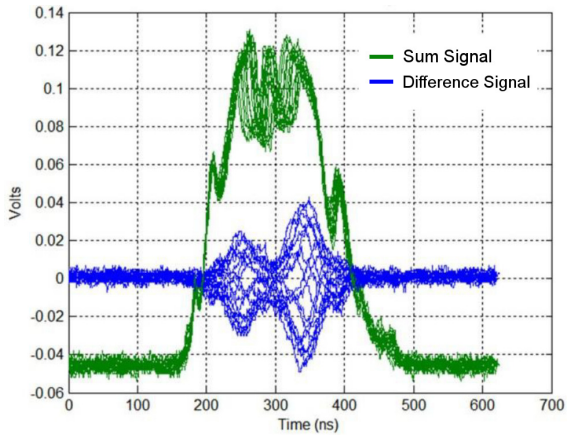

Figure 1: Sum and difference signals from a vertical BPM showing oscillations along a bunch [3].

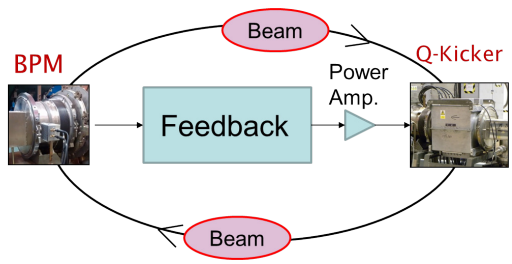

Figure 2: Set-up of the existing ISIS feedback system.

The Betatron Exciters

The ISIS betatron exciters; or "Q-Kickers", are window frame ferrite loaded kickers in the synchrotron which are ordinarily used for measurements of beam tune; there is one such kicker for each transverse plane. They are formed of two high-voltage plates opposite to one another and surrounded by ferrite yokes. The plates are both terminated with a high-power 10 Ω load resistor. The layout of the Q-kicker is shown schematically in Fig. 3.

The Q-kickers are normally excited with 4 kV pulses of opposite polarity sent to each plate. The resulting electric and magnetic fields kick the beam for only a single turn. This kick produces betatron oscillations which are observed on BPMs around the ring.

* alex.pertica@stfc.ac.uk

ISBN: 978-3-95450-192-2 doi:10.18429/JACoW-IBIC2017-TUPWC05

NEW RF FEEDBACK SYSTEM AND SIMULATIONS FOR SUPPRESSION OF COUPLED-BUNCH INSTABILITIES AT SuperKEKB

Kouki Hirosawa*, Kazunori Akai[1], Eizi Ezura[1], Tetsuya Kobayashi[1],
Kota Nakanishi[1], Michiru Nishiwaki[1], Shin-ichi Yoshimoto[1],
SOKENDAI (the Graduate University for Advanced Studies), Tsukuba, Japan
[1]also at High Energy Accelerator Research Organization (KEK), Tsukuba, Japan

Abstract

SuperKEKB is an asymmetric electron-positron circular collider based on nano-beam scheme at interaction region and large beam current. Longitudinal coupled-bunch instabilities (CBI) near RF frequency modes become bigger as the beam current increase. We developed new CBI damper to suppress newly arisen CBI modes (μ = -1, -2, -3) in SuperKEKB. The new damper will install in Low Level RF control system. LLRF control system was digitalized; it is a FPGA- based system on the microTCA for the high beam current operation of SuperKEKB. New CBI damper is independent of main LLRF control components. In test-bench measurements, our new CBI damper performed very well and satisfied required specifications. For SuperKEKB Phase-2 commissioning from January 2018, we calculated simple feedback model to estimate feedback loop gain of the new CBI damper.

INTRODUCTION

SuperKEKB is a high-luminosity asymmetric electron-positron collider upgraded from KEKB. The SuperKEKB Phase-1 commissioning was operated from February to June in 2016, and the Phase-2 will be carried out from January in 2018. Table 1 provides the main parameters of SuperKEKB [1] for this study. The SuperKEKB storage ring consists of a 7 GeV high-energy ring (HER) for electrons and a 4 GeV low-energy ring (LER) for positrons. One of the major differences between SuperKEKB and KEKB is increase of the beam current. In SuperKEKB design, longitudinal coupled-bunch instabilities (CBI) from the interaction between the beam and the accelerating mode of cavity will be serious, and there is every possibility of higher modes ($\mu = -2$ and -3) destabilized. So we need new mode-feedback system to counteract these multi-bunch oscillations.

Table 1: SuperKEKB and Cavity Parameter

parameters for SuperKEKB	value LER	HER
Energy: E	4.0 GeV	7.0 GeV
Beam current: I_0	3.6 A	2.62 A
Mom. compact.: α_c	3.25×10^{-4}	4.55×10^{-4}
Synch. freq.: f_s	2.43 kHz	2.78 kHz
Harmonic number: h	5120	
RF frequency: f_{rf}	508.877 MHz	
$f_0 = f_{rf}/h$	99.39 kHz	
Number of cavity	22	ARES 8, SC 8
for Cavity	**ARES**	**SC**
$V_c/cavity$	0.5 MV	1.5 MV
R_s/Q_0	15 Ω	93 Ω
Q_0	1.1×10^5	2.0×10^9
coupling factor: β	5.0	4.0×10^4

In the KEKB operation, the lowest mode of CBI called μ = -1 mode had been excited, and we suppressed it by using the CBI damper, which corresponds to only μ = -1 mode [2]. While upgrading to SuperKEKB, we predict that μ = -1, -2 mode instabilities will be excited at design beam current (LER: 3.6 A, HER: 2.6 A). To reach SuperKEKB design current, $\mu = -2$ mode will occur and $\mu = -1$ mode will become more serious (Figure 1). So we developed a new CBI damper as an RF feedback (FB) component [3]. We expect that CBI $\mu = -1, -2, -3$ mode will be suppressed by using this new damper in SuperKEKB operation.

COUPLED-BUNCH INSTABILITIES CAUSED BY ACCELERATING MODE

We reuse the KEKB RF system [4], which has two cavity types. One is a normal conducting (NC), and the other is superconducting (SC). In HER, a NC and SC cavity are used, and in LER, only NC cavity. The NC cavity is a unique cavity of KEKB and SuperKEKB called "ARES" [5]. ARES has a three-cavity structure: an accelerating cavity is coupled with an energy storage cavity via a coupling cavity in order to reduce cavity-detuning by beam loading [5]. The reason why CBI caused by accelerating mode become serious is that cavity detuning amount become larger as the beam current increases (following equation). $\Delta f = -(I_0 \sin\phi_s/2V_c) \cdot (R_{sh}/Q_0) \cdot f_{rf}$, where I_0 is beam current, ϕ_s is synchronous phase, V_c is accelerating voltage, R_{sh} is shunt impedance, Q_0 is unloaded quality factor, and f_{rf} is accelerating frequency.

To evaluate power of CBI, we use growth rate which is well known in Equation (1).

$$\tau_\mu^{-1} = AI_0 \sum_{p=0}^{\infty} \{ f_p^{(\mu+)} \mathrm{Re}Z^{\parallel}(f_p^{(\mu+)}) - f_p^{(\mu-)} \mathrm{Re}Z^{\parallel}(f_p^{(\mu-)}) \} \tag{1}$$

$$f_p^{(\mu+)} = (pM + \mu) f_0 + f_s, \quad f_p^{(\mu-)} = \{(p+1)M - \mu\} f_0 - f_s$$
$$f_{rf} = h f_0 \quad ,$$

* hirosawa@post.kek.jp

ISBN: 978-3-95450-192-2 doi:10.18429/JACoW-IBIC2017-TUPWC06

DEVELOPMENT OF KICKER FOR TRANSVERSE FEEDBACK SYSTEM IN BEPCII

J. S. Zhou, J. X. Zhao, Y. F. Sui, J. H. Yue, J. S. Cao, IHEP, Beijing, P. R. China
also at the University of Chinese Academy of Science, Beijing, P. R. China

Abstract

This paper introduces the necessary design parameters of transverse feedback system. Meanwhile, it mainly contains the design of stripline as feedback system kicker. The transverse kicker has 4 striplines, so that it can work in vertical and horizontal area. In the experiment, the shunt impedance is 1500 Ω which is simulated by HFSS and the system only needs 120 W to suppress the coupled beam bunch instabilities. According to the results of parameter S (1, 1) and S (2, 1), power loss and reflection is convenient. Recently, the prototype is calibrated.

INTRODUCTION

In order to receive more specific beam position instances and suppress beam instability as much as possible, we need to develop the kicker for BEPCII transverse bunch-by-bunch feedback system in storage ring. Comparing with the current transverse kicker, the new one provides superior dipole oscillation damping and detects the electrical field signal more sensitively [1]. According to calculation and simulation results, the amplitude reflection rate parameter is lower than 1% and a shunt impedance of 1500 Ω at 250 MHz working bandwidth can be reached. It needs 120 W power to suppress all unstable coupled bunch modes and the transmission efficiency is more than 99%. Meanwhile, this design aims to increase the space utilization rate in the storage ring, so the four-stripline-type kicker is adopted. This kicker tube consists of 2 striplines in horizontal and another 2 striplines in vertical direction. The important dimensions include the stripline length of 300 mm and the total length of the transverse kicker which is less than 500 mm. The innovation of this development is improving the beam intensity and lifetime, and the analysis and diagnosis ability of the beam detection system.

PARAMETER SIMULATION

Relevant Parameters Deduction

BEPCII has collide mode and synchrotron mode. At the beginning of the design of the transverse kicker, physics analysis needs to refer to some details of BEPCII in two different mode [2]. Table 1 shows the main parameters which play an important role in this work.

Table 1: Main Parameters of BEPCII

Parameters	Collide mode	Synchrotron mode
Energy E_0 (GeV)	1~2.1	2.5
Circumference (m)	234.53	241.13
RF frequency (MHz)	499.8	499.8
Harmonic number	396	402
Revolution frequency (MHz)	1.264	1.243
Revolution period (ns)	792	804

Table 2 shows the main parameters of the new transverse kicker, which is based on the relevant parameters in Table 1. The other part of this paper concerns the details of the design. Because of synchronous mode in BEPCII, the bucket will be filled by beam bunch one by one. So the system bandwidth is a half of RF frequency. The maximum output voltage is calculated by the Eq. (1):

$$V_{FB\perp} = 2\frac{T_0}{\tau_{FB}} \cdot \frac{E}{e} \cdot \frac{\Delta x}{\sqrt{\beta_m \beta_k}} \quad (1)$$

According to shunt impedance and maximum output voltage, the maximum power needed by this system is 120 W, and Eq. (2) shows how to calculate it

$$P = \frac{1}{2}\frac{\Delta V_{FB}^2}{R_k} \quad (2)$$

Table 2: Main Parameters Transverse Kicker

Parameters	Transverse Kicker
System Bandwidth (MHz)	250
Shunt Impedance (Ω)	1500
Maximum Feedback Voltage (V)	600
Maximum Output Power (W)	120
Stripline Length (mm)	305
Tube Inner Radius (mm)	50
Stripline Flare Angle	60°

* This work was supported by Accelerator Division, IHEP
† zhoujs@ihep.ac.cn

ISBN: 978-3-95450-192-2 doi:10.18429/JACoW-IBIC2017-TUPWC08

THE COLD BEAM POSITION MONITORS FOR THE C-ADS INJECTOR I PROTON LINAC*

Y.F. Sui, J.S. Cao, H.Z.Ma, Q. Ye, L.D. Yu, J.H. Yue
Institute of High Energy Physics, Beijing, China
also at Key Laboratory of Particle Acceleration Physics and Technology, IHEP, Beijing, China

Abstract

The injector I of China Accelerator Driven Subcritical system (C-ADS), which is composed of an ECR ion source, a low energy beam transport line (LEBT), a radio frequency quadrupole accelerator (RFQ), a medium energy beam transport line (MEBT) and cryomodules with SRF cavities to boost the beam energy up to 10 MeV. The injector linac is equipped with beam diagnostics. Cold beam position monitor (BPM) is one of instrumentations of the injector. This paper describes the design and fabrication of the cold BPM pick-ups, and also the application of the BPM in commissioning of SRF cavities. Discussion of the promotion and other aspect will also be presented.

INTRODUCTION

The Chinese ADS project is aimed to solve the nuclear waste problem and the resource problem for nuclear power plants in China. With its long-term plan lasting until 2030th, the project will be carried out in 3 phases: Phase I of R&D facility, Phase II of experiment facility and Phase III of industry demonstration facility. The driver linac of the CADS consists of two injectors to ensure its high reliability. Each of the two injectors will be a hot-spare of the other. Although the two injectors that are installed in the final tunnel will be identical, two different design schemes, named injector I and II respectively are being pursued in parallel by the Institute of High Energy of Physics (IHEP) and the Institute of Modern Physics (IMP). [1] The Injector I ion source is based on ECR technology. The beam will be extracted with an energy of 35 keV. The ion source will be followed by a Low Energy Beam Transport line (LEBT), which consists of 2 solenoids, a fast chopper system and a set of beam diagnostics including CTs and faraday cup. A Radio Frequency Quadrupole (RFQ) will accelerate the beam up to 3.2 MeV and will be followed by the first Medium Energy Beam Transport line (MEBT1), fully instrumented and also equipped. The next section is two cryogenic modules named CM1 and CM2 with seven cold beam position monitors in each, which accelerate beam up to about 10 MeV. The last section is the second Medium Energy Beam Transport line (MEBT2). The drift tubes between magnets provide the gap for diagnostics.

Table 1: The Beam Characteristics of CADS Injector I

Parameters	Value
Beam energy	3.5Mev~10MeV
Bunch frequency	325MHz
Beam pulse length	30us-CW
Peak current	10mA

To monitor the parameters of injector I, Several beam diagnostic and monitoring instruments are used. BPM as an essential part of beam diagnostics was designed and manufactured to measure the displacement of the beam. The BPMs provide the basic diagnostics tool for commissioning and operation of accelerators. The BPMs will provide information about both the transverse position of the beam and the beam phase that can be used to detect energy on line using the time-of-flight (TOF) method [2]. 27 BPMs including 14 cold BPMs are installed on the injector I. There are 7 cold BPMs, 7 superconducting quadruple magnet (SCQ) and 7 superconducting RF (SRF) cavities in each cryostat. The cold BPM is installed between SCQ and SRF cavity. So the SRF or SCQ is adjusted one to one based on BPM. The cold BPM is shown in Fig.1.

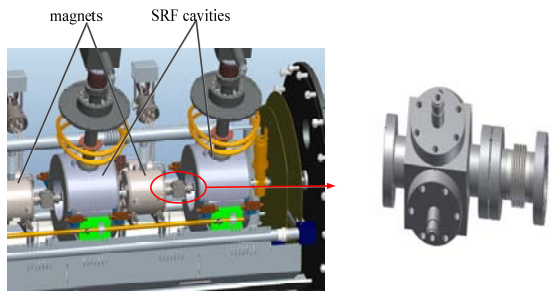

Figure 1: The position of the BPM in the cryostat and the structure of BPM.

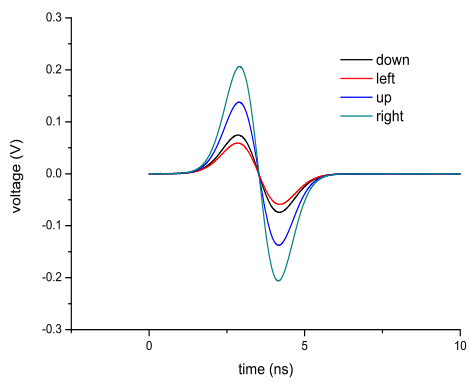

Figure 2: Voltages versus time during one period on four BPM electrodes from a passing transversely displaced (x = 2r/7; y =r/7) bunch.

*Work supported by China ADS Project (XDA03020000) and the National Natural Science Foundation of China (NO. 11205172, NO. 11475204)

ISBN: 978-3-95450-192-2 doi:10.18429/JACoW-IBIC2017-TUPWC09

REDUCING CURRENT DEPENDENCE IN POSITION MEASUREMENTS OF BPM SYSTEMS BY USING PILOT TONE: QUASI-CONSTANT POWER APPROACH

G. Brajnik*, S. Bassanese, G. Cautero,
R. De Monte, M. Ferianis, Elettra-Sincrotrone Trieste, Trieste, Italy
G. Rehm, Diamond Light Source, Oxfordshire, UK

Abstract

In BPM systems, the dependence of measured position on beam current is a well-known behaviour due to many factors. Measurements were carried out at Diamond Light Source with the pilot-tone compensated RF front end developed at Elettra and they evidenced a strong link between that issue and the integral non-linearity (INL) of the ADCs. A potential way to reduce this dependence is to change the gain of the preamplifiers following the beam current variation, trying to coerce the ADC into working as close as possible to a specific level. In this paper, along with the results of the tests performed at Diamond, which confirm once again the effectiveness of the front end and of the compensation strategy, an alternative technique is proposed to mitigate the current dependence by using the pilot tone itself. The idea is to maintain constant the total amplitude at the input of the ADCs, which is composed of the signal from the beam plus the pilot tone. Our data demonstrate how, by changing the latter in a convenient way during the current variations, we can achieve a reduction of the dependence by a factor of 10 considering an equivalent current ramp from 10 to 300 mA.

INTRODUCTION

The analog front end developed at Elettra for electron BPM applications has already been presented in previous papers [1, 2]. The proposed compensation strategy used has proven its effectiveness in several tests both on bench and on the storage ring during the normal operation of the machine.

In order to verify the excellent performances on different accelerators with different parameters, a new measurement session was carried out at Diamond Light Source. The results are reported in the first part of this manuscript, while the second part is focussed on some unexpected behaviours, mainly related to the integral non-linearity of the ADCs.

TESTS AT DIAMOND

A first test was realized in the laboratory of Diamond's Beam Diagnostics Group to ensure the correct operation of the system: a fixed beam was emulated by an RF generator and a 4-way splitter connected with semi-rigid coaxial cables to the front end. This last one was coupled with a Libera Spark as a fast 4-channel digitizer and the decimated IQ data were used for the analysis, calculating the FFT and working on carrier and pilot amplitudes.

* gabriele.brajnik@elettra.eu

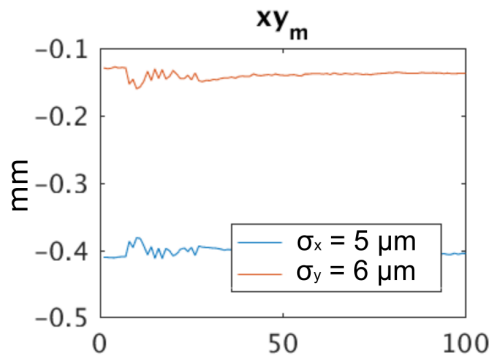

Figure 1: Calculated position while wobbling cables.

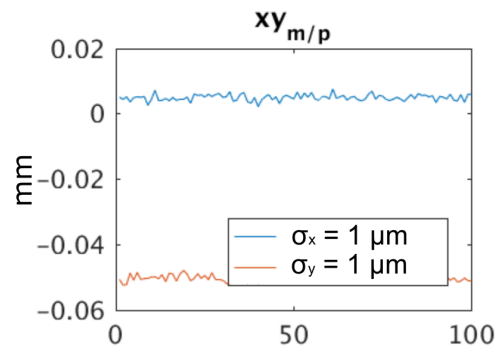

Figure 2: Compensated position while wobbling cables: note the different y scale.

During the acquisitions, the cables from the front end to the Libera Spark were twisted and wobbled: Figure 1 shows the calculated position with the movements due to the cables and Figure 2 illustrates the compensated position using the pilot tone. An improvement of a factor of 5 on the standard deviation has been obtained, and more than a factor of 10 considering the peak-to-peak value, virtually cancelling the shifts introduced by the cables. Note the different y scales of the two figures.

Results with Beam

The analog front end was subsequently placed in Diamond storage ring tunnel and connected to button BPMs (radius of 10.3 mm, scale factor $K_x = 10.3$ mm, $K_y = 10.4$ mm) by means of four 2-metres cables to detect the signal at 499.680 MHz. Power and communications were supplied by an Ethernet cable (PoE equipped). The output of the front

ISBN: 978-3-95450-192-2 doi:10.18429/JACoW-IBIC2017-TULAB1

DEVELOPMENT OF THE ELECTROMAGNETIC BOOM AND MOP SYSTEMS (EMOP)

A. Warner†[1], D. Cathey, G. Cullen, J. Nelson, Natural Science LLC., Big Rock IL, USA
P. Kasper, A. Lumpkin, Natural Science, LLC - Consultant
[1]also at Fermilab, Batavia IL, USA

Abstract

Several large-scale oil spills typically occur in the USA and other places around the world, and the Great Lakes are not immune from such threatening events. The clean-up process is inefficient and can have severe environmental impacts. An innovative, electromagnetic-based approach for oil spill remediation has been developed by Natural Science, LLC that uses micron-sized magnetite (Fe_3O_4) particles which are reusable, recoverable, and environmentally safe.

INTRODUCTION

In the past four decades, there has been an oil spill somewhere in the world each year, and in some years there are several. While many of these are small, larger spills are not uncommon. Though oil spills are inevitable, the techniques we use to combat them are choices based on available technologies, insight, and innovation.

Clean up of these spills is still largely inefficient, time-consuming, and expensive. One of the most widely used devices during an oil spill is the boom, which is supposed to provide a containment barrier for the spilled oil and to protect our shores. Although some effort has gone into the design of deployment mechanisms and designs aimed to improve the tow rates and buoyancies of these passive devices, no innovation has been made toward making these devices active. The ability to deploy a single device (system) that controls and efficiently removes spilled oil is a much-needed innovation to adequately protect and prepare for future oil spills worldwide.

In addition, standard oil booms and skimmer combinations generally target surface oil. However, a relatively recent complication is starting to emerge. The explosion in tar sands production in western Canada also means increasing amounts of heavy crude oil is making its way to the American Midwest via the Great Lakes. There is a growing concern regarding our ability to remediate spills for such heavy hydrocarbons that have the potential to sink. The magnetite particles used in our process have been demonstrated to target oil below the water surface. The particles will descend in pure water until they encounter and bond with oil. The electromagnetic field of our booms can extend some distance below the surface and will attract any magnetizable oil within its reach.

The likelihood for spills has increased over time, but environmentally safe methods of remediation, control and manipulation of oil have not been fully developed. The electromagnetic boom technology is a potentially game-changing advance [1]. The process works when micron-sized magnetite (Fe_3O_4) particles are dispersed in oil on water. The particles form a unique and preferential bond with the oil due to a combination of forces, dominated by the Van der Waals force. Magnetic fields can then be used to manipulate, trap and remove the oil with high efficiency. In the case of oil spills on water, the water becomes the primary transport medium for manipulating the oil. Both the particles and the oil are recaptured and separated for reuse. This process is being applied to electromagnetic systems that can replace and/or increase the efficiency of the passive boom and skimmer systems used today. In addition, the methods described can be used to remove oil from other surfaces and can target oil on the order of scale of the particles (micron scales).

THE FUNDAMENTAL CONCEPTS

The fundamental concepts involved in the seeding of oil with magnetite, the magnetic manipulation of the combination, the separation of the magnetite particles at the end of the process, and the magnetorheological effects are described in this section.

Seeding Process

This invention [2] provides a seeding process that preferentially targets oil on water by trapping the micron sized magnetite or iron oxide particles (the "particles") in the oil/water combination. The process is dominated by the Van der Waals force in the aqueous phase. The particles preferentially bond with the oil while passing through any water free of oil. As a result, this provides a method to determine where the oil is located at the micron scale (even when it is not visible to the naked eye). Figures 1 and 2 below illustrate the concept. The limiting scale is of the order of the size of the magnetite particles used. This method can therefore be used as a probe for targeting oil on water at the micron scale and above and thus

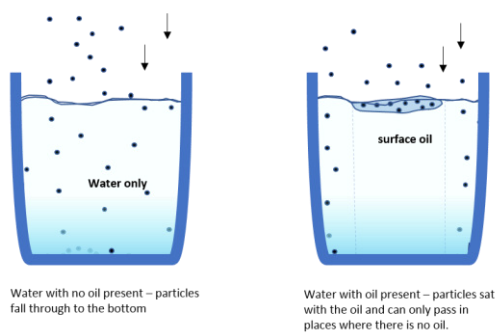

Figure1: Illustrating the fact that the particles preferentially stay with the oil.

† awarner@naturalscienceusa.com

ISBN: 978-3-95450-192-2 doi:10.18429/JACoW-IBIC2017-WE1AB1

THE SPS WIDEBAND FEEDBACK PROCESSOR: A FLEXIBLE FPGA-BASED DIGITAL SIGNAL PROCESSING DEMONSTRATION PLATFORM FOR INTRA-BUNCH BEAM STABILITY STUDIES

J. E. Dusatko#, J. D. Fox, C. H. Rivetta, O. Turgut (SLAC National Accelerator Laboratory, Menlo Park, California USA), E. Bjorsvik, W. Höfle (CERN, Geneva Switzerland)

Abstract

A flexible digital signal processing platform based on FPGA technology has been developed for vertical intra-bunch beam stability studies at the CERN SPS. This system is unique in that samples at a very high rate (4GSa/s) in order to measure and control motion within the 1.7ns proton beam bunch. The core of the system is an FPGA-based digital signal processor. Being programmable, it enables fast development of control algorithms. The processor, together with its supporting components forms a complete platform for demonstration studies of beam instability measurement and control. This system is capable of operation as either a stand-alone arbitrary waveform generator for driven mode instability studies, a closed-loop feedback control system for stability control and as a diagnostic instrument for measurement of beam motion. Recent measurements have shown the system is effective at damping single-bunch and bunch train intra-bunch instabilities with growth times of 200 turns. This paper summarizes the system design, provides some operational highlights, describes the upgrades performed to date and concludes with a description of the next generation processor now in development.

INTRODUCTION

The CERN Super Proton Synchrotron (SPS) accelerates protons for injection into the LHC. Control of performance-limiting transverse vertical bunch beam instabilities is normally handled a by dedicated transverse damper system [1]. For the planned High Luminosity LHC Upgrade (HL-LHC) [2], concerns have arisen that with the higher beam intensities, transverse intra-bunch motion driven by transverse mode coupling instability (TMCI) and the electron cloud instability (ECI), may become a limiting factor in the luminosity of the upgraded LHC [3,4]. Transverse beam instabilities within the SPS are being addressed in three ways: machine lattice configuration, vacuum chamber coating with amorphous carbon and active electronic feedback control, which is the role of the wideband feedback system (WBFB).

The hardware details of this system are described in another publication [5], presently we describe the design of the system with a focus on the signal processor.

SYSTEM DESCRIPTION

The comprehensive Wideband Transverse Feedback System (WBFB) consists of an ensemble of components. The system block diagram is shown in Figure 1.

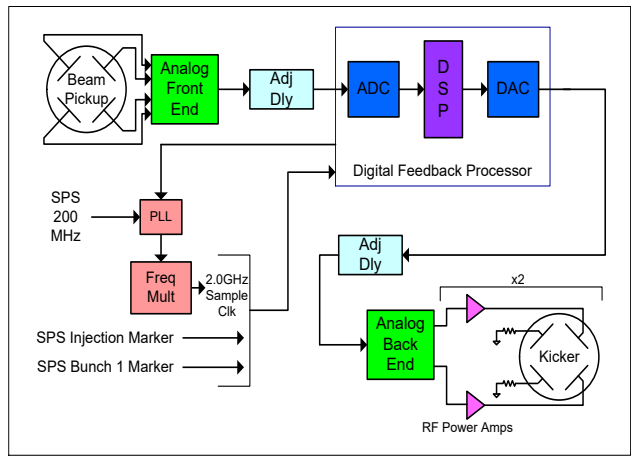

Figure 1: System Block Diagram.

DIGITAL FEEDBACK PROCESSOR

The Feedback Processor is designed as a general-purpose digital signal processing system with integrated data converters. A block diagram is shown in Figure 2. An FPGA implements all of the data formatting, system control and signal processing functions, as well as ancillary/support functions (e.g. control of the input trigger comparator threshold DACs). This is the most complex subsystem. Its functions and design will now be described.

Feedback Mode

In feedback mode, the processor can selectively compute corrections for [1…64] bunches or [1…32] scrubbing bunch doublets [6]. In non-doublet mode a 5ns sample window across the bunch takes 16 samples or slices (these parameters are 2x for doublets). The current control algorithm treats each slice as an independent signal and applies a non-recursive Finite Impulse Response (FIR) digital filtering function to that signal. Thus there are 16 FIR filters for each bunch, the filters have identical coefficients and are 16 taps long. The FIR filter is expressed as:

$$y(n) = \sum_{k=0}^{15} h(k)x(n-k)$$

*Work supported by the U.S. Department of Energy under contract DE-AC02-76SF00515, the US LHC Accelerator Research program (LARP), the CERN LHC Injector Upgrade Project (LIU) and the US-Japan Cooperative Program in High Energy Physics.
#jedu@slac.stanford.edu

ISBN: 978-3-95450-192-2 doi:10.18429/JACoW-IBIC2017-WE2AB3

A NANOFABRICATED WIRESCANNER: DESIGN, FABRICATION AND EXPERIMENTAL RESULTS

M. Veronese*, S. Grulja, G. Penco, M. Ferianis, Elettra-Sincrotrone Trieste, Trieste, Italy
S. Dal Zilio, S. Greco[1], M. Lazzarino, IOM-CNR Laboratorio TASC, Basovizza, Trieste, Italy
L. Fröhlich, Deutsches Elektronen-Synchrotron DESY, Hamburg, Germany
[1] also at Graduate School of Nanotechnology, University of Trieste, P.le Europa 1, Trieste, Italy

Abstract

Measuring the transverse size of electron beams is of crucial importance in modern accelerators, from large colliders to free electron lasers to storage rings. For this reason several kind of diagnostics have been developed such as: optical transition radiation screens, scintillating screens, laser scanners and wirescanners. The last ones although providing only a multishot profile in one plane have proven capable of very high resolution. Wirescanners employ thin wires with typical thickness of the order of tens of microns that are scanner across the beam, whilst ionizing radiation generated from the impact of the electrons with the wires is detected. In this paper we describe a new approach to wirescanners design based on nanofabrication technologies. This approach opens up new possibilities in term of wires shape, size, material and thickness with potential for even higher resolution and increase flexibility for instrumentation designers. We describe the device, the fabrication process and report measurement performed on the FERMI FEL electron beam.

INTRODUCTION

It is of importance for a wide variety of accelerators to have accurate control of machine optics to reach the desired high electron densities. This task is accomplished with the help of transverse profile instrumentation. Through the decades several concepts of transverse profile instrumentation has been explored depending on the specific parameters of the accelerator and the resolution requirements. Two of the most extensively deployed in electron accelerators are imaging screens and wirescanners (WSC). The imaging screens are capable of providing a two dimensional profile in a single shot but have resolution hardly better than 10 µm (scintillator screens) [1]. In the case of a metallic screen emitting transition radiation they may be plagued by coherent optical transition radiation (COTR) [2]. The wirescanners on the other side can provide only one dimensional multishot measurement of the profiles but can reach better resolution than screens. Typical WSC detection is based on measurement of the ionizing radiation dose produced by the electron beam hitting the wires. For high brightness electron beams where the beam sizes are below 100 µm, the wirescanner designer has the possibility to choose amongst wires of different materials, such as: tungsten, aluminum and carbon [3–5], and wire diameter to reach the needed compromise between signal, resolution and mechanical robustness. For a detection based on ionizing radiation the larger the atomic number and density of the material the larger the signal. The mechanical robustness of the wires equipped diagnostics is mostly related to the vibrations induced by the motorized actuator used for the scan while beam induced heating may be an issue mainly for high repetition rate machines. The resolution of a measurement performed with a wire of diameter d corresponds to the r.m.s. of the cylindrical distribution i.e. $d/4$ [5]. In practice the diameter of the wire is typically limited to about 5 µm. In this paper we describe a novel device manufactured using nanofabrication techniques providing several potential benefits in terms of instrumentation design including the potential for sub-micron resolution.

DEVICE DESIGN

The basic idea is to create thin bridges across a robust frame. By nanofabrication these structures can be made thinner and narrower than a traditional wire. For this purpose we use a silicon substrate (thickness 500 µm) coated by 2 µm low stress silicon nitride (SiN) film. After the patterning the SiN coating with suitable structures, the etching of the substrate allowed the release of suspended structures bridged on a 3x9 mm free window. The structures made in this way have a rectangular cross section and from now on we will refer to them as nanofabricated wires (NF wires). Their width w determines the resolution. It can be demonstrated that the r.m.s. of a rectangular distribution is $w/\sqrt{12}$. With nanofabrication the width can made as small as 0.5 µm and thus the resolution can potentially reach 0.15 µm. The energy loss per unit thickness of a high energy electron beam scales with the square of the atomic number Z of the target material and is linear in its density ρ [6]. While in general more signal is better, for potential applications such as intra undulator diagnostics having a lower ionizing dose is a beneficial property. SiN has a low density of $\rho(Si)$ =3 gcm^{-3}). Considering $Z(Si)$ = 14 and that $Z(N)$ = 7 an effective atomic number can be calculated for SiN according to [7] to be $Z(SiN)$ = 12.5. on the basis of this two quantities a first approximation of the relative yield between wires can be calculated. Considering for example a NF wire of width of 10 µm and a thickness of 2 µm the dose generated by a 2x10 µm SiN NF wires is calculated to be 929 times less the one generated by a 10 µm tungsten wire ($Z(W)$ = 74, $\rho(W)$ =19.35 gcm^{-3}).A comparison between cylindrical wires and NF wires can be found in Table 1. A benefit of the NF wires compared to a traditional

* marco.veronese@elettra.eu

ISBN: 978-3-95450-192-2 doi:10.18429/JACoW-IBIC2017-WE2AB5

FIRST RESULTS FROM THE OPERATION OF A REST GAS IONISATION PROFILE MONITOR BASED ON A HYBRID PIXEL DETECTOR

J.W. Storey, D. Bodart, B. Dehning, G. Schneider, R. Veness, CERN, Geneva, Switzerland
W. Bertsche, H. Sandberg, University of Manchester, Manchester, UK
S. Gibson, S. Levasseur, Royal Holloway, University of London, London, UK
M. Sapinski, GSI, Darmstadt, Germany
K. Satou, Accelerator Laboratory, KEK, Ibaraki-ken, Japan

Abstract

A novel rest gas ionisation profile monitor which aims to provide continuous non-destructive bunch-by-bunch measurement of the transverse emittance is currently under development for the CERN Proton Synchrotron (CPS). The instrument consists of an electric drift field to transport ionisation electrons onto a measurement plane, a self-compensating magnet to maintain the transverse position of the ionisation electrons and an imaging detector to measure the transverse position of the ionisation electrons. Uniquely for this type of instrument the imaging detector consists of an array of pixelated silicon sensors which are read-out using Timepix3 readout chips. This so-called hybrid pixel detector is sensitive to single ionisation electrons and therefore removes the need for electron amplification with Multi-Channel Plates which typically suffer from aging phenomena and distorts the measured profile. The use of a pixel detector also offers the promise to significantly improve the time and spatial resolution of the position measurement compared to existing instruments. An ambitious program has been undertaken to develop a pixel based imaging detector that is compatible with operation directly inside the beam pipe vacuum together with the necessary radiation hard control and data acquisition electronics. A prototype version of the instrument was recently installed in the CPS and first results from the operation of this novel instrument will be presented.

INSTRUMENT DESIGN & REALISATION

An overview of the instrument design is shown in Fig. 1. Rest gas ionisation electrons are accelerated by an electric drift field towards an electron imaging detector located beneath a honeycomb structured radio-frequency shield. A magnetic field parallel to the electric field, formed by a self-compensating 0.2 T dipole magnet, helps to maintain the transverse position of the ionisation electrons during transport to the measurement plane. The electric drift field is formed by a single -11 kV cathode, without side-electrodes. The cathode includes an ion trap that prevents ion induced secondary electrons from re-entering the vacuum chamber and reaching the imaging detector [1]. The instrument is mounted on a rectangular vacuum flange with a ConFLat-type seal [2].

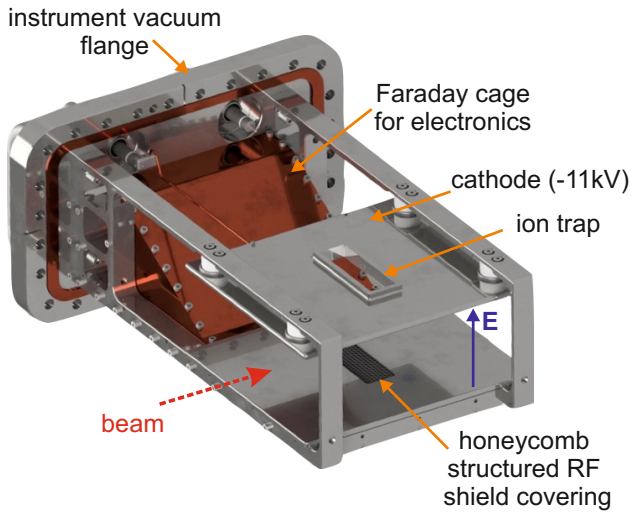

Figure 1: Rest gas ionisation profile monitor for the CERN PS.

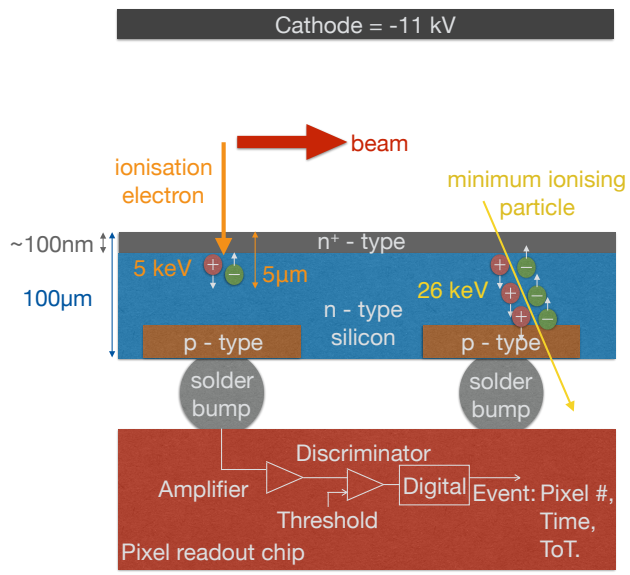

Figure 2: Detection of rest gas ionisation electrons with a hybrid pixel detector.

Detection of Rest Gas Ionisation Electrons With a Hybrid Pixel Detector

The ionisation electron imaging detector consists of four 14 × 14 mm hybrid pixel detectors mounted side-by-side creating a measurement plane 56 mm wide (transverse to the beam direction) and 14 mm long (in the direction of the

ISBN: 978-3-95450-192-2 doi:10.18429/JACoW-IBIC2017-WE3AB1

THE LHC BEAM GAS VERTEX DETECTOR - A NON-INVASIVE PROFILE MONITOR FOR HIGH ENERGY MACHINES*

S. Vlachos†, A. Alexopoulos, C. Barchel[1], E. Bravin, G. Bregliozzi, N. Chritin, B. Dehning‡, M. Ferro-Luzzi, M. Giovannozzi, R. Jacobsson, L. Jensen, R. Jones, V. Kain, R. Matev, M. Rihl, V. Salustino Guimaraes, R. Veness, B. Würkner, CERN, Geneva, Switzerland
A. Bay, F. Blanc, S. Giani, O. Girard, G. Haefeli, P. Hopchev, A. Kuonen, T. Nakada, O. Schneider, M. Tobin, Q. Veyrat, Z. Xu, EPFL, Lausanne, Switzerland
R. Greim, W. Karpinski, T. Kim, S. Schael, A. Schultz von Dratzig, G. Schwering, M. Wlochal, RWTH Aachen University, I. Physikalisches Institut, Aachen, Germany
[1]also at Cockcroft Institute and University of Liverpool, UK

Abstract

The Beam Gas Vertex (BGV) monitor is being developed as part of the High Luminosity LHC project with the aim of providing measurements with less than 5% error on the beam size with an integration time of 5 minutes. It will be an instrument capable of non-invasive beam size measurements throughout the LHC acceleration cycle with high intensity physics beams. A prototype BGV monitor has been installed in the LHC since 2016. Particles emerging from beam-gas interactions are recorded by two tracking stations made of scintillating fibres. Based on vertex reconstruction of the detected tracks, this monitor allows for a non-invasive measurement of the beam profile with bunch-by-bunch resolution. A dedicated computer farm performs track reconstruction and event analysis online so that real-time beam profile measurements can be provided. Data taken in 2016 and 2017 will be presented that demonstrate the potential of this method.

INTRODUCTION

The LHC Beam Gas Vertex (BGV) detector is a non-invasive beam profile monitor being developed for use as part of the high luminosity LHC upgrade (HL-LHC) [1]. The BGV system reconstructs the transverse beam profile by detecting particles from inelastic beam-gas collisions [2]. A gas tank is installed in the path of each circulating beam so that noble gas (initially Ne) is injected in the beam's trajectory. Particles emerging from the beam-gas collisions are detected by several planes of scintillating fibre detectors (SciFi) to enable a precise track reconstruction. These tracks are in turn used to reconstruct the vertex of each collision building-up a picture of the transverse beam profile. This method, originally developed for the LHCb experiment [3], allows profile measurements in real time. The pressure in the gas volume can be tuned to accommodate a large range of accelerator luminosity and/or inelastic beam-gas cross-section (i.e. beam energy). Using five minutes of beam time data, the BGV system is intended to provide an absolute measurement of the transverse beam profile with less than 10% error [4]. The transverse profile of individual bunches may also be reconstructed. Based on the beam width and given the β-function and dispersion of the magnetic lattice (measured independently), the emittance ϵ can be calculated. With enough statistics the detector can in addition measure beam tilt. Furthermore, relative bunch populations and ghost charges (beam intensity in nominally empty RF buckets) can be quickly estimated by using the BGV trigger system as for these measurements no precise tracking or vertex reconstruction is needed.

The addition of a precise timing detector (with a resolution of approximately 50 ps) would allow also the measurement of the longitudinal beam profile.

One BGV demonstrator is currently installed at Point 4 of the LHC on the beam 2 ring. A location where β_x and β_y are similar was selected, giving similar profiles in both planes and allowing the use of a reduced diameter beam pipe around the main detector so that it can sit as close as possible to the beam line. At the BGV location the 7 TeV beam to be monitored is expected to have a transverse profile with $\sigma_{x,y} \approx 0.22$ mm. The BGV system is composed of three independent parts: The gas target where beam-gas interactions occur, the trigger system that selects interactions originating from the volume of interest and the precise tracking system used to reconstruct tracks and vertices (Fig. 1).

THE GAS TARGET SYSTEM

The gas target vacuum system was designed to have a minimal impact both on the passing beam and on the particles emerging from the beam-gas interactions. It is made of aluminium (Al 2219) and is approximately 2 metres long. It consists of three parts: a 0.75 m long conical tube at the beam entry (to minimise beam impedance) followed by the gas target itself, a 1.25 m long cylinder with a diameter of 200 mm, and ending with a thin exit window towards the trigger and tracking detectors. The exit window has a thickness ranging from 3.25 mm at its edges to 1.15 mm close to the beam pipe, in order to minimise the multiple scattering of the emerging particles. The beam pipe around the end of the conical section has been reduced to a diameter of 58 mm (instead of the nominal 80 mm) and around the tracking detectors to a diameter of 52 mm. This serves two purposes. First of all it allows the BGV tracking detectors to be as

* Research supported by the HL-LHC project
† S.Vlachos@cern.ch
‡ Deceased January 14, 2017

ISBN: 978-3-95450-192-2 doi:10.18429/JACoW-IBIC2017-WE3AB3

COMMISSIONING AND FIRST RESULTS OF THE ELECTRON BEAM PROFILER IN THE MAIN INJECTOR AT FERMILAB*

R. Thurman-Keup†, M. Alvarez, J. Fitzgerald, C. Lundberg, P. Prieto, J. Zagel,
FNAL, Batavia, IL, 60510, USA
W. Blokland, ORNL, Oak Ridge, TN, 37831, USA

Abstract

The planned neutrino program at Fermilab requires large proton beam intensities in excess of 2 MW. Measuring the transverse profiles of these high intensity beams is challenging and often depends on non-invasive techniques. One such technique involves measuring the deflection of a probe beam of electrons with a trajectory perpendicular to the proton beam. A device such as this is already in use at the Spallation Neutron Source at ORNL and a similar device has been installed in the Main Injector at Fermilab. Commissioning of the device is in progress with the goal of having it operational by the end of the year. The status of the commissioning and initial results will be presented.

INTRODUCTION

Traditional techniques for measuring the transverse profile of proton beams typically involve the insertion of an object into the path of the proton beam. Flying wires for instance in the case of circulating beams, or secondary emission devices for single pass beamlines. With increasing intensities, these techniques become riskier both for the device and the radioactivation budget of the accelerator. Various alternatives exist including ionization profile monitors, gas fluorescence monitors, and the subject of this report, electron beam profile monitors.

The concept of a probe beam of charged particles to determine a charge distribution has been around since at least the early 1970's [1-3]. A number of conceptual and experimental devices have been associated with accelerators around the world [4-8]. An operational device is presently in the accumulator ring at SNS [9].

An Electron Beam Profiler (EBP) has been constructed at Fermilab and installed in the Main Injector (MI) [10]. The MI is a proton synchrotron that can accelerate protons from 8 GeV to 120 GeV. The protons are bunched at 53 MHz with a typical rms bunch length of 1-2 ns. In this paper, we discuss the design and installation of the EBP and present some initial measurements.

THEORY

The principle behind the EBP is electromagnetic deflection of the probe beam by the target beam under study (Fig. 1). If one assumes a target beam with $\gamma \gg 1$, no magnetic field, and $\rho \neq f(z)$, then the force on a probe particle is [11]

$$\vec{F}(\vec{r}) \propto \int d^2\vec{r}'\rho(\vec{r}')\frac{(\vec{r}-\vec{r}')}{|\vec{r}-\vec{r}'|^2}$$

and the change in momentum is

$$\Delta\vec{p} = \int_{-\infty}^{\infty} dt\ \vec{F}\left(\vec{r}(t)\right)$$

For small deflections, $\vec{r} \approx \{b, vt\}$, and the change in momentum is

$$\Delta\vec{p} \propto \int_{-\infty}^{\infty} dx' \int_{-\infty}^{\infty} dy'\ \rho(x',y') \cdot \int_{-\infty}^{\infty} dt\ \frac{\{b-x', vt-y'\}}{(b-x')^2+(vt-y')^2}$$

where {} indicates a vector. For small deflections, $\vec{p} \approx \{0, p\}$ and the deflection is $\theta \approx \frac{|\Delta\vec{p}|}{|\vec{p}|}$. The integral over time can be written as $\mathrm{sgn}(b - x')$ leading to an equation for the deflection

$$\theta(b) \propto \int_{-\infty}^{\infty} dx' \int_{-\infty}^{\infty} dy'\,\rho(x',y')\,\mathrm{sgn}(b-x')$$

where $\mathrm{sgn}(x) = -1$ for $x < 0$ and $+1$ for $x \geq 0$.

If one takes the derivative of $\theta(b)$ with respect to b, the sgn function becomes $\delta(b - x')$ leading to

$$\frac{d\theta(b)}{db} \propto \int_{-\infty}^{\infty} dy'\,\rho(b,y')$$

which is the profile of the charge distribution of the beam. Thus, for a gaussian beam, this would be a gaussian distribution and the original deflection angle would be the error function, $\mathrm{erf}(b)$.

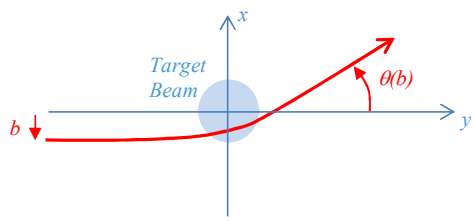

Figure 1: Probe beam deflection (red) for some impact parameter b.

EXPERIMENTAL TECHNIQUE

To obtain $\theta(b)$, one needs to measure the deflection for a range of impact parameters. This can be accomplished in a single shot by sweeping the electron beam through the proton beam provided the sweep time is much smaller than the r.m.s. bunch length of the proton beam to avoid coupling the longitudinal and transverse distributions. In the main injector, this would be challenging considering

* Operated by Fermi Research Alliance, LLC under Contract No. De-AC02-07CH11359 with the United States Department of Energy.
† keup@fnal.gov

ISBN: 978-3-95450-192-2 doi:10.18429/JACoW-IBIC2017-WEPCC02

UniBEaM - BEAM PROFILER FOR BEAM CHARACTERIZATION AND POSITION FEEDBACK

D. E. Potkins, M. P. Dehnel, D-Pace Inc., Nelson, BC, V1L 4B6, Canada
N. Lobanov, The Australia National University, Canberra, ACT 2601, Australia
T. Kubley, O. Toader, Michigan Ion Beam Laboratory, Ann Arbor, MI 48109, USA

Abstract

A beam profiler called UniBEaM is based on passing 200 micron cerium-doped optical fibers through a charged particle beam and measuring the scintillation light. In order to characterize UniBEaM over its entire kinetic energy range: keV to GeV; current range: pA to mA; and particle type range: light ions to heavy ions, and electrons, an Early Adopter Programme (EAP) was established to test UniBEaM's performance. EAP's: Australia National University (ANU) and Michigan Ion Beam Laboratory (MIBL) report on their use of UniBEaM at their facilities.

INTRODUCTION

A beam profiler based on doped SiO_2 optical fibers was designed and tested at the Albert Einstein Center for Fundamental Physics (AEC), Laboratory for High Energy Physics (LHEP), University of Bern, Switzerland [1]. This beam profiler, called the Universal Beam Monitor (UniBEaM™) was licensed and commercialized by D-Pace Inc., Canada. This paper provides example measurements made by two early adopters of this device: the Department of Nuclear Physics of the Australian National University (ANU), and the Michigan Ion Beam Laboratory (MIBL).

SYSTEM DESCRIPTION

D-Pace's commercial version of UniBEaM was described in detail by Potkins *et al*. [2].

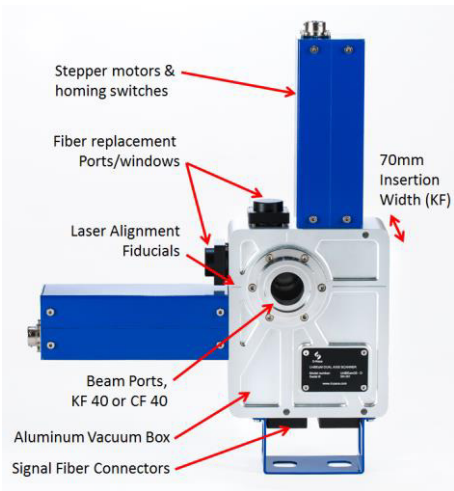

Figure 1: UniBEaM Probe.

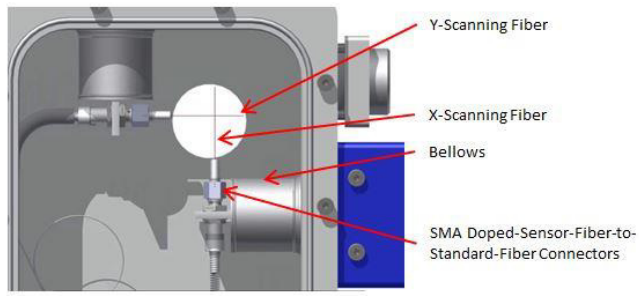

Figure 2: Internal view of UniBEaM showing the X & Y scintillating sensor fibers and fiber connector.

The UniBEaM probe (Figs. 1 & 2) has two sensing fibers; one for X-profiles and one for Y-profiles. The sensor fibers are moved through the beam by stepper motor actuators. The sensor fibers are made from SiO_2 doped with Ce^{+3} ions, and have a diameter of 200 µm. Silicon photo multipliers (SiPMs), located in the UniBEaM controller 10's of meters from the probe, measure the scintillation light, and subsequently amplify and digitize the signal. The UniBEaM software controls the scan resolution, and start and stop positions. X and Y beam profiles may be scanned separately or simultaneously. The software also calculates the beam centroid and the integral of the intensity profile.

The UniBEaM25 probe measures nominal 25 mm diameter beams, has a 35 mm aperture, and is provided with KF40 or CF40 flanges.

TESTING

Signal to Noise Assessment with 1MeV $16O^{+1}$

ANU installed UniBEaM on the beam line of a high energy ion implanter. The implanter utilizes an NEC 1.7 MV tandem accelerator able to reach energies up to 10 MeV. The BPM provides the feedback required for the operator to produce a well-focused and aligned beam on the target, and to measure the beam response to beam steering devices.

ANU utilized UniBEaM to measure beam profiles of a $16O^{+1}$, 1 MeV beam at low beam currents to investigate the noise floor of UniBEaM and compare the results with profiles acquired using an NEC BPM 80 helical wire scanner.

UniBEaM plots separate profiles for the orthogonal X and Y scans. The X and Y profiles may be scanned and displayed individually, or in the same plot. The horizontal axis of the UniBEaM plots are in mm. Figure 3 shows a scan of a $16O^{+1}$, 1 MeV, 80 pA beam to evaluate the noise floor of UniBEaM for this beam.

ISBN: 978-3-95450-192-2 doi:10.18429/JACoW-IBIC2017-WEPCC03

PERFORMANCE ASSESSMENT OF PRE-SERIES FAST BEAM WIRE SCANNER PROTOTYPES FOR THE UPGRADE OF THE CERN LHC INJECTOR COMPLEX

J. L. Sirvent, L. Garcia, J. Tassan-Viol, G. Trad, J. Emery, P. Andersson, F. Roncarolo, W. Andreazza, D. Gudkov, R. Veness, B. Dehning, CERN, Geneva, Switzerland

Abstract

A new generation of beam wire scanner (BWS), for transversal beam profile monitoring, is under development on the framework of the LHC Injector Upgrade project at CERN. Two pre-series prototypes have been built and installed in the Super Proton Synchrotron and Proton Synchrotron Booster, to assess the performance of the upgraded BWS concept.

This contribution shows the outcome of the measurement campaigns carried out on the first BWS prototypes, both in the laboratory and with proton beams. An evaluation of a high dynamic range acquisition system for the measurement of the secondary showers produced by the beam-wire interaction is also presented.

INTRODUCTION

The High Luminosity upgrade of the Large Hadron Collider (HL-LHC) will feature higher intensity proton beams in the whole injector chain. In addition, this upgraded scenario requires that the normalized transverse emittance of these beams be measured with a precision better than 5%. For beam wire scanners, the reference transverse beam profile monitors at CERN, this translates into a required wire position measurement uncertainty of a few micrometers.

The performance of the current operational beam wire scanners at CERN is limited by electronic noise on the signal from their position sensitive potentiometers, by the reproducibility of their motion mechanics and by the dynamic range of the acquisition system measuring the resulting secondary showers. The current wire position measurement uncertainty is in the order of ±100µm for the fast rotating scanners in the Proton Synchrotron (PS) and its Booster (PSB) at a speed of $15ms^{-1}$ [1], ±30µm for the rotating scanners ($6ms^{-1}$) in the Super Proton Synchrotron (SPS) and ±18µm for the linear scanners ($1ms^{-1}$) installed in the SPS and LHC [2]. The linear scanners are limited for use with low intensity beams as at higher intensity the deposited energy can lead to sublimation of the carbon wires used. In addition, all of these systems use bellows for motion transfer to the in-vacuum mechanics, this represent reliability issues when performing thousands of scans per year. The current scanners cannot therefore fulfill the HL-LHC specifications in terms of reliability and precision.

The need for higher measurement reproducibility at higher speeds has motivated the design of an innovative high precision beam wire scanner for the LHC Injectors Upgrade (LIU) project [3]. The upgraded concept is based on a rotational architecture with a frameless motor, where all mobile parts are located in vacuum on a shared shaft, eliminating the need of bellows. The wire position is determined through a high accuracy optical encoder [4], see schematic of Fig. 1. The secondary showers produced through the beam-wire interaction will be acquired using a high dynamic range acquisition system to eliminate the tedious set-up of operational parameters when switching between different beam configurations [5].

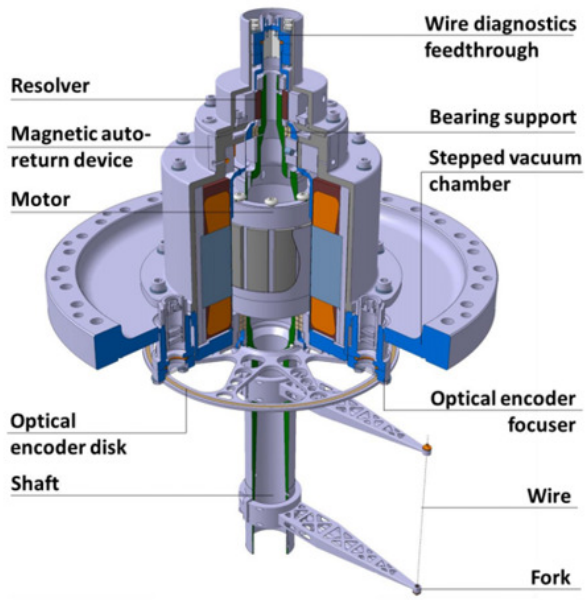

Figure 1: LIU beam wire scanner schematic.

SPS PROTOTYPE PERFORMANCE

The precision validation of the SPS BWS prototype [6] (BWS.51740.V) was carried out by measuring a single bunch with $2.3x10^{10}$ protons, during a period in which it was accelerated to 270 GeV and left circulating for several hours. Due to beam dynamic aspects, this beam suffers an emittance increase during this time and negligible beam intensity losses.

A standard linear scanner (BWS.51731.V) was operated in parallel with the prototype for performance comparison. The linear scanner performed scans at $1ms^{-1}$, while the nominal speed of the prototype was $20ms^{-1}$. With the circulating bunch interacting with the wire every 23µs (the SPS revolution period) and the prototype running 20 times faster than the linear scanner, the number of times the bunch intercepts the wire (points per sigma) is reduced for the prototype, thus providing less information for the Gaussian fitting routine used on the resulting profile.

ISBN: 978-3-95450-192-2 doi:10.18429/JACoW-IBIC2017-WEPCC04

AN OPTICAL AND TERAHERTZ INSTRUMENTATION SYSTEM AT THE FAST LINAC AT FERMILAB*

R. Thurman-Keup†, A. H. Lumpkin, J. Thangaraj, FNAL, Batavia, IL, 60510, USA

Abstract

FAST is a facility at Fermilab that consists of a photoinjector, two superconducting capture cavities, one superconducting ILC-style cryomodule, and a small ring for studying non-linear, integrable beam optics called IOTA. This paper discusses the layout for the optical transport system that provides optical radiation to an externally located streak camera for bunch length measurements, and THz radiation to a Martin-Puplett interferometer, also for bunch length measurements. It accepts radiation from two synchrotron radiation ports in a chicane bunch compressor and a diffraction/transition radiation screen downstream of the compressor. It also has the potential to access signal from a transition radiation screen or YAG screen after the spectrometer magnet for measurements of energy-time correlations. Initial results from both the streak camera and Martin-Puplett will be presented.

INTRODUCTION

The Fermilab Accelerator Science and Technology (FAST) facility has been constructed for advanced accelerator research [1-3]. It will eventually consist of 3 entities: a photoinjector-based linac followed by an ILC-type cryomodule, an RFQ-based proton injector, and a small ring called IOTA (Integrable Optics Test Accelerator) for studying non-linear optics among other things. Presently, the facility has the linac, cryomodule, and beamline to a high-energy dump. The IOTA ring is under construction and should be completed next year. The proton source is also under construction and will be completed in the next couple of years. When the full beamline to IOTA has been completed, the electron linac will provide beam to IOTA to map out the optics of the ring in preparation for injecting protons once the source is completed. In addition to the experiments in the IOTA ring, there are various experiments in the linac; both before the cryomodule and after. In support of these experiments, there is an optical / THz instrumentation system containing a a Hamamatsu streak camera and a Martin-Puplett interferometer. This paper will describe the system and present some initial measurements from it.

FAST FACILITY

The FAST injector starts with a 1.3 GHz normal-conducting rf photocathode gun with a Cs_2Te coated cathode. The photoelectrons are generated by irradiation with a YLF laser at 263 nm that can provide several μJ per pulse [4]. Following the gun are two superconducting 1.3 GHz capture cavities that accelerate the beam to its design energy of around 50 MeV. After acceleration, there is a section for doing round-to-flat beam transforms, followed by a magnetic bunch compressor and a short section that can accommodate small beam experiments. At the end of the experimental section is a spectrometer dipole which can direct the beam to the low energy dump. If the beam is not sent to the dump, it enters the ILC-type cryomodule where it receives up to 250 MeV of additional energy and is sent to either a high-energy dump or the IOTA ring. Table 1 lists the typical beam parameters.

Table 1: Beam Parameters for FAST

Parameter	Value
Energy	20 – 300 MeV
Bunch Charge	< 10 fC – 3.2 nC
Bunch Frequency	0.5 – 9 MHz
Macropulse Duration	≤ 1 ms
Macropulse Frequency	1 – 5 Hz
Transverse Emittance	> 1 μm
Bunch Length	0.9 – 70 ps

OPTICAL AND TERAHERTZ INSTRUMENTATION SYSTEM

The optical / THz instrumentation system (OTIS) [5] is located near the low energy dump. The transport system is constructed of stainless steel pipes and flanges connected between boxes containing mirrors for steering the light (Fig. 1).

There are currently three source points for the radiation. One each from the third and fourth dipoles in the bunch compressor, D3 and D4, and one from a cross downstream of the bunch compressor, X121. There is also the possibility of implementing one from the cross (X124) in the low energy dump beamline that normally measures the energy spread.

The source points D3 and D4 in the bunch compressor provide coherent synchrotron edge radiation (CSR) from the entrance of the corresponding dipole magnets. The CSR is generally in the high GHz / low THz region [6].

The source point at X121 consists of an aluminized, silicon wafer on a translatable actuator (Fig. 2). The wafer can be inserted all the way into the beam to generate both coherent transition radiation (CTR) and optical transition radiation (OTR). The screen can also be extracted partly, with its edge a few mm above the beam, to generate coherent diffraction radiation (CDR).

*Operated by Fermi Research Alliance, LLC under Contract No. De-AC02-07CH11359 with the United States Department of Energy.
† keup@fnal.gov

ISBN: 978-3-95450-192-2 doi:10.18429/JACoW-IBIC2017-WEPCC05

GAS JET PROFILE MONITOR FOR USE IN IOTA PROTON BEAM*

S. Szustkowski†[1], S. Chattopadhyay[1,2], D. Crawford[2], B. Freemire[1]
[1]Northern Illinois University, DeKalb, IL 60115, USA
[2]Fermi National Accelerator Laboratory, Batavia, IL 60510, USA

Abstract

The Integrable Optics Test Accelerator (IOTA) at the Fermilab Accelerator Science and Technology (FAST) Facility will attempt to demonstrate novel techniques for high current accelerators. An electron beam of 150 MeV/c momentum and a proton beam of 70 MeV/c momentum will be used for a number of experiments, including nonlinear focusing integrable optics, space charge compensation, and optical stochastic cooling. The low energy proton beam will provide a space charge dominated regime with which to investigate Hamiltonian diffusion and chaos. A non-invasive beam instrumentation device is needed to study emittance evolution and halo formation without destroying the beam. A supersonic gas jet curtain can be injected perpendicular to the proton beam, which will preserve the integrity of the beam and provide a two-dimensional turn-by-turn profile measurement. Currently, IOTA and the gas jet monitor are being built and commissioned at Fermilab.

INTRODUCTION

The Integrable Optics Test Accelerator (IOTA) is a storage ring designed to test novel high current accelerator techniques. A RFQ based proton source will provide a low energy beam for injection into IOTA. The ring will allow a sufficient number of turns to observe nonlinear effects in a space charge regime. Nonlinear decoherence in nonlinear integrable lattices will suppress halo formation of the beam. To preserve the lifetime of the beam, a non-invasive detector is required [1]. Simulation studies of the beam distribution, with various lattices, turn-by-turn are made using Synergia [2] code running on a server maintained by RadiaSoft [3]. The gas jet parameters, such as the gas density and the detector location, can be optimized for a higher resolution of the beam profile. A gas jet sheet is produced in the interaction chamber of the beam line. The beam ionizes the gas, producing an electron-ion pair. A transverse electric field will direct the electrons toward a micro-channel plate (MCP), which will provide a signal amplification of 10^6. Finally, a phosphor screen and CCD camera will image the signal.

IOTA PROTON BEAM PARAMETERS

The previously existing HINS (High Intensity Neutrino Source) RFQ will be used for injection of protons into the IOTA ring. The source will provide IOTA a beam energy of 2.5 MeV bunched at 325 MHz [4]. Bunches will spread out after a few turns due to the momentum spread and low energy. A dual purpose RF cavity will be used to bunch the beam at 2.18 MHz. The IOTA lattice (Fig. 1) has two integrable lattice sections (upper corners) where the transverse beta functions are matched and dispersion is zero (see Fig. 2). The lower left corner has a RF cavity and the lower right section will contain the electron lens/column. Table 1 provides a summary of HINS and IOTA main parameters.

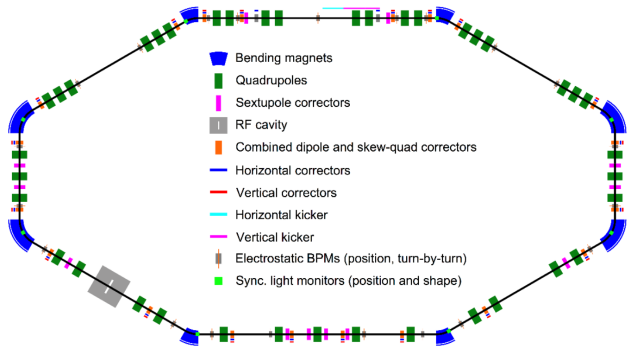

Figure 1: IOTA ring layout

Table 1: Summary of IOTA Proton Beam Parameters

PARAMETER	VALUE
Kinetic Energy	2.5 MeV
dp/p	0.1 %
Circumference, C_0	39.97 m
Revolution period, T_0	1.83 μs
RF bunching	2.18 MHz
Average beam current	8 mA
Vacuum	$6x10^{-10}$ Torr
Beam lifetime	300 s
Pulse rate	<1 Hz
Pulse width	1.77 μs

BEAM SIMULATIONS

The Synergia code has been used to simulate and propagate the beam including space charge effects. A lattice for IOTA with one nonlinear section was used. The nonlinear element in the lattice can be turned on and off. The initial KV beam is randomly distributed and propagated starting at the injection point (middle of the top section in Fig. 1). A virtual detector was placed s = 8.711 m from the right nonlinear section (middle of the lower right section in Fig. 1). The beam was propagated through the lattice for 200 turns with 10240 macro particles. A toolkit in Synergia, 2D

* Work supported by US Department of Energy, Office of High Energy Physics, General Accelerator Research and Development (GARD) Program.
† sszustkowski1@niu.edu

ISBN: 978-3-95450-192-2 doi:10.18429/JACoW-IBIC2017-WEPCC06

SIMULATION SUPPORTED PROFILE RECONSTRUCTION WITH MACHINE LEARNING

R. Singh, M. Sapinski and D. Vilsmeier, GSI, Darmstadt, Germany

Abstract

Measured IPM profiles can be significantly distorted due to displacement of residual ions or electrons by interaction with beam fields for high brightness or high energy beams [1–6]. It is thus difficult to deduce the characteristics of the actual beam profile from the measurements. Artificial neural network with multilayer perceptron (ANN-MLP) architecture is applied to reconstruct the actual beam profile from the measurement data. The MLP is trained using Virtual-IPM simulation program [7] developed under the IPMSim collaboration [8]. The first results are presented in this contribution.

INTRODUCTION

Ionization Profile Monitors (IPM) are used for non-destructive transverse beam profile measurements at many accelerator facilities. The principle of operation is the following; the primary beam ionizes the residual gas and the ionized particles (ions or electrons) are extracted via electric fields and sometimes in conjunction with magnetic fields to confine the movement of ionized particles in the plane transverse to the electric field. The profile of the extracted particles reflects the transverse profile of the primary beam with the assumption that ionized particles are created at rest and the effect of induced fields by the primary beam on ionized particles can be neglected. The choice between ions or electrons for profile reconstruction is based on the requirement for the speed of device operation and potential influence of beam space charge.

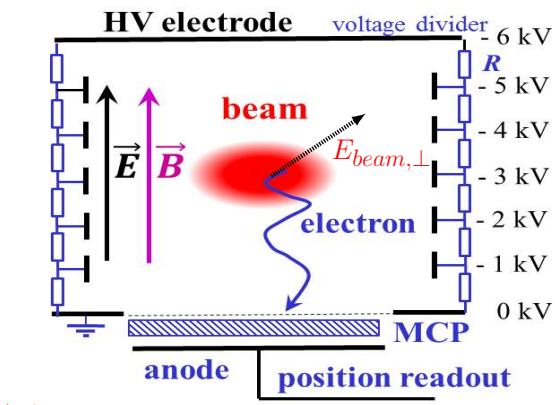

Figure 1: Operating principle of the IPM.

Figure 1 shows the typical components present in an IPM where both the electric and magnetic fields are utilized to confine the ionized particles [9]. The support electrodes/rods between the top and bottom electrodes are used to reduce the fringe fields and improve field homogeneity. The field homogeneity is important in order to avoid any distortion in the measured profile and therefore static EM simulations for the full geometry are usually performed. IPMs are often used for non-destructive measurements in low pressure conditions such as storage rings and hence they usually have to be equipped with a high amplification multi-channel plate (MCP) for obtaining sufficient signal to noise ratio. The output of MCPs are connected to data acquisition system directly or via phosphor screens and optical system. Figure 2 shows the image of the horizontal IPM formerly installed at LHC relevant to the discussions in this paper [4]. The dipole magnet has been moved in order to make the IPM chamber visible. In the next section, we will discuss the distortion in measured IPM profiles due to beam space charge and discuss previous efforts on correcting or reducing the distortion. Following that, the simulation tool and the beam and device parameters used to train the artificial ANN-MLP are discussed. Finally, the ANN-MLP parameters, training and validation are presented and the results are summarized.

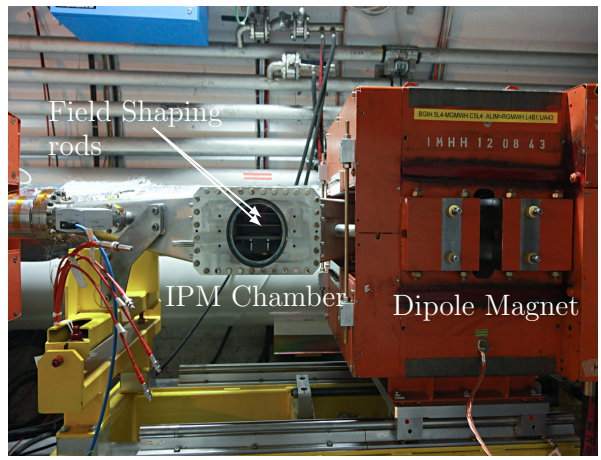

Figure 2: IPM installation at LHC. The dipole magnet (orange) has been shifted, revealing the IPM chamber.

SPACE CHARGE EFFECTS ON IPM PROFILE

IPM profile distortion due to beam fields depends on a variety of parameters such as device geometry, beam properties, extracted particle types (ions or electrons) and if IPM uses only electric field or also magnetic field. Initial IPM developments were focused around devices utilizing only electric fields. The distortion of IPM profiles has long been observed and the first attempt to make a simulation-based correction was by Thern [1] at AGS. Calculation of actual beam profile width from measured profile as a function of applied electric field and bunch population for coasting and bunched

ISBN: 978-3-95450-192-2 doi:10.18429/JACoW-IBIC2017-WEPCC07

A MODULAR APPLICATION FOR IPM SIMULATIONS

D. Vilsmeier, P. Forck, M. Sapinski, GSI, Darmstadt, Germany

Abstract

Simulating the electron and ion tracking in Ionization Profile Monitors is an important tool for specifying and designing new monitors. It is also essential for understanding the effects related to the ionization process, guiding field non-uniformities and influence of the beam fields which may lead to a distortion of measured profiles. Existing simulation codes are often tuned to the specific needs of a laboratory, are not well documented and lack a practical user interface. This work presents a generic simulation tool which combines the features of existing codes in order to provide a common standard for IPM simulations. The modular structure of the application allows for exchanging the computational modules depending on the use case and makes it extensible to new use cases. By this means simulations of Beam Induced Fluorescence monitors based on supersonic gas jets have been realized. The application and all involved methods have been tested and benchmarked against existing results. The code is well documented and includes a graphical user interface. It is publicly available as a git repository and as a Python package.

INTRODUCTION

Ionization Profile Monitors (IPM) allow for measuring the transverse profile of particle beams. They take advantage of the ionization process which is induced by the interaction of the particle beam with the (rest) gas and measure the resulting ionization products. An electric field is used for guiding ionized electrons or ions towards an acquisition system.

Several simulation codes have been developed at different accelerator laboratories in order to study effects which influence the quality of measured profiles or to design new devices [1, 2]. Two workshops dedicated to IPM simulations [3, 4] have shown a broad interest in this topic and also revealed the benefits of combining efforts and existing developments into a single application. For that reason the idea of a common, generic simulation tool was born. This application shall include the features of existing codes as well as be extensible to new methods.

USE CASES

While the motivation for such an application emerged mainly from simulations of IPMs it can be easily extended to other beam instruments such as Beam Induced Fluorescence monitors (BIF) or Electron Wire Scanners. Because such simulations involve many similarities it is useful to include them into a single application (in order to reuse the relevant parts for the different scenarios). For IPM simulations the influence of beam space charge [5, 6] or guiding field non-uniformities [7] are interesting subjects to study. Also the effect of secondary electrons emerging from ion impact on detector elements can be important to estimate. Other scenarios include the usage of supersonic gas jets for IPMs and BIFs or simulations of Electron Wire Scanners. Simulations involving the influence of multiple beams, for instance in case of diagnostics for electron lenses, are also of great interest.

MODULES

In order to fulfill the above mentioned use cases, common aspects have been separated into different modules and were realized in form of the following models. A model is a specific implementation for a given module, applicable to one or more specific use cases. The structure of the simulation framework, including the different modules and models, is shown in Fig. 1.

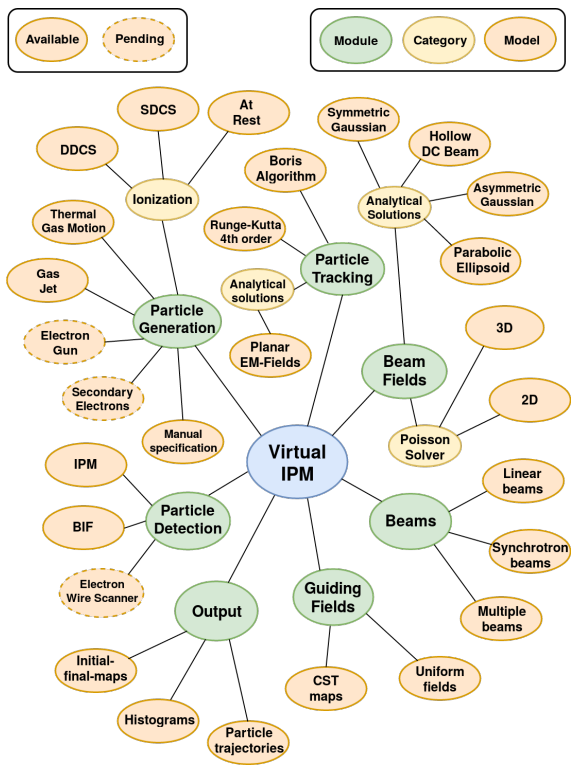

Figure 1: The different components (modules) of the simulation framework together with their corresponding models. Dashed ellipses indicate models in development.

Particle Generation

Particle generation models define the initial parameters for particles when they enter the simulation. Typically this involves the ionization or excitation process induced by the particle beam however other methods are possible (for example secondary electron generation). The following methods

ISBN: 978-3-95450-192-2 doi:10.18429/JACoW-IBIC2017-WEPCC08

DEVELOPMENT OF A FLUORESCENCE BASED GAS SHEET PROFILE MONITOR FOR USE WITH ELECTRON LENSES: OPTICAL SYSTEM DESIGN AND PREPARATORY EXPERIMENTS

S. Udrea†, P. Forck, GSI Helmholtzzentrum für Schwerionenforschung, Darmstadt, Germany
E. Barrios Diaz, N. Chritin, O. R. Jones, P. Magagnin, G. Schneider, R. Veness,
CERN, Geneva, Switzerland
V. Tzoganis, C. Welsch, H. Zhang, Cockcroft Institute, Warrington, United Kingdom

Abstract

A hollow electron lens is presently under study as a possible addition to the collimation system for the high luminosity upgrade of the LHC, while an electron lens system is also proposed for space charge compensation in the SIS-18 synchrotron for the high intensities at the future FAIR facility. For effective operation, a precise alignment is necessary between the high energy hadron beam and the low energy electron beam. In order to achieve this a beam diagnostics set-up based on an intersecting gas sheet and the observation of beam-induced fluorescence is under development. In this contribution we give an account of the design and performance of the optical detection system and report on recent preparatory experiments performed using a laboratory gas curtain set-up.

BEAM-INDUCED FLUORESCENCE SET-UP OVERVIEW

The beam-induced fluorescence (BIF) set-up for transverse beam diagnostics for electron lenses has as main components a supersonic gas sheet generator and an intensified camera system with an appropriate lens. The supersonic gas sheet is supposed to cross the charged particle beams under consideration and emit fluorescence radiation as a consequence of the interaction between the charged particles and the gas atoms or molecules. Part of the emitted radiation is collected by the lens and an image of the interaction region and thus of the transversal beam profiles is formed at the detector of the camera system.

The electron lens under study for the future high luminosity upgrade of the LHC (HL-LHC) will generate a hollow, 5 A, 10 keV electron beam which will be stabilized around the axis of the high energy proton beam by a 4 T magnetic field produced by a superconducting solenoid. Presently two BIF stations are foreseen, one at each end of the solenoid. At these positions the electron beam will not be in full compression, so is expected to have an outer diameter of approximately 10.5 mm and an inner one of about 7 mm, while the proton beam will have a sigma of approximately 0.3 mm. Thus the gas sheet is planned to have a width of about 11 mm and a thickness of less than 1 mm to allow for a proper interaction region. As working gases both Nitrogen [1] and Neon are presently under consideration. A 3D model of the diagnostics test set-up using a low current electron beam is shown in Fig. 1. This prototype is planned for commissioning at the Cockcroft Institute, UK towards the end of 2017.

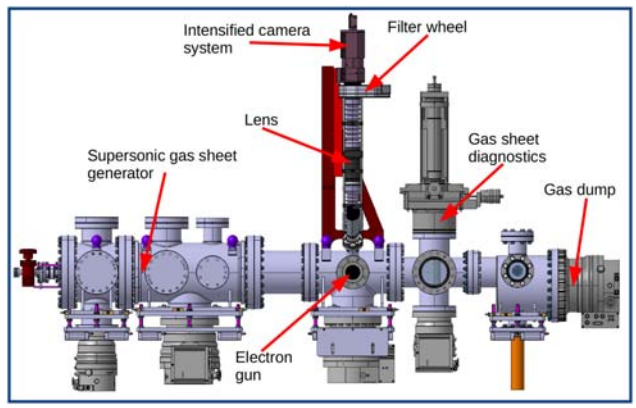

Figure 1: 3D model of the full prototype set-up to be commissioned end of 2017. An electron beam generated by a commercially available electron gun will be used for testing purposes.

THE INTESIFIED CAMERA SYSTEM

The cross-sections and integration times estimated for both Nitrogen [1] and Neon show that a camera system with the capability to detect single photons is required. Recent studies carried out at GSI [2] showed that an image intensifier based on MCP technology is currently still the best choice. Thus a ProxiKit PKS 2581 TZ-V image intensifier made by ProxiVision and using a Ø 1" double MCP in Chevron configuration has been acquired. Its main characteristics are:

- UV enhanced S20 photocathode, see Fig. 2 for sensitivity dependence upon wavelength
- P43 phosphor screen
- 28 lp/mm (line pairs per mm) maximum spatial resolution at the phosphor screen plane
- gated, TTL-triggered HV supply, minimum gate time 25 µs, no limit is imposed to the maximum, repetition rate up to 1 kHz
- Schneider Componon 12 35/2.8 lens system as optical relay to image the phosphor screen on a camera sensor
- C-mount adapters for objective and camera

† s.udrea@gsi.de

ISBN: 978-3-95450-192-2 doi:10.18429/JACoW-IBIC2017-WEPCC09

HORIZONTAL OPENING OF THE SYNCHROTRON RADIATION AND EFFECT OF INCOHERENT DEPTH OF FIELD FOR HORIZONTAL BEAM SIZE MEASUREMENT

T. Mitsuhashi†, KEK, Ibaraki, Japan
J. Corbett, SLAC, Menlo Park, CA, USA
M. J. Boland, SLSA, Clayton, Australia

Abstract

The incoherent depth-of-field due to the instantaneous opening angle of dipole SR emission can influence horizontal beam size measurements. In particular, for double-slit spatial interferometry, the opening angle introduces an intensity imbalance across the two slits that reduces interference contrast and therefore increases the apparent beam size. To investigate this effect, the instantaneous horizontal opening of the SR light must be known. Schwinger's theory gives the vertical opening angle and the qualitative theory of K.J. Kim gives an estimation for horizontal opening angle. An extension of Schwinger's theory to the horizontal plane by one of the authors leads to the same Bessel function distribution as the vertical plane using integration by parts. Neglecting the cubic phase term in the exponent, the expression agrees with Kim's diffraction theory. Using this result to correct for incoherent depth-of-field effects in double-slit measurements at the Australian Synchrotron, ATF and SPEAR3, the measured horizontal beam size is in good agreement with design values.

INTRODUCTION

For the measurement of horizontal beam size, the incoherent depth of field due to horizontal instantaneous opening of the Synchrotron Radiation will modify the spatial coherence in the horizontal direction. In particular, for double-slit spatial interferometry, the opening angle introduces an intensity imbalance across the two slits that reduces interference contrast and therefore increases the apparent beam size. To investigate this effect, the information of instantaneous horizontal opening of the SR light must be known. It is well known that the theory for the Synchrotron radiation which emitted from Circular trajectory is investigated by J. Schwinger, and he gives the vertical opening angle for the spectral density [1]. The qualitative theory of K.J. Kim gives an estimation for both of vertical and horizontal opening angle by using diffraction concept [2]. In this paper, a simple introduction for K.J. Kim's paradigm and Schwinger's theory, then we discuss an extension of Schwinger's theory to the horizontal plane using integration by parts. Using this result to correct for incoherent depth-of-field effects in double-slit measurements at the SPEAR3, Australian Synchrotron and ATF, the measured horizontal beam size is in good agreement with design values.

†email address: toshiyuki.mitsuhashi@kek.jp

EFFECT OF INCOHERENT DEPTH OF FILED FOR HORIZONTAL INTERFEROMETRY

In the horizontal plane, the interferogram includes the additional effect of incoherent depth of field (IDOF) by the instantaneous opening of the SR in the horizontal plane [3][4]. The IDOF has two effects, the first is the apparent horizontal beam size becomes bigger and the second is the visibility of the horizontal interferogram reduces by intensity imbalance at two opening of double slit. Using the instantaneous intensity distribution of SR in horizontal plane by $I(\theta)$ as a function of horizontal observation angle θ, the apparent beam shape $\sigma_\alpha(x)$ including the intensity imbalance factor is given by,

$$\sigma_a(x)=\int \frac{2\sqrt{I\left(\theta+\frac{D}{2R}\right)I\left(\theta-\frac{D}{2R}\right)}}{I\left(\theta+\frac{D}{2R}\right)+I\left(\theta-\frac{D}{2R}\right)}\cdot I(\theta)\cdot \frac{\exp\left[\frac{-\left[x-\rho\{1-\cos(\theta)\}\right]^2}{2\sigma^2}\right]}{\sigma\cdot\sqrt{2\pi}}d\vartheta \tag{1}$$

where the original beam profile is assumed to be ~~a~~ Gaussian. The visibility of the interferogram $\gamma_h(D)$ is given by Fourier cosine transform of the apparent beam shape as follows,

$$\gamma_h(D)=\int \sigma_a(x)\cdot\cos\left(\frac{2\pi\cdot D\cdot x}{R\cdot\lambda}\right)dx \tag{2}$$

For the discussion of horizontal spatial coherence, we need knowledge of instantaneous intensity distribution of SR in horizontal plane.

HORIZONTAL INSTANTANEOUS SR OPENING BY K.J.KIM

A horizontal instantaneous opening of the SR is qualitatively discussed by K. J. Kim [2]. He considers an apparent shape of circular trajectory by using time scale change factor (Doppler factor) as indicated in Fig. 1. According to his paradigm, the kink shaped apparent trajectory due to strong temporal squeezing in observer

ISBN: 978-3-95450-192-2 doi:10.18429/JACoW-IBIC2017-WEPCC10

ANALYSIS OF MIE SCATTERING NOISE OF OBJECTIVE LENS IN CORONAGRAPH FOR HALO MEASUREMENT

T. Mitsuhashi†, KEK, Accelerator Laboratory, Tsukuba, Ibaraki, Japan

Abstract

In beam halo measurements by means of a coronagraph viewing visible SR light, the theoretical image contrast is dominated by leakage of the diffracted fringe pattern from the Lyot stop. On other hand, the noise background in an actual coronagraph also contains light scattered from imperfections in the first objective lens. Most of this light is due to Mie-scattering from dig imperfections on the surface of objective which can reduce the image contrast to the 10-3 range for a lens with 60/40 scratch and dig figures. By introducing a high-quality objective lens into the system the theoretical value of 10-5-10-6 image contrast can be recovered for the Lyot coronagraph. In this paper, Mie-scattering due to dig imperfections is analyzed theoretically and results from measurements of the Mie scattering are presented.

INTRODUCTION

For high energy or high power accelerators such too much beam in the halo can lead to damage of accelerator components, either due to instantaneous beam loss or through long term irradiation. Beam halo control is essential and is best achieved by tuning the machine to avoid populating the tails of the bunch distribution. The beam diagnostic challenges here lie in developing non-invasive techniques with a high enough dynamic range to resolve a beam halo a factor 10^{-5} lower in intensity than that in the beam core. Synchrotron light sources, FELs and high energy hadron accelerators, such as the LHC, can all use synchrotron light to provide a non-invasive, transverse image of the beam distribution. To be able to measure the beam halo, however, requires an imaging system that eliminates the diffraction fringes created by the intense light from the beam core as is passes through the aperture of the first optical element. These fringes can have an intensity as high as 10^{-2} of the peak intensity and would hide any halo at the 10^{-5} level. To reduce this effect a coronagraph, developed by Lyot [1] in 1936 for solar astronomy, can be used. Such a technique has already been demonstrated by one of authors at the KEK Photon Factory to achieve a $6x10^{-7}$ ratio for background to peak intensity [2]. In this way, the coronagraph can escape from background due to diffraction fringe, but in other hand, strong illumination for objective lens can produce another background. The Mie scattering from digs on the surface of the objective lens. With typical commercial-available lens has scratch and dig 60/40 optical polishing quality, the Mie scattering background can make a background as like as intensity of diffraction fringe. In this paper, it is described analysis of Mie scattering from dig on the lens surface, and discuss the contribution to background in the coronagraph.

†email address: toshiyuki.mitsuhashi@kek.jp

CORONAGRAPH

The optical layout of the coronagraph is illustrated in Fig. 1 [2]. The objective lens makes a real image of the object (beam image) on to a blocking mask which makes artificial eclipse. Second lens (field lens) which is located just after the blocking mask makes a real image of the objective lens onto a mask so-called Lyot Stop. The diffraction fringes on focal plane of the objective lens is re-diffracted by field lens aperture and making a diffraction ring onto the focal plane of field lens. The Lyot's genius idea of the coronagraph is to remove this diffraction rings by a mask, so-called Lyot stop in today and relay the hidden image such as Sun corona by a third lens onto final observation plane. The background light on the final observation plane is now mainly come from the leakage of diffraction fringe inside of Lyot stop and the scattering of the input bright light by the objective lens. Theoretically, diffraction fringe leakage to next stage can reduce greatly, and we can reduce the background light less than 10^{-6} to the peak intensity of blocked main image at final stage. With this coronagraph, we can observe a hidden image of beam halo in accelerator surrounding from the bright beam core image.

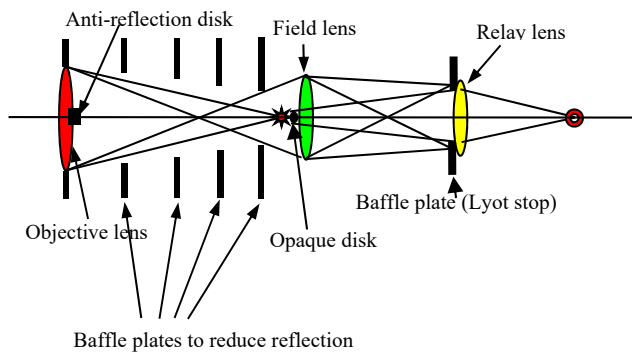

Figure 1: Layout of optical system of the coronagraph.

MIE SCATTERING SOURCE ON SURFACE OF OBJECIVE LENS

After blocking the central bright image and cutting the light from diffraction fringe, we have still scattered light (Mie scattering) from the defects in the objective lens such

ISBN: 978-3-95450-192-2 doi:10.18429/JACoW-IBIC2017-WEPCC11

PROFILE MONITOR ON TARGET FOR SPALLATION NEUTRON SOURCE

Shin-ichiro Meigo*, Hiroki Matsuda and Hayanori Takei
J-PARC center, Japan Atomic Energy Agency (JAEA), 319-1195, Japan

Abstract

Materials and Life Science Experimental Facility (MLF) in J-PARC is aimed at promoting experiments using the world highest intensity pulsed neutron and muon beams which are produced at a thick mercury target and a thin carbon graphite target by 3-GeV proton beams, respectively. Since damage due to the short pulsed proton beam at the mercury target vessel is proportional to the 4th power of the peak current density of the beam, decrease of the peak density is crucial for the beam injection system. To decrease peak density, a beam transport based on the nonlinear optics was developed. For reliable beam operation with the high-intensity beam, a reliable online 2D profile monitor with a long lifetime is indispensable to observe the beam introduced to the target. Furthermore, in J-PARC future facilities, high current density on the target will be required so that research and development have started to accept high density.

INTRODUCTION

In the Japan Proton Accelerator Research Complex (J-PARC) [1], a MW-class pulsed neutron source, the Japan Spallation Neutron Source (JSNS) [2], and the Muon Science facility (MUSE) [3] will be installed in the Materials and Life Science Experimental Facility (MLF) shown in Fig. 1. Since 2008, this source has produced a high-power proton beam of 300 kW. In 2015, we successfully ramped up beam power to 500 kW and delivered the 1-MW beam to the targets. To produce a neutron source, a 3 GeV proton beam collides with a mercury target, and to produce a muon source, the 3 GeV proton beam collides with a 2-cm-thick carbon graphite target. To efficiently use the proton beam for particle production, both targets are aligned in a cascade scheme, with the graphite target placed 33 m upstream of the neutron target. For both sources, the 3 GeV proton beam is delivered from a rapid cycling synchrotron (RCS) to the targets by the 3NBT (3 GeV RCS to Neutron facility Beam Transport) [4–6]. Before injection into the RCS, the proton beam is accelerated up to 0.4 GeV by a LINAC. The beam is accumulated in two short bunches and accelerated up to 3 GeV in the RCS. The extracted 3 GeV proton beam, with a 150 ns bunch width and a spacing of 600 ns, is transferred to the muon production target and the spallation neutron source.

Beam profile monitoring plays an important role in comprehending the damage to the target. Therefore it is very important to watch continuously the status of the beam at the target at the JSNS especially for the peak current density. We have developed a reliable beam profile monitor for the target by using Multi-Wire Profile Monitor (MWPM). In order to watch the two-dimensional profile on the target, we have also developed the profile monitor based on the imaging of radiation of the target vessel after beam irradiation. For observation beam introduced to the target, MWPM was placed at the proton beam window. In J-PARC center, facilities for research and development for Accelerator Driven System (ADS) is planned. Furthermore, to satisfy the demand of neutron and muon beam, second target facility is also expected. In those facilities, the beam will be more collimated than the JSNS so that a profile monitor will be required, which will stand higher current density than the JSNS.

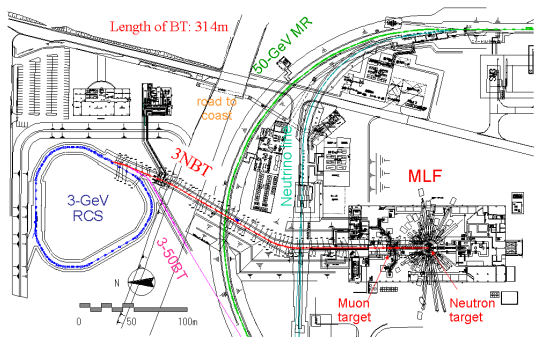

Figure 1: Plan of rapid cycling synchrotron (RCS) at the Materials and Life Science Experimental Facility (MLF) at J-PARC.

BEAM MONITOR SYSTEM AT THE BEAM TRANSPORT TO THE TARGET AT JSNS

Monitors Placed at Proton Beam Window

Continuously observing the characteristics of the proton beam introduced to the spallation target is very important. Due to the high activations caused by the neutron produced at the target, remote handling technique is necessary to exchange the beam monitor for the target. In order to decrease the radiation produced at the spallation neutron target, shielding above the monitor was required. To reduce the difficulties of the exchange work and decrease of the shielding, we combined the beam monitors with a Proton Beam Window (PBW) for separation between the vacuum region of the accelerator and the helium region around the neutron target. The PBW is better to be placed closer to the target where the distance between the target and the PBW is 1.8 m, which gives reliable profile at the target. In Fig. 2, the MWPM placed at the center of a vacuum chamber of the PBW is

* meigo.shinichiro@jaea.go.jp

ISBN: 978-3-95450-192-2 doi:10.18429/JACoW-IBIC2017-WEPCC12

MODIFICATION OF THE SYNCHROTRON RADIATION INTERFEROMETER AT THE TPS

M.L. Chen, K.H. Hsu, T.C. Tseng, S.Y. Perng, W.Y. Lai, H.C. Ho, H.S. Wang, C.J. Lin, D.G.Huang, C.Y.Liao, C.K. Kuan, NSRRC, Hsinchu, Taiwan

Abstract

During TPS operation, the stability of beam size measurement with the synchrotron radiation interferometer (SRI) does not compare well with the older SRI at the TLS. Ground vibrations appear to transmit to the SRI optics. This paper describes how to reduce the effect of vibration and improve the system stability to improve the stability of the SRI beam size measurement dramatically. To enhance the SRI sensitivity, an intensity imbalance method is incorporated and its results are discussed.

INTRODUCTION

The Taiwan Photon Source (TPS) was commissioned in 2015 and operates now routinely at 300 mA and 3 GeV energy. To measure the transverse beam size, two monitors are installed in the 40th beam port of the TPS. One is a synchrotron radiation interferometer (SRI) and the other a X-ray pinhole camera [1,2].

The SRI monitors horizontal and vertical beam sizes and its measurement results agree well with the pinhole camera, but the stability of the beam size measurements are not acceptable. In this paper, we present the recent work to stabilize the SRI beam size response.

PRINCIPAL FEATURES OF THE SYNCHROTRON RADIATION INTERFEROMETER

The synchrotron radiation interferometer, presented by Dr. T. Mitsuhasi in KEK, is now widely used to monitor beam sizes in synchrotron light sources [2,3,4,5]. The basic principle of a SR interferometer is to measure the profile of a small beam through the spatial coherence of light, and is based on the Van Citter-Zernike theorem. The distribution of intensity of the object is given by the Fourier transform of the complex degree of first-order spatial coherence. The intensity of the interferogram pattern is defined in Eq.1 as a function of position y1, where λ is the wavelength, R the distance from the light source to a double slit, D the double slit separation and a the half-height of the slits.

$$I(y1) = I_0 \left[sinc(\frac{2\pi a}{\lambda R} y_1)\right]^2 \left[1 + |v| \cos\frac{2\pi D}{\lambda R}\, y_1 + \varphi\right] \quad (1)$$

The visibility v is related to the complex degree of coherence by a factor involving the intensity of each beam.

The quantity ρ is the power imbalance ratio of the double slit defined by the ratio of the power intensities I1 and I2 from the double slits

$$\rho = \frac{I_1}{I_2} \quad (2)$$

The beam size is observed by the visibility of the interferogram and the beam size is given by

$$\sigma_{beam} = \frac{\lambda R}{\pi D}\sqrt{\frac{1}{2}\ln(\frac{1}{\gamma})} \quad (3)$$

where

$$\gamma = v\frac{1+\rho}{2\sqrt{\rho}} \quad (4)$$

Using the power imbalance method, the visibility γ can be reduced by lowering the imbalance ratio ρ while bringing the interferogram fringes above the noise level and increase the dynamic range of the SRI [6].

MONITOR SYSTEM SETUP

An SRI beam-size monitor is installed at the 40th beam port of the TPS and the beam line structure is shown in Fig. 1. The radiation produced from a dipole magnet propagates 19.2 m to pass through the shielding wall.

After a beryllium mirror in the vacuum chamber, the light passes through the extraction window and an aluminium reflection mirror, and then through the shielding wall. Outside of the shielding wall, two folding aluminium mirrors are used to deflect the synchrotron light to the optical table in the hutch.

The light is collected in the SRI beam size monitoring system by a diffraction-limited high-quality lens with 2 m focal length followed by a polarizer and a band-pass filter to obtain quasi-monochromatic light. The centre wavelength of the bandpass filter is 500 nm with 10 nm bandwidth. An eyepiece is applied to magnify the interferogram on the CCD; Two CCDs are used to separately observe the horizontal and vertical interferograms.

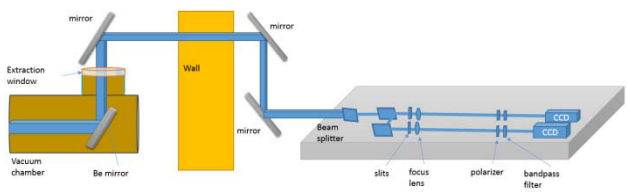

Figure 1: Optical set-up of the TPS SRI system at the 40th beam port.

VIBRATION MEASURMET

Since the stability of the TPS SRI does not match the stability achieved at the SRI in the TLS, laboratory ground vibrations are suspected and checked by an accelerometer (PCB393B31) and velocity sensor (MST-1031). As shown in Figs. 2 and 3, vibrations were observed not only on the ground but also on the optical table.

Observing the intensity variations of the interferograms on the CCD, we noted that the intensity variations are

ISBN: 978-3-95450-192-2 doi:10.18429/JACoW-IBIC2017-WEPCC13

PRELIMINARY STUDY ON IPM FOR CADS INJECTOR I*

J. He†, Z. Z. Wang, J. S. Zhou, Y. F. Sui, J. H. Yue, J. S. Cao
Key Laboratory of Particle Acceleration Physics & Technology,
Institute of High Energy Physics, Beijing 100049, China

Abstract

The Ionization Profile Monitor (IPM) based on the residual gas molecule is designed and fabricated for high power proton beam accelerator China Accelerator Driven Subcritical system injector I. The method of calculating the intensity of ionization signal is explored. The device uses the electric field generated by electrode to guide the ions, using Microchannel plates (MCP) to amplify ionization signals. A screen and a camera is used to detect the output electrons of the MCP, which present the distribution of the beam. The electric field distribution is optimized by CST ELECTROMAGNETIC STUDIO calculation. The IPM is installed on the ADS injector I and tested by beam. It measures the proton profile successfully during the CW commission. The experiment results agree well with the theoretical value which proves that the equipment can be used for CADS main linac in future.

INTRODUCTION

The Ionization Profile Monitor (IPM), also known as Residual Gas Monitor (RGM), is one of the most popular non-destructive profile detection device, mainly used for the machine which the beam size is in the range from mm to cm. High intensity and high power hadron accelerators usually implies the usage of non-destructive methods[1]. For the high power beam, the interception materials such as the phosphor screen [2], the wire target [3], the secondary electron grid may be damaged by the beam. Laser scanning [4], electron beam scanning [5] and residual gas detectors will not have this problem. There are a lot of IPM research experience in different lab, such as FNL [6, 7], KEK [8, 9], BNL [10], and CERN [11]. Several IPM systems have been installed and several workshops focus on this topic have been held in GSI [12, 13, and 14].

With the development of China high-power proton accelerator, there is a growing demand for non-destructive profile detection, such as Chinese Spallation Neutron Sources (CSNS) and Accelerator Driven Subcritical systems (ADS). There are several wires have been destroyed by beam both in CSNS and ADS. Two non-invasive beam profile measurement methods were developed including the electron scanner and IPM on ADS Injector I. The Fig.1 (a) shows the layout of the injector and the locations of both electron scanner and IPM. The Fig.1 (b) shows the RMS beam size from the exit of the ion source to the dump, the blue curve is the horizontal size and the red curve is vertical size. As shown in Fig. 1 (b), the theoretical beam size at the IPM location is 15 mm × 5mm.

The most important parameters that affects IPM systems is the ionization yield, which is how much electron-ion pairs are generated per second. It is determined by the beam parameters and the vacuum parameters, including the pressure and the composition of the residual gas. The Bethe-Bloch formula describes the energy loss caused by the collision between the beam and residual gas which is related to the energy of the beam. The total ionization number N can be expressed as: $N=\Delta E/I_0$, where the ΔE is the total energy loss in the gas volume, and I_0 is the average energy required to produce an electron-ion pair, also known as ionization energy, usually is about 20~30 eV. According $N_D = (-dE/dx)\cdot l \cdot I_{current} / I_0$, for the ADS beam, $I_{current}$=10 mA, assume that the residual gas is H_2 and the pressure is 1×10^{-5} Pa, the detector longitudinal length l = 3 cm, I_0 = 33 eV, the N_D is 3.86 x 10^7 pps for CW beam.

EXPERIMENT

The experiment set up is shown as Fig. 2. The device is working in ion collection mode. In order to produce a guild field of 1 kV / cm, ±4 kV is applied to the upper and lower oxygen-free copper electrodes, respectively.

Table 1: IPM Design Parameters for ADS Injector I

Parameters	Value
Electric field（V/m）	10^5
Distance of two plates（cm）	8
Size of MCP（mm）	Φ75
Size of EGA (mm)	Φ70
Detector	P43 +CCD
Work mode	Ions
Magnetic field	0

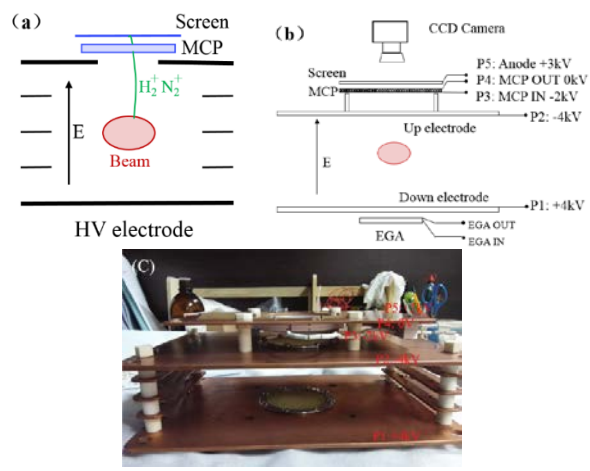

Figure 2: (a) Schematic of ion collection by E-field IPM (b) potential distribution MAP of IPM different components (c) picture of Oxygen-free copper electrodes and MCP.

* Work supported by the NSFC under grant No.11305186
† hejun@ihep.ac.cn

ISBN: 978-3-95450-192-2 doi:10.18429/JACoW-IBIC2017-WEPCC14

A STUDY OF THE EFFECT OF IMPERFECTIONS IN THE OPTICAL PATH OF THE SNS* TARGET IMAGING SYSTEM USING A MOCK-UP

W. Blokland†, F. Garcia[1], Oak Ridge National Laboratory, Oak Ridge, TN, USA
[1] also at the University of Tennessee, Knoxville, TN, USA

Abstract

The Spallation Neutron Source sends a 1 GeV proton beam to a mercury filled target to generate neutrons. The Target Imaging System (TIS) provides an image of this proton beam on the target to help center the beam and determine the peak density. Most of the TIS optical path is installed together with the proton beam window, which is replaced every two to three years. Using the next-to-be-installed proton beam window and a mock-up of the target and the beam pipe to the target, we have studied imperfections in the optical path to estimate their effect on the TIS measurements. In this paper, we show the effect of geometric distortion and light reflections, as well as the difference in the performance of two optical fiber bundles with different resolutions and contrasts.

INTRODUCTION

To produce the neutrons used for materials research, 1 GeV protons hit the stainless-steel target vessel filled with mercury. The Target Imaging System (TIS) helps optimize the target's lifetime by steering the beam to the center of the target's nose cone. The nose cone is coated with aluminum oxide doped with chromia. This layer luminesces when the protons hit, thus producing an image of the beam on the target. The light is collected by an off-axis parabolic mirror at the Proton Beam Window (PBW) and guided by optics and a radiation resistant high purity fused silica fiber bundle to a camera outside the high radiation area, see Fig. 1 and [1-3].

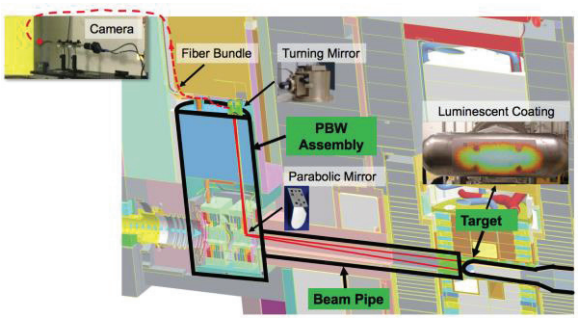

Figure 1: The layout of the TIS.

The TIS calculates the position of the beam to monitor that we are keeping the beam centered within ± 4 mm vertically and ± 6 mm horizontally. The beam can also be steered by equalizing the temperature read-backs from the thermocouples at the PBW. This method requires a symmetric beam halo and a flat orbit.

The TIS also provides estimates for the width of the beam, which is used to calculate the peak density. During operations, we must keep 90% of the beam within a 200 by 70 mm footprint and keep the peak density within certain limits, depending on beam power. A program called the RTBT Wizard (Ring to Target Beam Transferline) uses the beamline optics elements, 4 RTBT wire scanners, and the RTBT harp to predict the width of the beam on the target. The difference between the two width measurements has significantly varied, even more than 30%, with the Wizard usually providing a higher peak density. To be on the safe side, the higher number has been used for operations.

The difference in estimates can be due to the difference in analysis routines, imperfect knowledge of the magnetic fields of the quadrupole magnets, uncertainty in the calculation of the Proton Beam Window's beam scattering effect, widening of the TIS proton image by luminescence due to particles other than protons, a temperature gradient sensitivity in the luminescence across the coating, and imperfections in the TIS optical path. In this paper, we study the effects of imperfections of the optical path, specifically the reflections of light in the beam pipe and the geometric distortion by the optical elements. We will also show what effect the differences in the quality of the optical fiber bundles has on the TIS image.

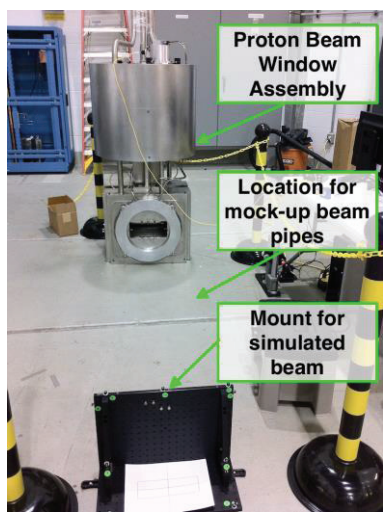

Figure 2: The proton beam window setup.

* This manuscript has been authored by UT-Battelle, LLC, under Contract No. DE-AC0500OR22725 with the U.S. Department of Energy.
† blokland@ornl.gov

ISBN: 978-3-95450-192-2 doi:10.18429/JACoW-IBIC2017-WEPCC16

FIRST EXPERIMENTAL RESULTS OF THE COMMISSIONING OF THE SwissFEL WIRE-SCANNERS

G.L. Orlandi*, A. Alarcon, S. Borrelli, A. Gobbo, P. Heimgartner, R. Ischebeck, D. Llorente, F. Loehl, C. Ozkan Loch, P. Pollet, B. Rippstein, V. Schlott,
Paul Scherrer Institut, 5232 Villigen PSI, Switzerland.
R. Vintar, Cosylab, Ljubljana, Slovenia.

Abstract

Several wire-scanners - 19 out of 22 - are presently installed in SwissFEL, the hard X-ray FEL facility under commissioning at Paul Scherrer Institut (www.psi.ch). Thanks to a wire-fork designed to be equipped with two different pairs of scanning wires (5 μm tungsten and 12.5 μm Al(99):Si(1)), high resolution measurements of the beam profile - and emittance - and, alternatively, a minimally-invasive beam monitoring during FEL operations can be performed. First experimental results of the SwissFEL wire-scanner commissioning will be presented as well as a summary of the prototyping design and characterization.

INTRODUCTION

SwissFEL is a Free Electron Laser (FEL) facility [1] presently under commissioning at Paul Scherrer Institut (www.psi.ch). Two undulator lines - so called ATHOS and ARAMIS - will provide X-rays pulses at a repetition rate of 100 Hz in the wavelength region $7 - 0.7$ nm and $0.7 - 0.1$ nm, respectively. The SwissFEL linear accelerator is a compact machine - the length of the entire facility including photon transfer lines and experimental hall is about 720 m - with a relatively moderate beam energy: 5.8 GeV being the maximum energy required to reach the saturation regime of coherent radiation emission in the given wavelength range. In order to meet such constraints of compactness and energy, the beam acceleration is mostly ensured by a C-band RF linac and the compression scheme is optimized to preserve the high brightness quality of the electron beam, which is characterized by a transverse normalized slice emittance of 0.4/0.2 mm.mrad for the two nominal charge operation modes 200/10 pC of the machine. The electron beam - emitted by a photo-cathode with an initial bunch length of 3/1 ps (rms) and with a two-bunch temporal macrostructure of 28 ns - is accelerated by a 2.5 cell S-band gun up to 7.1 MeV at a repetition rate of 100 Hz. The further acceleration of the electron beam is performed by a S-band RF linear booster - up to 330 MeV - and by a C-band linac up to $2.1 - 5.8$ GeV. During the transition from the S-band to the C-band RF sections, the S-Band induced energy chirp of the electron beam is linearized by a pair of X-band RF cavities and converted to a longitudinal compression of the electron beam - 300/200 fs (rms) - by a magnetic chicane. After a further compression stage in a second magnetic chicane - 20/3 fs (rms) - at a beam energy of about 2.1 GeV, an RF kicker and a magnetic switch-yard deviate the orbit of the second bunch of the two-bunch train from the ARAMIS arm to the ATHOS arm. After a further acceleration stage, the two bunches are separately injected at 100 Hz into the two undulator lines (ARAMIS and ATHOS).

In a FEL driver linac, wire-scanners (WSCs) [2, 3, 4, 5] complement view-screens to monitor the beam profile monitor. Compared to view-screens, WSCs are normally immune to non-linear effects of the signal response and can perform high resolution measurements which ultimately depends on the wire diameter and scanning speed. In SwissFEL, the WSCs are designed to absolve two main tasks [6, 7]: high resolution characterization of the beam profile for high precision measurement of the beam emittance and a routinely and minimally-invasive monitoring of the beam profile under FEL operations. Moreover, because of the afterglow characterizing the YAG:Ce crystals of the view-screens, in SwissFEL only WSCs can discriminate in time the two-bunch temporal macrostructure (28 ns) of the electron beam. The SwissFEL wire-fork is motorized by a stepper motor and equipped with two pairs of metallic wires, see Fig.1: 5 μm tungsten (W) and 12.5 μm Al(99):Si(1). As the wire scans the beam, a shower of primary scattered electrons and secondary emitted particles is produced in proportion to the fraction of the beam sampled by the wire. In SwissFEL, the forward - high energy and small scattering angle - component of the particle shower ("wire-signal") is out-vacuum detected by means of Beam-Loss-Monitors (BLMs) [8]. The beam-synchronous acquisition (BSREAD) [9] of both the encoder and the BLM readouts permits to reconstruct the one-dimensional transverse profile of the electron beam. The beam-loss sensitive material of the BLMs is a scintillator fiber (Saint Gobain BCF-20, decay time 2.7 ns) wrapped around the vacuum pipe. The scintillator fiber is matched by means of a Plastic Optical Fiber (POF) to a photomultiplier (PMT) having a remotely adjustable gain in the range $5 \times 10^3 - 4 \times 10^6$. The PMT signal is finally digitized and integrated in time by an ADC unit. In a WSC measurement, together with the signals from the encoder and the BLM, also the charge and position signals from Beam Position Monitors (BPMs) upstream and downstream the WSC are BSREAD acquired at every RF shot in order to correct the reconstructed beam

* gianluca.orlandi@psi.ch

ISBN: 978-3-95450-192-2 doi:10.18429/JACoW-IBIC2017-WEPCC17

2D NON-DESTRUCTIVE TRANSVERSE DIAGNOSTICS BY BEAM CROSS-SECTION MONITOR

S. Gavrilov[1,2†], P. Reinhardt-Nickoulin[1], A. Titov[1,2]
[1] Institute for Nuclear Research of the Russian Academy of Sciences, Moscow, Russia
[2] Moscow Institute of Physics and Technology (State University), Moscow, Russia

Abstract

Beam Cross-Section Monitors implemented at INR RAS proton linac provide an efficient non-destructive registration of real 2D beam cross section, beam position and profiles, phase space ellipses reconstructed from profiles data as well as real-time evolution of these parameters in the entire range of beam energies and intensities. Features of the monitor's design and image processing system are described. Measurement accuracy and precision analysis are discussed. A variety of available experimental results are presented.

INTRODUCTION

The reconstruction technique of a two-dimensional beam density distribution *I(x, y)* through a residual gas ionization was initially proposed by V. Mihailov et al. [1] in Kurchatov institute. Beam Cross-Section Monitors (BCSMs) [2], based on ion components of a residual gas ionization, were implemented later and upgraded at INR RAS linac for in-flight non-destructive diagnostics. The general principle of BCSM has been described many times previously and is clear from Fig. 1.

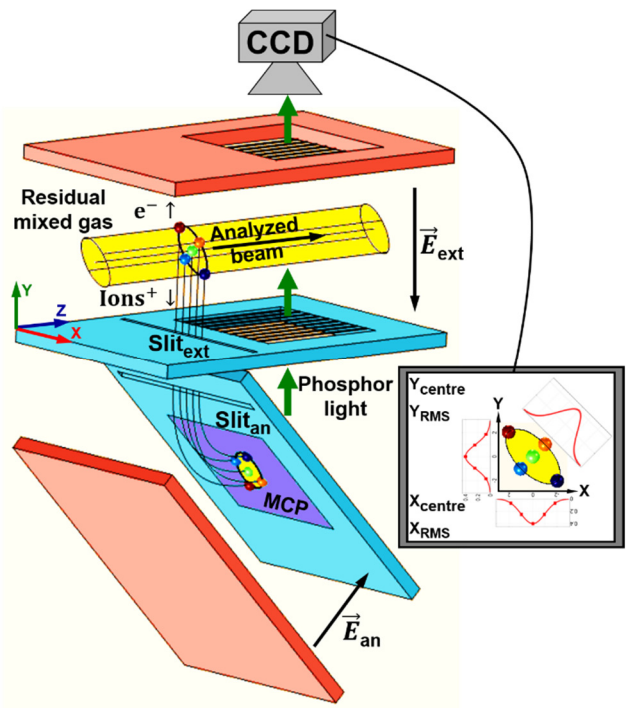

Figure 1: BCSM scheme.

The beam under study passes the area of a quasi-uniform electrostatic field and ionizes molecules of a residual gas. The energy of extracting ions in a double slit filter depends on their original Y-coordinates, so their energy distribution reproduces the transverse density distribution of the analyzed beam along Y-axis, while the distribution of the ions along X-axis keeps the same as that in the beam. Due to a potentiality of electric fields all types of ions, regardless of a specific charge: H_2^+, N_2^+, H_2O^+, etc. contribute to a 2D image formation of particle density distribution in analyzing beam cross-section (BCS).

DESIGN FEATURES

There are four main components of BCSM measurement errors. Two physical: thermal motion of ions and beam space charge and two technical: optical image processing system and internal mechanical design.

The design defines uniformity of extracting and analyzing fields as well as an Y-scale of the BCS image at electro-optical converter (MCP + phosphor). In case of uniform fields, the original distance Y_{ext} from the ion to extracting slit and converted distance L_{an} from the ion image to analyzing slit along the electrode are related as $L_{an} = 2 \cdot Y_{ext} \left({}^{E_{ext}}/_{E_{an}} \right)$. The image on the phosphor screen is detected by CCD-camera directed parallel to Y-axis. In case ${}^{E_{an}}/_{E_{ext}} = \sqrt{2}$ the detected image is identical to the analyzed BCS.

The fields in a simple, but effective, design (Fig. 2a) can be improved by several times with multiple extra correction electrodes (Fig. 2b), which decrease a non-uniformity of extracting and analyzing fields down to less than 1%. For Z-axis field symmetry extra cuts with special calculated forms can be implemented.

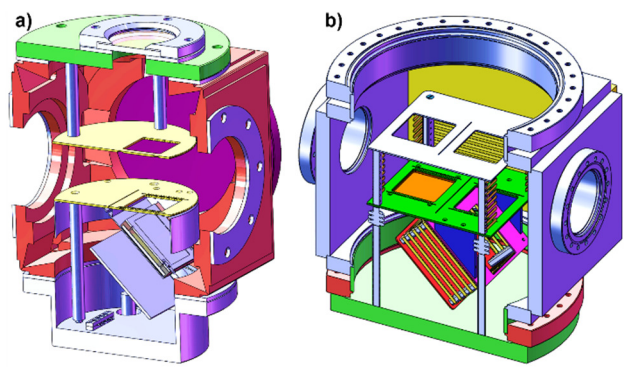

Figure 2: BCSM internal designs: a) used one (initial), b) improved one by extra correction electrodes and cuts.

† s.gavrilov@gmail.com

ISBN: 978-3-95450-192-2 doi:10.18429/JACoW-IBIC2017-WEPCC18

AN UPGRADED SCANNING WIRE BEAM PROFILE MONITORING SYSTEM FOR THE ISIS HIGH ENERGY DRIFT SPACE

D. M. Harryman*, C. C. Wilcox†, STFC Rutherford Appleton Laboratory, Didcot, UK

Abstract

The ISIS Neutron and Muon Source, based at the Rutherford Appleton Laboratory, begins with an injector line that accelerates an H^- ion beam to 70 MeV. The beam then travels through a High Energy Drift Space (HEDS) before passing through an electron stripping foil upon injection into the proton synchrotron, which provides acceleration up to 800 MeV.

During machine setup, beam profile measurements in the HEDS are taken using scanning wire monitors, which drive a single pair of measuring wires, one per plane, through the beam aperture using an analogue servo motor. Many of these monitors have been in operation since ISIS was commissioned in 1984 and as such are coming to the end of their operational lifetimes, meaning a new suite of monitors is required.

A prototype monitor has been developed along with new electronics and a control system to test the operation of a new drive mechanism based around a stepper motor and resolver, providing increased precision and reliability. This paper discusses the development of a new multi-wire monitor design, and the associated upgrade to the electronics and control system.

INTRODUCTION

The ISIS linac accelerates H^- ions to 70 MeV, producing a 50 Hz pulsed beam with a pulse length of 200 µs. This beam travels through a HEDS before injection into an 800 MeV proton synchrotron. After acceleration, protons are transferred into one of two Extracted Proton Beamlines (EPBs) and delivered to a tungsten target, driving the neutron spallation process.

Measurement of the beam's profile throughout the accelerator is vital during machine setup, whilst also providing valuable information during accelerator studies, and for understanding beam loss mechanisms. Three types of profile monitor are in use around ISIS: wire scanners and wire grid ('harp') monitors, which are both destructive to the beam [1]; and Ionisation Profile Monitors (IPMs), which provide non-destructive measurements. IPMs are used for profile measurements around the synchrotron ring, as any induced beam loss would quickly build to unsustainable levels over multiple orbits. Non-destructive profile monitoring at ISIS is described in further detail in [2] [3].

Destructive profile monitors are installed around the HEDS and EPBs and are crucial during machine setup, providing trusted and reliable measurements of the beam. Profiles are taken by moving conducting wires into the path of the beam and measuring the current generated by secondary electron emission, induced as beam particles pass through the wires. ISIS is operated at a slower rate of 1.6 Hz while these monitors are in use, reducing both the levels of induced beam loss and the risk of damage to the measuring wires.

Harp monitors are installed along both EPBs, consisting of retractable grids of wires which are inserted into the beam aperture using a pneumatic system. The grids contain 24 wires per plane with spacing set to either 6 mm or 10 mm, depending on the beam distribution in each location. Along the HEDS the beam is significantly smaller, with beam widths typically between 10-30 mm. As a result wire scanners are used here instead to allow higher resolution profiles to be measured, in addition to being cheaper to manufacture and causing less beam loss.

A single pair of measuring wires is scanned across the beam aperture by a motor driven linear stage, mounted at 45° to the beam (Fig. 1). As a result, wire displacement in both the horizontal and vertical planes is equal when the wire head is moved, with the distance travelled along each plane inversely proportional to the linear stage motion by a factor of $\sqrt{2}$. The wires are moved through the beam in horizontal and vertical steps, typically of 4 mm, and a reading is taken at each position to build up a 2D profile measurement over multiple beam pulses.

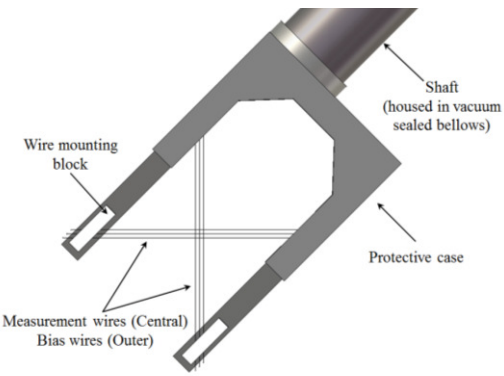

Figure 1: Orientation of a wire scanner head, with a signal wire and pair of bias wires mounted in each plane.

There are currently 15 wire scanners installed along the ISIS HEDS, many of which have been operational for over 30 years and have surpassed their design lifetimes. As a result a replacement programme is now underway, and a new monitor design has been developed alongside an upgraded control system and electronics.

MONITOR DESIGN

A prototype monitor of the new design has been built, tested and recently installed in the ISIS HEDS. The monitor offers improved measurement resolution and precision compared with existing monitors, in addition to enhanced reliability. As the motion undergone during measurement

* daniel.harryman@stfc.ac.uk
† christopher.wilcox@stfc.ac.uk

ISBN: 978-3-95450-192-2 doi:10.18429/JACoW-IBIC2017-WEPCC19

A FAST WIRE SCANNER FOR THE TRIUMF ELECTRON LINAC

P. Dirksen, M. Lenckowski, W.R. Rawnsley, M. Rowe, V. Verzilov,
TRIUMF, Vancouver, Canada

Abstract

The superconducting CW LINAC presently being commissioned at TRIUMF will accelerate up to 10mA of electrons to the energy of 30 – 50 MeV. Thus, beam powers up to 0.5 MW are eventually expected. To support high beam power operation modes, a Fast Wire Scanner (FWS) capable of velocities up to 3 m/s over a 70 mm range was developed. A stepper motor driven helical cam allows for a long stroke enabling two orthogonal wires to scan both axes in one scan. The radiation produced when the wires pass through the beam is detected by a BGO scintillator coupled to a photomultiplier (PMT), while wire position is measured with a precision linear potentiometer. A Struck SIS3302 VME transient recorder, synchronized to the beam pulses, simultaneously captures both signals to produce the beam profiles in the EPICS control system. The design of the FWS and initial beam measurements will be presented.

INTRODUCTION

As a part of the effort to substantially expand the Rare Radioactive Isotope Beam (RIB) program, TRIUMF is currently in a construction phase of a 50 MeV 10 mA CW superconducting electron LINAC, to act as a driver for production of neutron-rich isotopes via photo-fission reactions [1]. The electron accelerator comprises a gridded 10 mA 300 keV thermionic gun operated at 650 MHz, a 50 MeV superconducting CW LINAC and a 70 m long beam transport line to deliver the electron beam to RIB production targets. The LINAC presently consists of two cryomodules housing three 1.3 GHz 9-cell cavities of TESLA type. Two additional cavities in a separate cryomodule will be added to the setup in the future. The first beam was accelerated to 22 MeV in 2014 and presently various accelerator systems are still undergoing commissioning to prepare the machine for high beam power operation.

Although the beam tuning is typically done with beam currents of a few microamperes using diagnostic devices such as view screens and Faraday cups [2], the actual RIB production will require monitoring of beam parameters at the full beam current. To support production modes several diagnostic devices have been developed including the FWS.

Calculations show that a carbon wire needs to travel at speeds of about 3 m/s to survive the 10 mA and 50 MeV electron beam with the size of about 0.5 mm FWHM [3]. Wire scanners operated at even higher speeds exist [4] but employ a rotary motion of the wire. For the sake of compatibility with the standard diagnostics vacuum chamber, the TRIUMF design is based on a linear motion. The linear motion allows both X- and Y-plane scans in a single pass using two orthogonally mounted wires on the same frame. To our knowledge this is the fastest linear wire scanner presently in operation.

MECHANICAL DESIGN

The FWS design was inspired by the wire scanner developed for FLASH at DESY [5], which utilizes a slot winding cylinder that engages a follower to produce a 48 mm stroke with 24 mm working range at speeds of 1 m/s. The short travel range of the DESY design requires a dedicated device for measuring each plane. For the TRIUMF FWS (Fig. 1) we required a longer working range of 70 mm to allow one FWS to scan both planes, and a speed up to 3 m/s which resulted in an overall stroke of 170 mm. To achieve the longer stroke in a compact device, a multi-turn helical cam was developed.

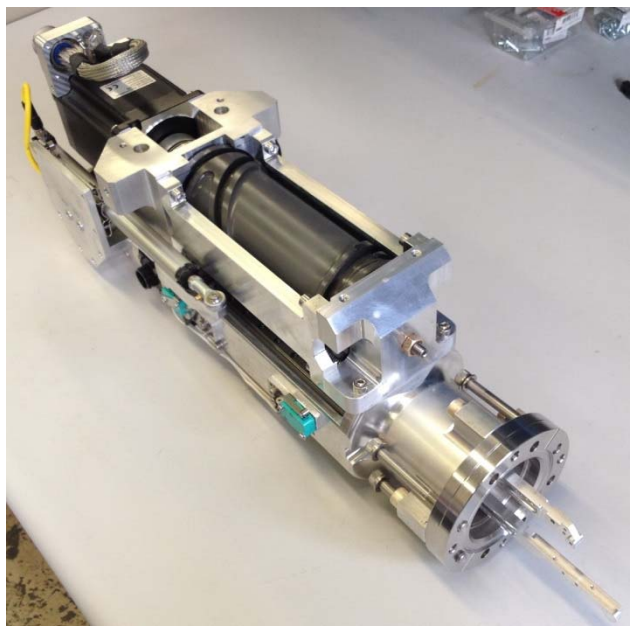

Figure 1: TRIUMF Fast Wire Scanner assembly.

The TRIUMF FWS mounts a wire fork assembly to a carriage which is supported on the main frame by linear bearings, and is driven in and out by the cam. To minimize the momentum generated at high accelerations, the mass of the moving parts is minimized where possible to a total of 816 grams.

Cam Design

The cam is a hollow 75 mm diameter cylinder constructed of aluminium and is hard anodized after machining. The 170 mm stroke includes two 70 mm ramps, and 30 mm of constant 168 mm/rev pitch in the middle. The motion of the FWS minimizes jerk by using a sinusoidal velocity ramp which is machined into the cam profile. The flat section at the end allows the cam to reach full speed before the carriage motion begins.

ISBN: 978-3-95450-192-2 doi:10.18429/JACoW-IBIC2017-WEPCC20

RF DEFLECTOR BASED MEASUREMENTS OF THE CORRELATIONS BETWEEN VERTICAL AND LONGITUDINAL PLANES AT ELI–NP–GBS ELECTRON LINAC

L. Sabato*, University of Sannio, Benevento, Italy
P. Arpaia, A. Liccardo, University of Naples Federico II, Napoli, Italy
A. Giribono, A. Mostacci, L. Palumbo, University of Rome La Sapienza, Roma, Italy
C. Vaccarezza, A. Variola, INFN/LNF, Frascati (Roma), Italy
A. Cianchi, University of Rome Tor Vergata, Rome, Italy

Abstract

The correlations between vertical and longitudinal planes at the Radio Frequency Deflector (RFD) entrance can be introduced by misalignments of accelerating sections or quadrupoles upstream of the RFD. These correlations are undesired effects and they can affect the RFD based bunch length measurements in high–brightness electron LINAC. In this paper, an RFD based measurement technique for vertical and longitudinal planes is proposed. The basic idea is to obtain information about the correlations between vertical and longitudinal planes from vertical spot size measurements varying the RFD phase, because they add contributions on this quantity. In particular, considering a small RFD phase range centred in 0 or π rad, the correlations between the particle longitudinal positions and the vertical plane are constant with the deflecting voltage phase, on the contrary, the correlations between the particle energies and the vertical plane vary linearly with the deflecting voltage phase. The simulations are carried out by means of ELEctron Generation ANd Tracking (ELEGANT) code in the case of the Gamma Beam System (GBS) at the Extreme Light Infrastructure–Nuclear Physics (ELI–NP).

INTRODUCTION

RFD or Transverse Deflecting Structure (TDS) [1] are very common in high–brightness LINACs in order to measure the ultra–short electron bunch length since they allow to achieve very good resolutions, lower than other state–of–the–art measurements, such Electro Optical Sampling [2]: at SLAC [3, 4], at SPARC_LAB [5, 6], at DESY [7], at MIT PSFC [8], and so on. An RFD provides a transverse kick to the electron bunch introducing a relationship between the bunch longitudinal dimension and the bunch vertical dimension at a screen, placed after the RFD. Therefore, the electron bunch length can be obtained through vertical spot size measurements on a screen, placed after the RFD [9, 10], after an appropriate calibration measuring the vertical bunch centroid varying the deflecting voltage phase [11].

The correlations between vertical and longitudinal planes at the RFD entrance can be introduced by misalignments of accelerating sections or quadrupoles upstream of the RFD [12]. These correlations are undesired effects and they can affect the bunch length measurements based on the usage of the RFD in high–brightness electron LINAC. The contribution of strong correlations between vertical and longitudinal are not taken into account by means of the standard bunch length measurement technique [4, 5, 11] and, therefore, they can be sources of systematic error. On the other hand, the variations of the squared value of vertical spot size due to these correlations can be used in order to take information about them. In this paper, a measurement technique for the correlations between the vertical and the longitudinal planes by means of an RFD is proposed. First of all, the theory behind the working principle is explained in section **BASIC IDEA**. Secondly, every step of the proposed measurement technique is detailed (section **MODEL OF MEASUREMENT PRODUCTION**) and, then, the simulation results are compared with the theoretical predictions (section **NUMERICAL RESULTS**). The simulations are carried out by means of ELEGANT code [13] in the case of GBS at ELI–NP facility [14].

BASIC IDEA

Modelling the L_{RFD}–long RFD as a $L_{RFD}/2$–long drift space, a vertical kicker, and another $L_{RFD}/2$–long drift space [15, 16], and assuming *(i)* the particle energy can be written in Taylor series stopped at first order around the particle energy average $\langle E \rangle$, and *(ii)* considering an RFD phase range small and centred in 0 rad (or π rad), the contribution of the correlations between longitudinal and vertical planes on the squared value of the vertical spot size at screen after the RFD is:

$$cor_{l_0 v_0}(\varphi) = 2K_{cal}(0) cor_{t_0 v_0} - 2\frac{K_{cal}(0)}{2\pi f_{RF}} cor_{\delta_0 v_0}\varphi, \quad (1)$$

where f_{RF} and φ are the deflecting voltage frequency and phase, respectively, t_0 is the particle longitudinal position in seconds when the bunch centroid is at RFD centre, $\delta_0 = (E_0 - \langle E_0 \rangle)/\langle E_0 \rangle$, E_0 is the particle energy, $cor_{t_0 v_0}$ and $cor_{\delta_0 v_0}$ are *(i)* the correlation term between the particle longitudinal positions and the vertical plane and *(ii)* the correlation term between the particle energies and the vertical plane, respectively:

$$cor_{t_0 v_0} = \sigma_{y_0 t_0} + L\sigma_{y'_0 t_0}, \quad (2)$$

$$cor_{\delta_0 v_0} = \sigma_{y_0 \delta_0} + L\sigma_{y'_0 \delta_0}, \quad (3)$$

* luca.sabato@unisannio.it

ISBN: 978-3-95450-192-2 doi:10.18429/JACoW-IBIC2017-WEPCC21

BEAM SIZE MONITOR BASED ON MULTI-SILT INTERFEROMETER AT SSRF*

B.Gao†[1], Y.B. Leng‡, J.Chen, H.J.Chen[1], K.R.Ye
Shanghai Institute of Applied Physics, Chinese Academy of Sciences, Shanghai 201800, China
[1]also at University of Chinese Academy of Sciences, Beijing 100049, China

Abstract

Double-silt synchrotron radiation interferometer is a common and useful tool to measure transverse beam size around the world. In order to satisfy the requirement of high speed measurement and improve the accuracy of BSM (beam size monitor), multi-silt interferometers have been designed and tested at SSRF. Multi-silt mask pattern has characteristics of high flux throughput and high SNR of the interferogram, which is very useful at high-speed beam size measurement. This technique has a relative complex algorithm to deconvolve the result image and figure out the beam size. Principle of the multi-silt SR interferometer, mask design and experiment will be present detailed in this paper.

INTRODUCTION

The emittance of an electron beam,which is inversely proportional to the brilliance of the synchrotron radiation, is one of the most important characteristics of a storage ring operated as a synchrotron light source. To monitor degradation of the emittance, which could be caused by beam instabilities or ion-trapping phenomena, it is necessary to observe the transverse profile of the electron beam in real time. Third-generation synchrotron light sources such as the SSRF storage ring are designed to achieve low emittance and a small emittance-coupling ratio. To measure the small beam size in few tens micro meters level is very necessary. Visible light interferometer, developed by T. Mitsuhashi [1] has high resolution in beam size measurement, which has been used in different facilities around the world. However, each method has advantages but also limitations, Double-silt synchrotron radiation interferometer is limited at high speed measurement. A novel approach was proposed to satisfy the requirement of high speed measurement. Multi-silt mask pattern has characteristics of high flux throughput and high SNR of the interferogram, which is very useful at high-speed beam size measurement. A prototype 3-silt mask has been designed and test at SSRF.

DOUBLE-SILT INTERFEROMETER AT SSRF

The arrangement of double-silt interferometer at SSRF is shown in Fig. 1. The measuring interferogram is fitted by the intensity distribution of the form. The image analysis system works extracting the orthogonal profile, centre position, and least square fit to evaluate the beam sizes. The 800Mb/s interface enables full frame rate and even more cameras on the same bus. The IEEE-1394b cable with jack screws allows a more secure connection to the camera. 12-bit A/D converter, Via external trigger, software trigger (on same bus), This equipment has been tested and found to comply with the limits for a Class A digital device, have good linearity It provide reasonable protection against harmful interference when the equipment is operated in experimental environment.

After all environments and system calibration, Interferometer is good enough for the measurement of a few micro meters small beam size [2]. But the data refresh rate is 2Hz, which is not able to meet the demand of high speed measurement.

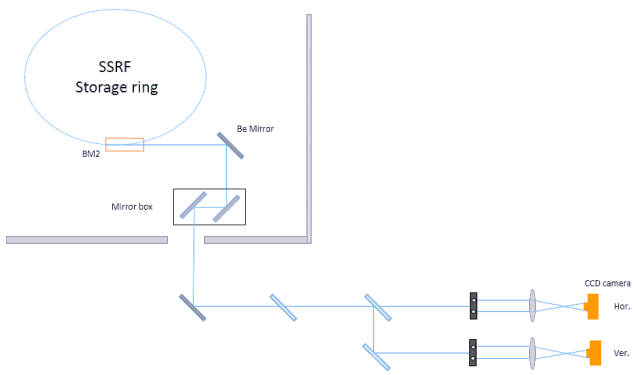

Figure 1: Layout of double-silt interferometer at SSRF.

MULTI-SILT INTERFEROMETER

The N-slit interferometer was first applied in the generation and measurement of complex interference patterns [3]. A demo beam size monitor(BSM) based on multi-silt interferometer has been proposed and developed for high speed measurements at SSRF. Multi-silt mask has characteristics of high flux throughput. A 3 silts mask for use at SSRF has been installed for demo tests, intercepting the synchrotron radiation fan at the location of an existing double-silt interferometer. In order to verify the performance of Multi-silt interferometer, images have been observerd through both double-silt and 3-silt mask using same CCD camera for a variety of beam size at same exposure times. For simplicity of demo experiments, 3-silt masks have been produced for beam size measurements.The beam size can be controlled via adjustment of the emittance coupling ratio. Figure 2 shows the prototype 3-silt mask installed at SSRF.

* Work supported by National Natural Science Foundation of China (No.11375255)
† gaobo@sinap.ac.cn
‡ leng@sinap.ac.cn

ISBN: 978-3-95450-192-2 doi:10.18429/JACoW-IBIC2017-WEPCF01

BEAM CHARGE MEASUREMENT USING THE METHOD OF DOUBLE-CAVITY MIXING *

J. Chen, Y.B. Leng†, L.W. Lai, R.X. Yuan, N. Zhang, S.S. Cao
SSRF, SINAP, Shanghai, China

Abstract

The measurement of beam charge is a fundamental requirement to all particle accelerators facility. In this paper, using the TM010 mode of the cavity BPM to measure the beam charge will be introduced. The data processing methods including harmonic analysis, time domain analysis and principle component analysis (PCA) are used and compared in evaluating the resolution of the beam charge. On the basis of this, the results of the evaluation at a ultra-low charge are also given and indicates the superiority of the cavity probe in the measurement of lower beam charge. In addition, the use of double-cavity mixing method to measure the beam charge will be proposed as well.

INTRODUCTION

Beam charge is a fundamental parameter for the particle accelerator facility; therefore, the beam current detector is a very important diagnostic means. There exist many methods such as various types of current transformers (CT), faraday cup (FC), etc.

In addition to that, using the sum signal of the beam position monitor (BPM) four electrodes and the TM010 mode of the cavity BPM can also to achieve the relative measurement of the beam charge. Using the reference cavity of the CBPM to measure the beam charge will be discussed in this paper. Based on this, the method of double cavity mixing to measure beam charge will be proposed and the result indicating that this method can achieve a higher beam charge resolution.

PRINCIPLE OF THE MEASURMENT

For a cylindrical pill-box cavity, when the beam source runs along the z-axis, the bunch does not lose energy in the transverse electric field of the TE mode. However, because of the longitudinal electric field of the TM mode, the bunch loses energy in the longitudinal electric field excited by itself and effectively induces the excitation mode. Therefore, only the TM modes are excited and the amplitude is determined by the bunch energy that is lost. Considering the asymmetric characteristics of TM110 dipole mode which has a strong linear dependencies to the beam offset and the beam charge, whereas TM010 monopole mode unaffected by the beam offset but it is proportional to the bunch charge and bunch length. Electric fields of the TM010 and TM110 mode are shown in Fig. 1.

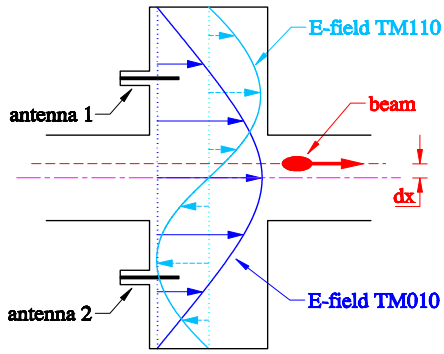

Figure 1: Electric fields of the TM010 and TM110 mode.

According to this characteristic, the beam charge can be measured using the TM010 mode of the cavity BPM. The TM010 mode signal coupled from the cavity can be expressed by Eq. (1):

$$V_p^{010} = \frac{q\omega_{010}}{2} * \sqrt{\frac{Z}{Q_{ext}^{010}} * \frac{2LT^2}{\varepsilon\omega_{010}\pi a^2 J_1^2(\chi_{01})}} * J_0\left(\frac{\chi_{01}}{a}\rho\right) * e^{-\frac{t}{\tau_{010}}} * \sin(\omega_{010}t + \varphi) \quad (1)$$

where the q is the beam charge we want to get, J_1 is the first-order Bessel function of the first kind, ω_{010} is the resonant angular frequency of the TM010 mode, χ_{01} is the first root of $J_0(\rho) = 0$ and a is the cavity radius. Since $J_0(\frac{\chi_{01}}{a}\rho)$ is appropriately equal to 1 when ρ is small. Thus, when the beam deviates from the electric centre within a small range, the signal amplitude is independent of the beam offset but dependent on the beam charge and the beam length. If we assume that the beam length is constant during the measurement process, the coupled signal strength is related to the beam charge only and proportional to it [1].

MIXING WITH LOCAL OSCILLATOR

For the beam experiment in Dalian Coherent Light Source (DCLS) [2], the reference cavities of the cavity BPM are used to measure the beam charge. The system diagram is illustrated in Fig. 2.

*Work supported by National Natural Science Foundation of China (No.11575282No.11305253)
†lengyongbing@sinap.ac.cn

ISBN: 978-3-95450-192-2 doi:10.18429/JACoW-IBIC2017-WEPCF02

A STUDY ON THE RESOLUTION OF BUNCH LENGTH MEASUREMENT SYSTEM USING HARMONIC METHOD*

Q. Wang, B. G. Sun†, Q. Luo‡
NSRL, University of Science and Technology of China, Hefei 230029, China
Y. B. Leng, B. Gao[1]
Shanghai Institute of Applied Physics, Chinese Academy of Sciences, Shanghai 201800, China
[1]also at University of Chinese Academy of Sciences, Beijing 100049, China

Abstract

Harmonic method is very useful when we try to obtain the bunch length, while its resolution is always influenced by many factors. In this paper, the relations between resolution and working frequencies of two cavities are given by mathematical deduction. The laws of resolution change caused by some decisive factors such as beam position, working frequency, electromagnetic mode and probe position are obtained through simulation on computer. An improved measurement method utilizing TM020 mode is presented based on the theory above. The simulation results show that the improved method can enhance the resolution capability of the bunch length monitor and these analyses can provide references for the design of cavity bunch length monitor.

INTRODUCTION

Harmonic method is used to quantify the bunch length with RF pick-up. The RF pick-ups for linacs are usually cavities. The monitors consisting of the cavities have been constructed to measure the bunch length in the CLIC (Compact Linear Collider) Test Facility (CTF) at CERN [1] and the BEPCII [2]. The electromagnetic fields can be induced when the beam passes through the cavity, and the monitor achieves its function by picking up information about bunch length contained in the electromagnetic fields. It has many advantages such as simple structure, wide application rage, and high signal-to-noise ratio. But the resolution of the cavity bunch length monitor is seriously limited by the system signal-to-noise ratio (SNR) [3, 4]. In this paper, the relationship between resolution and SNR is deduced primarily and then the factors which make an impact on the system SNR is analyzed. Finally, an improved measurement method utilizing TM020 mode is proposed.

THEORETICAL ANALYSIS

Cavity bunch length monitor is usually composed of two cavities with different working frequencies. The schematic is shown in Fig. 1.

When a Gaussian bunch passed through the center of the vacuum chamber, the oscillating electromagnetic fields could be excited in the cavities. The power of the field can be written as [2]

$$\begin{cases} P_1 = [I_0 \exp(-\frac{\omega_1^2 \sigma_\tau^2}{2})]^2 R_1 \\ P_2 = [I_0 \exp(-\frac{\omega_2^2 \sigma_\tau^2}{2})]^2 R_2 \end{cases} \quad (1)$$

Where the subscripts stand for the cavities' serial number, σ_τ is the bunch length, I_0 is pulse current, ω is resonance frequency of the mode, and R is cavity shunt impedance. The σ_τ and I_0 are quantified by solving this two simultaneous power equations. I_0 is eliminated and the equation is derived as follows

$$\sigma_\tau{}^2 = \frac{1}{\omega_2^2 - \omega_1^2} \ln \frac{P_1 R_2}{P_2 R_1} \quad (2)$$

Take the derivative of both sides,

$$2\sigma_\tau \Delta\sigma_\tau = \frac{1}{\omega_2^2 - \omega_1^2} (\frac{\Delta P_1}{P_1} - \frac{\Delta P_2}{P_2}) \quad (3)$$

is easily shown. The resolution of the system can be expressed as

$$\Delta\sigma_\tau = \frac{(10^{-SNR/10})}{4\pi^2 (f_2^2 - f_1^2)\sigma_\tau} \quad (4)$$

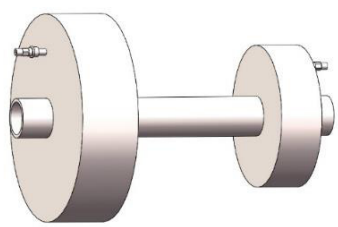

Figure 1: The schematic diagram of cavity bunch length monitor.

From the Eq. (4), it can be seen that the resolution depends on the system SNR and the difference of the square of working frequencies. As far as actual cavity is concerned, without regard to the electronics noise, the decisive factor affecting the resolution is beam position. When passing through the cavity with a position offset, the bunch will

* Supported by The National Key Research and Development Program of China (Grant No. 2016YFA0401900, 2016YFA0401903), the National Science Foundation of China (Grant No. 11575181, 11375178) and the Fundamental Research Funds for the Central Universities (WK2310000046).
† Corresponding author (email: bgsun@ustc.edu.cn)
‡ Corresponding author (email: luoqing@ustc.edu.cn)

ISBN: 978-3-95450-192-2 doi:10.18429/JACoW-IBIC2017-WEPCF04

THE SE-CpFM DETECTOR FOR THE CRYSTAL-ASSISTED EXTRACTION AT CERN-SPS

F.M Addesa*, G. Cavoto, F. Iacoangeli, INFN Sezione di Roma, Rome, Italy
S.Montesano, W. Scandale, CERN, 1211 Geneva 23, Switzerland
L. Burmistrov, S. Dubos, V. Puill, A. Stocchi, LAL, Orsay, France

Abstract

The UA9 experiment at CERN-SPS investigates the manipulation of high energy hadron beams using bent silicon crystals since 2009. Monitoring and characterization of channeled beams in the high energy accelerators environment ideally requires in-vacuum and radiation hard detectors. For this purpose the Cherenkov detector for proton Flux Measurement (CpFM) was designed and developed. It features a fused silica bar in the beam pipe vacuum which intercepts charged particles and generates Cherenkov light. In this contribution the SE-CpFM (Slow Extraction CpFM) detector is described in detail. It has been installed in early 2016 in the TT20 extraction line of SPS to study the feasibility of the crystal-assisted extraction from the SPS. Before the installation the detector has been fully characterized in 2015, during the UA9 data taking in the H8-SPS extraction line with 180 GeV pions. The single particle detection efficiency and the photoelectron yield per proton have been estimated and are shown in this contribution.

INTRODUCTION

Presently the SPS accelerator provides the beam for Fixed Target physics in the North Area (NA) using a slow resonant process and through electrostatic septa (ZSs). The main problematic issue of the resonant slow extraction process regards the small fraction of the beam that is unavoidably lost on the ZS wires. These losses produce both limitation to the delivered beam intensity and a strong activation of the SPS. Bent crystal technology applied in different configurations [1] offers promising solutions for the losses issue in the SPS LSS2 extraction region.

The UA9 experiment [2–7] and the CERN Accelerator Beam Transfer group are working together to demonstrate the feasibility of a crystal-assisted slow extraction toward the NA of the SPS. As a first step, a "proof of principle" experimental campaign started in 2016 during dedicated Machine Development (MD) sessions of the SPS and it is still ongoing. In this frame the installation of the SE-CpFM was needed to detect and measure the crystal-assisted extracted beam flux directly in the TT20 extraction line (Fig.1).

THE CHERENKOV DETECTOR FOR PROTON FLUX MEASUREMENTS

A "proof of principle" experiment basically consists of a very low intensity and bunched extraction from the SPS to the TT20 extraction line. The halo of a low intensity LHC-type bunch ($\sim 1.6 \times 10^{10}$) is extracted at each turn (every 23 μsec) from the circulating beam by a bent crystal located in the UA9 experimental area in LSS5 [8] and then reaches, with the right phase advance, the ZS through a closed orbit bump [9]. The flux of protons expected on the detector in TT20 ranges from 1 up to about 200 protons per turn (from 10^5 up to 10^7 p/s). Such a low flux doesn't allow to use the standard SPS instrumentation like for example BCTs (Beam Current Transformer [10]). During its collimation tests, the UA9 experiment uses to deal with a proton flux of the same order and since 2014 a Cherenkov detector (CpFM, **C**herenkov detector for **p**roton **F**lux **M**easurement) has been installed in LSS5 to measure the proton flux extracted by crystals [11, 12]. Therefore to design the SE-CpFM (**S**low **E**xtraction-CpFM) we started from the CpFM concept using the experience collected by UA9.

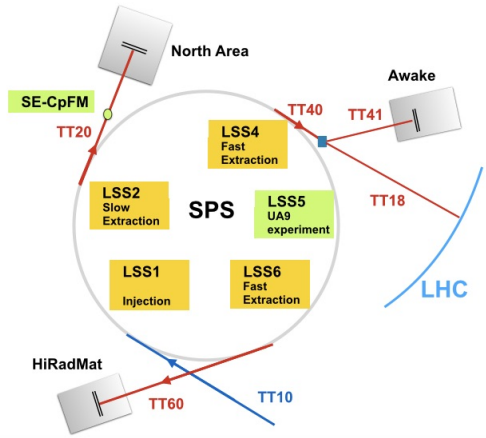

Figure 1: Conceptual sketch of the injection and extraction lines of the SPS.

SE-CpFM Requirements & Layout

The SE-CpFM detector has been devised as an ultra-fast and high resolution proton flux monitor. It has to provide the measurement of the extracted beam directly inside the beam pipe vacuum of the TT20 line, discriminating the signals coming from different proton bunches in case of multibunch beam in the SPS, with a 25 ns bunch spacing. The sensitive part of the detector is located in the beam pipe vacuum in order not to deteriorate the resolution of the flux measurement, avoiding the interaction of the protons with the vacuum-air interface. All the design choices are explained in details in [11, 12]. They were lead by the need to get very high performances matching at the same time the

* francesca.maria.Addesa@cern.ch

ISBN: 978-3-95450-192-2 doi:10.18429/JACoW-IBIC2017-WEPCF05

LOW FIELD NMR PROBE COMMISSIONING IN LEReC ENERGY SPECTROMETER*

T. Miller†, M. Blaskiewicz, A. Fedotov, D. M. Gassner, J. Kewisch, M. Minty, S. Seletskiy, H. Song, P. Thieberger, P. Wanderer, BNL, Upton, NY, USA
R. Boucher[1], C. Germain, JC. Germain, CAYLAR SAS, Villebon-sur-Yvette, FRANCE
[1]also at POLYTECH, Paris-Sud University, Orsay, FRANCE

Abstract

Low Energy RHIC electron Cooling (LEReC) [1] is planned during a 7.7 – 20 GeV/u run with Au^{+79} starting in 2019 (typically 200 GeV/n center-of-mass), to explore the existence and location of the QCD critical point. An electron accelerator for LEReC is being constructed to provide a beam to cool both the "blue" and "yellow" RHIC ion beams by co-propagating a 30 – 50 mA electron beam of 1.6 – 2.7 MeV. For effective cooling of the ion beam, the electron and ion beam energies must be matched with 10^{-4} accuracy. As the energy of the RHIC ion beam can be known to $< 1\times10^{-4}$ [2], the absolute energy of the electron beam can also be found to 10^{-4} accuracy with energy matching techniques. A 180° bend transport magnet will be used as an energy spectrometer for the electron beam providing fields in the range of 180 – 325 gauss. A Nuclear Magnetic Resonance (NMR) gaussmeter has been customized to measure the field in the magnet and tested to as low as 143 gauss with an accuracy of 50 milligauss and a noise floor of < 10 milligauss. The concept of the magnetic spectrometer with details and commissioning performance of the NMR instrument are presented in this paper.

INTRODUCTION

As the commissioning phase of the LEReC gun test beam line [3] finishes in August 2017, work continues through the RHIC shutdown to complete the construction of the beam transport, diagnostic beam line, cooling sections and high power dump sections of LEReC. Specifically, in preparation of implementing a magnetic energy spectrometer for the electron beam using the 180° dipole magnet in the cooling section, field mapping of the magnet, using integrated Hall and NMR sensors, approaches completion; while efforts to implement remote control of the NMR sensor and the magnet power supply continue in parallel. After field mapping, the dipole will be assembled on a stand with Beam Position Monitors (BPM) and Profile Monitors (PM). These are combined into Hybrid Horizontal-BPM + PM (HyPM) [4] devices that will provide calibrated on-line beam position measurement as part of the spectrometer.

The foremost challenge of the spectrometer, and the field mapping, was an absolute field measurement at the low operating field value of 196 Gauss (for 1.6 MeV operation). Most of the NMR probes available today are for the magnetic fields above ~430 Gauss, and making the NMR for the low field range of 180 Gauss – 350 Gauss is very challenging. This was accomplished by R&D efforts at CAYLAR [5] to fine-tune their model NMR20 Nuclear Magnetic Resonance (NMR) Gaussmeter for a low field range. The adapted NMR20 was acceptance tested to perform over 146 – 561 Gauss.

Energy Matching

For successful e-beam cooling of the RHIC beam, the energies of the two beams must be matched with an accuracy of 10^{-4}. Several steps of energy matching will be employed to approach the proper electron beam energy, as illustrated in Fig. 1. In order to get the electron beam energy to such a precise energy, the electron energy will be initially set to within 5% of the ion beam energy by adjusting the RF voltage and then to within 0.3% with feedback from the magnetic spectrometer. Observing recombination monitors [4], finer e-beam energies to within 0.1% will be attained; where the recombination rate will be maximized with further alignment and scanning of the RF phase. By observing the ion beam Schottky spectrum while further adjusting the beam position and RF phase, the final e-beam energy will be set to match to within 0.01%, required for cooling.

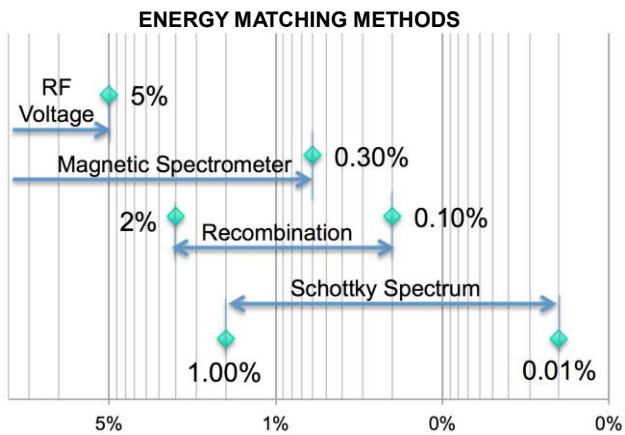

Figure 1: Several methods of energy matching will be employed as a strategy to reach the requirement for cooling. Each method spans a different range of energy matching precision.

MAGNETIC SPECTROMETER

The spectrometer is composed of the 180° dipole magnet and three BPMs [6], as shown in Fig. 2. The 180° dipole magnet design parameters are shown in Table 1 below. The magnet design was tailored for its role as a bending magnet but will be measured for use as a sensitive low field spectrometer magnet.

* Work supported by BSA under DOE contract DE-AC02-98CH10886
† tmiller@bnl.gov

ISBN: 978-3-95450-192-2 doi:10.18429/JACoW-IBIC2017-WEPCF06

R&D PROGRESS ON PRECISION CURRENT MONITORING AND CALIBRATION SYSTEMS FOR THE APS UPGRADE UNIPOLAR MAGNET POWER SUPPLIES*

R. Keane#, J. Carwardine, B. Deriy, T. Fors, J. Wang,
Argonne National Laboratory, Lemont, IL

Abstract

The APS Upgrade storage ring multi-bend acromat lattice uses 1000 individually-powered multi-pole magnets operating at current levels to ~260 A. Requirements for power-supply stability, repeatibility and reproducibility are of the order of 10 ppm. MBA SR quad magn et and Q-bend dipole magnet current regulation will require a higher level of accuracy, precision, stability, and independent control than existing APS systems. In order to meet these requirements, the upgrade will include the installation of 1000 new unipolar power supplies. To monitor and ensure the performance of the power supplies, an independent precision current measurement system is under development, based on a commercially available DCCT sensor. An in-situ calibration system is also required that will maintain the ensemble accuracy of the measurement system and magnet-to-magnet relative calibration by providing precise known calibration current to each of the 1000 DCCTs distributed around the 1100-meter ring. R&D on the in-situ cross-calibration scheme is being performed using a network of 6-8 full-spec DCCTs. This paper discusses the proposed approach, and results and lessons from the R&D program.

INTRODUCTION

Figure 1 shows the conceptual design of the external precision current measurement and calibration system. An interface chassis will provide connections for six DCCTs and will house the current-to-voltage converting circuitry and ADC required to produce a digital current reading. Each power supply cabinet will contain one interface chassis; approximately 200 chassis will be needed for the entire system. The raw digital data is sent to the Power Supply Controller (PSC) through an SPI link, and will be available to the system over Ethernet. A calibration circuit will also be housed in the interface chassis to allow in-situ calibrations of each DCCT through built-in calibration windings. Calibration factors will be applied in the PSC FPGA, or in software, to provide calibrated current read-outs. Calibration will be fully automated and performed remotely, at intervals to be determined by data gathered during further performance testing on the preliminary design hardware.

* Work supported by the U.S. Department of Energy, Office of Science, Office of Basic Energy Sciences, under Contract No. DE-AC02-06CH11357.
#keane@anl.gov

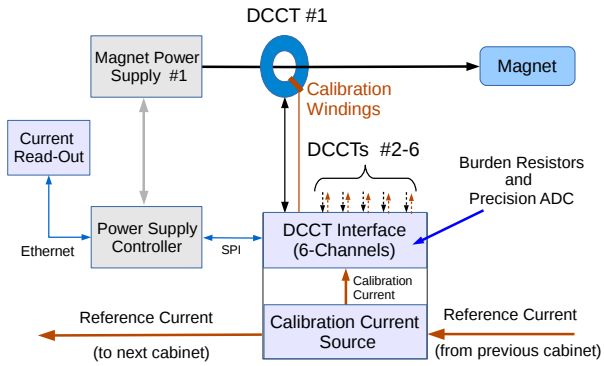

Figure 1: Current measurement and calibration system.

CURRENT MEASUREMENT SYSTEM

DCCT Current Sensor and Burden Resistor

DCCT technology is considered the standard for high-precision current measurement[1], and is capable of very high levels of accuracy, precision and stability. The DCCT is an active, non-interrupting device that produces an output current proportional to the primary DC current. The DCCT under investigation (DaniSence DS200CLSA- 1000) uses a 1:500 ratio, i.e. a 200 A primary current results in a 400 mA secondary output current. This DCCT model has excellent stability and linearity specifications, and includes a built-in calibration winding of 1000 turns. The secondary current is converted to a voltage using a precision burden resistor, and read-out by a precision voltmeter or ADC. Some DCCT models incorporate the burden resistor in the internal circuitry to provide a direct voltage output. Performance of the DCCT system depends strongly on burden resistor performance, so using an external burden resistor allows for better control of the resistor parameters and environmental conditions, particularly thermal conditions. Figure 2 shows the basic components of a DCCT-based current measurement channel.

ISBN: 978-3-95450-192-2 doi:10.18429/JACoW-IBIC2017-WEPCF07

CRYOGENIC CURRENT COMPARATORS FOR 150 mm BEAMLINE DIAMETER*

V. Tympel†, Th. Stoehlker[1, 2], Helmholtz Institut Jena, 07743 Jena, Germany
F. Kurian[1], M. Schwickert[1], T. Sieber[1]
R. Neubert, F. Schmidl, P. Seidel, Institute of Solid State Physics, 07743 Jena, Germany
M. Schmelz, R. Stolz, Leibniz Institute of Photonic Technology IPHT, 07745 Jena, Germany
V. Zakosarenko, Supracon AG, 07751 Jena, Germany
[1]also at GSI Helmholtzzentrum für Schwerionenforschung, 64291 Darmstadt, Germany
[2]also at Institute for Optics and Quantum Electronics, 07743 Jena, Germany

Abstract

New versions of Cryogenic Current Comparator (CCC) sensors with eXtended Dimensions (CCC-XD) for beamline diameters of up to 150 mm – necessary for the planned Facility for Antiproton and Ion Research (FAIR) at GSI (Gesellschaft für Schwerionenforschung) – have been realized. These non-destructive charged particle beam monitoring systems are able to measure intensities in the nA-range with a white noise level below 5 pA/√(Hz). The systems are sensitive from DC to several hundred kilohertz and can be linked up in a traceable way with national and international ampere-standards.

In its present design, the base body consists of a highly-permeable, nano-crystalline core optimized for low-temperatures (ready for superfluid He-II applications) [1] and a niobium shielding/pickup-coil unit. The flexible SQUID (Superconducting Quantum Interference Device) - cartridge allows tuning for application. Three cartridge versions (direct, balanced and enhanced) are presented, discussed and results of electrical laboratory measurements of the noise behaviour and the frequency response are given.

OPERATION PRINCIPLE

The key to measure the beam intensity non-destructively is to measure the magnetic field component created by the charged particle. The main parts of a CCC are shown in Fig. 1.

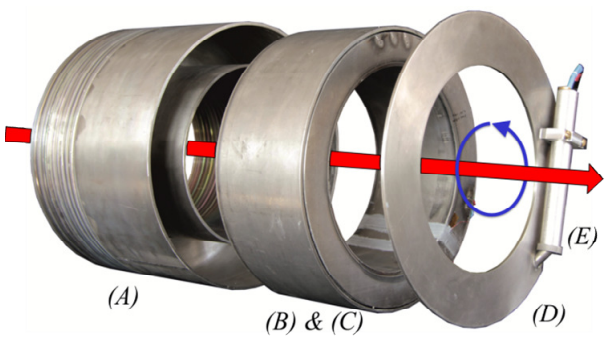

Figure 1: Exploded view of classical meander design CCC as used at CERN; red: charged particle beam; blue: magnetic field, courtesy of R. Geithner.

* Work supported by the BMBF, project number 05P15SJRBA.
† volker.tympel@uni-jena.de

(A) Superconducting Meander Shielding

This shielding separates the concentric magnetic field component created by the charged particle from the interference created by surroundings. Two long coaxial tubes – shorted by a complex meander structure – act as a filter [2, 3]. The meander structure has no electrical connection between both parts and creates a frequency-independent parasitic capacity C_m in the nF-range. For the CCC-XD shielding – consisting of about approximately 65 kg niobium – the measured parasitic capacity is about 40 nF.

(B) Flux Concentrator

A special, highly-permeable, nano-crystalline core – optimized for low-temperature applications – concentrates the magnetic field at the end of the tubes. In cooperation with MAGNETEC GmbH the GSI328plus core was developed and used for CCC-XD [4].

(C) Superconducting Pickup Coil

A full faced, one-turn, superconducting pickup coil covers the flux concentrator and creates a frequency-dependent inductance L_{pu} in the range of (10 to 100) µH at a temperature of 4 K. The pickup coil inductance of the CCC-XD is about 80 µH at 4.2 K and 1 kHz.

(D) Top Cover

A superconductive connection between both parts of the meander shielding tubes completes the shielding and also creates a full faced, one-turn frequency-dependent coupling coil inductance L_m – similar to the pickup coil. This inductance and the parasitic capacity C_m produce a LC-resonator which can be simulated for example with LTspice.

(E) SQUID-Cartridge

The cartridge includes the SQUID as the current meter and additional components like the matching transformer for inductance coupling.

Benefit of Superconductivity

The superconductivity with Meissner effect, Josephson effect and the flux quantization are necessary to realize shielding, DC-transformer and an extreme high sensitive current meter [5].

ISBN: 978-3-95450-192-2 doi:10.18429/JACoW-IBIC2017-WEPCF08

BEAM EXTRACTION BY THE LASER CHARGE EXCHANGE METHOD USING THE 3-MEV LINAC IN J-PARC*

H. Takei†, K. Hirano, and Shin-ichiro Meigo, J-PARC Center, Japan Atomic Energy Agency, Tokai, Ibaraki, JAPAN
K. Tsutsumi, Nippon Advanced Technology Co., Ltd., Tokai, Ibaraki, Japan

Abstract

The Accelerator-driven System (ADS) is one of the candidates for transmuting long-lived nuclides, such as minor actinide (MA), produced by nuclear reactors. For efficient transmutation of the MA, a precise prediction of neutronics of ADS is required. In order to obtain the neutronics data for the ADS, the Japan Proton Accelerator Research Complex (J-PARC) has a plan to build the Transmutation Physics Experimental Facility (TEF-P), in which a 400-MeV negative proton (H^-) beam will be delivered from the J-PARC linac. Since the TEF-P requires a stable proton beam with a power of less than 10 W, a stable and meticulous beam extraction method is required to extract a small amount of the proton beam from the high power beam using 250 kW. To fulfil this requirement, the Laser Charge Exchange (LCE) method has been developed. The LCE strips the electron of the H^- beam and neutral protons will separate at the bending magnet in the proton beam transport. To demonstrate the charge exchange of the H^-, a LCE experiment was conducted using a linac with energy of 3 MeV in J-PARC. As a result of the experiment, a charge-exchanged H^+ beam with a power of 7.99±0.22 W equivalent was obtained under the J-PARC linac beam condition, and this value almost satisfied the power requirement of the proton beam for the TEF-P.

INTRODUCTION

The Accelerator-driven System (ADS) is one of candidates for transmuting long-lived nuclides such as minor actinide (MA) produced by nuclear reactors [1]. For the efficient transmutation of MA, precise prediction of the neutronic performance of ADS is required. In order to obtain the neutronics data for the ADS, the Japan Proton Accelerator Research Complex (J-PARC) has a plan to build the Transmutation Physics Experimental Facility (TEF-P) [2], one of the two buildings of the Transmutation Experimental Facility (TEF) [3]. The critical assembly installed in the TEF-P, which is a small and low power reactor, operates below 500 W to prevent excessive radio-activation. To perform the experiments at the TEF-P with such reactor power, with an effective neutron multiplication factor (k_{eff}) of around 0.97, the incident proton beam power must be less than 10 W. Because the J-PARC accelerators focus on much higher beam power, a low power proton beam extraction device of high reliability is indispensable.

The development of a laser charge exchange (LCE) technique for extraction of the low power proton beam from the high power proton beam is now underway. The LCE technique was originally developed to measure the proton beam profile [4] and applied to the beam forming device [5]. To apply the LCE technique to the beam extraction device for the TEF-P, it is important to evaluate the efficiency of conversion to the low power proton beam and the long-term power stability of the low power proton beam in order to keep the thermal power of the assembly constant. Thus, a LCE experiment to measure the power of the low power proton beam was conducted using a linac with energy of 3 MeV in J-PARC. As already mentioned the preliminary results of the LCE experiment [6], the latest results are presented in this paper.

LCE DEVICE IN THE MAGNETIC FIELD

Figure 1 illustrates the concept of the LCE device for the TEF-P [7]. When a laser beam is injected into a negative proton (H^-) beam with energy of 400 MeV from the J-PARC linac, the charge of the H^- beam crossed with the laser beam becomes neutral (H^0). Here, the remaining H^- beam is introduced to the lead-bismuth spallation target in the ADS Target Test Facility (TEF-T) [3], other building of the TEF.

Since the outer electron of the H^- is very weakly bound to the atom, it can easily be stripped by a laser light in the wavelength range of 800~1100 nm as shown in Fig.2 [8].

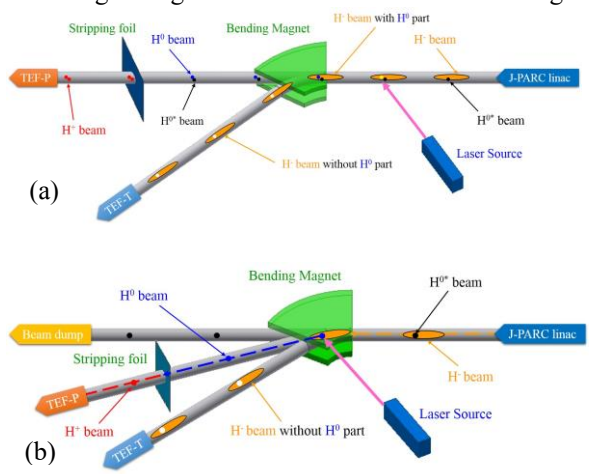

Figure 1: Conceptual diagram of the LCE device for TEF-P. For (a), the laser light is injected in the straight section of the H^- beam line. On the other hand, for (b), the laser light is injected in the bending section of the magnet. The neutralized proton due to interaction by the laser light is written as "H^{0*}", and the pre-neutralized proton due to interaction by the remaining gas in accelerator tubes is written as "H^{0*}".

* This paper summarizes results obtained with the Subsidy for Research and Development on Nuclear Transmutation Technology.
† takei.hayanori@jaea.go.jp

ISBN: 978-3-95450-192-2 doi:10.18429/JACoW-IBIC2017-WEPCF09

THE OPTIMIZATION DESIGN AND OUTPUT CHARACTERISTIC ANALYSIS OF IONIZATION CHAMBER DOSE MONITOR IN HUST-PTF*

H.D. Guo, P. Tan†, X. Liu, X.Y. Li, Y.J. Lin, Y.C. Yu, Y.Y.Hu
State Key Laboratory of Advanced Electromagnetic Engineering and Technology,
School of Electrical and Electronic Engineering,Huazhong University of Science and Technology,
Wuhan 430074, China

Abstract

An air parallel-plate ion chamber, which acts as a dose monitor for the beam delivery system in Huazhong University of Science and Technology Proton Therapy Facility (HUST-PTF), is designed as a redundant twin ionization chamber in order to meet the security requirements. In this paper, the characteristics of the designed ionization chamber are studied by using Boag theory and Monte Carlo simulation. Geant4 and SRIM are applied to simulate the energy loss and gain of 70-230MeV proton beam in parallel-plate ionization chamber. The influences of different sensitive regions and different gases on the performance of proton beam are discussed, moreover the structure of ionization chamber is optimized. According to the theory of Boag, the collection efficiencies of ionization chamber under different bias are calculated. The results show that the secondary particle collection efficiency of ionization chamber can reach above 99% when the air gap of ionization chamber is 5mm and bias voltage is above 100V. By the calculated gain of the ionization chamber, the output current of the detector can reach the order of 10nA when the proton beam intensity is 0.1nA.

INTRODUCTION

Nowadays, proton therapy facility is one of the most effective radiation therapy methods for cancers which use the Bragg peak characteristic of proton to achieve the precise irradiation of the tumor. The proton beam is tested with a dose detector in the nozzle before treating the patient, to ensure the efficacy of the treatment and the patient's safety. An air ionization chamber is used as a dose detector in Huazhong University of Science and Technology Proton Therapy Facility（HUST-PTF）.

The ionization chamber is composed of the cathode plate, the anode plate and the filling gas between the plates. When a proton beam passes through the gas, it disassociates the gas molecules, producing positive ions and electrons. Under the action of electric field, the positive ions move to the cathode while electrons move to the anode, and the secondary particles collected on cathode plate or anode plate reflect the magnitude of the beam current. The charge collected on the electrode plate is amplified and processed by peripheral electronics to obtain the dose of the proton beam.

In this paper, the structure and principle of plate ionization chamber are introduced. The energy loss and gain of different energy proton beams in ionization chamber are calculated by using the Monte Carlo software SRIM [1] and Geant4 [2]. According to Boag theory [3], the collection efficiency of ionization chamber under different bias voltages is calculated.

STRUCTURE AND PRINCIPLE OF PLATE IONIZATION CHAMBER

The structure of plate ionization chamber in HUST-PTF is shown in Fig. 1. The chamber consists of two windows, two cathode plates, an anode plate, and filling gas between plates. The entrance window acts as a seal and supports the ionization chamber. The material for the electrode background and window is Polyimide [4], with a thickness of 10μm. Polyimide has the characteristics of strong radiation resistance, high mechanical strength and high penetrability, and it has little influence on the beam. The gaps between the plates is filled with air, which is the sensitive volume of the ionization chamber. In order to meet the security requirements, the chamber is designed as a redundant twin ionization chamber.

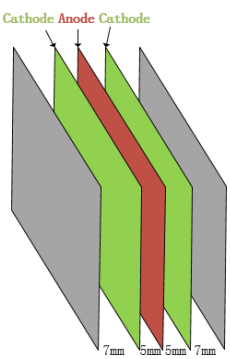

Figure 1: The structure of plate ionization chamber.

When the high-energy proton beam passes through the ionization chamber, the gas molecule is ionized. Due to the composite effect, the secondary particle produced by ionization cannot completely move to the electrode. With the increase of the bias voltage of the anode plate, the positive ions and electrons produced by the proton beam and the ionization of the air are completely collected and saturated. The principle of the ionization chamber is presented in Fig. 2.

* Work supported by the Fundamental Research Funds for the Central Universities (2014TS146), and by National Key R&D Plan (2016YFC0105308).
† Corresponding author, tanping@mail.hust.edu.cn

ISBN: 978-3-95450-192-2 doi:10.18429/JACoW-IBIC2017-WEPCF11

A PRELIMINARY STUDY OF A CURRENT TRANSFORMER BASED ON TMR SENSOR*

Ying Zhao, Yaoyao Du, Jun He, Lin Wang, Ijanshe Cao
Institute of High Energy Physics CAS, Beijing, China

Abstract

As Tunnel Magneto Resistance (TMR) sensor reaches high resolution and low noise, a new principle CT based on TMR sensor is developed. Simulations and other methods for improving the resolution and accuracy are done .The linearity and bandwidth of the sensor are test in the lab.

INTRODUCTION

A TMR (Tunnel Magneto Resistance) is a new generation of magnetic sensor devices after Holzer devices, AMR (anisotropic magneto resistance) and GMR (giant magneto resistance). TMR has low power consumption; high sensitivity and temperature drift characteristics. In the current sensor, the use of TMR instead of Holzer device can significantly improve the sensitivity of the current sensor, which can significantly improve the sensitivity and temperature characteristics of the current sensor.

Dowaytech has developed a TMR sensor, which has better temperature stability compared with higher sensitivity, lower power consumption and better linearity [1].

Based on the GSI's experiment [1], a new current transformer has been developed in IHEP.

BASIC DESIGN

The basic design of the TMR current transformer is something like clamp ammeter. Beam pass through a magnetic ring with a gap, a TMR sensor is put in a gap of the ring. The output of the sensor changes with the beam current.

A TMR's principle is based on tunnel effect of MTJs (magnetic tunnelling junctions). General MTJs is like a sandwich that consists of ferromagnetic layer, nonmagnetic insulating layer and ferromagnetic layer. The magnetization direction of the two ferromagnetic layer changes when the external magnetic field varies, which cause the tunnelling resistance changes. The resistances' change breaks the balance of the MJTs Bridge, and the bridge's output is linear relation with the magnetic field.

Early TMR sensor performance is limited by the sensitivity and background noise, Figure 1. As the advance of manufacture, the sensor now can measure very low field and reach high resolution for the background noise can be reduced to Pico Tesla. The typical parameter and spectral curve of the background noise with frequency of the sensors is shown in Table 1 [2].

Table 1: TMR9002 Parameter(temperature 25° C)

Parameter	Data
sensitivity	100mV/V/Oe
nonlinearity	1%Fs
noise	150pt/ √ Hz
V_{offset}	15mV/V
hysteresis	0.1Oe

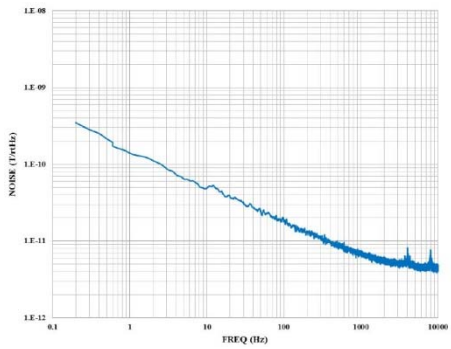

Figure 1: Background noise of TMR9002.

A high permeability nanocrystal soft material is chosen for the magnetic core, the primary μ_r is about 2e+5 and the coercive force is low. When the air gap meets the following requirements：g/a<0.2,g/b<0.2, Figure 2, the filled in the gap is approximate uniform [3].The B_g and H_g of the gap can be calculated as follow:

$$B = I/r[(2\pi - \theta)/\mu_r + \theta/\mu_0]$$

$$B \approx \mu_0 I/d$$

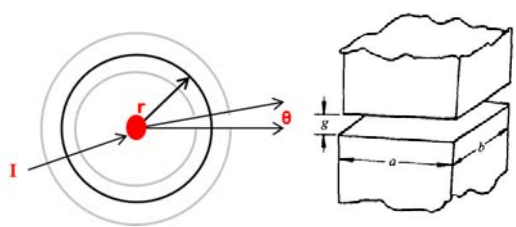

Figure 2: Calculate the B_g of the gap.

B is proportional to μ_0 and inversely proportional to the gap length when μ_r is much greater than μ_0. The dynamic range of TMR can be pre-estimated.

In this case, TMR9002 is chosen for the first prototype. For the extra power supply is needed and it is related to the sensitivity of the sensor. In first type of the electron-

* Work supported Key Laboratory of Particle Acceleration Physics & Technology,

ISBN: 978-3-95450-192-2 doi:10.18429/JACoW-IBIC2017-WEPWC01

OPTICAL BEAM LOSS MONITOR FOR RF CAVITY CHARACTERISATION*

A. Alexandrova†[1], E. N. del Busto, L. Devlin[1], M. Kastriotou[2], V. Tzoganis[1], C. P. Welsch[1],
University of Liverpool, Liverpool, UK
A. Brynes[1], F. Jackson[1], D. J. Scott[1] STFC Daresbury Laboratory, Warrington, UK
E. Effinger, E. B. Holzer, CERN, Geneva, Switzerland
[1]also at Cockcroft Institute, Warrington, UK
[2]also at CERN, Geneva, Switzerland

Abstract

Beam Loss Monitors (BLMs) based on optical fibres have been under development for many years as an alternative solution to commonly used methods, such as ionisation chambers. Optical BLMs (oBLMs) maintain standard BLM functionality but can also be used for machine and personal protection. They can be implemented over the entire beam line providing excellent position and time resolution, while being insensitive to radiation induced damage. This contribution describes how oBLMs can also assist in the characterisation of RF cavities during commissioning and operation. It first presents the design principle of highly compact monitors and the underpinning theory for particle loss detection, before discussing data obtained in experimental tests at the electron accelerator CLARA. It then shows how a 4-channel oBLM can be applied for efficient cavity monitoring. Finally, the results are put into a broader context underlying the application potential in accelerators and light sources.

INTRODUCTION

Optical fibre-based beam loss monitors (oBLMs) have been developed as a comprehensive low-cost solution for beam loss detection in an accelerator [1]. An oBLM system consists of one or more fibres running along a beamline with fast photodetectors at the end of the fibre. The front end readout electronics convert the light signals to electrical pulses followed by high-speed analogue-to-digital converters. The operating principle of an oBLM is based on Cherenkov radiation emitted as a result of a charged particle crossing the fibre. This charged particle originates from beam losses which occur when the charged particle beam impinges on any obstacles along the accelerator, including the beampipe itself. For electrons, the threshold energy to produce Cherenkov radiation in a quartz fibre is 175 keV. The oBLM system is completely insensitive to magnetic fields, so it can be installed inside a magnet, or close to it, without any restrictions. When compared with standard beam loss monitoring methods, an oBLM can monitor the entire beamline and localise the losses with a resolution of up to 10 cm instead of detecting losses only at specific locations. Moreover, on-line oBLM systems can be integrated with the machine and personnel protection systems of an accelerator reducing the probability of losses not being detected early and thus ensuring safer operation.

CLARA (Compact Linear Accelerator for Research and Applications) is a Free-Electron-Laser (FEL) test facility under construction at Daresbury Laboratory [2]. CLARA is based on a 250 MeV electron linac capable of producing short, high-brightness electron bunches. The CLARA front end, on which the oBLM system has been installed, consists of a 2.5 cell RF photocathode gun, and a 2 m S-band (2998.5 MHz) accelerating structure.

For the CLARA front end, in the area marked in Fig. 1 by red lines, four oBLM units have been installed, using two different types of fibres: 600 µm and 400 µm core. Two types of different core fibres provide different sensitivities to ensure the detection of a range of beam loss intensities. Combining four sensors instead of one, oBLMs can collect more information on losses and on their origin, including the estimation of the deviation from the 'golden orbit'. Additionally, four oBLMs allow the reliability of each oBLM system to be cross-checked. Moreover, this configuration allows the potential of localising the losses regarding the symmetry of the beampipe to be thoroughly explored. As can be seen from the marked locations on Fig. 1, fibres are installed in the locations of south, north, west and east of the pipe. The photodetectors installed at the fibre ends are silicon photomultipliers (SiPMs), which are an array of avalanche photodiodes operating in Geiger mode. SiPMs are insensitive to magnetic fields, unlike standard photomultiplier technology and so they do not require additional shielding. This allows for compact installation behind the gun without impeding other systems. Each SiPM, four in total connected to each fibre end, is biased from a custom made power supply to just above the Geiger-breakdown voltage of 70 V, and the charge produced in each SiPM is collected by a transimpedance amplifier and converted to a voltage signal [3].

LINAC CONDITIONING: LOADED AND UNLOADED RF STRUCTURE

Imperfections on the RF cavity surface can cause the field emission of electrons [4]. A travelling RF wave can accelerate these electrons up to energies of tens of MeV, depending on the available distance for the electrons to travel, the accelerating gradient and the RF phase. When colliding with the

* Work supported by STFC Cockcroft Institute core Grant No. ST/G008248/1
† A.Alexandrova@liverpool.ac.uk

ISBN: 978-3-95450-192-2 doi:10.18429/JACoW-IBIC2017-WEPWC02

CONSTRUCTION OF A MOBILE IRRADIATION INSTRUMENT FOR THE VERIFICATION OF THE CERN LHC BEAM LOSS MONITORING SYSTEM

D. Gudkov, V. Grishin, R. Veness, C. Zamantzas, CERN, Geneva, Switzerland

Abstract

The strategy for machine protection and quench prevention of the super-conducting elements of the Large Hadron Collider (LHC) at the European Organisation for Nuclear Research (CERN) is heavily reliant on its beam loss monitoring (BLM) system. This is one of the most complex and large-scale beam instrumentation systems deployed anywhere in the world.

In order to augment the system's dependability and verify the correct connection of each of the approximately 4000 detectors distributed around the 27 km LHC ring to its assigned channel in the electronic system, a mobile irradiation instrument has been designed and built. This instrument can be easily and safely transported along the LHC tunnel and imitate a localised beam loss at each BLM detector.

This paper describes the concept of the instrument, its engineering design, the safety measures included and recent upgrades. Possible future improvements of the device are also considered.

INTRODUCTION

There are approximately 4000 beam loss detectors using the ionization chamber principle installed next to areas where losses can take place in the LHC [1]. It is necessary to periodically verify the connection to the corresponding channels of the electronic system and the signal quality of all detectors. The purpose of the mobile irradiation device is to mimic a beam loss at a given detector using a ^{137}Cs radioactive source, and in so doing verify the complete detection chain for that particular channel. The instrument described here is designed to safely transport the ^{137}Cs radioactive source along the tunnel inside a lead safety container and then to perform the required tests. The equipment functions by pushing the compact radioactive source out from its lead safety container towards a defined end position located several millimetres from an ionization chamber and then to pull it back into the container after the tests are complete. The operators manipulate the device remotely, always remaining at least 5 meters from the radioactive source such that the dose rate does not exceed 1.5 µSv/h. The instruments currently used for BLM system validation have several reliability and safety issues related to the electromechanical system that lead to an increased risk of unnecessary radiation exposure for operators. The new device is therefore designed to be highly reliable during operation to avoid any requirement for human intervention close to the radioactive source

As this validation process is normally conducted as close as possible to the end of machine shutdowns, the transportation and manipulation of the source should be fast and easy.

ELECTRO-MECHANICAL DESIGN

The instrument consists of a metal box trolley with dimensions 1000 mm x 600 mm x 800 mm with all the equipment located inside for safe transportation along the tunnel, that can be towed by a standard LHC electric car. Figure 1 shows the general view of the instrument (opened). In order to safely transport the radioactive source a lead safety container is required. The thickness of the lead must be at least 100 mm to provide sufficient shielding from the source to the outer surface of the container, such that the dose rate on the surface does not exceed 2.5 µSv/h [2]. The radioactive source is attached to the end of a long, ny-

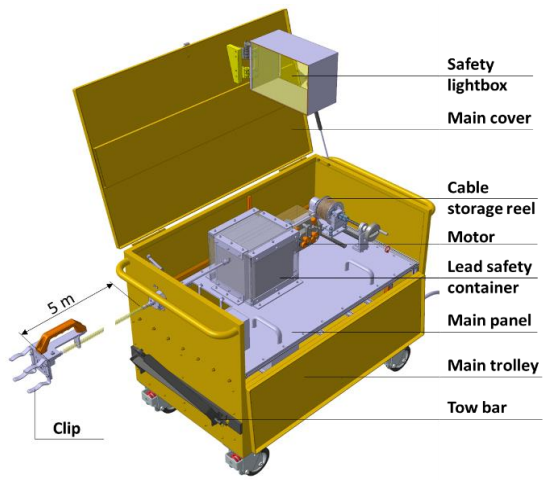

Figure 1: General view of the mobile irradiation instrument.

lon-coated steel cable stored on a reel. This cable is pushed by electric motor rollers through a 5 m long hose. Nylon coating helps to reduce friction between the cable and the hose to ensure low motor loads. It also protects the cable from possible mechanical damage. The hose is connected at one end to the lead safety container and at the other to a clip which is clamped on the detector under verification. When the source arrives at its end position inside the clip it activates an end-switch and the motor stops automatically. It is not then possible to push the source further. When the source is retracted to its home position it activates another end-switch located outside the lead safety container, again automatically stopping the motor.

The cable is stored on a compact reel that houses up to 5.6 m of cable. The reel has an auto-return spring mechanism that will retract the source back into the lead safety container in case of electric motor failure.

The irradiation instrument clip can be easily attached to the BLM thanks to spring-type clamps. These clamps pro-

ISBN: 978-3-95450-192-2 doi:10.18429/JACoW-IBIC2017-WEPWC03

IONIZATION CHAMBERS AS BEAM LOSS MONITORS FOR ESS LINEAR ACCELERATOR

V. Grishin, European Spallation Source ERIC, Lund, Sweden
B. Dehning, CERN, Geneva, Switzerland
A. Koshelev, A. Larionov, V. Seleznev, M. Sleptsov, Institute for High Energy Physics, Protvino, Russia

Abstract

The European Spallation Source (ESS) to be under construction in Lund, Sweden, will provide a highest average intensity beam from a 5 MW superconducting proton linear accelerator to produce spallation neutrons. A serious problem for high current accelerators is the high density of the beam, which is able to destroy the equipment, to make a quench of super conductive magnets.
Loss of even a small fraction of this intense beam would result in high radiation and destruction of the equipment. The Beam Loss Monitor (BLM) system must be sensitive to different level of losses in different accelerator locations. BLM system protection should limit the losses to a level which ensures hands-on-maintenance or intervention. From another side, the BLM system should be sensitive enough to enable machine fine tuning and machine studies with help of BLM signals, including mobile detectors.

The main ESS beam loss detector type is ionization chamber (icBLM). The detector is originally designed for CERN LHC and 4250 monitors were produced in 2006-2008, now widely used in almost all accelerators at CERN (figure 1), in IHEP (Protvino, Russia). In 2014-2017 a new production of 830 icBLM was performed to replenish spares for LHC and to make series for ESS, GSI. The requirements, design, testing and layout for ESS accelerator are presented.

INTRODUCTION

Parallel plate gas ionization chambers developed by CERN for LHC [1] and manufactured and tested at the Institute for High Energy Physics (IHEP) in Protvino, Russia, are chosen as beam loss detectors for the ESS linear accelerator due to their fast response, no gain variation (with possible exception of the target region), the robustness against aging, large dynamic range 10^8 (pA-mA), the little maintenance required.

Figure 1: icBLM at LHC.

The icBLM have a fast reaction time, which implies a detector gas with high ion mobility. The 99.9999 % nitrogen filled at 1.1 bar detector is permanently sealed inside a stainless-steel cylinder. Should a leak occur in a detector and air enter the chamber, the detection properties would not change severely as air consist 79% of nitrogen, therefore not leading to system immediate failure. In systematic system testing with a radioactive source, a lower signal due to lower gas pressure will be detected. The composition of the chambers gas is very important so as this is the only component in the icBLM which is not remotely monitored.

The icBLM is very sturdy, offering a good radiation hardness. The consistent, long-term (20 years of operation) high quality of icBLM requires materials testing and various tests during and after production in IHEP, after reception at CERN and ESS. IHEP designed and built the UHV production stand [2], shown in figure 2.

Figure 2: IHEP production stand.

DETECTORS PRODUCTION

The detectors active zone consists of 61 parallel electrodes with a 5.75 mm distance between electrodes in the ionization chambers produced in 2008 (ic08). The gap between electrodes in the ionization chambers produced in 2017 (ic17) is reduced to 5.71 every 2 electrodes, keeping the same spacer length. The electrodes are indeed made of a 0.5 mm thick aluminium in ic08 and 0.54 mm thick aluminium in ic17 (figure 3). The gap between electrodes is built to reduce the drift path and the recombination probability of the ions and electrons, and hence to get the requested linearity.

ISBN: 978-3-95450-192-2 doi:10.18429/JACoW-IBIC2017-WEPWC07

BEAM TRIP DIAGNOSTICS FOR THE TPS

C. Y. Liao, C. Y. Wu, Y. S. Cheng, C. H. Huang, K. H. Hu, K. T. Hsu
NSRRC, Hsinchu 30076, Taiwan

Abstract

The Taiwan Photon Source (TPS) is available to users since March 2016. A beam trip diagnostic system is used as an important tool to analyze the cause of beam trip events since the beginning of 2017. The main function of the system is to record relevant signals when the stored beam is suddenly lost. In the past few months, some useful features have been added, such as capturing trigger signals for pulsers, power line voltage, and auto generated beam trip reports. A detailed system architecture, implementation and progress will be summarized in this report.

INTRODUCTION

The Taiwan Photon Source (TPS) is a low emittance, high brightness synchrotron light source, located in Hsinchu, Taiwan. After commissioning [1], the TPS became available for user service in September 2016. During oper-ation, inevitably there will be unexpected beam trips due to subsystem failure or other abnormal circumstances. In or-der to find out the reason for such an event, a beam trip diagnostic system is developed to serve as an important tool for beam trip analysis. In the past few months, some useful features have been added, such as capture of the pulser trigger signals in case of spontaneous firing of the pulser, capturing the 3-phase power line voltage for power quality monitoring, auto generated beam trip reports, and web-based interface allowing for a quick review of the trip event through the web browser. The main system features are: Generate a trigger signal to subsystems when the stored beam current is lost abnormally; Record relevant signals when a beam trip occurs; View the report from the GUI tool or web browser to analyze each event for cause and effect. Reliability and availability of the TPS operation improved dramatically with the help of this beam trip di-agnostics.

SYSTEM DESCRIPTION

The architecture of the TPS beam trip diagnostic system is shown in Fig. 1. A trigger signal is generated through the beam trip detector when the stored beam current suddenly drops. This trigger is sent to many places (here to the data acquisition system) through an evented-based timing system (EVG/EVR) [2]. The data recorders will be updated on receiving this trigger. After a few seconds delay, all data from the recorders and subsystem parameters of interest will be saved through a PV access. The probable cause of the event will be analyzed by the program and identified by a simple description. Then, a beam trip report will be generated and saved as a web page. After that, operators can access and analyze the event data from the viewer GUI or web browser at any time.

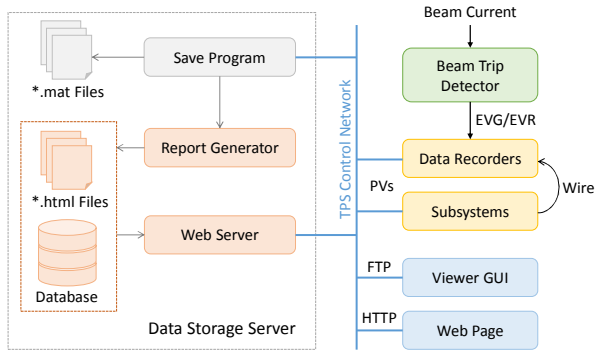

Figure 1: Schematic layout of the TPS beam trip diagnostic system.

Beam Trip Detection and Trip Trigger Generation

A beam trip detector is configured to generate a beam trip trigger signal, when the stored beam current drops abnormally more than 25 mA within 0.1 milliseconds (configurable). This trigger signal is broadcast via the event-based timing system to all data acquisition nodes (BPM platforms and data recorders) to synchronize the data captured. So far, known possible causes for the stored beam trip include: RF system trips, BPM orbit and angle interlock, vacuum interlock, front-end interlock, and abnormal firing of the injection pulse magnets.

Data Recorder

The TPS BPM system [3] provides turn-by-turn orbit post-mortem data which can be used to analyze beam positions during the trip event. In addition, several EPICS embedded standalone data recorders support distributed data acquisition capability to collect data from different subsystems. The quantity and parameters of the data recorders are shown in Table 1. Each data recorder has eight input channels with two types of configurations. These recorders provide waveform type signals which can be captured by many subsystems, including the storage ring beam orbit, machine protection system (MPS), RF and pulsed magnet system. In addition to these signals, some subsystem parameter set values need to be logged when an event occurs. The data to be saved are compiled in Table 2.

Table 1: List of Data Recorder Units used in TPS

Device	BPM platform	Data recorder (8ch)	
Quantity	173	4	1
Sampling rate (kHz)	~578	100	50,000
Time span (ms)	~17.28	100	6
Data length (point)	10,000	10,000	300,000

ISBN: 978-3-95450-192-2 doi:10.18429/JACoW-IBIC2017-WEPWC09

NEW SCINTILLATION TYPE BEAM LOSS MONITOR TO DETECT SPOT AREA BEAM LOSSES IN THE J-PARC RCS

M. Yoshimoto†, H. Harada, S. Kato, M. Kinsho, K. Okabe
J-PARC, JAEA, Tokai, Ibaraki, Japan

Abstract

In the J-PARC RCS, a large fraction of our effort has been concentrated on reducing and managing beam losses to achieve 1MW high power proton beam operation. Standard beam loss monitor (BLM), which is installed outside of the magnet in every cell of beam optics and detect the beam loss at wide area in each cell, is insufficient to investigate finer beam loss mechanism in the ring. Thus we developed new scintillation type BLM to detect the spot area beam losses on the vacuum chamber inside the magnet. The new BLM isolates a photomultiplier (PMT) from a plastic scintillator, and connects it with optical fibres. Because small plastic scintillator is set on the vacuum chamber directly, it has capability to have high sensitivity for a beam loss at localized spot area. On the other hand, the PMT can precisely be operated without being affected by a magnetic field because it can be kept keeping away from the magnet. In this paper, we report the detail of the performance of the new BLM.

INTRODUCTION

The 3-GeV Rapid Cycling Synchrotron (RCS) of the Japan Proton Accelerator Research Complex (J-PARC) accelerates protons from 400MeV to 3GeV kinetic energy at 25 Hz repetition rate. The average beam current is 0.333 mA and the design beam power is 1 MW. The RCS has two functions as a proton driver for neutron/muon production at the Material and Life science experimental Facility (MLF) and as a booster of the Main Ring synchrotron (MR) for the Hadron experimental facility (HD) and Neutrino experimental facility (NU) [1].

The most important issue in achieving such a MW-class high power routine beam operation is to keep machine activations within a permissible level, that is, to preserve a better hands-on maintenance environment. Therefore we adopt the ring collimator system to remove the beam halo and to localize the beam loss at the collimator area [2]. In addition, a large fraction of our effort has been concentrated on reducing and managing beam losses, in the J-PARC RCS. As a result, we have successfully achieved acceptable low-loss 1-MW beam acceleration [3]. Until now, the highest radio-activation area confines to an injection section, and then the beam loss localization by using the ring collimator is functioned. On the other hand, we surveyed residual doses on the vacuum ducts along the ring and mapped residual dose distributions in detail. The detailed dose distributions give key information about sources and mechanisms of the beam losses [4]. To move on the next step, we developed a new beam loss monitors (BLM) to detect the spot area beam loss, especially in the magnet. This paper presents details of the new BLM.

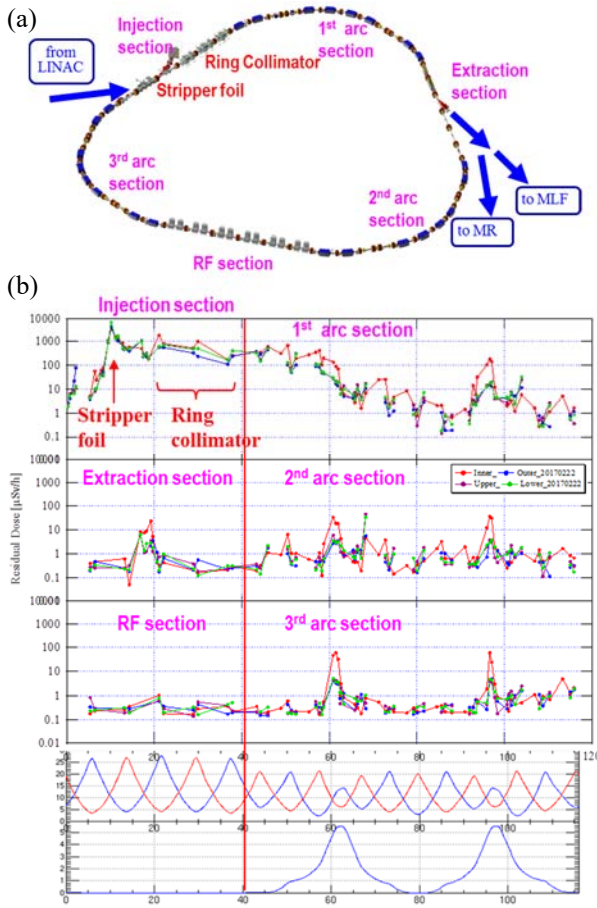

Figure 1: Schematic view of the RCS ring and measured residual dose distributions along the ring.

RESIDUAL DOSE SURVEY AND BEAM LOSS DETECT

Residual Dose Distribution along the Ring

Figure 1 shows the schematic view of the RCS ring and a typical surveying and mapping result of the residual dose distributions along the ring. The residual doses are measured by using the Geiger–Muller (GM) counter. We contact it on a surface of a vacuum duct because the sensitivity to the radio-activation at the contacted local spot can be enhanced drastically. In order to obtain the detailed distribution, we measure the residual dose on inner, .outer, upper, and lower sides of the vacuum duct at upstream and downstream of all magnets.

† yoshimoto.masahiro@jaea.go.jp

ISBN: 978-3-95450-192-2 doi:10.18429/JACoW-IBIC2017-WEPWC10

BEAM LOSS MONITORING SYSTEM FOR THE RARE ISOTOPE SCIENCE PROJECT*

Yoolim Cheon, Changkyu Sung, Kookjin Moon,
Chulun Choi, Dongnyung Choe, Moses Chung†, UNIST, Ulsan 44919, Korea
Yeonsei Chung‡, Gidong Kim, Hyung Joo Woo, IBS, Daejeon 34047, Korea
Chanmi Kim, Korea University, Sejong 30019, Korea

Abstract

A heavy ion accelerator facility called RAON is being constructed in Korea to produce various rare isotopes for the Rare Isotope Science Project (RISP). This facility is designed to use both In-flight Fragment (IF) and Isotope Separation On-Line (ISOL) techniques in order to provide a wide variety of RI beams for nuclear physics experiments. One of the biggest challenges in operating such a high beam power facility (~400 kW) is to monitor beam loss accurately and to execute the machine protection system reasonably quickly whenever necessary. In this work, we report the conceptual design of the RAON beam loss monitoring system. Monte Carlo simulations using MCNPX code have been performed to generate radiation dose maps for 1 W/m losses of proton and uranium beams. The required machine protection time has been estimated from the yield time of the stainless steel beam line components including the beam grazing angle dependence. Types of the detectors have been determined based on the radiation levels of the gammas and neutrons, and the minimum sensitivity and response time requirements.

INTRODUCTION

The RISP project [1] will be composed of a 70 kW proton cyclotron as a low-power ISOL driver, an 18 MeV/u linac for ISOL post-accelerator and a 200 MeV/u main linac for high-power ISOL and IFF driver. The main driver linac named RAON will accelerate all elements up to uranium with beam power up to 400 kW. To maximize the average currents of the primary beam on target, continuous wave (CW) operation is preferred, and therefore superconducting RF (SCRF) technology has been adopted for the linac design. One of the biggest challenges in operating such a high beam power facility (~400 kW) is to monitor beam loss accurately and to execute the machine protection system (MPS) reasonably quickly whenever necessary.

The role of the dedicated beam loss monitors (BLMs) includes 1) to protect beam line components from fast or irregular beam losses, 2) to minimize activation of the components for maintenance, and 3) to provide information for beam tuning and optimization. The BLM should provide the amount of beam loss, beam loss location, and fast interlock signal to inhibit the beam. The (preliminary) requirements of the RAON BLM system are summarized as follows:

- It should detect beam losses not only from proton beam, but also from heavier ion beams such Oxygen and uranium ion beams.
- It should have a high dynamic range to cover both slow (<1 W/m level) and fast (significant fraction of total beam power) beam losses.
- It should provide the interlock signal within $< 15\mu s$ (overall MPS time would be $< 35\mu s$).

MPS REQUIREMENTS

It has been known that the yield stress of the beam line components (copper, stainless-steel, or niobium etc.) indeed determines the maximum allowable beam injection time, which is given by [2–6]

$$T_{\max} \approx \frac{4\pi}{\sqrt{3}} \frac{\sigma_x \sigma_y}{I} \frac{\rho C_v}{\alpha E} \sigma_m \frac{1}{R_{ave}}, \quad (1)$$

where $\sigma_x(\sigma_y)$ is the rms beam radius in $x(y)$-direction, I is the beam current in pps, ρ is the mass density of the material, C_v is the specific heat, α is the coefficient of linear expansion, E is the Young's modulus, σ_m is the yield strength, and R_{ave} is the average stopping power of the Bragg curve which is estimated from the SRIM code. Because the stopping power of a heavy ion beam is a few ten times larger than proton or electron beams, a fast response of the MPS (faster than the material damage time) is even more important in heavy ion machines.

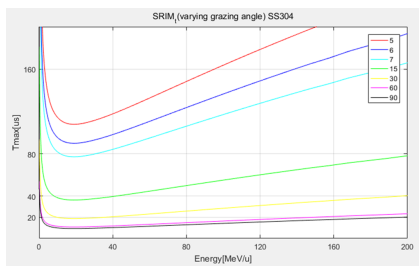

Figure 1: The maximum allowable injection time depends on the incidence angle (~2 orders of magnitude difference).

The required response time strongly depends on incident angle of the beam (θ) as well. Figure 1 shows $T_{\max}$ for the case of uranium beam injecting into stainless-steel (SS) along the RISP linac (see the linac structure in Fig. 2). For incident angles larger than 60 degrees, the damage may happen in less than 20 μs, which is beyond the capability of

* Work supported by the National Research Foundation of Korea (Grants No. NRF-2017M7A1A1019375 and No. NRF-2017M1A7A1A02016413).
† mchung@unist.ac.kr
‡ yschung@ibs.re.kr

ISBN: 978-3-95450-192-2 doi:10.18429/JACoW-IBIC2017-TH1AB1

FIELD EMISSION IN SRF ACCELERATORS: INSTRUMENTED MEASUREMENTS FOR ITS UNDERSTANDING AND MITIGATION*

R. L. Geng†, A. Freyberger, R. Legg, R. Suleiman, JLAB, Newport News, VA, USA
A. S. Fisher, SLAC, Menlo Park, CA, USA

Abstract

Several new accelerator projects are adopting superconducting RF (SRF) technology. When accelerating SRF cavities maintain high RF gradients, field emission, the emission of electrons from cavity walls, can occur and may impact operational cavity gradient, radiological environment via activated components, and reliability. In this talk, we will discuss instrumented measurements of field emission from the two 1.1 GeV superconducting continuous wave (CW) linacs in CEBAF. The goal is to improve the understanding of field emission sources originating from cryomodule production, installation and operation. Such basic knowledge is needed in guiding field emission control, mitigation, and reduction toward high gradient and reliable operation of superconducting accelerators.

INTRODUCTION

Field emission (FE) is a well-known phenomenon in both normal conducting and superconducting RF cavities. Its impact to SRF cavities is far more profound owing to the fact that the surface power dissipation in SRF cavities is smaller by many orders of magnitude as compared to their normal-conducting counterparts. Therefore, there is significant interest in its understanding and control for SRF accelerator design, construction and operation.

Despite the continued progress in understanding and control of FE over decades, the challenge remains as the specification of operation gradients has been on the rise too. By using today's state-of-the-art cavity surface processing and assembly techniques, FE is controlled satisfactorily in qualified individual cavities. This has been demonstrated in SRF accelerator projects requiring large numbers of multi-cell cavities prepared and assembled in laboratories as well as in industry [1,2]. However, preserving the cavity performance from qualification testing of individual cavities to SRF cryomodule operation with beam remains an issue of interest. One cause for cavity performance loss is the degradation of FE onset and this has provoked lots of recent discussions [3].

It is generally believed that the current understanding of the basic physics of FE in SRF cavities is adequate [4-6]. The challenge lies largely in the engineering aspects of controlling *field emitter input or activation* over the course of constructing, shipping, commissioning and operating the SRF cavities at an increasingly complex level of cryomodules, segments, and linacs. In such a situation, opportunities for learning and improving are rather scarce because of limited number of large-scale SRF projects and yet a closed loop is required to allow understanding and testing. Fortunately, some recently completed SRF projects, such as CEBAF 12 GeV upgrade and E-XFEL, have provided new opportunities. Looking forward, several new accelerator projects are adopting SRF technology, such as ESS, FRIB, LCLS-II etc., one may anticipate a continued progress in our understanding and mitigation of FE in SRF accelerators. In this paper, we present our instrumented measurements of FE from the two 1.1 GeV superconducting CW linacs in CEBAF. This work is based on and an extension of the previous work in our effort of FE understanding for its ultimate control, in particular for large scale CW SRF accelerators [7].

FE THEORETICAL AND PRACTICAL

FE Theory

The original theory of FE was developed by Fowler and Nordheim [8]. It describes electron emission in electric fields at the interface of a metal and a vacuum based on the quantum mechanical tunnelling process. The potential barrier at the interface prevents electrons in the metal from escaping. The work function ϕ, a material dependent property, is the measure of this barrier. ϕ = 3-5 eV for most metals. When no external electric field is applied to the metal surface, electrons in the metal are confined as they are at the Fermi energy level which is below the vacuum energy level by an amount of the work function and the thickness of the potential barrier is infinite. An external electric field applied to the metal surface E_s deforms the original rectangular potential barrier of infinite thickness into a triangular barrier of finite thickness, thus permitting electron tunnelling with finite probability. The salient result of the FN theory is that the FE current density j_{FN} rises exponentially with an increasing electric field: $j_{FN}=(AE_s^2/\phi)\exp(-B\phi^{3/2}/E_s)$, where A and B are constants.

The agreement between experimental results and the FN theory is quite satisfactory provided the surface electric field E_s is replaced by $\beta_{FN}E_s$, where β_{FN} is the field enhancement factor [9,10]. E_s and β_{FN} are typically in the range of 10-100 MV/m and 50-1000, respectively in SRF cavities. Besides β_{FN}, the effective emitting area A_e is a parameter useful for fitting the total FE current $I_{FN}=j_{FN}A_e$ against the FN law.

FE in SRF Cavities

The estimated time for an electron to tunnel through the potential barrier is on the order of fs, orders of magnitude smaller than the ns RF period for typical SRF applications

* Authored by Jefferson Science Associates, LLC under U.S. DOE Contract No. DE-AC05-06OR23177. The U.S. Government retains a non-exclusive, paid-up, irrevocable, world-wide license to publish or reproduce this manuscript for U.S. Government purposes.
† geng@jlab.org

ISBN: 978-3-95450-192-2 doi:10.18429/JACoW-IBIC2017-TH1AB2

BEAM CONTAINMENT AND MACHINE PROTECTION FOR LCLS-2*

Alan S. Fisher†, Christine Clarke, Clive Field, Josef Frisch, Ryan Herbst,
Ruslan Kadyrov, Bobby McKee, Feng Tao, James Welch,
SLAC National Accelerator Laboratory, Menlo Park, California 94027, USA

Abstract

The first km of the 3-km SLAC linac is being replaced by LCLS-2, a superconducting linac with continuous RF and a maximum beam rate of 1 MHz. The beam will have an energy of 4 GeV and a maximum power of 250 kW, with an upgrade to 8 GeV and 1.2 MW in planning. The beam will be transported through the accelerator tunnel, passing over the future 1-km FACET-2 and the existing 1-km LCLS linacs, both using normal-conducting copper cavities at repetition rates of up to 30 and 120 Hz respectively. The LCLS and LCLS-2 beams will continue together through the Beam Transport Hall to two new undulators, for hard and soft x rays. Kickers will direct individual pulses to either undulator or to a dump. The high power in the beam and potentially in field emission necessitates integrating losses over 500 ms but responding within 0.1 ms. A capacitor for integration and a comparator for the threshold give a simple and robust approach over a wide dynamic range. We plan both long loss monitors covering regions of typically 100 m and point monitors. In regions with two or more beamlines, the system will attempt to determine the line that caused a loss, so that only one is shut off.

INTRODUCTION

LCLS, LCLS-2, and FACET-2

The LCLS x-ray free-electron laser (FEL) at SLAC National Accelerator Laboratory began operation in 2009 [1] using the third kilometre of SLAC's 3-km linear accelerator. It retains the original 2856-MHz copper linac, but with a 1.6-cell copper radio-frequency (RF) photocathode gun at 2856 MHz. Both are pulsed at 120 Hz.

LCLS-2 [2] will replace the first km of the copper linac, removed one year ago, with a superconducting linac using continuous RF at 1300 MHz. Laser pulses at rates of up to 1 MHz will emit electrons from a normal-conducting photocathode gun with 186-MHz (1300/7) continuous RF. Operation will begin at an electron energy of 4 GeV and a maximum beam power of 250 kW. Upgrades will raise the beam energy to 8 GeV and the power to 1.2 MW, as shown in Table 1. This high beam power demands fast but accurate response to beam losses.

The middle km of the linac tunnel will be occupied by FACET-2, a user facility mainly for advanced acceleration studies [3]. The LCLS-2 beam will bypass both FACET-2 and LCLS in a transport line suspended from the tunnel ceiling and only 125 cm from the two linac beams, which may make it difficult at times to determine unambiguously the source of a loss signal.

* SLAC is supported by the U.S. Department of Energy under contract DE-AC02-76SF00515.
† afisher@slac.stanford.edu

Table 1: Parameters for LCLS and LCLS-2

Parameter	LCLS	LCLS-2
Electron energy	15 GeV	4 (later 8) GeV
Bunch charge	20 to 250 pC	20 to 300 pC
Beam power	450 W	**0.25 (later 1.2) MW**
Gun frequency	2856 MHz	185.7 MHz
Linac frequency	2856 MHz	1300 MHz
RF pulse rate	120 Hz	Continuous
e^- bunch rate	120 Hz	92.9 (later 929) kHz
Photon energy	0.2 to 12 keV	1 to 15 (later 25) keV

Safety Systems for Beam Loss

SLAC uses a three-tier protection system. The highest, the Personnel Protection System (PPS), prevents unsafe machine access. The Beam Containment System (BCS) stops the accelerator if a loss of beam current or radiation from beam loss indicates possible harm to people or to safety devices like protection collimators. It must be robust and simple, with no knowledge of bunch timing and no software. As safety systems, both have rigorous configuration control. The Machine Protection System (MPS) is more flexible. When triggered—for example, by high losses, the insertion of an obstacle such as a valve, an excessive temperature—MPS can insert a beam stop, lower the beam rate, block the photocathode laser, or halt the beam. Recovery from an MPS event is faster than from a BCS trip, and so its thresholds are set lower.

LCLS-2 beam-loss detectors will serve three purposes: BCS, MPS, and beam diagnostics. Losses below the trip thresholds will provide diagnostic information to operators for tuning the machine and locating high-loss points to avoid or recover from a rate limit or trip.

Trip specifications vary with the tunnel depth and other shielding and are given in joules of beam loss within an integration time of 500 ms. BCS thresholds range from 500 to 17.5 J. MPS thresholds are generally set 10 times lower. This loss can arrive in a fast burst of lost photocurrent or slowly over the full integration time. The repetition rate of the losses can be at any beam rate from 10 Hz to 1 MHz; a full loss of 1-Hz beam is permitted for tuning. Field emission (dark current) from the gun or linac may generate loss in every RF period (Table 1) and would appear as a DC signal in the loss detectors.

LCLS BEAM-LOSS MONITORS

BCS and MPS at SLAC have long used ionization chambers. A Protection Ion Chamber (PIC), an array of interleaved circular parallel plates, is placed at each expected loss point. A long ionization chamber (LION)

ISBN: 978-3-95450-192-2 doi:10.18429/JACoW-IBIC2017-TH1AB3

BEAM LOSS MONITORS FOR ENERGY MEASUREMENTS IN DIAMOND LIGHT SOURCE

N. Vitoratou*, P. Karataev
John Adams Institute at Royal Holloway, University of London, Egham, UK
G. Rehm, Diamond Light Source, Oxfordshire, UK

Abstract

Resonant Spin Depolarization is a high precision technique for beam energy measurement employed in the Diamond Light Source storage ring. The relation between spin tune and beam energy can be used to determine the energy of a transversely polarized beam. Vertical oscillations excite the beam at frequencies that match the fractional part of the spin tune and the beam loss rate is used to monitor the beam depolarization. However, the standard procedure of these measurements is intrusive and not compatible with user operation of a light source. The Advanced Resonant Spin Depolarization (AdReSD) project aims to extend and improve the method with the goal of making the measurements compatible with the user operation, for instance by acting only on a small fraction of the stored beam. As a first step, we are investigating the beam loss monitors that will be used to detect beam depolarization. The material, location and optimal geometry of the detector to capture the largest fraction of the radiation footprint resulting from beam losses are studied. Results and designs are presented and future work is discussed.

INTRODUCTION AND MOTIVATION

Diamond Light Source is a 3 GeV, 561m circumference synchrotron light source in operation since 2007. The precise energy of the stored beam has been measured in 2011 [1], and at an infrequent rate thereafter.

More recently, motivation was given to an increased rate of measurements to check for correlation with photon energy fluctuations. Ultimately, this lead to the project presented here, which aims to determine the stored beam energy precisely and at the same time in a way that is not interfering with ongoing 'user operations'.

RESONANT SPIN DEPOLARIZATION

Beam Polarization

The spin of electrons in a storage ring will start to be randomly oriented after injection. The spin vector of individual electrons will develop an overall polarization due to spin flip radiation emission according to the Sokolov - Ternov effect. The spin will gradually align antiparallel with the main guide field of the bending magnets leading to a polarization build up that is given by the equation [2] :

$$P(t) = P_0(1 - e^{t/\tau_0}) \quad (1)$$

where the maximum polarization for an ideal flat storage ring without field errors is $P_0 = 8/5\sqrt{(3)} = 0.9238$ and the time constant of the exponential build-up process is:

$$\tau_0 = [\frac{5\sqrt{3}}{8}\frac{e^2\hbar\gamma^5}{m^2c^2\rho^3}]^{-1} \quad (2)$$

For Diamond Light Source, considering the depolarizing effects for a non-ideal ring, the polarization time has been calculated 27.7 minutes with a maximum polarization of 85.4 % [1]

Spin Precession

The spin precession frequency for a light source storage ring where there are no significant solenoid magnetic fields, nor transverse electric fields, is described by:

$$\Omega_z = \omega_0(1 + \alpha\gamma) \quad (3)$$

where ω_0 is the revolution frequency, α the gyromagnetic anomaly and γ the relativistic factor. The product $\alpha\gamma$ is the number of revolutions the spin vector makes about the vertical axis in one revolution of the storage ring defined as the spin tune. Since α and ω_0 are known, the beam energy can be calculated.

In order to measure the spin tune and calculate the energy of the beam, a polarized beam is needed. The beam is then excited by a horizontal magnetic field produced using a vertical stripline. The magnetic field is set to oscillate at a frequency f_{dep} which matches the fractional part of the spin tune:

$$f_{dep} = (\alpha\gamma - k) \cdot f_{rev} \quad (4)$$

where k is the integer part of the spin tune. When the horizontal excitation frequency is in resonance with the spin tune, the spin-vector is tilted away from the vertical axis by a small amount in successive revolutions of the storage ring, gradually reducing the beam polarization. This is were the term Resonant Spin Depolarization (RSD) has its origin.

Touschek Scattering

Touschek effect is a Möller scattering collision process between two electrons of the bunch. The collision can transfer momentum from transverse to longitudinal motion, and both the electrons can exceed the longitudinal acceptance, in which case they are lost. The scattering cross section is spin dependent hence the particle loss rate depends on the beam polarization.

For a stored beam with equal current in several bunches the bunch population $N(t)$ is proportional to the current $I(t)$

* Niki.Vitoratou.2016@live.rhul.ac.uk

ISBN: 978-3-95450-192-2 doi:10.18429/JACoW-IBIC2017-TH1AB4

STATUS OF THE BNL LEReC MACHINE PROTECTION SYSTEM*

S. Seletskiy†, Z. Altinbas, D. Bruno, M. Costanzo, A. Fedotov, D. M. Gassner, X. Gu, L. Hammons, J. Hock, P. Inacker, J. Jamilkowski, D. Kayran, J. Kewisch, C. Liu, K. Mernick, T. Miller, M. Minty, M. Paniccia, W. Pekrul, I. Pinayev, V. Ptitsyn, K. Smith, Y. Than, P. Thieberger, J. Tuozzolo, W. Xu, Z. Zhao
BNL, Upton, USA

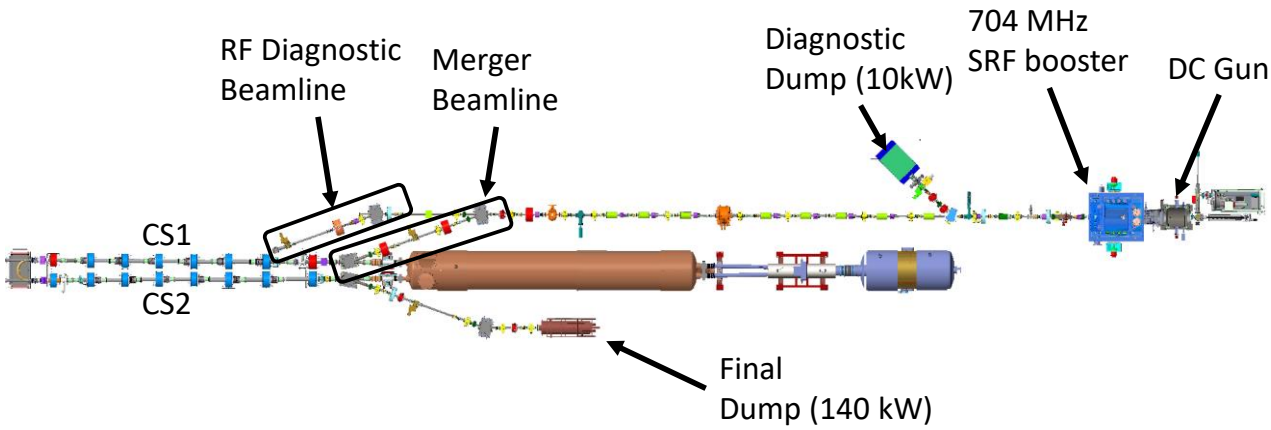

Figure 1: LEReC layout.

Abstract

The low energy RHIC Electron Cooler (LEReC) will be operating with 1.6-2.6 MeV electron beams having up to 140 kW power. It was determined that the missteered electron beam can damage the vacuum chamber and in-vacuum components within 40 us. We protect our accelerator against such a catastrophic scenario by a dedicated machine protection system (MPS). In this paper we describe the current status of the LEReC MPS design. We share our recent experience in commissioning and operation of the scaled down MPS used for the LEReC gun test beamline and discuss the status of the MPS designed for the commissioning of the full LEReC facility planned for next year.

LEREC LAYOUT AND PARAMETERS

The LEReC accelerator [1] consists of the 400 keV DC photo-gun followed by the 1.2-2.2 MeV SRF Booster, the transport line, the merger that brings the beam to the two cooling sections (CS1 and CS2) and the cooling sections followed by the 140 kW dump. The LEReC also includes two dedicated diagnostic beamlines: the low-power beamline capable of accepting 10 kW beam and the RF diagnostic beamline.

The LEReC layout is schematically shown in Fig. 1.

The LEReC beam train consists of 9 MHz macro-bunches. Each macro-bunch (MB) consists of N_b=30 bunches repeated with 704 MHz frequency. The length of each bunch at the cathode is 80 ps. The charge per bunch (Q_b) can be as high as 200 pC.

We will have the ability to work with macro-bunch trains of various length (Δt), various number of macro-bunches per train (N_{mb}), and various time delay (T) between the trains.

In addition to baseline operational modes listed in Table 1 the LEReC might also be operated with CW 704 MHz beam of 85 mA (at 1.6 MeV) and 68 mA (at 2 MeV).

The LEReC beam modes and their use are summarized in Table 1.

Table 1: LEReC Beam Modes

Beam Modes	Goals
Low Current Mode (LCM) N_b = 30; N_{mb} = 1; T = 1 s Q_b = 30 – 200 pC	Optics commissioning; Rough RF settings; Emittance measurement
RF Studies Mode (RFSM) N_b = 10,15,20,25,30; $\Delta t \leq$ 250 us; T = 1s – 5s; $Q_b \leq$ 200 pC	RF fine-tuning. Study beam longitudinal phase space.
Transition Mode (TM) N_b = 30; $\Delta t = T$; $Q_b \leq$ 200pC	Transition from LCM to HCM with gradual adjustment of Q_b.
High current Mode (HCM) N_b = 30; $\Delta t = T$; Q_b = 130 – 200 pC	Getting nominal e-beam parameters in the CS.
CW Mode (CWM) 704 MHz CW; Q_b = 95 – 120 pC	Alternative to HCM.

* Work supported by Brookhaven Science Associates, LLC under Contract No. DE-AC02-98CH10886 with the U.S. Dept. of Energy.
† seletskiy@bnl.gov

ISBN: 978-3-95450-192-2 doi:10.18429/JACoW-IBIC2017-TH2AB1

MINIMIZING ERRANT BEAM AT THE SPALLATION NEUTRON SOURCE*

C. Peters, W. Blokland, A. Justice, T. Southern, Spallation Neutron Source, Oak Ridge National Laboratory, Oak Ridge, TN, 37831, USA

Abstract

Since beginning neutron production operation in 2006 at the Spallation Neutron Source (SNS), one of the goals for the Accelerator Operations group has been to minimize beam trips. The beam trips which occur with the highest frequency are due to errant beam in the Super Conducting Linac (SCL). The process of minimizing the amount of errant beam and the frequency of faults will be described.

DESCRIPTION OF THE SNS LINAC

The linear accelerator at the SNS consists of (in order of beam acceleration) an H^- Ion Source (H^-IS), Low Energy Beam Transport (LEBT) which contains an electrostatic beam chopper (LEBT chopper), Radio Frequency Quadrupole (RFQ), Medium Energy Beam Transport (MEBT), Drift Tube Linac (DTL), Coupled Cavity Linac (CCL), Medium Beta Super Conducting Linac (MB SCL) (3 cavities per cryomodule), and High Beta Super Conducting Linac (HB SCL) (4 cavities per cryomodule). The fundamental RF frequency in the RFQ-DTL is 402.5 MHz, and 805 MHz for the CCL-SCL.

The SCL is physically the longest accelerating component of the linac, and also performs the majority of the beam acceleration. The nominal beam energy for the current SNS linac is 1 GeV, and the energy acceleration by the SCL is from 186 MeV to the design 1 GeV. Of the 96 RF structures used for accelerating, 81 are superconducting [1].

All systems (H^-IS and RF) are pulsed at a 60 Hz repetition rate for approximately 1 millisecond, for a duty factor of about 6%. Figure 1 shows the linac arrangement and relative lengths of the different structures.

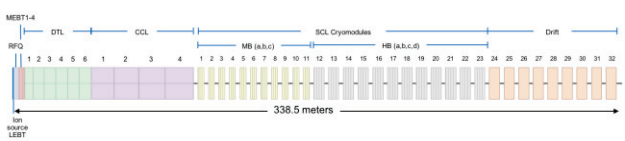

Figure 1: Ion source through SCL schematic.

*This manuscript has been authored by UT-Battelle, LLC under Contract No. DE-AC05-00OR22725 with the U.S. Department of Energy. The United States Government retains and the publisher, by accepting the article for publication, acknowledges that the United States Government retains a non-exclusive, paid-up, irrevocable, worldwide license to publish or reproduce the published form of this manuscript, or allow others to do so, for United States Government purposes. The Department of Energy will provide public access to these results of federally sponsored research in accordance with the DOE Public Access Plan (http://energy.gov/downloads/doe-public-access-plan).

ERRANT BEAM AND BEAM TRIPS

Errant beam is the resulting beam produced by malfunctioning accelerator equipment. When a glitch occurs, this errant beam does not transport through the accelerator properly (see Fig. 2). This beam typically triggers the Machine Protection System (MPS) to stop beam acceleration resulting in what is termed a beam trip. In general, errant beam trips typically take only a few seconds to reset. Occasionally errant beam events induce an SCL RF cavity trip which can take a few minutes to recover. If the frequency of errant beam trips is high enough, it can reduce the overall 60 Hz beam even with the relatively quick recovery.

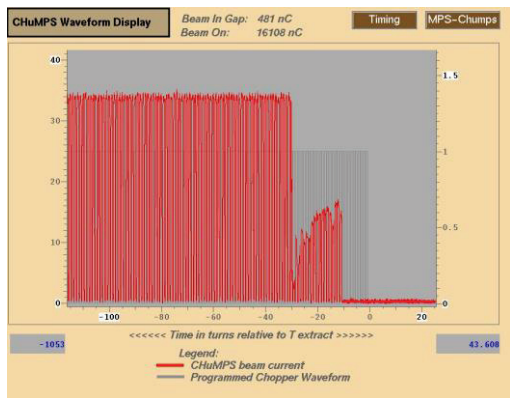

Figure 2: Example of LEBT high voltage malfunction.

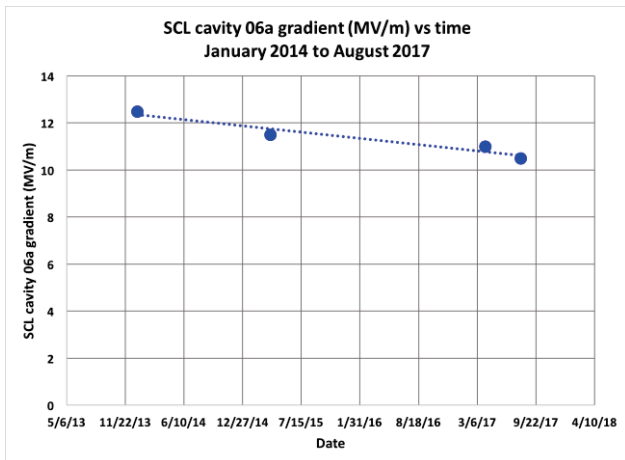

Figure 3: SCL cavity 06a gradient is declining at about 0.6 MV/m per year even with reduced errant beam frequency.

Additionally, repeated errant beam events over weeks, months, and years degrade SCL cavity performance [2,3]. Degradation of cavity performance means that over time

ISBN: 978-3-95450-192-2 doi:10.18429/JACoW-IBIC2017-TH2AB2

BUNCH-BY-BUNCH BEAM LENGTH MEASUREMENT USING TWO-FREQUENCY SYSTEM AT SSRF*

H. J. Chen†,1, L. W. Duan, Y. B. Leng‡, B. Gao[1], L. W. Lai, N. Zhang
Shanghai Institute of Applied Physics, Chinese Academy of Sciences, Shanghai, China
[1]also at University of Chinese Academy of Sciences, Beijing, China

Abstract

A Two-frequency method has been implemented for bunch length measurement at Shanghai Synchrotron Radiation Facility (SSRF). It is based on the information from two harmonic frequencies of Flourier Transformation of longitudinal charge distribution. We select 500MHz and 3GHz as working frequency and the system consists of power splitters, band-pass filters and a mixer. Raw data are acquired by a digital oscilloscope and analyzed by MATLAB code. The system has been calibrated by Steak Camera in single-bunch experiment environment with bunch charge from 0.23nC to 6.05nC. The paper also shows bunch length synchronous oscillation phenomenon during injection period.

INTRODUCTION

Shanghai Synchrotron Radiation Facility (SSRF) is a third-generation light source facility in Shanghai ,China, which has been operating about 8 years. With the second phase construction and more inserts in storage ring, the longitudinal instabilities will raise up including bunch-length diversity. Moreover, bunch length should be regulated within appropriate ranges for high brilliance pulses producing, which leads it as an important factor of overall beam performance.

Bunch length is now precisely measured by Streak Camera in SSRF with bunch-by-bunch capability and resolution of 2 ps [1]. However, the data reputation rate of Streak Camera is low about 2 Hz, and it requires complicated optical structures. A two-frequency system for bunch-by-bunch bunch length measurement has been implemented in SSRF for real-time measurement and data analysis of SSRF daily operation.

The two-frequency method picks up longitudinal distribution information from Beam Position Monitors (BPMs).The bunch length could be calculated through the intensity radio at two harmonic frequencies of Fourier component in Gaussian longitudinal charge distribution.It is a indirectly way in Frequency domain and had been used for average bunch length measurement at CERN with a resolution about 0.7 ps [2].Bunch-by-bunch data acquisition and analysis techniques have been developed at SSRF for many years with successfully implemented for position measurement [4] [5].It could also applied for the two-frequency system to approach bunch-by-bunch results.

* Work supported by National Natural Science Foundation of China (No. 11375255 and No. 11375254)
† chenhanjiao@sinap.ac.cn
‡ Corresponding author:lengyongbing@sinap.ac.cn

Two harmonic frequency detection point is selected as 500 MHz and 3 GHz in the two-frequency system. It employs radio-frequency (RF) electronics, a high sampling rate and multi channels oscilloscope as data acquisition module. Data analysis is under Matlab environment. In this paper, we will discuss the principle, system setup, system calibration using Streak Camera and bunch length synchronous oscillation phenomenon during injection period.

PRINCIPLES

A typical bunch longitudinal charge distribution is Gaussian and its Fourier component of m_i-th harmonic is given as:

$$V(m_i\omega_0) = 2V_0 exp\ -\frac{m_i^2\omega_0^2\sigma_0^2}{2} \quad (1)$$

where ω_0 is the RF frequency 499.654 MHz of SSRF, V_0 is the DC component, σ_0 is the bunch length considered as a constant at one time. Hence, the σ could be obtained with voltage radio between two different harmonic frequency points as follows:

$$\sigma = \sqrt{\frac{2}{m_2^2\omega_0^2 - m_1^2\omega_0^2} ln\left(\frac{KV_1(m_1\omega_0)}{V_2(m_2\omega_0)}\right)} \quad (2)$$

where V_1 and V_2 are experimental measured value at two m_i-th harmonic frequencies, m_2 is larger than m_1 and K is a coefficient calculated by two-frequency results. To calculate the resolution of bunch length σ, we could get the equation as follows:

$$\frac{\Delta\sigma}{\sigma} \simeq \frac{\sqrt{2}}{\left|m_1^2 - m_2^2\right|\omega_0^2\sigma^2}\left[\left(\frac{\Delta V_1}{V_1}\right)^2 + \left(\frac{\Delta V_2}{V_2}\right)^2\right] \quad (3)$$

The $\Delta V/V$ is equal to the signal-to-noise ratios(SNR)of V_1 and V_2 signal, which are close enough at most occasions. From Eq. (3), the resolution of bunch length will suffer a severe enlargement when the two frequencies are too close: $\left|m_1^2 - m_2^2\right| \to 0$. As RF components bandwidth limitation, m_1=1 and m_2=6 (about 500 MHz and 3 GHz) are selected for this application.

SYSTEM SETUP

The two-frequency bunch-by-bunch bunch length measurement system is comprised of RF conditioning module, time module and real-time oscilloscope acquisition module, the detail block diagram is shown in Figure 1.

The signal from BPM button is divided into two channels by a two-way zero-degree power splitter. One channel passes

ISBN: 978-3-95450-192-2 doi:10.18429/JACoW-IBIC2017-TH2AB3

OPTIMIZATION OF THE CRYOGENIC CURRENT COMPARATOR (CCC) FOR BEAM INTENSITY MEASUREMENT*

T. Sieber[1†], H. De Gersem[7], J. Golm[3], M. Fernandes[2, 8], R. Jones[2], P. Kowina[1], F. Kurian[1], N. Marsic[7], R. Neubert[3], H. Reeg[1], M. Schmelz[6], F. Schmidl[3], M. Schwickert[1], P. Seidel[3], L. Soby[2], T. Stoehlker[1,4,5], R. Stolz[6], J. Tan[2], G. Tranquille[2], V. Tympel[5], C.P. Welsch[8], V. Zakosarenko[6]
[1]GSI Helmholtz Center for Heavy Ion Research, Darmstadt, Germany
[2]CERN European Organization for Nuclear Research, Geneva, Switzerland
[3]Institute for Solid State Physics, Friedrich-Schiller-University Jena, Germany
[4]Institute for Optics and Quantum Electronics, Friedrich-Schiller-University Jena, Germany
[5]HIJ, Helmholtz-Institute Jena, Germany
[6]IPHT, Leibniz Institute of Photonic Technology, Jena
[7]TEMF, Institute for Theory of Electromagnetic Fields, Technical University, Darmstadt
[8]University of Liverpool, Liverpool

Abstract

Triggered by the need for nA current measurement of slow extracted beams and in the storage rings at FAIR and CERN, the idea of the CCC as a current transformer has been revitalized during the last ten years. Compared to the first prototype, developed at GSI in the 90s, the second generation of CCCs is based on the possibility of detailed simulation of superconducting magnetic shielding properties, new nanocrystalline materials for the magnetic ring-cores and on superior commercially available SQUID systems. In 2014, nA resolution measurements at 2 kHz bandwidth demonstrated the possibility of spill analysis at slow extracted beams from GSI SIS18. In the following year, the first stand-alone CCC system, including a cryostat with separate He liquefier, started operation in the CERN AD. Although the existing systems show outstanding current resolution, their cost efficiency and robustness, as well as noise- and vibration sensitivity can still be improved, which is subject of ongoing research.

In this paper, recent results of our CCC tests are shown and future developments are discussed.

INTRODUCTION

Beam intensity measurement with a Cryogenic Current Comparator is based on the detection of the azimuthal magnetic field of the particle beam. This field is measured by using a pickup coil wound around a high permeability ring core which acts as a flux concentrator, an arrangement which ensures efficient coupling of the azimuthal magnetic field to the pickup. The signal from the pickup coil is fed (via a transformer for impedance matching) to a dc SQUID (Superconducting Quantum Interference Device) current sensor, which is operated in a compensation circuit, using a so called Flux Locked Loop (FLL) electronics [1]. In order to suppress disturbing magnetic noise from external fields, the pickup coil and ring core are embedded in a superconducting meander-shaped magnetic shield, providing attenuation of non-azimuthal field components of < -100 dB. Figure 1 shows the currently used arrangement, originally developed at the PTB (Physikalisch-Technische Bundesanstalt) [2].

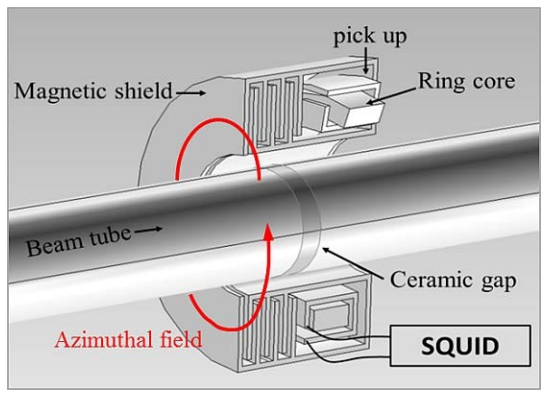

Figure 1: Principle of the CCC, shielding with radial meanders.

Following earlier work by Grohmann, Kuchnir and Peters et al. [2, 3, 4], the most recent and also most detailed investigations of the practical aspects of CCC operation in accelerators were performed in 2014 at GSI in a SIS18 extraction beamline, and in the CERN Antiproton Decelerator, where a CCC started its operation in 2015. Both systems were/are equipped with state of the art commercial SQUID systems (Magnicon© [5] and Supracon© [6] SQUIDs respectively).

While the GSI CCC basically consisted of a prior GSI prototype, equipped with a lead shielding and a VITROVAC© ring core, housed in a comparatively simple high vacuum cryostat, the AD CCC represents the first stand-alone device (including a UHV beam tube and a He reliquefier), which has been extensively optimized with respect to mechanical vibrations and slew rate limitations. For the pickup coil, a different material of the ring core was chosen, since a study at Jena University concluded that the so called NANOPERM© material had a more

* Work supported by the BMBF under contract No. 05P15SJRBA
† T.Sieber@gsi.de